INVESTIGATION OF NOVEL APPROACHES FOR IMPROVED AMPHIPHILIC FOULING-RELEASE COATINGS

A Dissertation
Submitted to the Graduate Faculty
of the
North Dakota State University
of Agriculture and Applied Science

By

Alireza Rahimi

In Partial Fulfillment of the Requirements
for the Degree of
DOCTOR OF PHILOSOPHY

Major Department:
Coatings and Polymeric Materials

April 2020

Fargo, North Dakota

North Dakota State University
Graduate School

Title

Investigation of Novel Approaches for Improved Amphiphilic Fouling-release Coating

By

Alireza Rahimi

The Supervisory Committee certifies that this ***disquisition*** complies with North Dakota State University's regulations and meets the accepted standards for the degree of

DOCTOR OF PHILOSOPHY

SUPERVISORY COMMITTEE:

Dr. Dean C. Webster
Chair

Dr. Ghasideh Pourhashem

Dr. Bakhtiyor Rasulev

Dr. Andrew B. Croll

Dr. Ronald Degges

Approved:

4/24/2020
Date

Dr. Dean Webster
Department Chair

ABSTRACT

Marine biofouling has troubled mankind, both environmentally and economically, since they set sail, resulting in many undesired consequences such as increased drag, reduced maneuverability, increased fuel consumption and greenhouse gas emissions, and heightened maintenance costs. This problem is highly complex as it involves more than 4000 marine organisms with varying modes of adhesion and surface preferences as well as many aquatic environments. The common state-of-the-art approaches to contend with marine biofouling on the submerged surfaces of ships in seawater has antifouling (AF) and fouling-release (FR) surfaces.

As AF coating systems utilize biocides which are often toxic to the environment to prevent settlement of biofoulants, the endeavors have been shifted towards non-toxic FR marine system. Many FR systems take advantage of low surface energy and modulus polydimethylsiloxane (PDMS) on their surface, while the recent attempts explored the simultaneous effect of PDMS and hydrophilic moieties (i.e. polyethylene glycol (PEG) or zwitterionic polymers) on an FR surface, known as amphiphilic surfaces. Thus, the work in this dissertation focused on attaining amphiphilic surfaces with desirable FR performance.

The studies in this dissertation were investigated to deliver two goals: 1) Enhancing the (FR) fouling-release performance of previously developed coating systems; 2) Introducing novel fouling-release marine coatings with set criteria. To address the former, a series of amphiphilic additives containing PDMS and hydrophilic polymers (zwitterionic-based or PEG) were prepared in chapters two-five. These additives were incorporated in several previously developed FR coating systems in order to modify their surfaces and enhance their FR performance. To address the latter, two amphiphilic marine coating systems were explored for accessing durable, non-toxic, and effective FR surfaces using epoxy-amine crosslinking chemistry. Overall, the studies in this dissertation not only demonstrated viable FR surfaces with desirable performance against several representative marine organisms such as *N. incerta*, *U. linza*, *C. lytica*, barnacles, and mussels but also contributed a deeper understanding about the effect of amphiphilicity concentration/balance on surface and FR properties.

ACKNOWLEDGMENTS

As I am writing this page to complete the assembly of my Ph.D. dissertation, I would like to express my extreme gratefulness and humility to every individual who supported me throughout this journey and celebrated my attained milestones with me.

Foremost of all, I would like to thank my advisor, Dr. Dean C. Webster for his continuous mentoring and teaching. I will always cherish your endeavors for locating resources to let me learn, grow as a scientist, and be part of your group – your efforts to fund me for summers 2014 and 2015 as well as securing a fund so I could pursue this Ph.D. Your leadership style and humbleness trained me to be a scientist with integrity and humility. When I completed my summer 2014 internship in your lab, I knew that I would like to be your student. Today, I am honored and privileged that I have had this opportunity of being your student and carry your name as my mentor throughout my professional career and personal life.

To my Ph.D. committee members, Dr. Ghasideh Pourhashem, Dr. Bakhtiyor Rasulev, Dr. Andrew B. Croll, and Dr. Ronald Degges: I truly appreciate your timely advice and support throughout these years. Your inputs not only helped me to direct my research towards clear goals but also trained me to be a well-rounded student. Thanks to Dr. Pourhashem for never minding my long conversations in her office concerning research, personal and career opportunities. Thanks to Dr. Rasulev for always being available to assist me in learning new computational skills and collaborating with me on our attempt to create predictive models for my projects. Thanks to Dr. Croll for being accessible to discuss AFM images and training me to understand the fundamentals of the AFM technique better. And finally, thanks to Dr. Degges for his applied statistics class that motivated me to obtain a graduate certificate in statistics which greatly contributed to design objective-oriented projects.

To my parents, Mohammad Kabir Rahimi and Marzia Rahimi, and my brothers, Taha and Mehrdad: My words can never express my gratitude to you as you unconditionally supported me to pursue my education and never allowed me to be saddened for being away as the oldest son/brother for more than ten years. Mom and dad, I vividly recall you praying for me since my childhood to access world-class education and be successful while I was thinking about how that would be possible considering our weak financial status and the treacherous condition of Afghanistan. Today, I am very

happy that your prayers paid off as I present you this Ph.D. I will always remember that you sacrificed many things for me and my brothers to have a bright future. Hence, I am always indebted to your kindness and support while unfortunately many kids in Afghanistan lacked such parents. You raised me to have integrity and value and be honest, and I am glad I became an individual who you can be proud of. Moreover, I would like to thank my grandparents, uncles, aunts, and cousins who often brightened my days by calling me and letting me be part of their lives.

To my best friend Kinza F., I would like to acknowledge you for your unconditional support that I am always thankful for. Your strong personality and unstoppable motivations pushed me to be a better person every day. When I did not believe in myself, you believed in me. When many mocked me, you encouraged me. I am extremely grateful for the significant role that you played throughout my undergraduate and graduate school.

To my wonderful mentors, I would like to thank you all for equipping me with lifelong skills, ranging from technical skills in a lab to soft skills like project management and public speaking. Dr. Jeannette Garcia from IBM Almaden Research Center, you were one of the greatest mentors I could ask for – you taught me many instrumental skills and expanded my scientific horizon. Dr. Bob Allen from IBM Almaden Research Center, I am very thankful for your encouraging conversations and letting me be involved in some projects with you – your wise words opened my eyes to choose a great Ph.D. advisor over a “school name.” Thank you, Dr. Ahmad F Samin, for guiding me to pursue a career in physical sciences when you met me at the American University of Afghanistan in Kabul, Afghanistan – knowing you was a blessing that changed the course of my life. I also express gratitude to Dr. Arvin Yu, Dr. Adlina Paramarta, Dr. Craig Jasperse, Dr. Gary Edvenson, and Dr. Asoka Marasinghe as well as other teachers and mentors in Enghelab High School (Herat, Afghanistan), the American University of Afghanistan, and Minnesota State University Moorhead (Moorhead, MN, USA).

A special thank you to Azita M. whose kindness and great personality guided me to worry less and appreciate life more; your presence brought joy always. Also, I would like to thank my great friend as well as a mentor Dr. Morteza Farrahmand – words cannot express the gratitude I have for our friendship and I greatly appreciate that you always shared with me without hesitation your experiences and words of wisdom that you gained over the 25 years of life ahead of me.

Furthermore, I would like to thank my friends that our connection was beyond the lab perimeter including Dr. Alison Rohly, Dr. Teluka G., Dr. Arvin Yu, Dr. Eric Krall, Jonah Karanja, Jackson Benda, Raul Setien, Kweeni Iduoku, Taysir Bader, Faraz A., Anas KK., Oksana Z., Tanya, Zoriana, Gwen, Michael, Alex, Kristen, Joey, Zach, and Marta (and many others which I could not name). Additionally, I am grateful for my friends during Salsa/Bachata/Kizomba sessions in Fargo – you expanded my social network far beyond NDSU.

My appreciation goes to Shane Stafslien, Lyndsi Vanderwal, and Jim Bahr for their collaborations to assess the fouling-release performance of my coatings and their compositions. Thanks to Dr. Chunju Gu for always being helpful in the characterization lab. Thanks to Maryam S. and Morgan M. at NDSU and Abe H. at IBM for being wonderful interns/students who assisted me to accomplish more in less time. Also, my gratitude goes to our collaborators in the UK, Dr. John A. Finlay and Dr. Anthony S. Clare, as well as other collaborators Dr. Daniel Rittschof and Beatriz Orihuela. Also, special thanks to Janice and Ben for doing a fabulous job in the office and letting us have a great experience as students who would go to conferences.

Finally, I am extremely grateful to the Office of Naval Research for providing financial support for this research under grant number N00014-16-1-3064. I also appreciate all the scholarships and opportunities from the Department of Residence Life at NDSU, SSPC, Valspar, American Coatings Association, and NDSU College of Science and Mathematics. I am very grateful for the opportunities that this great land offered to me, the USA – I will always be thankful and dedicate my bests for this great country.

DEDICATION

I would like to dedicate this dissertation to my parents, Mohmmad Kabir Rahimi and Marzia Rahimi who dedicated their life for me and my brothers to be successful and continued their unconditional support when I moved to the US, to my supportive best friend who always encouraged me and believed in me, and to two great countries which are very close to my heart, the US and Afghanistan.

TABLE OF CONTENTS

LIST OF TABLES

LIST OF FIGURES

LIST OF SCHEMES

LIST OF APPENDIX TABLES

LIST OF APPENDIX FIGURES

CHAPTER 1. GENERAL INTRODUCTION

Marine Biofouling – Process, Impact, and Challenges

The undesirable settlement/attachment of marine organisms like barnacles or mussels on submerged surfaces in seawater, marine biofouling is a challenging problem that pressures the shipping/maritime industry.[1] Marine biofouling results in increased surface roughness on ship hulls, contributing to increased drag and decreased maneuverability. Due to these effects, fuel costs for a ship may increase up to 45% (depending on vehicle's size) that would surge the overall expense of a voyage up to 77%.[2] Additionally, marine biofouling requires frequent dry-docking of the ships which leads to further undesirable results such as damaging's ship hull coatings which will be prone to corrosion, penalizing ship owners with a higher maintenance cost, and generating toxic waste from cleaning.[1, 3] The US Navy spends $1 billion per year to maintain their ships from the undesired effects of biofouling; for example, it costs roughly $56 million in a year to clean ship hull of a USS Arleigh Burke class Navy destroyer.[4] Furthermore, marine biofouling takes the blame for transportation of invasive species to new aquatic locations around the world that misbalance marine ecosystem and for elevated greenhouse gas emissions (due to more fuel consumption).[1, 3] Thus, these examples portray marine biofouling poses both economic and environmental challenges that need to be addressed.

Marine biofouling is a complex problem that a sole answer cannot entail its complete solution due to many variables including diversity of biofoulants, differences in fouling behaviors, and a variety of aquatic zones. There are about 4000 marine organism that can potentially settle on a surface,[1] ranging from macrofoulants like diatoms and algae to macrofoulants like mussels and barnacles. As a result, this staggering number of biofoulants results in many remarkably different modes of adhesion and surface preferences for colonization. The presence of many aquatic zones with substantial differences such as salinity, micronutrient, and temperature further complicate the biofouling dilemma, while marine trade routes introduce new organisms to aquatic zones continuously.[1, 5] Therefore, finding a solution to address all these variables is very challenging, and an ideal coating surface should be economically sound, environmentally friendly (non-toxic), and durable to tackle as many biofoulants as possible in various aquatic zones.

Biofouling Processes and Mechanisms

The complicated nature of the marine biofouling issue restricts the development of a valid model for the biofouling process. The general perception is that marine biofouling starts as soon as a surface is submerged in seawater by the formation of conditioning film composed of organic molecules such as proteins, polysaccharides, and glycoproteins.[1] Microfoulants such as bacteria and diatoms subsequently colonize the surface,[6, 7] forming a microbial biofilm, followed by settlement of multicellular species (i.e. spores of macroalgae) that sustains on the biofilms as a food source.[5] Macrofoulants such as macroalgae, barnacles, and mussels further settle on the surface, resulting in an unaesthetic surface.[5, 8] However, this linear process may be limited to a few marine organisms while many circumvent this predicted scenario. For example, species like macroalgae *Ulva linza* and barnacle *Amphibalanus amphitrite* can settle on pristine unconditioned surfaces.[1, 9, 10] Regardless of the settlement order, one inevitable fact is that biofouling process starts seconds after the submergence of a surface in seawater (Figure 1.1).

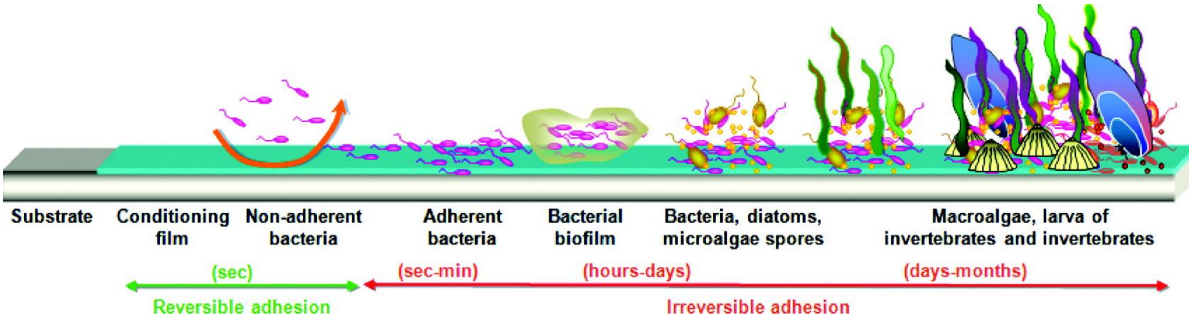

Figure 1.1. Development processes of marine fouling. Reproduced from reference 1.

Mechanisms of adherence vary greatly among marine organisms and is a significant factor that complicates marine biofouling, ranging from passive to active settlements. Diatoms and bacteria approach a surface when they are passively carried around by water movement or gravity forces,[5, 11] occupy a surface by secreting high amounts of polysaccharide-based polymeric substances, and rapidly colonize a surface via cell division, forming biofilms that can be as thick as 500 µm. In contrast, barnacles undergo a series of life phases before settling on a surface permanently. They start life as larvae that feed on plankton, followed by the formation of a cyprid barnacle with an approximate size of 500 µm that freely swims to settle on a surface. The juvenile cyprid barnacles explore and “walk” on a surface with the ability to detach/reattach using a bio-adhesive until a permanent location is selected and then they

metamorphose into calcified adult barnacles.[1, 12] These two organisms, out of many biofoulants, exemplify the significant variations among biofouling mechanisms of marine organisms. Therefore, it can be summed up marine biofouling organisms do not follow a straight, linear and regulated process and do not employ a single mechanism for adhesion and colonization, requiring a surface technology with the ability to defeat settlements of “all organisms” simultaneously.

Approaches to Contend with Marine Biofouling

Historically, ship hulls were made of wood and they were protected with sheaths and alloys of copper, lead, wax, or asphalt depending on location.[1, 13] These solutions emerged to be unviable over time due to limited availability of resources and proneness to corrosion with the advent of steel hulls. To address these concerns, paints with biocides were introduced as anti-fouling coating systems to prevent biofouling. In the 1960s-1980s, tributyl-tin (TBT)-based antifouling paints offered the marine industry a superior performance against biofoulants.[1, 13] However, as TBT was criticized for its potential toxicity,[14] the efforts concurrently were applied to find systems antifouling systems as contact leaching coatings, soluble/controlled depletion polymer coatings, and self-polishing copolymer coatings (Figure 1.2) – these systems also incorporated toxins and TBT as active biocides.[1]

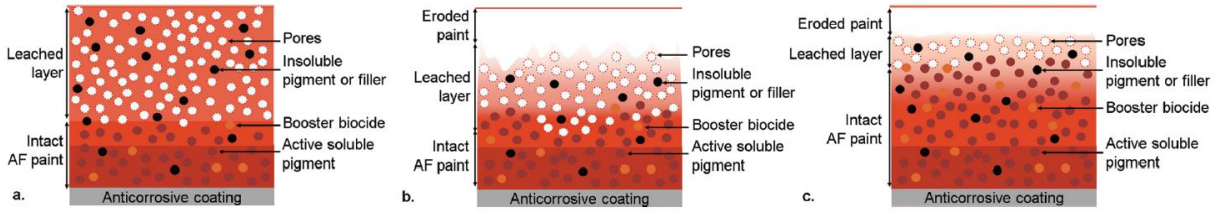

Figure 1.2. Schematic illustration of biocide-based containing antifouling paints after exposure to seawater. (a) Contact leaching coatings; (b) Soluble/controlled depletion polymer coatings; (C) self-polishing copolymer coatings. Reproduced from reference 1.

The TBT-based coatings exhibited highly desirable performance, but their toxic effects on aquatic environments and eventually humans could not be ignored. TBT resulted in shell thickening of oysters, extinction of *Nucella* marine organisms, and accumulation of tin in fish, seals, and ducks over the years.[14, 15] The negative consequences forced a worldwide ban on tin-containing paints in 2003 and obliged marine vessels to remove tin-based paints from their hulls by 2008. Therefore, the regulations accelerated further investigations that started in 1970s for finding alternative marine paints that were non-toxic and effective. The investigated approaches include, but not limited to, biomimetic systems,[16-19]

hydrophobic fluoropolymer networks,[20-22] self-stratifying siloxanes,[23-26] hydrogels,[27] xerogels,[28-34] zwitterionic polymers,[35-44] layer-by-layer assemblies.[45-48] The general characteristics of these diverse systems are briefly discussed under three umbrellas in the following sections: antifouling (AF) systems, bio-inspired systems, and fouling-release (FR) systems.

Antifouling (AF) coatings prevent the attachment of marine organisms while FR coatings decrease the adhesion strength of biofoulants on the surface, resulting in easy removal. In response to finding TBT alternatives, AF coatings currently utilize copper oxides (it was also used before and during TBT period as well), zinc oxides, and organic molecules as alternative biocides.[15, 16, 49-51] While these alternatives are not considered very “toxic”, they still have a potential to poison ecosystems. As a result, the number of universally accepted copper/zinc-based or organic biocides is limited to less than 20, suggesting the stringent regulations and assessments for their selection and the need for non-toxic non-leaching/biocide-free systems.

Fouling is not a problem limited only to marine vehicles or other manmade submerged surfaces in seawater, but many organisms such as fish and aquatic plants could also be prone to it; however, their intrinsic natural defense mechanisms deter biofouling.[3, 52] The defense mechanisms of marine organisms/plants against biofouling are diverse, including replenishing surfaces by sloughing skin layers, releasing bioactive molecules or enzymes, possessing structural topographies, and secreting of oils or mucus. These organisms often combine several defense mechanisms to fight against biofoulants, utilizing chemical, physical, mechanical and behavioral strategies. Thus, biomimicking fouling-release systems have been explored to find other alternatives in the fight against biofouling. Bio-mimicked surfaces have been prepared following an array of natural organisms and observations. With inspiration from sharks that utilize their skin topography against biofoulants, surfaces were prepared using PDMS in the early 2000s to generate morphologies of varying sizes and patterns to combat marine biofouling.[53, 54] It was noted that the degree of biofouling was affected by differences in surface topographies. For example, *U. linza* showed better release on 2 μm wide rod-like pattern than other patterns such as triangles and pillars as well as smooth PDMS coatings. In other approaches, surface patterns have been inspired from the skin of pilot whales or prepared as a honeycomb.[55] Although engineered topographies showed promising

results, the feasibility for their mass production is costly and limited while a specific pattern cannot deliver FR of all biofoulants.

Slippery liquid infused porous surfaces (SLIPS) were investigated with inspiration from pitcher plants as non-toxic fouling-resistant and FR coatings and showed promising output due to their highly smooth, dynamic, and liquid-like surface (Figure 1.3).[18, 56] However, this technology lacked long-term stability as infused liquid depletes, requiring further modifications for commercial applications. Silicone oils have also been explored to attain slippery surfaces for better fouling-release performance.[57, 58] As another bio-mimicked example, lotus leaf effect encouraged the preparation of superhydrophobic surfaces that typically possess very low surface energy and water contact angles greater than 150°, resulting in superior repellence of water (and other objects) due to trapped air pockets resulted from micro/nano-scale roughness (known as Cassie-Baxter state).[19] As AF/FR performance of superhydrophobic surfaces diminished quickly after submergence in seawater due to potential conversion of the surface from Cassie-Baxter state to Wenzel state, there were efforts to create superhydrophobic surfaces with stable air pockets, but it was noted the fouling-resistant of such surfaces depends on the pocket-size rather than their wettability.[59] The other examples of nature-inspired systems include mechano-responsive silicone or graphene-silicone elastomer coatings[60] and self-healing silicone-polyurea coatings.[61]

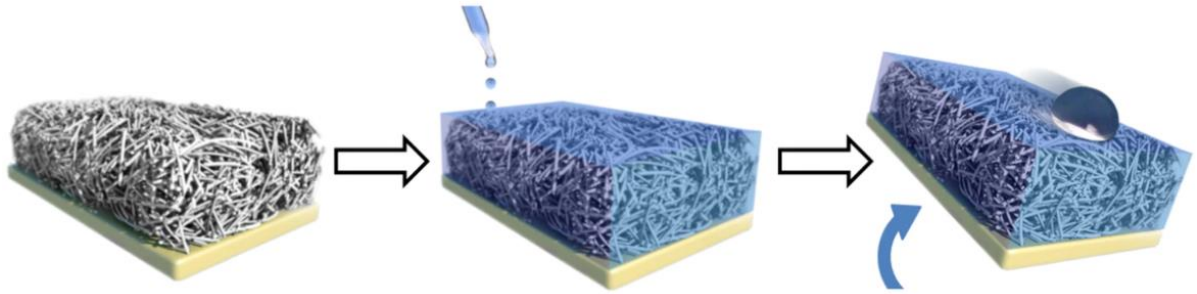

Figure 1.3. Illustration of slippery liquid infused porous surfaces (SLIPS) technology. Reproduced from reference 56.

Fouling-release coatings are recognized as another major type of marine systems. FR coatings fight biofouling by offering an ultra-smooth, uninhabitable surface for marine organisms that weakens their adhesion strength and facilitates their release under low hydrodynamic pressure (i.e. due to ship movement) or light cleaning/brushing.[1] Additionally, the competitive advantages of FR marine coatings

include several remarkable points such as their non-leachate or biocide-free property, prolonged service life (5-10 years with a reduced maintenance cost, extended dry-docking intervals, and chemically metal-free high-solid content systems (Figure 1.4).[62]

Figure 1.4. Economic and ecological advantages of fouling-release marine coatings. Reprinted from reference 62.

Traditional FR systems are mainly made of elastomeric materials such as polydimethylsiloxane (PDMS), fluoropolymers, or other organo-silicones, though it is noteworthy that siloxane-containing systems have shown better FR performance over years than fluorine-based surfaces.[1, 3] Generally, these materials possess low surface energy and low modulus. The former results in minimized interfacial bond between the foulants and the surface while the latter presents “mobile” chains in the bulk that limits effectiveness of bio-adhesives, thus facilitating the release of biofoulants.[63, 64] To this effect, the Baier curve was developed that indicated surfaces with surface energy values between 20-30 mN/m are ideal for minimal bioadhesin.[65] (It should be noted this does not hold true for several marine systems throughout this chapter such as self-stratified hydrophobic/amphiphilic siloxane-polyurethane or xerogels.)

The desirable properties of PDMS results from its molecular structure in terms of bond length and angles. The length of Si-O-Si and C-C bonds are 1.64 Å and 1.53 Å, respectively, and bond angles for Si-O-Si and tetrahedral C-C are 143° and 110°, respectively.[66] The longer bonds and higher bond angles

contribute to easier rotation and lower rotational free energy, resulting in high structural mobility, low glass transition (T_g -120 °C), and low interfacial energy (20-24 mJ/m^2). Besides, methyl groups on silicone atom protect the -Si-O- groups in the PDMS backbone which are reactive due to their polar nature while oxygen atoms in the backbone are not encumbered by any side chains, thus promoting further configurational flexibility. Therefore, PDMS possess great properties that rank it as a great choice for FR application such as smoothness, hydrophobicity, rotating/mobile molecular structure, low surface energy, and low porosity. PDMS also holds desirable anti-oxidation/ozone properties, heat resistance, and durability against UV (ultraviolet) radiations.[66] Thus, the characteristics of PDMS contributes to its selection as a top candidate for FR purposes.[1, 3, 5, 62] Although PDMS-base FR coatings are environmentally friendly and chemically stable, these systems suffer from poor mechanical durability and require a tie-coat to achieve proper adhesion to a substrate (which increases costs and operation time). While hydrophobic surfaces like PDMS-based coatings that can combat some biofouling species effectively, there are still marine organisms that can attach firmly on such surfaces. The difference in adherence of foulants to FR coating surfaces is not surprising given the wide variety of marine fouling organisms (~4000 species) with differing surface affinities for settlement, from hydrophilic to hydrophobic surfaces, and adhesion mechanisms. For example, *U. linza* and mussels attach strongly to hydrophilic surfaces, diatom, and bacterium *N. incerta* stick to hydrophobic surfaces and the marine bacterium, and *C. lytica* settles on a variety of surfaces.[1] Furthermore, the hydrophobic FR systems have poor antifouling performance under static conditions, allowing the growth of a slime layer composed of bacteria and diatoms which is very hard to remove at high ship speeds (>30 knots).[60, 62] Hence, there has been a need to improve adhesion/mechanical properties and FR performance of hydrophobic FR coatings.

Advancing Adhesion/Mechanical Properties of Fouling-release Coatings

Hydrophobic fouling-release (FR) marine coatings suffer from weak adhesion/mechanical strength and ability to tackle marine organisms that settle on hydrophobic surfaces, so efforts have been carried out to improve these properties utilizing physical and chemical modifications in a system. The incorporation of nanomaterials to a system or chemical moieties to a polymeric backbone has been investigated to improve mechanical and adhesion properties. Nanomaterials such as carbon nanotubes (CNTs), graphene oxide sheets, alumina nanorods, titanium dioxide (TiO_2) nanospheres, and zirconium

oxide (ZrO_2) are few examples that have been added to silicone-based FR coatings, contributing to improved mechanical and fouling-release properties.[67-70] For example, the addition of multi-walled CNTs at ~0.1 wt.% improved its storage modulus and fouling-release performance.[71] Chemical moieties such as epoxy, urea, and urethane have also boosted properties of silicone-based FR coatings where these linkages deliver better adhesion and increase system toughness. Self-stratifying hydrophobic siloxane-polyurethane (SiPU) FR coatings have been developed that display FR performance comparable to or better than commercially available products with strong adhesion to a substrate and a magnitude higher bulk modulus.[72, 73] The self-stratified SiPU coatings benefit from the combination of two incompatible materials: polyurethane (PU), which is polar with high surface energy, and PDMS, which is non-polar with low surface energy. The incompatibility as well as low surface energy causes self-stratification of components with PDMS segregating to the surface, tackling the biofouling issue, while the PU remains in contact with the substrate offering good mechanical strength and strong adhesion. XPS (X-ray photoelectron spectroscopy) experiments with ion milling showed that the distribution of siloxane varied from the surface into the bulk of the coatings, supporting the self-stratification of the engineered coating formulations (Figure 1.5). Following the same self-stratifying technique, there also has been reported the explorations of siloxane-glycidyl-carbamate coatings via epoxy crosslinking.[74, 75] The self-stratifying systems eliminate the need for a tie-coat and allow for mass-scale production of these systems with fewer labor requirements. Besides, the incorporation of urea groups in silicone backbone resulted in enhanced adhesion and mechanical properties where the coating possessed adhesion strength of 2 MPa in comparison to commercial PDMS Slygard® 184 with adhesion strength of 0.4 MPa.[76]

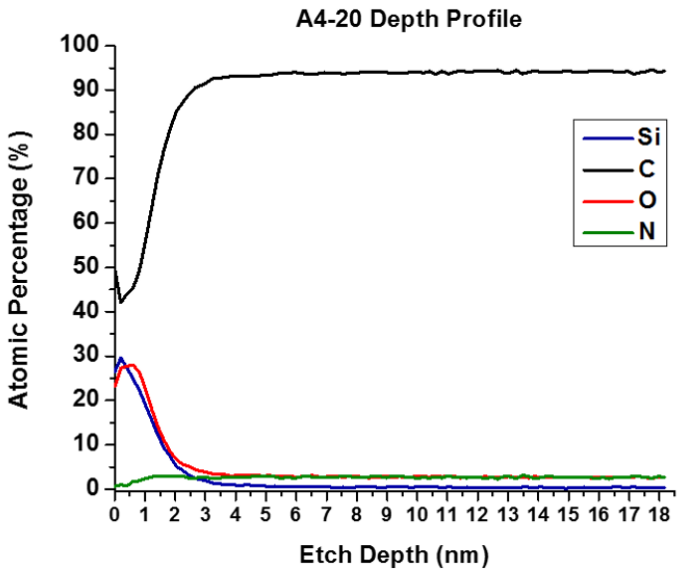

Figure 1.5. XPS depth profiling using argon ion milling for siloxane-polyurethane coating. This data confirms the self-stratification of the system and compositional variations on the surface and in the bulk. Reproduced from reference 73.

Amphiphilic Surfaces: Boosting Performance of Fouling-release Coatings

The restrictions of hydrophobic FR systems to tackle all biofouling of a wider range of marine organisms has always been a challenge since there are organisms like *N. incerta* diatom that settle on hydrophobic surfaces. The difference in adherence of foulants to FR coating surfaces is not surprising given the wide variety of marine fouling organisms with differing surface affinities, from hydrophilic to hydrophobic surfaces, and adhesion mechanisms.[1] Thus, amphiphilic FR surfaces that contain both hydrophilic and hydrophobic moieties have been explored as an alternative to combat marine biofouling.[3] Amphiphilic systems also have been explored for other applications including medical implants and devices, drug and gene delivery, texturing, petroleum recovery, and membrane separation recovery.[77]

An amphiphilic system contains both hydrophobic and hydrophilic segments. PDMS and fluoroalkyl polymers are common hydrophobic moieties for FR applications because of their desired characteristics. As discussed previously, PDMS, for example, possesses many great properties including smoothness, hydrophobicity, rotating/mobile molecular structure, low surface energy, low porosity, anti-oxidation/ozone properties, heat resistance, and durability against UV radiation.[66] On the other side of the spectrum, hydrophilic materials have shown a promising ability to discourage biofouling due to their protein-resistant ability,[78] thus they have been explored as modifiers for marine coatings as well.[1]

Polyethylene glycol (PEG) is one of the commonly investigated materials as it resists protein absorption and possesses non-toxic and nonimmunogenic properties. PEG-modified surfaces interfere with protein binding through hydrophilic interactions of the surface with water to form a hydration layer. This layer serves as an energetic barrier that prevents nonspecific protein absorption. Also, PEG polymer brushes on a surface block potential sites for protein adsorption due to their flexible chains and configurational mobility that results in steric excluded volume, thus requiring too much entropic energy from proteins in order to favorably adsorb to the surface (Figure 1.6).[79] Zwitterionic materials are recognized as another major category of hydrophilic, protein-resistant and ultra-low fouling materials that can bind water molecules even more strongly and offer prolonged stability.[38, 40] Phosphobetaine, sulfobetaine, and carboxybetaine are examples of zwitterionic candidates. A study reported zwitterionic poly (sulfobetaine methacrylate) absorbed up to eight times more water than PEG (Figure 1.7),[80] forcing biofoulants to dislike the coating surface due to their inability to surpass the required entropic energy for displacing the water molecules which is much higher than PEG-based hydration layer.[81] Overall, hydrophilic polymers have demonstrated promising results in a wide range of applications due to their biomimetic and low biofouling properties, stability, and commercial availability.

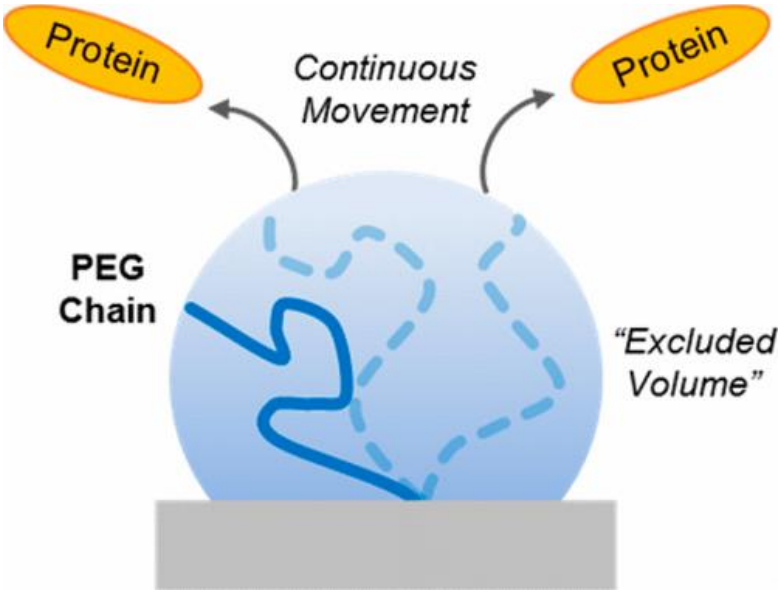

Figure 1.6. Schematic of the steric excluded volume effects of surface grafted PEG chains. Flexible and continuously moving PEG chains create a physical barrier to protein adsorption. Reprinted from reference 79.

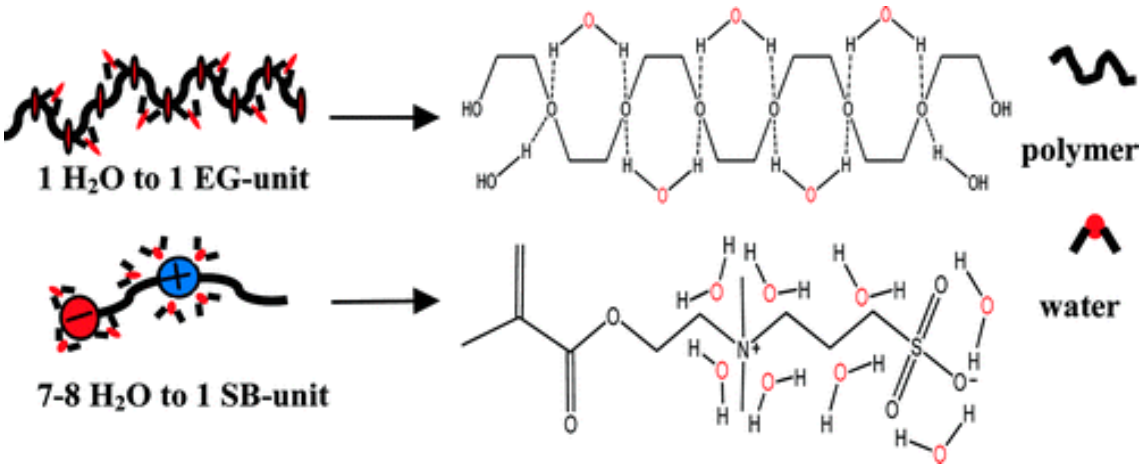

Figure 1.7. Schematic illustration of the extent of hydration for poly (ethylene glycol) (Top) and poly (sulfobetaine methacrylate) (Bottom). The zwitterionic group results in water absorption up to eight times higher. Reprinted from reference 80.

Amphiphilic surfaces provide a heterogeneous nanoscale surface that is a combination of both hydrophobic and hydrophilic patterns, or one can think of amphiphilic surfaces as platforms that present chemically ambiguous surfaces composed of both polar and non-polar functionalities to the marine organisms.[82] Though little is understood about the defense mechanisms of amphiphilic surfaces towards biofoulants, the general theory is that these surfaces "confuse" organisms during settlement and adhesion,[5, 20] resulting in the observed desirable antifouling/fouling-release properties. A variety of amphiphilic marine surfaces/networks has been explored that include several categories, such as surface-active, hyperbranched, UV-cured, condensation-cured, layer-by-layer, and polypeptides/peptide-mimic.

Surface-active Networks

Polymers with potential surface activity have been explored as an approach to attain amphiphilic surfaces, where these polymers self-segregate and self-assemble to the surface-environment interface and function as surface modifiers or additives. Amphiphilic copolymers have been utilized for AF/FR applications as either sole systems or booster in an elastomeric matrix and they are physically dispersed in, not chemically/covalently linked to, the elastomeric matrices. The matrices for these amphiphilic copolymers are mainly poly(styrene-b-(ethylene-co-butylene)-b-styrene) (SEBS) and PDMS.[22, 83]

For the SEBS matrix, the initial work included copolymers that typically contained PEG and fluorinated alkyl chains (**1-2,** Figure 1.8).[82] The incorporation of these copolymers resulted in suggestions

that the surfaces become more hydrophilic upon exposure to water, because of surface rearrangements due to hydrophilic/hydrophobic swelling/deswelling behavior as confirmed by AFM experiments. The PEG-fluorinated copolymers improved the performance of the base SEBS towards diatom *N. perminuta* and macroalgae *U. linza* biofoulants, thus encouraging further exploring these amphiphilic copolymers.[84] However, perfluorocarbon chains with seven or more CF_2 repeating groups raised the possible issue of environmental (bio)accumulation due to biodegradation products such as perfluorooctanoic acid.[85] The environmental concerns directed focus towards fluorine-free surface-active amphiphilic copolymers such as PDMS and PEG chains attached on a polymeric backbone, non-ionic amphiphiles, and PEGylated hydrocarbon side chains (**3,** Figure 1.8).[82, 86] These fluorine-free copolymers exhibited desirable performance as their fluorine-based counterparts as well as surface rearrangements in response to immersion in water. Surface-active copolymers were introduced to PDMS based matrices as well. The first attempt was the introduction of a di-block copolymer composed of a PDMS block and a PEGylated-fluoroalkyl modified polystyrene block, opening the door for new opportunities where amphiphilic copolymers of ranging lengths of PEGylated and Fluro-based blocks, fluorine-free copolymers, and hybrid SEBS and PDMS matrices were assessed.[87-89]

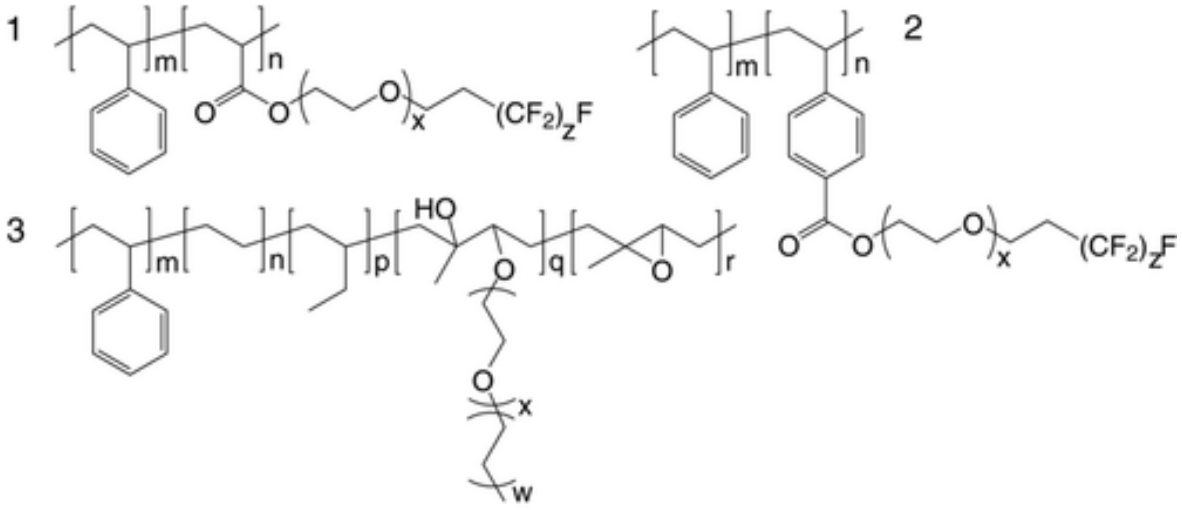

Figure 1.8. Illustrations of surface-active (co)polymers containing amphiphilic moieties. Hydrophilic PEG segments, hydrophobic alkyl segments and hydrophobic/lipophobic fluorinated segments of varying length (x, w, and z, respectively) for introduction into SEBS-based systems. Reproduced from references 82.

Hyperbranched Surfaces

Hyperbranched polymers have intrigued interests in engineering surfaces that have environmental-responsive domains ranging from nano to micro scales. A hyperbranched polymer combining hyperbranched fluoropolymer (HBFP) and polyethylene glycol (PEG) was the first system to pioneer amphiphilic surfaces for marine applications (Figure 1.9).[90] The films displayed surfaces with heterogeneous phase due to incompatibility of HBFP and PEG chains while the surface responded to changes in the surrounding environment dynamically and reversibly (i.e. changes in contact angle or swelling/deswelling domains in dry state vs wet state). This system demonstrated a specific concentration of PEG (~40 wt.%) contributed to better fouling-release than PDMS control film. Due to brittleness of the hyperbranched HBFP-PEG films, second and third generations of this system were developed to improve its mechanical properties by decreasing the glass transition temperature.[91, 92] Moreover, an array of HBFP and PEG combinations along with noradrenaline (bioactive fouling-deterrent molecule) were explored to assess the physical-chemical effect of each factor on FR performance.[93, 94] The studies showed higher PEG resulted in higher surface hydrophilicity until a “contraphilic” behavior was observed by larger contact angles due to the presence of increasing HBFP content. The introduction of PDMS into the structure of HBFP-PEG, resulting in HBFP-PEG-PDMS hyperbranched molecule, was another step to access better-performing surfaces.[95] Additionally, highly branched and dendritic (i.e. polyglycerol based) amphiphilic marine networks were investigated using thiolene click chemistry.[96] Overall, the hyperbranched surfaces indicated the amount of PEG played a major role in the formation of the observed surface topographies, roughness, and extent of fouling-release performance, suggesting the tunability of these systems.

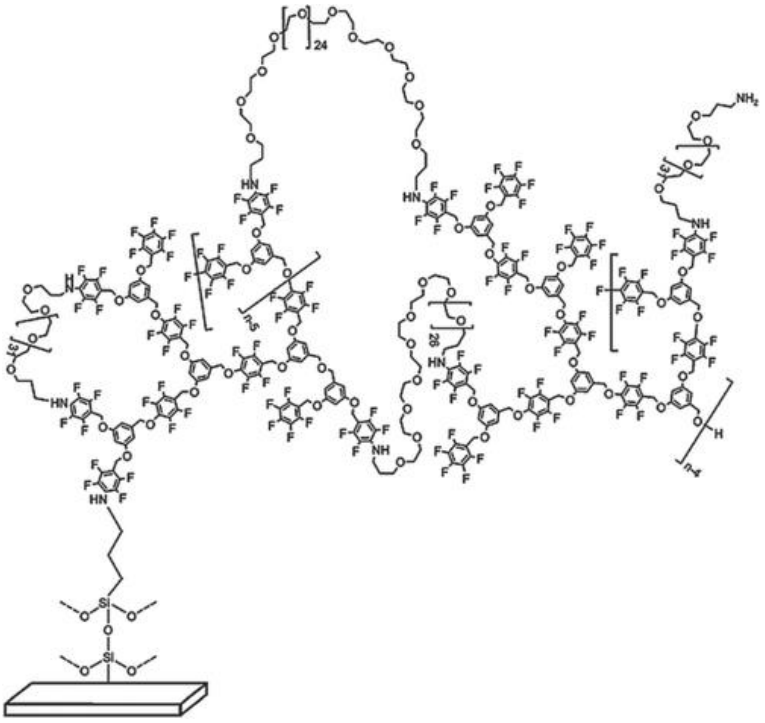

Figure 1.9. Schematic of an HBFP-PEG polymer network deposited on an amine-functionalized glass substrate. Reprinted from reference 90.

UV-cured Networks

UV photopolymerization delivers amphiphilic surfaces by combining (macro)monomers that undergo the same polymerization technique. The UV-based approach discards the limitations of complex synthesis procedures to prepare block copolymers or hyperbranched polymers, though this approach restricts the ability to easily tune the surfaces. Methacrylated (MA) macromonomers containing perfluoropolyether and PEG backbones were UV-cured as fouling-release coatings, where one system utilized mono-MA PEG (PEG-MA) and the other system used di-MA PEG (PEG-DMA) (Figure 1.10).[97] While the performance of these systems was comparable to control PDMS, it was noteworthy that films based on PEG-MA performed better than PEG-DMA. This behavior was attributed to greater flexibility and freedom of the PEG chains of PEG-MA to access the surface-water interface as they were tethered at one end only, while PEG chains of PEG-DMA were locked more strictly due to being crosslinked from both ends which impeded the effective migration of these moieties to the surface. In another study, PEG, PDMS, and perfluorohexylethyl (macro)monomers with (meth)acrylate functional groups were photopolymerized too.[98] These films possessed elastomeric behavior as they contained up to 90 wt.%

PDMS. The FR results indicated amphiphilic surface impacts performance, where at least 5 wt.% PEG was needed in a system to attain relatively better FR than PDMS films.

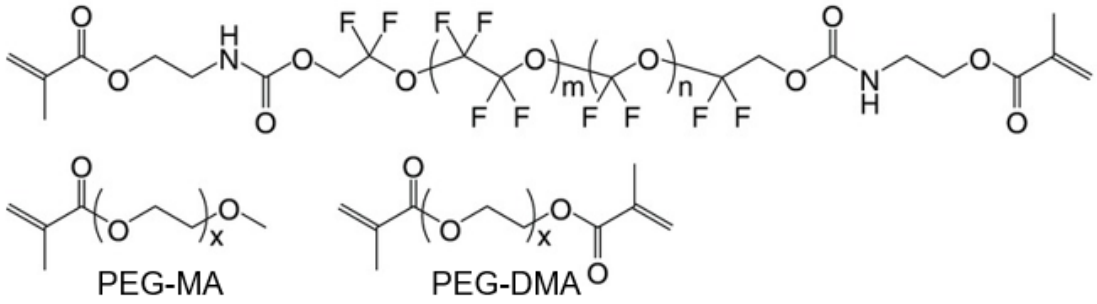

Figure 1.10. Chemical structures of building blocks for UV-photocured amphiphilic system. Reprinted from reference 97.

Condensation-cured Networks

Hydrophobic siloxane-polyurethane (SiPU) coatings were a major step to attain durable well-performing FR surfaces (Figure 1.11).[23, 24, 73, 74, 99] To expand the performance of these self-stratified surfaces against a wider range of marine organisms, their amphiphilic versions were investigated as new domains of surfaces that showed not only desired durability of the conventional formulations but also delivered promising fouling-release performance. The initial attempts crosslinked a PDMS functionalized with pendant hydrophilic carboxylic acid groups with the polyurethane bulk, resulting in a self-stratified surface composed of PDMS and carboxylic acid moieties.[100] This system improved the release of *N. incerta* biofilm, but it slightly reduced the release of barnacles and *U. linza* in comparison to the control SiPU system. In another zwitterionic-based approach, amine-containing block copolymers of poly(sulfobetaine methacrylate) (poly(SBMA)) and PDMS were crosslinked with polyurethane bulk.[36] This zwitterionic SiPU network resulted in a better release of *N. incerta* while it delivered comparable performance to conventional SiPU formulation.

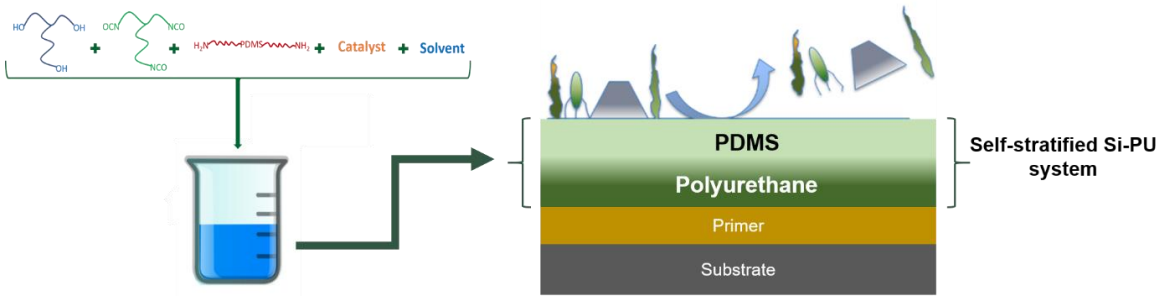

Figure 1.11. Schematic illustration of self-stratified hydrophobic SiPU fouling-release coating.

Furthermore, amphiphilic isocyanate-based prepolymers containing PEG and PDMS chains were prepared and crosslinked within a polyurethane network.[101] The amphiphilic isocyanate-based prepolymer, isocyanate resin, and acrylic polyol constituted the coating system. These PEG-PDMS coatings demonstrated the presence of amphiphilic domains on the surface and very promising performance towards all assessed marine biofoulants (*N.* incerta, *U.* linza, *C.* lytica, barnacles, mussels), outperforming both internal SiPU control and commercial controls like Intersleek® 900 and 1100SR. PEG-PDMS-PU surfaces indicated the presence of at least 10 wt.% amphiphilic moieties resulted in the sought FR performance.

Isocyanates are often flagged for their effects of workers' health while it is challenging to discard their desired properties that roots from the urethane linkages,[102] thus glycidyl carbamate (GC) coatings were introduced to deliver both urethane linkage and epoxy chemistry for crosslinking.[103-105] GC coatings are composed of a GC resin which can undergo either polycondensation curing with an amine[105] or self-crosslinking.[103] A GC resin is easily synthesized by the reaction of polyisocyanate resin with glycidol, generating a urethane/carbamate linkage and introducing epoxy functional groups. Utilizing the glycidyl carbamate chemistry, self-stratified hydrophobic and amphiphilic coatings based on PDMS and PEG moieties were extensively explored (Figure 1.12).[74, 75] The initial explorations suggested the potential of these novel marine coatings as fouling-release surfaces, but not as great as conventional SiPU formulation. The lagging performance of FR GC coatings may be attributed to restricted freedom of PEG/PDMS chains to migrate to the surface due to their crosslinked chains from two ends instead of one.

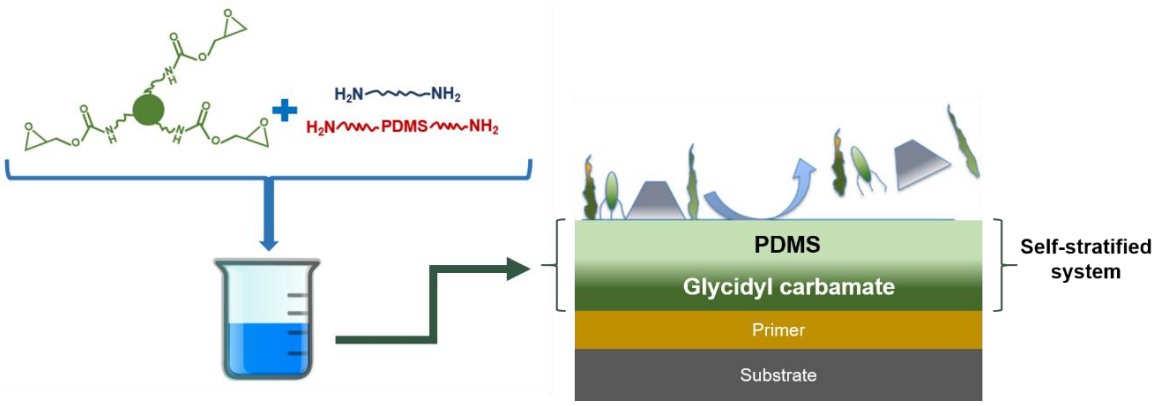

Figure 1.12. Schematic illustration of self-stratified hydrophobic GC fouling-release coating.

Amphiphilic fouling-release networks based on the polycondensation reaction of silanol has also been explored. For example, a combinatorial approach was used to explore films derived from condensation reactions between silanols, methoxy silane, and acetoxy silane functional groups of four coating components: silanol-terminated PDMS, silanol-terminated CF_3-PDMS (Silanol-terminated polytrifluorpropylmethylsiloxane), TMS-PEG (2-[Methoxy(polyethyleneoxy)propyl]-trimethoxysilane), and a crosslinker. Amphiphilicity was tuned by changing CF_3-PDMS/TMS-PEG ratio, and it was concluded the highest amount of these moieties resulted in 100% removal of *C. lytica* and *H. pacifica* and lowest adhesion strength of adult barnacles.[106]

Other Amphiphilic Surfaces

Amphiphilic surfaces for marine applications have garnered the attention of other creative approaches as well such as layer-by-layer, zwitterionic, polysaccharide, or polypeptides/peptide-mimic. The layer-by-layer technique has been investigated via covalent or electrostatic approaches, such as a combination of partially ionized poly(isobutylene-alt-maleic anhydride) (PIAMA)- perfluoroalkyl-PEG with polyethyleneimine (PEI) polycation that was crosslinked with amide bonds (Figure 1.13). Polyelectrolyte films composed of hyaluronic acid (HA) and chitosan (Ch) were composed following the layer-by-layer technique as well, demonstrating the potential for fouling-release applications after assessments against *U. linza*.[45]

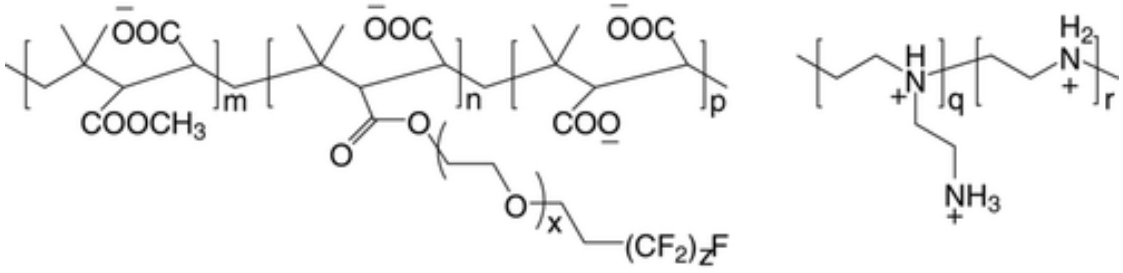

Figure 1.13. PIAMA polyanion-PEI polycation system for deposition of an amphiphilic layer-by-layer film. Reprinted from reference 82.

Zwitterionic materials are another major hydrophilic component that have proven to be advantageous for preparing amphiphilic films. Zwitterionic polymers are highly effective against marine biofouling which is attributed to their strong hydration layer (up to 8 times more water uptake than PEG-based systems).[80] Hydrophilic surfaces with brushes of poly(sulfobetaine methacrylate) were first reported

for their desirable release of spores of the green marine alga, *Ulva*, and diatom *N. incerta* compared to untreated glass.[40] Zwitterionic polymers based on sulfobetaine and carboxybetaine end groups have been explored for marine applications. Furthermore, efforts to understand the effect of changes in zwitterionic groups or their structural arrangements on fouling-release of coatings have been carried out, indicating relative negligible importance.[107]

Polysaccharides are hydrophilic natural polymers that have been studied as alternatives to PEG for marine coating purposes due to their ability to store more water owing to the high concentration of hydroxyl groups.[108, 109] Several works have highlighted the potential protein resistance of polysaccharides. For example, amphiphilic polysaccharide-based coatings composed of hyaluronic acid and chondroitin resulted in improved removal of *U. linza* and *N. incerta* respect to untreated glass. In another work, surfaces made of alginic acid (AA) functionalized with hydrophobic trifluoroethylamine reduced the critical adhesion strength of *C. marina* and *N. incerta* by 50%.[110]

The availability of many natural and non-natural amino acids offers a tunable polypeptide platform that has been utilized to design a series of amphiphilic marine surfaces.[111, 112] Oligopeptide-based systems containing either block or alternating hydrophilic/hydrophobic amino acids where prepared, and these surfaces inhibited the settlement of *U. linza* sporelings with respect to the unmodified surface.[113] The results suggested the sequence of amino acids had no influential effect on fouling-release output but affected the wettability of the surfaces. In another route, polypeptoids, the constitutional isomers of polypeptides, have also been investigated as a based for amphiphilic surfaces.[114, 115] The sequence and amount of the hydrophilic N-(2-methoxyethyl)glycine and the hydrophobic N-(2,2,3,3,4,4,4-heptafluorobutyl)glycine in an amphiphilic polypeptoid-based coating influenced the surface and fouling-release properties.[115] When the fluorine-based moieties were located at the end of polypeptoid chain instead of the middle (Figure 1.14), *U. linza* settled less on the surface.

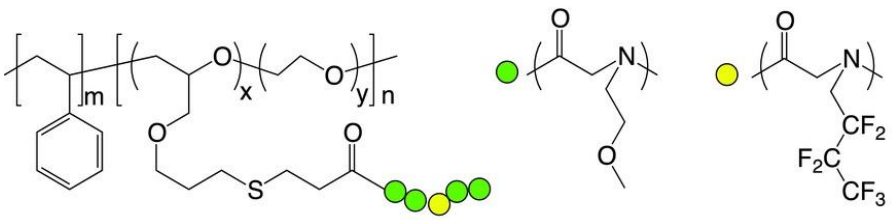

Figure 1.14. Schematic of a block copolymer functionalized with amphiphilic polypeptoid tethers. Reprinted from reference 115.

Design Considerations for Amphiphilic Networks

The discussed amphiphilic systems, ranging from their foundation on neutral polymers to zwitterionic and natural polymers, all share a common goal, delivering heterogeneous surfaces composed of hydrophilic and hydrophobic domains that can potentially "confuse" or tackle as many marine biofouling organisms as possible. Amphiphilic approaches allow future designs to be tailored and tuned as needed by understanding the effect of molecular and higher-level structures on the surface and fouling-release/antifouling (FR/A) properties. The overall considerations for designing for amphiphilic surfaces include four major factors: surface activity, surface functionality, surface structure, and surface reconstruction, while there are sub-levels for each of these driving factors as illustrated in **Figure 1.15** that contribute to a desirable engineered marine surface.[82] Therefore, these factors can be utilized as general guidelines to design and access unprecedented improved amphiphilic AF/FR coatings, although more thorough knowledge is needed to comprehend the complexity and interaction of these novel amphiphilic surfaces with marine biofoulants and explain better the fundamentals behind the "confusion" of marine organisms.

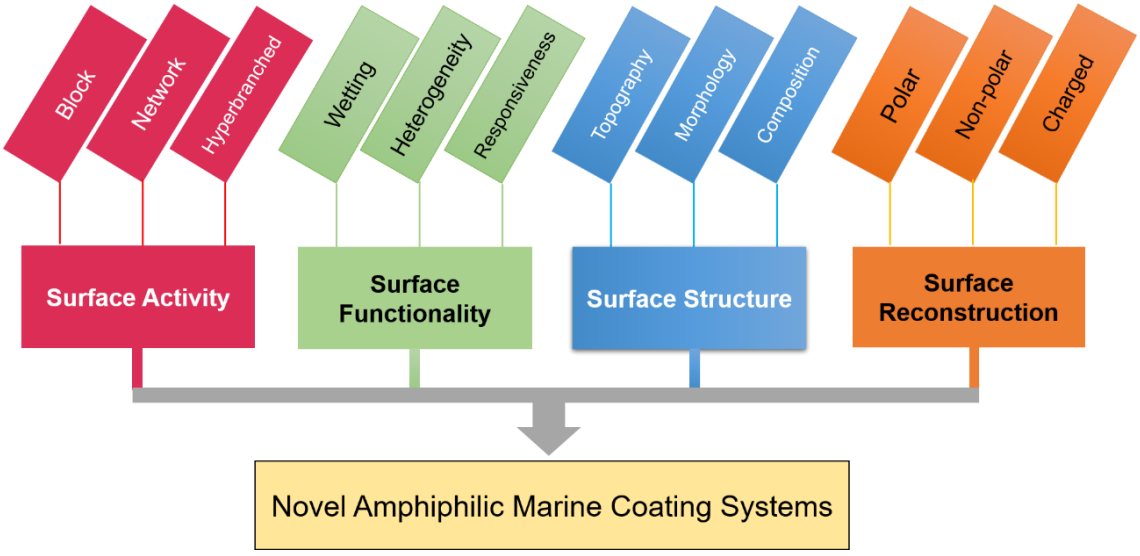

Figure 1.15. Surface design parameters for attaining novel amphiphilic marine coating systems.

Research Scope and Purpose

This research aimed to attain novel amphiphilic fouling-release surfaces by either enhancing the performance of previously established coating systems and/or investigating novel polymeric networks. The previously established fouling-release systems in Webster Group have been hydrophobic SiPU

coatings,[73] glycidyl-carbamate (GC) based coatings,[75] and amphiphilic SiPU coatings.[101] All systems are designed as self-stratifying networks that take advantage of incompatibility between siloxane and urethane components. As mentioned, each of these systems faced limitations that needed to be addressed. Hydrophobic SiPU system suffers from a PDMS-based surface that is preferred by some organisms for settlement due to its hydrophobic nature. The recent amphiphilic SiPU systems developed by Galhenage et al. delivered highly desired fouling-release coatings with improved performance against a wider range of marine organisms concerning original SiPU formulation, but it still contained isocyanate-based resins in the final formulation. As a result, GC-based coatings were explored to attain fouling-release performance, benefits of urethane linkages, and use epoxy chemistry for network crosslinking. Although GC-based systems tackled the presence of isocyanate resins in the final formulation, their fouling-release performance has not been ideal in respect to hydrophobic SiPU and amphiphilic SiPU systems. Therefore, to address the limitations of the aforementioned coating systems in terms of expanding FR array or discarding health-concerning components, there is a compelling reason to explore new avenues for improving these coating systems and/or introducing novel marine formulations. This research can be divided to two main sections: 1) Incorporation of amphiphilic additives in marine coating systems of interest to modify surface and boost fouling-release properties; 2) Investigations of novel amphiphilic fouling-release marine surfaces.

Chapters two through five of this dissertation focus on amphiphilic additives and their effects on the modified systems while the last two chapters introduce novel amphiphilic surfaces without the shortcomings of the previously developed coatings. Marine coatings have benefited from additives to access better antifouling/fouling-release performance towards marine biofoulants. The additives for marine purposes are mostly designed as surface-modifying agents to alter the surface of coatings, resulting in tuned AF/FR properties. There are many types of marine additives such as copper/zinc-based,[49, 50, 116] amphiphilic copolymers (i.e. PEG[22, 95, 117-121] or zwitterionic-based[42, 43, 122-125]), or hydrogel-like polymers.[126] The horizon of explored marine additives also covers silicone oils[57, 58, 127, 128] and specialty additives such as sephiolite nanofibers, modified graphite, and carbon nanotubes and pigments (i.e. TiO2 and ZnO).[129-133]

A major advantage of additives is their facile addition to any system without requiring any major changes for the base matrices/formulations. Therefore, we considered amphiphilic additives as a great tool to boost the performance of the established systems such as hydrophobic SiPU and amphiphilic SiPU without changing the chemistries. In this dissertation, the second chapter investigated the preparation of zwitterionic poly(SBMA)-PDMS additives and their effect on surface and FR properties of hydrophobic SiPU system. This study aimed to achieve a stable amphiphilic surface for the SiPU system, theorizing poly(SBMA) possesses long-term stability and forms strong hydration layers that require costly energy from biofoulants for attachment. With promising results from zwitterionic-based additives, we aspired to access amphiphilic additives with alternative hydrophilic materials like PEG.

Even though amphiphilic additives are explored as viable modifiers, but one of the major drawbacks for such additives is their complex synthesis and purification processes. To this effect, chapters three to five not only examined PEG-PDMS-based additives, but they also introduced a facile chemistry to access these highly sought additives. The third chapter incorporated the PEG-PDMS additives into a non-marine polyurethane coating to determine the concentration of amphiphilic moieties in that system for reaching desirable fouling-release performance, introducing the “critical amphiphilic concentration” concept. Chapters four and five subsequently explored the addition of PEG-PDMS additives to hydrophobic SiPU and amphiphilic SiPU systems, respectively, assessing the contribution of additives to surface and FR properties.

Furthermore, the need for alternative amphiphilic systems was also followed. As the previously established systems (i.e. hydrophobic SiPU, amphiphilic SiPU, and Si-GC) either suffered from isocyanate-related health concerns or poor FR performance, the sixth chapter investigated a novel marine system combining the founding theories from amphiphilic SiPU and Si-GC systems, introducing GC coatings composed of amphiphilic prepolymers. This novel amphiphilic GC system delivered all targeted goals including isocyanate-free final formulations and well-performing FR surfaces with respect to both internal and commercial controls.

While all the urethane-based marine systems (i.e. hydrophobic SiPU, amphiphilic SiPU, and Si-GC) have been stable in field tests lasting up to two years,[134] they have been questioned for their stability in aquatic environments. Hence, the seventh chapter searched for an alternate amphiphilic urethane-free

system with desired stability, health considerations, and FR performance, resulting in a formulation composed of PEG-containing acrylate epoxy resin crosslinked with amine-terminated PDMS and amine curing agents. This study was designed as a primary investigation to open future explorations for this urethane-free epoxy-based amphiphilic FR marine coating.

References

1. Lejars, M.; Margaillan, A.; Bressy, C., Fouling release coatings: A nontoxic alternative to biocidal antifouling coatings. *Chemical Reviews* **2012,** *112* (8), 4347-4390.

2. Magin, C. M.; Cooper, S. P.; Brennan, A. B., Non-toxic antifouling strategies. *Materials Today* **2010,** *13* (4), 36-44.

3. Callow, J. A.; Callow, M. E., Trends in the development of environmentally friendly fouling-resistant marine coatings. *Nature Communications* **2011,** *2* (1), 244-244.

4. Schultz, M. P.; Bendick, J. A.; Holm, E. R.; Hertel, W. M., Economic impact of biofouling on a naval surface ship. *Biofouling* **2011,** *27* (1), 87-98.

5. Callow, M. E.; Callow, J. E., Marine biofouling: a sticky problem. *Biologist* **2002,** *49* (1), 10-14.

6. Hunsucker, K. Z.; Koka, A.; Lund, G.; Swain, G., Diatom community structure on in-service cruise ship hulls. *Biofouling* **2014,** *30* (9), 1133-1140.

7. Zargiel, K. A.; Coogan, J. S.; Swain, G. W., Diatom community structure on commercially available ship hull coatings. *Biofouling* **2011,** *27* (9), 955-965.

8. Rittschof, D.; Costlow, J. D., Bryozoan and barnacle settlement in relation to initial surface wettability: A comparison of laboratory and field studies. *Sci. Mar.* **1989,** *53* (2), 411-416.

9. Petrone, L.; Di Fino, A.; Aldred, N.; Sukkaew, P.; Ederth, T.; Clare, A. S.; Liedberg, B., Effects of surface charge and Gibbs surface energy on the settlement behaviour of barnacle cyprids (Balanus amphitrite). *Biofouling* **2011,** *27* (9), 1043-1055.

10. Aldred, N.; Gatley-Montross, C. M.; Lang, M.; Detty, M. R.; Clare, A. S., Correlative assays of barnacle cyprid behaviour for the laboratory evaluation of antifouling coatings: a study of surface energy components. *Biofouling* **2019,** *35* (2), 159-172.

11. Chiovitti, A.; Dugdale, T. M.; Wetherbee, R., Biological Adhesives. Springer Berlin: 2006.

12. Schmidt, M.; Cavaco, A.; Gierlinger, N.; Aldred, N.; Fratzl, P.; Grunze, M.; Clare, A. S., In situ imaging of barnacle (Balanus amphitrite) cyprid cement using confocal Raman microscopy. *The Journal of adhesion* **2009,** *85* (2-3), 139-151.

13. Yebra, D. M.; Kiil, S.; Dam-Johansen, K., Antifouling technology—past, present and future steps towards efficient and environmentally friendly antifouling coatings. *Progress in Organic Coatings* **2004,** *50* (2), 75-104.

14. Champ, M. A., A review of organotin regulatory strategies, pending actions, related costs and benefits. *Science of the total Environment* **2000,** *258* (1-2), 21-71.

15. Konstantinou, I. K.; Albanis, T. A., Worldwide occurrence and effects of antifouling paint booster biocides in the aquatic environment: a review. *Environment International* **2004,** *30* (2), 235-248.

16. Nurioglu, A. G.; Esteves, A. C. C., Non-toxic, non-biocide-release antifouling coatings based on molecular structure design for marine applications. *Journal of Materials Chemistry B* **2015,** *3* (32), 6547-6570.

17. Lafuma, A.; Quéré, D., Slippery pre-suffused surfaces. *EPL (Europhysics Letters)* **2011,** *96* (5), 56001.

18. Wong, T.-S.; Kang, S. H.; Tang, S. K. Y.; Smythe, E. J.; Hatton, B. D.; Grinthal, A.; Aizenberg, J., Bioinspired self-repairing slippery surfaces with pressure-stable omniphobicity. *Nature* **2011,** *477* (7365), 443.

19. Genzer, J.; Efimenko, K., Recent developments in superhydrophobic surfaces and their relevance to marine fouling: a review. *Biofouling* **2006,** *22* (5), 339-360.

20. Martinelli, E.; Pelusio, G.; Yasani, B. R.; Glisenti, A.; Galli, G., Surface Chemistry of Amphiphilic Polysiloxane/Triethyleneglycol-Modified Poly (pentafluorostyrene) Block Copolymer Films Before and After Water Immersion. *Macromolecular Chemistry and Physics* **2015,** *216* (21), 2086-2094.

21. Martinelli, E.; Pretti, C.; Oliva, M.; Glisenti, A.; Galli, G., Sol-gel polysiloxane films containing different surface-active trialkoxysilanes for the release of the marine foulant Ficopomatus enigmaticus. *Polymer* **2018,** *145*, 426-433.

22. Martinelli, E.; Suffredini, M.; Galli, G.; Glisenti, A.; Pettitt, M. E.; Callow, M. E.; Callow, J. A.; Williams, D.; Lyall, G., Amphiphilic block copolymer/poly (dimethylsiloxane)(PDMS) blends and nanocomposites for improved fouling-release. *Biofouling* **2011,** *27* (5), 529-541.

23. Ekin, A.; Webster, D. C.; Daniels, J. W.; Stafslien, S. J.; Cassé, F.; Callow, J. A.; Callow, M. E., Synthesis, formulation, and characterization of siloxane–polyurethane coatings for underwater marine applications using combinatorial high-throughput experimentation. *Journal of Coatings Technology and Research* **2007,** *4* (4), 435-451.

24. Majumdar, P.; Webster, D. C., Surface microtopography in siloxane–polyurethane thermosets: The influence of siloxane and extent of reaction. *Polymer* **2007,** *48* (26), 7499-7509.

25. Majumdar, P.; Webster, D. C., Preparation of Siloxane−Urethane Coatings Having Spontaneously Formed Stable Biphasic Microtopograpical Surfaces. *Macromolecules* **2005,** *35* (18).

26. Pieper, R. J.; Ekin, A.; Webster, D. C.; Cassé, F.; Callow, J. A.; Callow, M. E., Combinatorial approach to study the effect of acrylic polyol composition on the properties of crosslinked siloxane-polyurethane fouling-release coatings. *Journal of Coatings Technology and Research* **2007,** *4* (4), 453-461.

27. Coneski, P. N.; Wynne, J. H., Zwitterionic Polyurethane Hydrogels Derived from Carboxybetaine-Functionalized Diols. *ACS Applied Materials & Interfaces* **2012,** *4* (9), 4465-4469.

28. Sokolova, A.; Bailey, J. J.; Waltz, G. T.; Brewer, L. H.; Finlay, J. A.; Fornalik, J.; Wendt, D. E.; Callow, M. E.; Callow, J. A.; Bright, F. V., Spontaneous multiscale phase separation within fluorinated xerogel coatings for fouling-release surfaces. *Biofouling* **2012,** *28* (2), 143-157.

29. Bennett, S. M.; Finlay, J. A.; Gunari, N.; Wells, D. D.; Meyer, A. E.; Walker, G. C.; Callow, M. E.; Callow, J. A.; Bright, F. V.; Detty, M. R., The role of surface energy and water wettability in

aminoalkyl/fluorocarbon/hydrocarbon-modified xerogel surfaces in the control of marine biofouling. *Biofouling* **2009,** *26* (2), 235-246.

30. Evariste, E.; Gatley, C. M.; Detty, M. R.; Callow, M. E.; Callow, J. A., The performance of aminoalkyl/fluorocarbon/hydrocarbon-modified xerogel coatings against the marine alga Ectocarpus crouaniorum: relative roles of surface energy and charge. *Biofouling* **2013,** *29* (2), 171-184.

31. Tang, Y.; Finlay, J. A.; Kowalke, G. L.; Meyer, A. E.; Bright, F. V.; Callow, M. E.; Callow, J. A.; Wendt, D. E.; Detty, M. R., Hybrid xerogel films as novel coatings for antifouling and fouling release. *Biofouling* **2005,** *21* (1), 59-71.

32. Gunari, N.; Brewer, L. H.; Bennett, S. M.; Sokolova, A.; Kraut, N. D.; Finlay, J. A.; Meyer, A. E.; Walker, G. C.; Wendt, D. E.; Callow, M. E., The control of marine biofouling on xerogel surfaces with nanometer-scale topography. *Biofouling* **2011,** *27* (2), 137-149.

33. Sokolova, A.; Cilz, N.; Daniels, J.; Stafslien, S. J.; Brewer, L. H.; Wendt, D. E.; Bright, F. V.; Detty, M. R., A comparison of the antifouling/foul-release characteristics of non-biocidal xerogel and commercial coatings toward micro-and macrofouling organisms. *Biofouling* **2012,** *28* (5), 511-523.

34. Finlay, J. A.; Bennett, S. M.; Brewer, L. H.; Sokolova, A.; Clay, G.; Gunari, N.; Meyer, A. E.; Walker, G. C.; Wendt, D. E.; Callow, M. E., Barnacle settlement and the adhesion of protein and diatom microfouling to xerogel films with varying surface energy and water wettability. *Biofouling* **2010,** *26* (6), 657-666.

35. Anthony Yesudass, S.; Mohanty, S.; Nayak, S. K.; Rath, C. C., Zwitterionic–polyurethane coatings for non-specific marine bacterial inhibition: A nontoxic approach for marine application. *European Polymer Journal* **2017,** *96*, 304-315.

36. Bodkhe, R. B.; Stafslien, S. J.; Daniels, J.; Cilz, N.; Muelhberg, A. J.; Thompson, S. E. M.; Callow, M. E.; Callow, J. A.; Webster, D. C., Zwitterionic siloxane-polyurethane fouling-release coatings. *Progress in Organic Coatings* **2015,** *78*, 369-380.

37. Liu, P.; Huang, T.; Liu, P.; Shi, S.; Chen, Q.; Li, L.; Shen, J., Zwitterionic modification of polyurethane membranes for enhancing the anti-fouling property. *Journal of Colloid and Interface Science* **2016,** *480*, 91-101.

38. Jiang, S.; Cao, Z., Ultralow-fouling, functionalizable, and hydrolyzable zwitterionic materials and their derivatives for biological applications. *Advanced Materials* **2010,** *22* (9), 920-932.

39. Xin, X.; Wang, Y.; Liu, W., Synthesis of zwitterionic block copolymers via RAFT polymerization. *European Polymer Journal* **2005,** *41* (7), 1539-1545.

40. Zhang, Z.; Finlay, J. A.; Wang, L.; Gao, Y.; Callow, J. A.; Callow, M. E.; Jiang, S., Polysulfobetaine-grafted surfaces as environmentally benign ultralow fouling marine coatings. *Langmuir* **2009,** *25* (23), 13516-13521.

41. Wang, C.; Ma, C.; Mu, C.; Lin, W., A novel approach for synthesis of zwitterionic polyurethane coating with protein resistance. *Langmuir* **2014,** *30* (43), 12860-12867.

42. Yeh, S.-B.; Chen, C.-S.; Chen, W.-Y.; Huang, C.-J., Modification of silicone elastomer with zwitterionic silane for durable antifouling properties. *Langmuir* **2014,** *30* (38), 11386-11393.

43. Shivapooja, P.; Yu, Q.; Orihuela, B.; Mays, R.; Rittschof, D.; Genzer, J.; López, G. P., Modification of silicone elastomer surfaces with zwitterionic polymers: short-term fouling resistance and triggered biofouling release. *ACS Applied Materials & Interfaces* **2015,** *7* (46), 25586-25591.

44. Leigh, B. L.; Cheng, E.; Xu, L.; Derk, A.; Hansen, M. R.; Guymon, C. A., Antifouling photograftable zwitterionic coatings on PDMS substrates. *Langmuir* **2018,** *35* (5), 1100-1110.

45. Yu, W.; Koc, J.; Finlay, J. A.; Clarke, J. L.; Clare, A. S.; Rosenhahn, A., Layer-by-layer constructed hyaluronic acid/chitosan multilayers as antifouling and fouling-release coatings. *Biointerphases* **2019,** *14* (5), 051002.

46. Chen, D.; Wu, M.; Li, B.; Ren, K.; Cheng, Z.; Ji, J.; Li, Y.; Sun, J., Layer-by-Layer-Assembled Healable Antifouling Films. *Advanced Materials* **2015,** *27* (39), 5882-5888.

47. Li, S.; Huang, P.; Ye, Z.; Wang, Y.; Wang, W.; Kong, D.; Zhang, J.; Deng, L.; Dong, A., Layer-by-layer zwitterionic modification of diverse substrates with durable anti-corrosion and anti-fouling properties. *Journal of Materials Chemistry B* **2019,** *7* (39), 6024-6034.

48. Xu, G.; Pranantyo, D.; Xu, L.; Neoh, K.-G.; Kang, E.-T.; Teo, S. L.-M., Antifouling, Antimicrobial, and Antibiocorrosion Multilayer Coatings Assembled by Layer-by-layer Deposition Involving Host–Guest Interaction. *Industrial & Engineering Chemistry Research* **2016,** *55* (41), 10906-10915.

49. Pérez, M.; Blustein, G.; García, M.; del Amo, B.; Stupak, M., Cupric tannate: a low copper content antifouling pigment. *Progress in Organic Coatings* **2006,** *55* (4), 311-315.

50. Claisse, D.; Alzieu, C., Copper contamination as a result of antifouling paint regulations? *Marine Pollution Bulletin* **1993,** *26* (7), 395-397.

51. Dafforn, K. A.; Lewis, J. A.; Johnston, E. L., Antifouling strategies: History and regulation, ecological impacts and mitigation. *Marine Pollution Bulletin* **2011,** *62* (3), 453-465.

52. Darmanin, T.; Guittard, F., Recent advances in the potential applications of bioinspired superhydrophobic materials. *Journal of Materials Chemistry A* **2014,** *2* (39), 16319-16359.

53. Schumacher, J. F.; Carman, M. L.; Estes, T. G.; Feinberg, A. W.; Wilson, L. H.; Callow, M. E.; Callow, J. A.; Finlay, J. A.; Brennan, A. B., Engineered antifouling microtopographies–effect of feature size, geometry, and roughness on settlement of zoospores of the green alga Ulva. *Biofouling* **2007,** *23* (1), 55-62.

54. Carman, M. L.; Estes, T. G.; Feinberg, A. W.; Schumacher, J. F.; Wilkerson, W.; Wilson, L. H.; Callow, M. E.; Callow, J. A.; Brennan, A. B., Engineered antifouling microtopographies–correlating wettability with cell attachment. *Biofouling* **2006,** *22* (1), 11-21.

55. Xiao, L.; Thompson, S. E. M.; Röhrig, M.; Callow, M. E.; Callow, J. A.; Grunze, M.; Rosenhahn, A., Hot embossed microtopographic gradients reveal morphological cues that guide the settlement of zoospores. *Langmuir* **2013,** *29* (4), 1093-1099.

56. Wilson, P. W.; Lu, W.; Xu, H.; Kim, P.; Kreder, M. J.; Alvarenga, J.; Aizenberg, J., Inhibition of ice nucleation by slippery liquid-infused porous surfaces (SLIPS). *Physical Chemistry Chemical Physics* **2013,** *15* (2), 581-585.

57. Wei, C.; Zhang, G.; Zhang, Q.; Zhan, X.; Chen, F., Silicone oil-infused slippery surfaces based on sol–gel process-induced nanocomposite coatings: A facile approach to highly stable bioinspired surface for biofouling resistance. *ACS Applied Materials & Interfaces* **2016,** *8* (50), 34810-34819.

58. Galhenage, T. P.; Hoffman, D.; Silbert, S. D.; Stafslien, S. J.; Daniels, J.; Miljkovic, T.; Finlay, J. A.; Franco, S. C.; Clare, A. S.; Nedved, B. T., Fouling-release performance of silicone oil-modified siloxane-polyurethane coatings. *ACS Applied Materials & Interfaces* **2016,** *8* (42), 29025-29036.

59. Scardino, A. J.; Zhang, H.; Cookson, D. J.; Lamb, R. N.; Nys, R. d., The role of nano-roughness in antifouling. *Biofouling* **2009,** *25* (8), 757-767.

60. Selim, M. S.; El-Safty, S. A.; Shenashen, M. A., Chapter 8 - Superhydrophobic foul resistant and self-cleaning polymer coating. In *Superhydrophobic Polymer Coatings*, Samal, S. K.; Mohanty, S.; Nayak, S. K., Eds. Elsevier: 2019; pp 181-203.

61. Chen, K.; Zhou, S.; Wu, L., Self-healing underwater superoleophobic and antibiofouling coatings based on the assembly of hierarchical microgel spheres. *Acs Nano* **2016,** *10* (1), 1386-1394.

62. Selim, M. S.; Shenashen, M. A.; El-Safty, S. A.; Higazy, S. A.; Selim, M. M.; Isago, H.; Elmarakbi, A., Recent progress in marine foul-release polymeric nanocomposite coatings. *Progress in Materials Science* **2017,** *87*, 1-32.

63. Brady Jr, R. F.; Singer, I. L., Mechanical factors favoring release from fouling release coatings. *Biofouling* **2000,** *15* (1-3), 73-81.

64. Brady Jr, R. F., A fracture mechanical analysis of fouling release from nontoxic antifouling coatings. *Progress in Organic Coatings* **2001,** *43* (1-3), 188-192.

65. Baier, R. E., Surface behaviour of biomaterials: The theta surface for biocompatibility. *Journal of Materials Science: Materials in Medicine* **2006,** *17* (11), 1057-1062.

66. Brook, M. A., *Silicon in organic, organometallic, and polymer chemistry*. Wiley New York: 2000; Vol. 123.

67. Schmidt, D.; Shah, D.; Giannelis, E. P., New advances in polymer/layered silicate nanocomposites. *Current Opinion in Solid State and Materials Science* **2002,** *6* (3), 205-212.

68. Derbalah, A.; El-Safty, S. A.; Shenashen, M. A.; Abdel Ghany, N. A., Mesoporous alumina nanoparticles as host tunnel-like pores for removal and recovery of insecticides from environmental samples. *ChemPlusChem* **2015,** *80* (7), 1119-1126.

69. Dalton, H. M.; Stein, J.; March, P. E., A biological assay for detection of heterogeneities in the surface hydrophobicity of polymer coatings exposed to the marine environment. *Biofouling* **2000,** *15* (1-3), 83-94.

70. Wouters, M.; Rentrop, C.; Willemsen, P., Surface structuring and coating performance: novel biocidefree nanocomposite coatings with anti-fouling and fouling-release properties. *Progress in Organic Coatings* **2010,** *68* (1-2), 4-11.

71. Cavas, L.; Yildiz, P. G.; Mimigianni, P.; Sapalidis, A.; Nitodas, S., Reinforcement effects of multiwall carbon nanotubes and graphene oxide on PDMS marine coatings. *Journal of Coatings Technology and Research* **2018,** *15* (1), 105-120.

72. Sommer, S.; Ekin, A.; Webster, D. C.; Stafslien, S. J.; Daniels, J.; VanderWal, L. J.; Thompson, S. E. M.; Callow, M. E.; Callow, J. A., A preliminary study on the properties and fouling-release performance of siloxane–polyurethane coatings prepared from poly(dimethylsiloxane) (PDMS) macromers. *Biofouling* **2010,** *26* (8), 961-972.

73. Bodkhe, R. B.; Thompson, S. E. M.; Yehle, C.; Cilz, N.; Daniels, J.; Stafslien, S. J.; Callow, M. E.; Callow, J. A.; Webster, D. C., The effect of formulation variables on fouling-release performance of stratified siloxane–polyurethane coatings. *Journal of Coatings Technology and Research* **2012,** *9* (3), 235-249.

74. Pade, M.; Webster, D. C., Self-stratified siloxane-polyurethane fouling-release marine coating strategies: A review. In *Marine Coatings and Membranes*, Mittal, V., Ed. Central West Publishing: Australia, 2019; pp 1-36.

75. Pade, M. Influence of Surface Topography and Curing Chemistry on Fouling-Release Performance of Self-Stratified Siloxane-Polyurethane Coatings. North Dakota State University, 2017.

76. Liu, C.; Xie, Q.; Ma, C.; Zhang, G., Fouling release property of polydimethylsiloxane-based polyurea with improved adhesion to substrate. *Industrial & Engineering Chemistry Research* **2016,** *55* (23), 6671-6676.

77. Alexandridis, P., Amphiphilic copolymers and their applications. *Current Opinion in Colloid & Interface Science* **1996,** *1* (4), 490-501.

78. George, B. S.; Mathai, M.; Georg Dahmann, a.; Whitesides*, G. M., Polyacrylamides Bearing Pendant α-Sialoside Groups Strongly Inhibit Agglutination of Erythrocytes by Influenza Virus: The Strong Inhibition Reflects Enhanced Binding through Cooperative Polyvalent Interactions. *J. Am. Chem. Soc.* **1996,** *118* (16), 3789-3800.

79. Ngo, B. K. D.; Grunlan, M. A., Protein Resistant Polymeric Biomaterials. *ACS Macro Letters* **2017,** *6* (9), 992-1000.

80. Wu, J.; Lin, W.; Wang, Z.; Chen, S.; Chang, Y., Investigation of the hydration of nonfouling material poly(sulfobetaine methacrylate) by low-field nuclear magnetic resonance. *Langmuir* **2012,** *28* (19), 7436-7441.

81. Wu, J.; Chen, S., Investigation of the hydration of nonfouling material poly(ethylene glycol) by low-field nuclear magnetic resonance. *Langmuir* **2012,** *28* (4), 2137-2144.

82. Galli, G.; Martinelli, E., Amphiphilic polymer platforms: surface engineering of films for marine antibiofouling. *Macromolecular rapid communications* **2017,** *38* (8), 1600704.

83. Martinelli, E.; Guazzelli, E.; Bartoli, C.; Gazzarri, M.; Chiellini, F.; Galli, G.; Callow, M. E.; Callow, J. A.; Finlay, J. A.; Hill, S., Amphiphilic pentablock copolymers and their blends with PDMS for antibiofouling coatings. *Journal of Polymer Science Part A: Polymer Chemistry* **2015,** *53* (10), 1213-1225.

84. Andersen, M. E.; Butenhoff, J. L.; Chang, S.-C.; Farrar, D. G.; Kennedy Jr, G. L.; Lau, C.; Olsen, G. W.; Seed, J.; Wallace, K. B., Perfluoroalkyl acids and related chemistries—toxicokinetics and modes of action. *Toxicological sciences* **2008,** *102* (1), 3-14.

85. Dimitriou, M. D.; Zhou, Z.; Yoo, H.-S.; Killops, K. L.; Finlay, J. A.; Cone, G.; Sundaram, H. S.; Lynd, N. A.; Barteau, K. P.; Campos, L. M., A general approach to controlling the surface composition of poly (ethylene oxide)-based block copolymers for antifouling coatings. *Langmuir* **2011,** *27* (22), 13762-13772.

86. Sundaram, H. S.; Cho, Y.; Dimitriou, M. D.; Weinman, C. J.; Finlay, J. A.; Cone, G.; Callow, M. E.; Callow, J. A.; Kramer, E. J.; Ober, C. K., Fluorine-free mixed amphiphilic polymers based on PDMS and PEG side chains for fouling release applications. *Biofouling* **2011,** *27* (6), 589-602.

87. Martinelli, E.; Sarvothaman, M. K.; Galli, G.; Pettitt, M. E.; Callow, M. E.; Callow, J. A.; Conlan, S. L.; Clare, A. S.; Sugiharto, A. B.; Davies, C.; Williams, D., Poly(dimethyl siloxane) (PDMS) network blends of amphiphilic acrylic copolymers with poly(ethylene glycol)-fluoroalkyl side chains for fouling-release coatings. II. Laboratory assays and field immersion trials. *Biofouling* **2012,** *28* (6), 571-582.

88. Atlar, M.; Ünal, B.; Ünal, U. O.; Politis, G.; Martinelli, E.; Galli, G.; Davies, C.; Williams, D., An experimental investigation of the frictional drag characteristics of nanostructured and fluorinated fouling-release coatings using an axisymmetric body. *Biofouling* **2013,** *29* (1), 39-52.

89. Yasani, B. R.; Martinelli, E.; Galli, G.; Glisenti, A.; Mieszkin, S.; Callow, M. E.; Callow, J. A., A comparison between different fouling-release elastomer coatings containing surface-active polymers. *Biofouling* **2014,** *30* (4), 387-399.

90. Gudipati, C. S.; Finlay, J. A.; Callow, J. A.; Callow, M. E.; Wooley, K. L., The antifouling and fouling-release perfomance of hyperbranched fluoropolymer (HBFP)− poly (ethylene glycol)(PEG) composite coatings evaluated by adsorption of biomacromolecules and the green fouling alga Ulva. *Langmuir* **2005,** *21* (7), 3044-3053.

91. Cheng, C.; Wooley, K. L.; Khoshdel, E., Hyperbranched fluorocopolymers by atom transfer radical self-condensing vinyl copolymerization. *Journal of Polymer Science Part A: Polymer Chemistry* **2005,** *43* (20), 4754-4770.

92. Powell, K. T.; Cheng, C.; Wooley, K. L., Complex Amphiphilic Hyperbranched Fluoropolymers by Atom Transfer Radical Self-Condensing Vinyl (Co)polymerization. *Macromolecules* **2007,** *40* (13), 4509-4515.

93. Imbesi, P. M.; Finlay, J. A.; Aldred, N.; Eller, M. J.; Felder, S. E.; Pollack, K. A.; Lonnecker, A. T.; Raymond, J. E.; Mackay, M. E.; Schweikert, E. A.; Clare, A. S.; Callow, J. A.; Callow, M. E.; Wooley, K. L., Targeted surface nanocomplexity: two-dimensional control over the composition, physical properties and anti-biofouling performance of hyperbranched fluoropolymer–poly(ethylene glycol) amphiphilic crosslinked networks. *Polymer Chemistry* **2012,** *3* (11), 3121-3131.

94. Imbesi, P. M.; Gohad, N. V.; Eller, M. J.; Orihuela, B.; Rittschof, D.; Schweikert, E. A.; Mount, A. S.; Wooley, K. L., Noradrenaline-Functionalized Hyperbranched Fluoropolymer–Poly(ethylene glycol) Cross-Linked Networks As Dual-Mode, Anti-Biofouling Coatings. *ACS Nano* **2012,** *6* (2), 1503-1512.

95. Pollack, K. A.; Imbesi, P. M.; Raymond, J. E.; Wooley, K. L., Hyperbranched fluoropolymer-polydimethylsiloxane-poly(ethylene glycol) cross-linked terpolymer networks designed for marine and biomedical Applications: heterogeneous nontoxic antibiofouling surfaces. *ACS Applied Materials & Interfaces* **2014,** *6* (21), 19265-19274.

96. Wanka, R.; Finlay, J. A.; Nolte, K. A.; Koc, J.; Jakobi, V.; Anderson, C.; Clare, A. S.; Gardner, H.; Hunsucker, K. Z.; Swain, G. W.; Rosenhahn, A., Fouling-release properties of dendritic polyglycerols against marine diatoms. *ACS Applied Materials & Interfaces* **2018,** *10* (41), 34965-34973.

97. Wang, Y.; Betts, D. E.; Finlay, J. A.; Brewer, L.; Callow, M. E.; Callow, J. A.; Wendt, D. E.; DeSimone, J. M., Photocurable amphiphilic perfluoropolyether/poly (ethylene glycol) networks for fouling-release coatings. *Macromolecules* **2011,** *44* (4), 878-885.

98. Martinelli, E.; Del Moro, I.; Galli, G.; Barbaglia, M.; Bibbiani, C.; Mennillo, E.; Oliva, M.; Pretti, C.; Antonioli, D.; Laus, M., Photopolymerized Network Polysiloxane Films with Dangling Hydrophilic/Hydrophobic Chains for the Biofouling Release of Invasive Marine Serpulid Ficopomatus enigmaticus. *ACS Applied Materials & Interfaces* **2015,** *7* (15), 8293-8301.

99. Majumdar, P.; Stafslien, S.; Daniels, J.; Webster, D. C., High throughput combinatorial characterization of thermosetting siloxane–urethane coatings having spontaneously formed microtopographical surfaces. *Journal of Coatings Technology and Research* **2007,** *4* (2), 131-138.

100. Bodkhe, R. B.; Stafslien, S. J.; Cilz, N.; Daniels, J.; Thompson, S. E. M.; Callow, M. E.; Callow, J. A.; Webster, D. C., Polyurethanes with amphiphilic surfaces made using telechelic functional PDMS having orthogonal acid functional groups. *Progress in Organic Coatings* **2012,** *75* (1-2), 38-48.

101. Galhenage, T. P.; Webster, D. C.; Moreira, A. M. S.; Burgett, R. J.; Stafslien, S. J.; Vanderwal, L.; Finlay, J. A.; Franco, S. C.; Clare, A. S., Poly(ethylene) glycol-modified, amphiphilic, siloxane–polyurethane coatings and their performance as fouling-release surfaces. *Journal of Coatings Technology and Research* **2017,** *14* (2), 307-322.

102. Sonnenschein, M. F., *Polyurethanes : science, technology, markets, and trends*. Hoboken, NJ, 2015.

103. Edwards, P. A.; Striemer, G.; Webster, D. C., Synthesis, characterization and self-crosslinking of glycidyl carbamate functional resins. *Progress in Organic Coatings* **2006,** *57* (2), 128-139.

104. Edwards, P. A.; Striemer, G.; Webster, D. C., Novel polyurethane coating technology through glycidyl carbamate chemistry. *JCT research* **2005,** *2* (7), 517-527.

105. Harkal, U. D.; Muehlberg, A. J.; Webster, D. C., Linear glycidyl carbamate (GC) resins for highly flexible coatings. *Journal of Coatings Technology and Research* **2013,** *10* (2), 141-151.

106. Stafslien, S. J.; Christianson, D.; Daniels, J.; VanderWal, L.; Chernykh, A.; Chisholm, B. J., Combinatorial materials research applied to the development of new surface coatings XVI: fouling-release properties of amphiphilic polysiloxane coatings. *Biofouling* **2015,** *31* (2), 135-149.

107. Koc, J.; Schönemann, E.; Amuthalingam, A.; Clarke, J.; Finlay, J. A.; Clare, A. S.; Laschewsky, A.; Rosenhahn, A., Low-fouling thin hydrogel coatings made of photo-cross-linked polyzwitterions. *Langmuir* **2019,** *35* (5), 1552-1562.

108. Cao, X.; Pettit, M. E.; Conlan, S. L.; Wagner, W.; Ho, A. D.; Clare, A. S.; Callow, J. A.; Callow, M. E.; Grunze, M.; Rosenhahn, A., Resistance of Polysaccharide Coatings to Proteins, Hematopoietic Cells, and Marine Organisms. *Biomacromolecules* **2009,** *10* (4), 907-915.

109. Morra, M.; Cassineli, C., Non-fouling properties of polysaccharide-coated surfaces. *Journal of Biomaterials Science, Polymer Edition* **1999,** *10* (10), 1107-1124.

110. Bauer, S.; Arpa-Sancet, M. P.; Finlay, J. A.; Callow, M. E.; Callow, J. A.; Rosenhahn, A., Adhesion of Marine Fouling Organisms on Hydrophilic and Amphiphilic Polysaccharides. *Langmuir* **2013,** *29* (12), 4039-4047.

111. Cavalli, S.; Albericio, F.; Kros, A., Amphiphilic peptides and their cross-disciplinary role as building blocks for nanoscience. *Chemical Society Reviews* **2010,** *39* (1), 241-263.

112. Parrish, B.; Breitenkamp, R. B.; Emrick, T., PEG- and Peptide-Grafted Aliphatic Polyesters by Click Chemistry. *Journal of the American Chemical Society* **2005,** *127* (20), 7404-7410.

113. Calabrese, D. R.; Wenning, B.; Finlay, J. A.; Callow, M. E.; Callow, J. A.; Fischer, D.; Ober, C. K., Amphiphilic oligopeptides grafted to PDMS-based diblock copolymers for use in antifouling and fouling release coatings. *Polymers for Advanced Technologies* **2015,** *26* (7), 829-836.

114. van Zoelen, W.; Zuckermann, R. N.; Segalman, R. A., Tunable Surface Properties from Sequence-Specific Polypeptoid–Polystyrene Block Copolymer Thin Films. *Macromolecules* **2012,** *45* (17), 7072-7082.

115. Van Zoelen, W.; Buss, H. G.; Ellebracht, N. C.; Lynd, N. A.; Fischer, D. A.; Finlay, J.; Hill, S.; Callow, M. E.; Callow, J. A.; Kramer, E. J., Sequence of hydrophobic and hydrophilic residues in amphiphilic polymer coatings affects surface structure and marine antifouling/fouling release properties. *ACS Macro Letters* **2014,** *3* (4), 364-368.

116. Turner, A., Marine pollution from antifouling paint particles. *Marine Pollution Bulletin* **2010,** *60* (2), 159-171.

117. Cai, L.; Liu, A.; Yuan, Y.; Dai, L.; Li, Z., Self-assembled perfluoroalkylsilane films on silicon substrates for hydrophobic coatings. *Progress in Organic Coatings* **2017,** *102*, 247-258.

118. Noguer, A. C., *Experimental investigation of the behaviour and fate of block copolymers in fouling-release coatings*. Technical University of Denmark (DTU): Kgs. Lyngb, Denmark, 2016.

119. Murthy, R.; Bailey, B. M.; Valentin-Rodriguez, C.; Ivanisevic, A.; Grunlan, M. A., Amphiphilic silicones prepared from branched PEO-silanes with siloxane tethers. *Journal of Polymer Science Part A: Polymer Chemistry* **2010,** *48* (18), 4108-4119.

120. Røn, T.; Javakhishvili, I.; Hvilsted, S.; Jankova, K.; Lee, S., Ultralow friction with hydrophilic polymer brushes in water as segregated from silicone matrix. *Advanced Materials Interfaces* **2016,** *3* (2), 1500472.

121. Rufin, M. A.; Barry, M. E.; Adair, P. A.; Hawkins, M. L.; Raymond, J. E.; Grunlan, M. A., Protein resistance efficacy of PEO-silane amphiphiles: Dependence on PEO-segment length and concentration. *Acta biomaterialia* **2016,** *41*, 247-252.

122. Liu, Y.; Leng, C.; Chisholm, B.; Stafslien, S.; Majumdar, P.; Chen, Z., Surface structures of PDMS incorporated with quaternary ammonium salts designed for antibiofouling and fouling release applications. *Langmuir* **2013,** *29* (9), 2897-2905.

123. Wan, F.; Pei, X.; Yu, B.; Ye, Q.; Zhou, F.; Xue, Q., Grafting polymer brushes on biomimetic structural surfaces for anti-algae fouling and foul release. *ACS Applied Materials & Interfaces* **2012,** *4* (9), 4557-4565.

124. Zhang, L.; Sha, J.; Chen, R.; Liu, Q.; Liu, J.; Yu, J.; Zhang, H.; Lin, C.; Wang, J., Three-dimensional flower-like shaped Bi5O7I particles incorporation zwitterionic fluorinated polymers with synergistic hydration-photocatalytic for enhanced marine antifouling performance. *Journal of Hazardous Materials* **2020,** *389*, 121854.

125. Sun, D.; Li, P.; Li, X.; Wang, X., Protein-Resistant Surface Based on Zwitterion-Functionalized Nanoparticles for Marine Antifouling Applications. *New Journal of Chemistry* **2020**.

126. Ciriminna, R.; Bright, F. V.; Pagliaro, M., Ecofriendly antifouling marine coatings. *ACS Sustainable Chemistry & Engineering* **2015,** *3* (4), 559-565.

127. Kavanagh, C. J.; Swain, G. W.; Kovach, B. S.; Stein, J.; Darkangelo-Wood, C.; Truby, K.; Holm, E.; Montemarano, J.; Meyer, A.; Wiebe, D., The effects of silicone fluid additives and silicone elastomer matrices on barnacle adhesion strength. *Biofouling* **2003,** *19* (6), 381-390.

128. Tamaev, N.; Kiil, S.; Noguer, A. C.; Olsen, S. M. In *Use of Fillers, Pigments and Additives in Fouling-Release Coatings: A Literature Review*, 2015.

129. Selim, M. S.; El-Safty, S. A.; Azzam, A. M.; Shenashen, M. A.; El-Sockary, M. A.; Abo Elenien, O. M., Superhydrophobic silicone/TiO2–SiO2 nanorod-like composites for marine fouling release coatings. *ChemistrySelect* **2019,** *4* (12), 3395-3407.

130. Beigbeder, A.; Mincheva, R.; Pettitt, M. E.; Callow, M. E.; Callow, J. A.; Claes, M.; Dubois, P., Marine fouling release silicone/carbon nanotube nanocomposite coatings: on the importance of the nanotube dispersion state. *Journal of Nanoscience and Nanotechnology* **2010,** *10* (5), 2972-2978.

131. Beigbeder, A.; Labruyère, C.; Viville, P.; Pettitt, M. E.; Callow, M. E.; Callow, J. A.; Bonnaud, L.; Lazzaroni, R.; Dubois, P., Surface and fouling-release properties of silicone/organomodified montmorillonite coatings. *Journal of Adhesion Science and Technology* **2011,** *25* (14), 1689-1700.

132. Selim, M. S.; El-Safty, S. A.; El-Sockary, M. A.; Hashem, A. I.; Elenien, O. M. A.; El-Saeed, A. M.; Fatthallah, N. A., Smart photo-induced silicone/TiO2 nanocomposites with dominant [110] exposed surfaces for self-cleaning foul-release coatings of ship hulls. *Materials & Design* **2016,** *101*, 218-225.

133. Arukalam, I. O.; Oguzie, E. E.; Li, Y., Fabrication of FDTS-modified PDMS-ZnO nanocomposite hydrophobic coating with anti-fouling capability for corrosion protection of Q235 steel. *Journal of Colloid and Interface Science* **2016,** *484*, 220-228.

134. Stafslien, S. J.; Sommer, S.; Webster, D. C.; Bodkhe, R.; Pieper, R.; Daniels, J.; Vander Wal, L.; Callow, M. C.; Callow, J. A.; Ralston, E., Comparison of laboratory and field testing performance evaluations of siloxane-polyurethane fouling-release marine coatings. *Biofouling* **2016,** *32* (8), 949-968.

CHAPTER 2. AMPHIPHILIC, ZWITTERIONIC-PDMS-BASED SURFACE-MODIFYING ADDITIVES TO IMPROVE FOULING-RELEASE OF MARINE COATINGS

Introduction

Marine biofouling is the undesirable accumulation of marine micro- and macro-organisms on submerged structures in seawater.[1] Biofouling imposes a complex problem that not only causes unappealing aesthetic effects, but it also has penalized the marine industry for centuries through significant economic and environmental drawbacks. The estimates report that biofouling costs $1 billion per year to the United States Navy alone.[2] The continuous settlement of marine organisms on ships' hulls creates frictional drag, which eventually leads to reduced speed and maneuverability, resulting in increased fuel consumption and gaseous emissions.[3] Estimates have shown that even a 2% reduction in ship speed can drop fuel efficiency significantly.[4] A biofouled ship, therefore, should undergo frequent dry-docking, enforcing severe economic penalties on ship owners. Additionally, given the global nature of shipping routes, biofouling also threatens natural environments through transportation of invasive species.[2]

The process of marine biofouling is a complex phenomenon of multiple stages that worldwide involves more than 4000 marine organisms with varying sizes, surface type affinities, and mechanisms of adhesion. The process starts immediately when a structure is immersed in seawater – proteins, nutrients, and other small molecules settle on the surface and form a conditioning film. This is followed by marine bacteria as well as slime forming algae (diatoms), which colonize within minutes and form a biofilm. Alongside the micro-organisms macro-organisms such as barnacles and mussels will settle on the surface too, but at a slower rate. While marine biofouling is often viewed as a linear chain of fouling events, from micro- to macro-organisms, this is not necessarily the case and macro-foulants, such as the barnacle *A. amphitrite* and the green alga *U. linza* are known to adhere to clean or newly immersed surfaces without the presence of microbial films[1, 3]

Historically, the protection of ships' hulls has taken many forms, with copper alloys and lead sheathing giving way to biocide-containing antifouling paints by the 1900s. The effectiveness of these

peaked with the introduction of tributyl tin-based self-polishing copolymer coatings in the 1970s. However, the paints were toxic to non-targeted marine species,[5] resulting in a worldwide ban of organotin-based coatings by the International Marine Organization (IMO) due to their harmful effects to aquatic ecosystems.[3, 6] Therefore, to address regulations, the focus of many recent studies has been to develop antifouling (AF) coatings and fouling-release (FR) coatings that are non-toxic.

The most common antifouling coatings used today contain copper oxide-based components, which although less toxic than organotin materials, release metal ions into aquatic environments with potential negative impact on marine ecosystems. FR systems offer a completely non-toxic and eco-friendly approach to combat biofouling. FR coatings do not release any chemicals, rather they prevent strong adhesion of marine organisms to the surface of structures, which facilitates easy removal of the foulants when subjected to hydrodynamic pressure upon movement of ships or light cleaning.[1, 3] As a result, FR systems have remained of special interest to avoid application of biocide-containing paints.

Traditional FR systems are mainly made of elastomeric materials such as polydimethylsiloxane (PDMS), fluoropolymers, or other silicones.[3] Additionally, PDMS and materials similar to it, possess low surface energy, which acts as a driving force for weak adhesion of organisms, introducing the fouling release mechanism upon exposure of settled foulants to hydrodynamic pressure.[3] Nevertheless, commercial coatings made of these low surface energy components suffer from poor mechanical durability and require a tie-coat to achieve proper adhesion to a substrate.[3, 7] To address the durability and tie-coat limitations while ensuring desirable FR performance is met, hydrophobic siloxane-polyurethane (SiPU) FR coatings have been developed that display FR performance comparable to or better than commercially available products with strong adhesion to a substrate and a magnitude higher bulk modulus. The SiPU coatings benefit from the combination of two incompatible materials: polyurethane (PU), which is polar with high surface energy, and PDMS, which is non-polar with low surface energy. The incompatibility causes self-stratification of components with PDMS segregating to the surface, tackling the biofouling issue, while the PU remains in contact with the substrate offering good mechanical strength and strong adhesion.[8-10]

Hydrophobic FR systems, like SiPU, can combat some biofouling species effectively, but there are still organisms that can settle firmly on such surfaces. The difference in adherence of foulants to FR

coating surfaces is not surprising given the wide variety of marine fouling organisms with differing surface affinities, from hydrophilic to hydrophobic surfaces, and adhesion mechanisms.[7] For example, *U. linza,* mussels, and barnacles attach strongly to hydrophilic surfaces, while the diatom, *N. incerta*, attaches strongly to hydrophobic surfaces and the marine bacterium, *C. lytica*, settles on a variety of surfaces.

Hydrophilic, protein-resistant materials have shown a promising ability to deter biofouling.[11] Polyethylene glycol (PEG) is one of the commonly investigated materials as it resists protein absorption and possesses non-toxic and nonimmunogenic properties. PEG-modified surfaces interfere with protein binding through hydrophilic interactions of the surface with water.[12-14] Self-assembled monolayers (SAM) containing PEG are commonly explored as protein-resistant materials for biomedical applications,[15] but the application of SAMs as marine coatings is not feasible. As a viable approach, PEG-modified amphiphilic siloxane-polyurethane coatings were designed to benefit from properties of PEG, which resulted in broadened performance against marine organisms.[16] However, PEG experiences rapid autoxidation in the presence of transition metals in both the biological and marine environments, appearing as a less suitable candidate for long-term use in marine coatings.[17] Zwitterionic materials are recognized as another major category of hydrophilic, protein-resistant and ultra-low fouling materials that can bind water molecules even more strongly and offer prolonged stability.[18, 19] Phosphobetaine, sulfobetaine, and carboxybetaine are examples of zwitterionic candidates. Sulfobetaine-based polymers have demonstrated promising results in a wide range of applications due to their biomimetic and ultra-low biofouling properties, stability, and commercial availability of the monomer, sulfobetaine methacrylate.[20-25]

This study evaluated a series of amphiphilic surface-modifying additives that can be non-covalently added into a hydrophobic SiPU coating system to tailor its fouling-release performance. Amphiphilic zwitterionic additives are composed of both hydrophilic and hydrophobic segments that are poly (sulfobetaine methacrylate) (poly(SBMA)) and polydimethylsiloxane (PDMS), respectively. The PDMS segment of such amphiphilic additives should facilitate its self-stratification to the coating/air interface as a result of its low surface energy as well as its incompatibility with the coating composition (Figure 2.1).[8, 9] In water, poly(SBMA) zwitterionic segment of the additive will form a highly hydrated aqueous structure (up to 8 times more than PEG) at the surface.[24, 25] The hydrated layer will not be readily displaced by marine organisms, limiting their ability to settle on the surface of a coating. Thus, a

combination of both PDMS and poly(SBMA) will potentially form a coating surface that has both hydrophobic and hydrophilic characteristics, respectively, to combat settlement of a wider range of organisms.

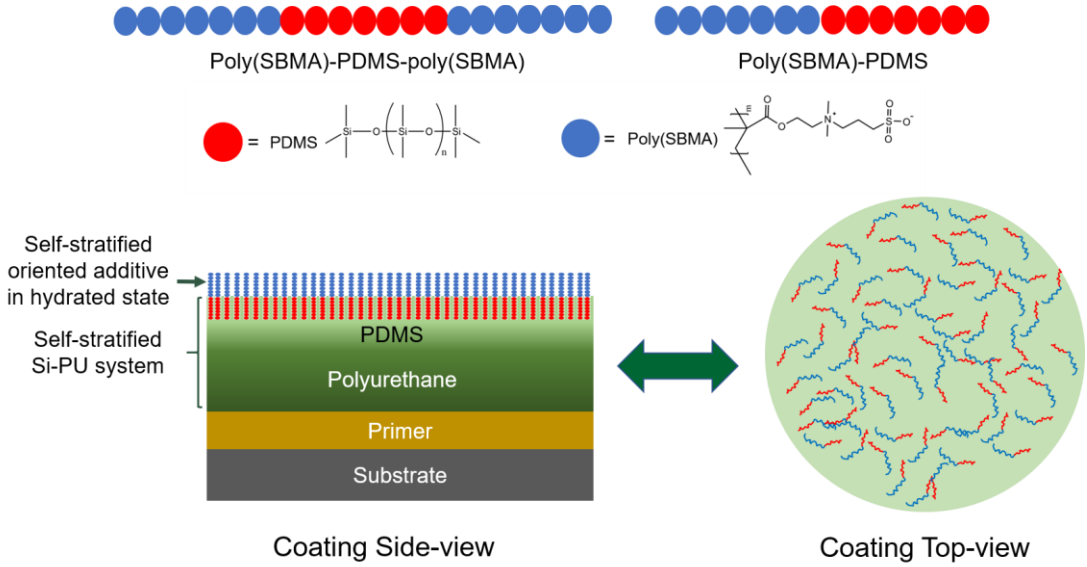

Figure 2.1. Illustration of amphiphilic zwitterionic-PDMS-based surface-modifying additives to improve fouling-release performance of the hydrophobic SiPU marine coating system.

Experimental

Materials

Desmodur Z4470 BA (isophorone diisocyanate-based polyisocyanate (IPDI)) was provided by Covestro LLC. All monofunctional carbinol-terminated polydimethylsiloxane (CT-PDMS) and difunctional CT-PDMS were purchased from Gelest Inc. Copper (II) chloride, 2-(dimethylamino) ethyl methacrylate, 1-3-propane sultone, ascorbic acid (vitamin C), 2,2'-bipyridine, α-bromoisobutyryl bromide (BIBB), triethylamine, dibutyltin diacetate (DBTDAc), deuterated dimethyl sulfoxide (DMSO), tetrahydrofuran (THF), toluene, chloroform, acetone, acetylacetone, and methyl amyl ketone (MAK), drying molecular sieves of 4 Å size were purchased from Sigma-Aldrich. A solution of DBTDAc was prepared by mixing 1% by wt. in MAK. An acrylic polyol composed of 80% butyl acrylate and 20% 2-hydroxyethyl acrylate was synthesized via conventional free radical polymerization and diluted to 50% with toluene. Aminopropyl-terminated polydimethylsiloxane (APT-PDMS) with molecular weight (MW) of 20,000 $\bar{M}_n$ was also synthesized through a ring-opening equilibration reaction. Detailed descriptions of synthesis procedures for both the acrylic polyol and APT-PDMS can be found elsewhere.[9]

AkzoNobel, International Paint Ltd. provided the commercial FR standards Intersleek® 700 (IS 700), Intersleek® 900 (IS 900), and Intersleek® 1100SR (IS 1100). The silicone elastomer, Silastic® T2 (T2), and polyurethane standard was provided by Dow Corning. Aluminum panels (4" x 8" in., 0.6 mm thick, type A, alloy 3003 H14) purchased from Q-lab were sandblasted and primed with Intergard 264 (International Paint) using air-assisted spray application. Multi-well plates were modified using circular disks (1-inch diameter) of primed aluminum.[26]

Synthesis of Sulfobetaine Methacrylate (SBMA) Monomer

In a 250-mL one-neck round-bottom flask equipped with a magnetic stirrer and a thermocouple, 2-(dimethylamino) ethyl methacrylate (30.0 g; 0.19 mole) and acetone (90.0 mL) were charged, and the contents were stirred at 30 °C. A solution of 1,3-propane sultone (23.3 g; 0.19 mole) and acetone (10 mL) was added dropwise, over 30 minutes, to the flask. After the addition of the solution, the reaction was stirred at 30 °C for four hours and then allowed to stand at room temperature for one week. The monomer precipitated out as white crystals and was collected by filtration, washed with dry acetone three times, and dried under vacuum overnight to obtain sulfobetaine methacrylate **(Scheme 2.1).** The product was confirmed by proton nuclear magnetic resonance (^{1}H-NMR) and Fourier transform infrared spectroscopy (FTIR).

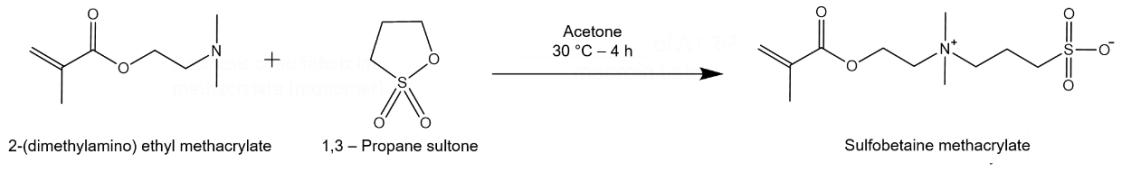

Scheme 2.1. Synthesis of SBMA monomer

Synthesis of ARGET-ATRP Macroinitiator (Br-terminated PDMS)

The reaction to synthesize the macroinitiator is shown in **Scheme 2.2**.The mole ratio of CT-PDMS: triethylamine: BIBB was 1.00:1.00:1.16 and 1.00:2.00:2.30 for mono-functional CT-PDMS and di-functional CT-PDMS, respectively. In a 500-mL three-neck round-bottom flask equipped with an addition funnel, magnetic stirrer, and thermocouple, CT-PDMS and triethylamine were dissolved in 200 mL dry THF solvent. The flask was placed in an ice bath and the contents were stirred at 0 - 5 °C. A solution of BIBB and 10 mL THF was added dropwise to the flask while maintaining the temperature at 0 - 5 °C. After the addition of the solution, the reaction was stirred at room temperature overnight. Next, the generated

white precipitate was removed using a fritted funnel, and solvent was removed under vacuum. Then, 100 mL of dichloromethane was added to the condensed contents, and they were washed with water 3 times (100 mL each time). The organic layer was collected, dried over $MgSO_4$, filtered, condensed in a rotary evaporator, and dried *in vacuo* overnight. The synthesized macroinitiator was characterized by ^{1}H-NMR and FTIR.[27]

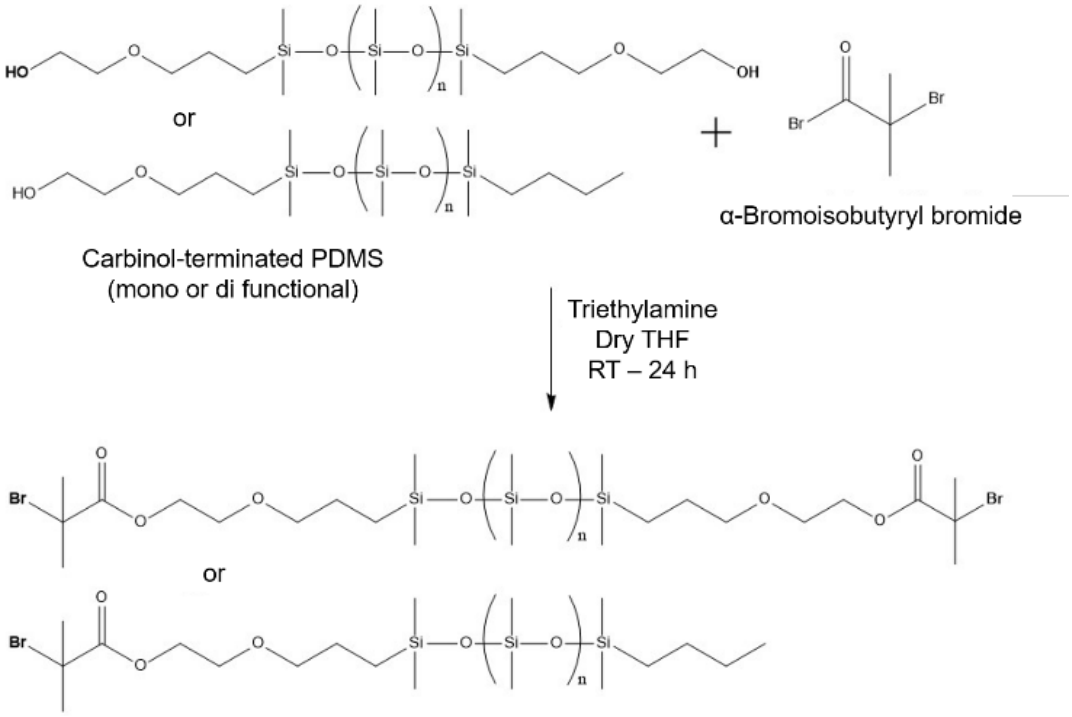

Scheme 2.2. Synthesis of Br-PDMS macroinitiator for ARGET-ATRP polymerization technique

Synthesis of Amphiphilic Additives

Amphiphilic additives that contained zwitterionic poly(SBMA) block(s) and PDMS block were synthesized through the ARGET-ATRP technique, which provided the advantage to control chain length of poly(SBMA) attached to the PDMS block.[27-29] This polymerization technique allows synthesis of polymers with targeted chain lengths, requires negligible catalyst content (ppm concentration) and utilizes vitamin C (ascorbic acid) as a reducing agent. Also, there is no need for a glove box to run this polymerization since the catalyst precursor is more stable for ARGET ATRP than conventional ATRP. ARGET ATRP requires solvent plus five components including monomer, macroinitiator, catalyst, reducing agent, and a ligand: sulfobetaine methacrylate (SBMA), Br-terminated PDMS, Cu(II) Cl, vitamin C (ascorbic acid), and 2,2'-bipyridine, respectively.

The ratio of $[SBMA]_0/[Br\text{-}PDMS\text{-}Br]_0/[CuCl_2]_0/[bpy]_0/[Vitamin\ C]_0$ for the polymerization was 100/0.2/0.01/0.05/0.15. For example, to synthesize 10 g of triblock additive 2500-1000-2500 (where 2500 is $\bar{M}_n$ molecular weight of each poly(SBMA) chain attached on a di-functional 1000 $\bar{M}_n$ CT-PDMS), the mentioned reagents were added in 10,000 mg/ 2596 mg/ 13 mg/ 78 mg/ 264 mg. The reaction is illustrated in **Scheme 2.3** In a 100-mL one-neck round-bottom flask equipped with a magnetic stirrer, Br-PDMS macroinitiator and 40 mL methanol was charged and stirred at room temperature. A solution of SBMA monomer dissolved in 5 mL methanol was added to the flask. The contents were stirred for 5 minutes to obtain a homogenous mixture. A solution of 2,2'-bipyridine and Cu(II) Cl in 5 mL methanol was added to the flask. The flask was sealed, and a flow of nitrogen gas was injected into the flask for 30 seconds. A solution of ascorbic acid in 2 mL water was injected into the flask using a syringe to initiate the polymerization reaction. The reaction was stirred at room temperature for 48 hours. After this time, the polymer was precipitated in methanol. The solvent was removed by a rotary evaporator. Then, as the amphiphilic product was not soluble in water or common organic solvents, the contents were washed with both water and dichloromethane 3 times (50 mL each time). The remaining residual solvent was removed using a rotary evaporator and the product was dried *in vacuo* at 40 °C overnight. The synthesized macroinitiator was characterized by ^{1}H-NMR and FTIR. GPC could not be run on these block copolymers also due to their insolubility limitations in common solvents like THF or water; however, ARGET-ATRP polymerization was conducted using the same procedure with butyl methacrylate and Br-PDMS and GPC confirmed a tri-block copolymer of targeted 6000 $\bar{M}_n$ (PDI 1.12). Poly (SBMA) with no PDMS in the backbone was also synthesized using the same procedure as a control additive to compare results with; BIBB initiator was used instead of Br-terminated PDMS macroinitiator.

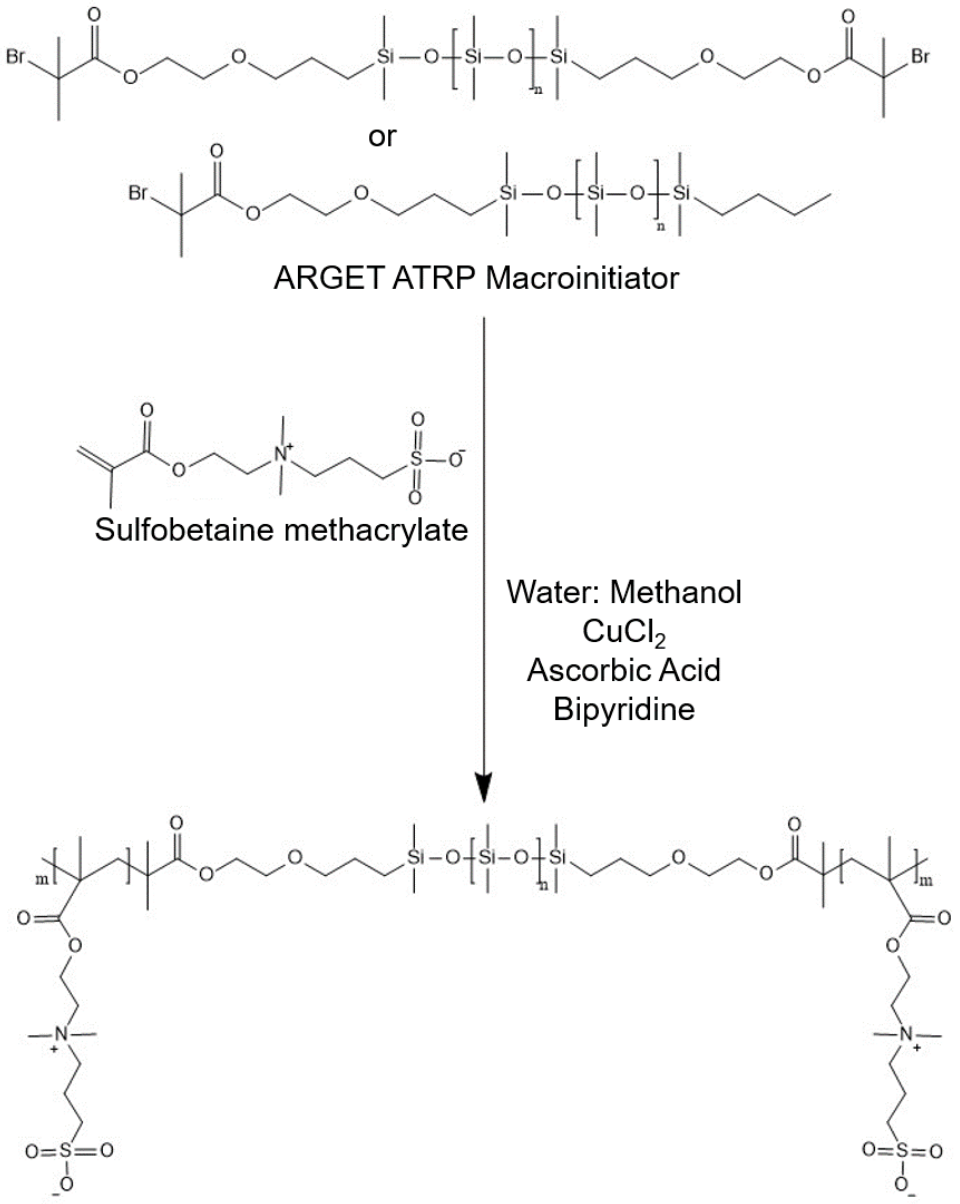

Scheme 2.3. Synthesis of amphiphilic copolymeric additive via ARGET ATRP polymerization method

Coating Formulations

All synthesized additives in this study were added to the SiPU A4-20 formulation to tune its marine performance. The A4-20 formulation consists of an IPDI trimer isocyanate resin that is crosslinked with an acrylic polyol and an amine-terminated PDMS, being an inherently hydrophobic fouling-release coating. An amphiphilic additive was the only variable that was added to SiPU A4-20 system for a studied formulation. Additives were added in wt. % of total solid content of the A4-20 system. For example, to formulate a formulation with 1 wt.% of additive, acrylic polyol (16.71 g) and additive (0.17 g) were added

in a vial, sonicated for 15 minutes and magnetically stirred at ambient condition for 24 hours. APT-PDMS (3.34 g) and acetylacetone (1.65 g) were added to the vial. The mixture was sonicated for 15 minutes and was magnetically stirred at ambient condition for another 24 hours. IPDI trimer Desmodur Z4470 BA resin (7.41 g) and DBTDAc catalyst solution (0.66 g) were added to the vial, and the mixture was stirred for another hour. After mixing, coating formulations were deposited into multi-well plates using an automatic repeat pipette (250 µL of formulation was deposited into each well in multi-well plate). Drawdowns were made on primed 8' x 4' aluminum panels using a wire-wound drawdown bar with a wet film thickness of 80 µm. All coatings were cured under ambient conditions for 24 hours followed by oven curing at 80 °C for 45 min.

Experimental Design

This study was designed to assess 12 additives **(**Table 2.1**).** Additives are labeled based on the MW of their polymeric blocks, where the first and third number (applicable for triblock additives) is always MW of poly(SBMA) chain(s) and the second number is MW of PDMS.

Four variables were evaluated to establish an understanding and correlation between a designed additive and fouling-release performance. The variables were PDMS average molecular weight (1,000 $\bar{M}_n$, 5,000 $\bar{M}_n$, 10,000 $\bar{M}_n$), poly(SBMA) molecular weight (500 $\bar{M}_n$, 1,000 $\bar{M}_n$, 2,500 $\bar{M}_n$), additive type (di-blocks vs tri-blocks) and addition amount to a coating (0.2, 1, and 5 wt. % in relation to non-volatile coating ingredients). A total of 44 coatings were formulated **(**Table A1**).** Formulations are labeled based on the type and amount of incorporated additive. For example, formulation "500-1k 1%" refers to an additive with 500 $\bar{M}_n$ poly(SBMA) block and 1,000 $\bar{M}_n$ PDMS block that is added in 1 wt. % to A4-20 coating system. Eight formulations were shortlisted and discussed in this paper **(**Table 2.2**)** after preliminary fouling-release assessments against *C. lytica* (Figure A1) and *U. linza* (Figure A2), and these eight were further investigated against *U. linza*, barnacles, and mussels. Table 2.2 also outlines the percentage of hydrophilic portion for an additive, which is calculated by dividing the MW of hydrophilic block(s) by the total molecular weight of an additive and then multiplying by 100.

Table 2.1. Synthesized copolymeric additives

Additive ID	Additive Type	MW of a poly(SBMA) Block ($\bar{M}_n$)	MW of PDMS Block ($\bar{M}_n$)
500-1k	Di-block	500	1000
1k-1k		1000	1000
2.5k-1k		2500	1000
500-1k-500	Tri-block	500	1000
1k-1k-1k		1000	1000
2.5k-1k-2.5k		2500	1000
500-5k-500		500	5000
1k-5k-1k		1000	5000
2.5k-5k-2.5k		2500	5000
500-10k-500		500	10000
1k-10k-1k		1000	10000
2.5k-10k-2.5k		2500	10000

Table 2.2. Selected formulations

Formulation ID	Incorporated Additive & Percent Amount	Hydrophilic Content % of Used Additive
3	500-1k 1%	33.3
6	1k-1k 1%	50.0
9	2.5k-1k 1%	71.4
15	1k-1k-1k 1%	66.6
18	2.5k-1k-2.5k 1%	83.3
26	2.5k-5k-2.5k 1%	50.0
35	2.5k-10k-2.5k 1%	33.3
42	polySBMA 1%	100.0

Control and Standard Coatings

Commercial standards were prepared following manufacturer's specifications. Control SiPU A4-20 was prepared following the procedure outlined in a previous study.[9] Similar to experimental coatings all control and standards were also prepared on 4" x 8" primed aluminum panels and multi-well plates. Table 2.3 contains detailed descriptions of the control and standard coatings used for this study.

Table 2.3. List of control and standard coatings

Control Name	Control ID	Description
A4-20%	1	Internal Si-PU FR Control
Standard PU	PU	Pure Polyurethane Standard
Dow T2	T2	Silicone Elastomer Standard
Intersleek® 700	IS 700	Commercial FR Standard
Intersleek® 900	IS 900	Commercial FR Standard
Intersleek®1100SR	IS 1100	Commercial FR Standard

Fourier Transform Infrared Spectroscopy

Fourier transform infrared (FTIR) spectroscopy was utilized to characterize the monomer, macroinitiators and block copolymers, using a Thermo Scientific Nicolet 8700 FTIR. The liquid resin or prepolymer was spread as a thin layer on a potassium bromide (KBr) plate to collect the spectrum.

^{1}H-NMR

^{1}H-NMR spectra for a synthesized additive were collected using a Bruker Avance 400 MHz instrument and processed with Topspin software. Peak shifts were calibrated based on residual solvent peaks. Additive samples for NMR experiment were dissolved in deuterated DMSO solvent.

Surface Characterization

All experimental coatings were characterized using a Symyx®/First Ten Angstroms system to measure the contact angles and surface energy of the coatings before and after water immersion. Water contact angles (WCA) and diiodomethane contact angles (MICA) for each coating were obtained at 0, 3, 6, 9, 15-minute time intervals to assess changes to measured values over time. Three measurements of contact angles were obtained using First Ten Angstroms™ software. Surface energy for each formulation was calculated using the Owens-Wendt method.[30] Three replicates were recorded for each sample at the above-mentioned time intervals.

Atomic force microscopy (AFM) offered insights into the surface topography of the studied coatings. A Dimension 3100 microscope with Nanoscope controller scanned the surface of experimental coatings, collecting images on a sample area of 100 µm x 100 µm in tapping mode. The experiment was done in air under ambient conditions, using a silicon probe with a spring constant of 0.1-0.6 N/m and 15-39 kHz resonance frequency.

Attenuated total reflectance-Fourier transform infrared spectroscopy (ATR-FTIR) was used to characterize the surfaces of the coatings. A Bruker Vertex 70 with Harrick's ATR™ accessory using a hemispherical Ge crystal was used to collect ATR-FTIR spectra for a coating.

Water Aging

All the prepared coatings were pre-leached for 28 days in running tap water. The water tanks were equipped to automatically fill and empty every 4 hours. Water aging of the coatings was carried out to meet two objectives: 1) to leach out any impurities that might interfere with fouling-release assessments; 2) to determine if there was any significant surface rearrangement of the coatings, or whether the additives leach out. All biological laboratory assays were carried out after the pre-leaching water aging process was completed.

Biological Laboratory Assays

Growth and Release of Macroalgae (*Ulva linza*)

A set of multiwall plates was sent to Newcastle University, following water-immersion for 28 days, to assess fouling-release performance of coatings against *U. linza*. A detailed description of the method of assessment can be found elsewhere.[31] Briefly, after leaching, all multi-well plates were equilibrated in 0.22 µm filtered artificial seawater (Tropic Marin) for 2 hours. To each well, 1 mL of spores of *U. linza* suspension was added, adjusted to 3.3 x 10^5 spores/mL in enriched seawater medium.[32] Spores settled on the coated discs were grown for 7 days inside an illuminated incubator at 18°C with a 16:8 light: dark cycle (photon flux density 45 µmol.m^{-2}.s^{-1}). There was no washing to remove unsettled spores after settlement. After 7 days, the biomass generated was assessed from a single row of wells (6) from each plate. Relative adhesion strength was evaluated by exposing two other rows of wells to two different water pressures using a waterjet.[33]. Chlorophyll was extracted by adding 1 mL DMSO to each well and followed by measuring the fluorescence at 360 nm excitation and 670 nm emission. Fluorescence is directly proportional to the biomass present on each coating surface. The removal of *U. linza* at each pressure was compared with the unsprayed wells that were used to determine initial growth.[33-35]

Growth and Release of Microalgae (*Navicula incerta*)

A laboratory biological assay to evaluate FR properties of coatings towards diatom cells (*Navicula incerta*) was conducted at NDSU following a similar procedure to that described previously.[31, 36] Briefly, a

suspension with 4×10^5 cells/mL of *N. incerta* (adjusted to 0.03 OD at absorbance 660 nm) in Guillard's F/2 medium was deposited into each well (1 mL per well) and cell attachment was stimulated by static incubation for 2 hours, under ambient conditions, in the dark. Coating surfaces were then subjected to water-jet treatments.[33] The first column of wells (3 wells) was not water-jetted so that initial cell attachment could be determined and the next column of wells (3 wells) was water-jetted at 20 psi for 10 seconds. Microalgae biomass was quantified by extracting chlorophyll using 0.5 mL of DMSO and measuring fluorescence of the transferred extracts at an excitation wavelength of 360 nm and an emission wavelength at 670 nm. The relative fluorescence units (RFU) measured from the extracts was considered to be directly proportional to the biomass remaining on the coating surfaces after water-jetting. Percent removal of attached microalgae was determined from RFUs of non-jetted and water-jetted wells.

Bacterial (*Cellulophaga lytica*) Biofilm Adhesion

Fouling-release properties towards bacteria were evaluated using retention and adhesion assays described previously.[33-35] A suspension consisting of the marine bacterium *C. lytica* at 10^7 cells/mL concentration, in artificial seawater (ASW), containing 0.5 g/L peptone and 0.1g/L yeast extract was deposited into 24-well plates (1 mL/well). The plates were then incubated statically at 28°C for 24 hours. The ASW growth medium was then removed and the coatings were subjected to water-jet treatments. The first column of each coating (3 replicate wells) was not treated and served as the initial amount of bacterial biofilm growth. The second column (3 replicate wells) was subjected to water-jetting at 10 psi for 5 seconds. Following water-jet treatments, the coating surfaces were stained with 0.5 mL of a crystal violet solution (0.3 wt. % in deionized water) for 15 minutes and then rinsed three times with deionized water. After 1 hour of drying at ambient laboratory conditions, the crystal violet dye was extracted from the coating surfaces by adding 0.5 mL of 33% acetic acid solution for 15 minutes. The resulting eluates were transferred to a 96-well plate (0.15 mL/coating replicate) and subjected to absorbance measurements at 600nm wavelength using a multi-well plate spectrophotometer. The absorbance values were considered to be directly proportional to the amount of bacterial biofilm present on coating surfaces before and after water-jetting treatments.[33]

Adult Barnacle (*Amphibalanus amphitrite*) Adhesion

An adult barnacle reattachment and adhesion assay was used to evaluate the FR properties of the coatings towards macrofoulers.[37, 38] Coatings prepared on 4" x 8" panels after water aging were utilized for this laboratory assay. Barnacles were dislodged from silicone substrates sent from Duke University Marine Laboratory (DUML) in Beaufort, North Carolina, USA, and immobilized on experimental coatings (6 barnacles per coating) using a custom-designed immobilization template. The immobilized barnacles were allowed to reattach and grow for 2 weeks while immersed in an ASW aquarium tank system with daily feedings of brine shrimp *Artemia* nauplii (Florida Aqua Farms). After the 2-week attachment period, the number of non-attached barnacles was recorded, and the attached barnacles were pushed off (in shear) using a hand-held force gauge mounted onto a semi-automated stage. Once the barnacles were dislodged, their basal plate areas were determined from scanned images using Sigma Scan Pro 5.0 software program. Barnacle adhesion strength (MPa) was calculated by taking the ratio of peak force of removal to the basal plate area for each reattached barnacle. To ensure consistency, barnacles of similar sizes were tested. The average barnacle adhesion strength for each coating was reported as a function of the number of barnacles released with a measurable force and that exhibited no visible damage to the basis or shell plates.

Mussels (*Geukensia demissa*) Adhesion

Marine mussels were used to evaluate fouling-release performance of the coating using 4" x 8" coated panels. Marine mussels (*G. demissa*) were provided by the DUML. Each mussel was further prepared for testing purposes by attaching a 4-cm-long acetal plastic rod (product # 98873A105, McMaster-Carr) perpendicular to the ventral edge, with a 3M® acrylic adhesive (product # 7467A135, McMaster-Carr). A total of six mussels were allowed to explore the surface of a coating for settlement, followed by placing custom-designed PVC sheets against plastic rods so that mussels were in contact with the surface of a coating. Coatings were analyzed after 3 days of attachment with two feedings of phytoplankton. The total number of mussels that attached by byssus threads was recorded for each surface. A tensile force gauge (mounted to an automated stage, moving at 1 mm/s pull rate) attached to a mussel's plastic rod was used to measure the force (Newtons). required to completely remove attached mussels from coating surfaces. The average force for all mussels that were removed from a surface was

recorded. The presence of nonattached mussels after a 3-day period indicated good mussel deterrence properties.[31-33]

Statistical Analysis

Analysis of variance for completely randomized design (CRD) (all experimental and control coatings included in this design) was performed in SAS software, version 9.4. The GLM procedure with least-squares means (LS-means) methods was used to determine the difference between means for each treatment group under the CRD design. The analysis compared two response values of interest, fouling-release performance of coatings against barnacles and *U. linza*.

Results and Discussions

Amphiphilic coatings have shown an enhanced ability to deter the attachment of a wide range of marine organisms. Therefore, we hypothesized that the addition of amphiphilic additives to a hydrophobic system will modify its surface to become amphiphilic, resulting in improved performance. This study investigated the synthesis of a series of amphiphilic additives based on building blocks of poly (SBMA) and PDMS and their incorporation in a well-established hydrophobic marine coating system the A4-20 siloxane-polyurethane coating.[9]

To synthesize the amphiphilic additives, two components were prepared and characterized beforehand, SBMA monomer and Br-PDMS macroinitiator. SBMA was prepared by the reaction of 2-(dimethylamino) ethyl methacrylate with 1,3-propane sultone as illustrated in Scheme 2.1. The synthesized monomer was characterized by ^{1}H-NMR, FTIR and melting point. The ^{1}H-NMR data shows all the expected signals corresponding to the structure of the monomer. These include signals from the proton of the carbon-carbon double bond appearing at 5.7 ppm and 6.15 ppm, along with other characteristic peaks (Figure A3). The FTIR spectrum showed signals for $^{+}NR_4$ (960 cm^{-1}), SO_3 (1060 cm^{-1}), C=C (1640 cm^{-1}), and C=O (1740 cm^{-1}) as shown in Figure A4, further confirming successful synthesis of the SBMA monomer. A OH shift at 3500 cm^{-1} was observed due to the hygroscopic nature of the monomer.[39] Also, the melting point of the monomer was 150 °C, which is within reported values.[40]

Br-terminated PDMS that functions as the ARGET-ATRP macroinitiator was synthesized by substituting the hydroxy functional groups with BIBB as outlined in Scheme 2.2. A comparison of ^{1}H-NMR between virgin PDMS and modified PDMS confirmed the transformation of hydroxyl end groups to

bromine as the -OH signal disappeared at 4 ppm, signals for two methyl groups of BIBB appeared at 1.9 ppm (Signal “a” in Figure A5), and signals of hydrogen on α-carbon of original hydroxyl group further de-shielded due to electronegative nature of introduced bromine (signal “b” in Figure A5). Furthermore, the transformation of end groups to bromine was supported by the appearance of C=O (1740 cm^{-1}) and disappearance of OH (3500 cm^{-1}) signals in FTIR (Figure A6).

After the SBMA monomer and Br-terminated PDMS macroinitiator were synthesized, amphiphilic additives were synthesized as shown in Scheme 2.3. The characteristic ^{1}H-NMR spectrum of a representative tri-block ABA additive is shown in Figure A7. The nearly disappeared peaks of the proton of the carbon-carbon double bond in SBMA at 5.5 – 6.5 ppm as well as broad peaks confirmed the polymerization of SBMA with the PDMS macroinitiator. The formation of additive is confirmed by FTIR data in Figure A8 that has indicative signals for both poly(SBMA) and PDMS segments: C=O at 1740 cm^{-1}, Si-O at 1164 cm^{-1}, SO_3 at 1060 cm^{-1}, and $^{+}NR_4$ at 960 cm^{-1}.

The synthesized additives were then added into the A4-20 SiPU system in 0.2 wt.%, 1 wt.%, and 5 wt.%. A series of contact angle measurements offered insights into the effect of the additives on surface properties. The water contact angles (WCAs) of all the coatings were dynamic in nature dropping as a function of time within a 15-minute period (Figure 2.2A). We attribute the change in WCAs to the interaction of the water droplet with hydrophilic poly (SBMA) chains that started to swell after being exposed to a “good” solvent,[41] facilitating the spreading of the water droplet. In contrast, the unmodified A4-20 control coating did not show any dynamic behavior as its WCA remained almost unchanged over the same time period. This observation supports the theory that amphiphilic additives self-stratified to the surface and modified the surface properties of the A4-20 system. Also, the data indicates that higher MW poly(SBMA) chains on an additive lead to a more dynamic surface. This trend can be observed among coatings containing additives 500-1k, 1k-1k, and 2.5k-1k (systems 3, 6, and 9), where poly(SBMA) MW increases from 500 $\bar{M}_n$ to 2500 $\bar{M}_n$. The higher amount of an additive in a system (i.e. 1 wt.% vs 5 w.%) results in a lower initial WCA and more change over time as exemplified for additive 1k-1k-1k (Figure A9). Methylene iodide contact angles (MICA) were slightly less dynamic as expected due to its nonpolar properties, but additive-containing systems still displayed changes in comparison to the A4-20 system (Figure 2.2A). Surface energy values for the coatings initially lay between 22-27 mN/m and increased

considerably after 15 minutes, unlike the A4-20 system. This increase correlates with the WCAs and MICAs; the higher the change in contact angle values over time, the higher the change in surface energy for a coating (Figure 2.2B). An unchanged or slightly marginal increase of surface energy for all the coatings was observed after 28 days of water aging, indicating that the coatings were stable, and the additives did not leach out (Figure 2.2B). Overall, the contact angle data suggested that the poly(SBMA)-based additives are accessible on the surface since the non-dynamic hydrophobic surface of SiPU A4 exhibits a dynamic characteristic after introduction of amphiphilic additives.

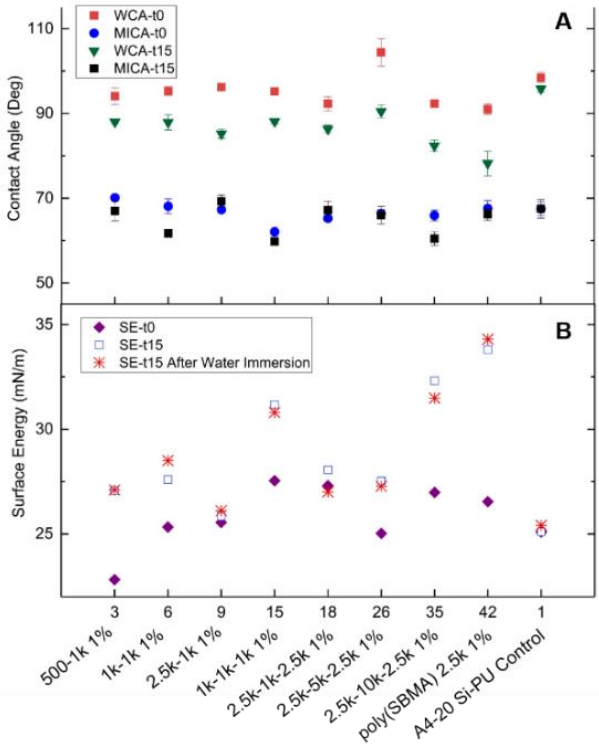

Figure 2.2. Contact angle data for selected additive-containing A4-20 systems. (A) Water contact angles (WCA) and methylene iodide contact angles (MICA) as a function of time at 0 minute and 15 minutes. (B) Surface energy (SE) values at 0 minute and 15 minutes before water immersion and at 15 minutes after 28 days water immersion, calculated by Owens-Wendt method utilizing average WCAs and MICAs for each coating. The X-axis is labeled to indicate both the coating number and additive type/composition.

All selected coatings were analyzed by AFM to determine morphology of the surfaces. Figure 2.3 and Figure A10 display phase and height AFM images, respectively. Theoretically, lighter areas with higher phase angles indicate the presence of softer materials like PDMS, while darker areas suggest the presence of harder materials like poly(SBMA) or polyurethane. To this effect, the AFM phase images for additive-containing coatings show very heterogeneous surfaces that possess many microdomains in

comparison to the A4-20 system. These images support the presence of the incorporated additives on the surface as is evident through differences in surface morphology compared to that of the A4-20 system. Coatings that contain 2.5k poly(SBMA) blocks as part of their incorporated additives show domains that are stretched throughout the surface, while coatings with shorter poly(SBMA) chains (500 and 1k $\bar{M}_n$) show domains that are smaller, localized and circular. We attempted to capture AFM images in the hydrated state but it was not feasible after many unsuccessful trials, while systems with poly(ethylene glycol) (PEG)-based moieties on the surface did not exhibit this problem. It is likely that the reason for the difficulties in taking hydrated AFM images occurs because the poly(SBMA) attracts up to 8 times more water molecules than PEG, indirectly suggesting SBMA-based domains are present on the surface as expected.

The surfaces of the coatings were also characterized with ATR-FTIR. The spectra for all of the additive-containing coatings were very similar. As an example, Figure 2.4 shows plots for coating 9 containing 2.5k-1k additive (blue line) and unmodified A4-20 system (black line). The definitive signal that indicated the presence of poly(SBMA)-containing additives on a surface was for SO_3 at 1060 cm^{-1} (Figure 2.4) in correlation with SBMA monomer FTIR (Figure A4). This conclusive SO_3 peak appeared as a stretching between the two well-recognized peaks of siloxane (Si-O-Si). The remaining characteristic peaks of A4-20 were observed for coating 9 as well including (NH) at 3350 cm^{-1}, due to the formation of urethane linkage by crosslinking of isocyanate and hydroxyl groups.

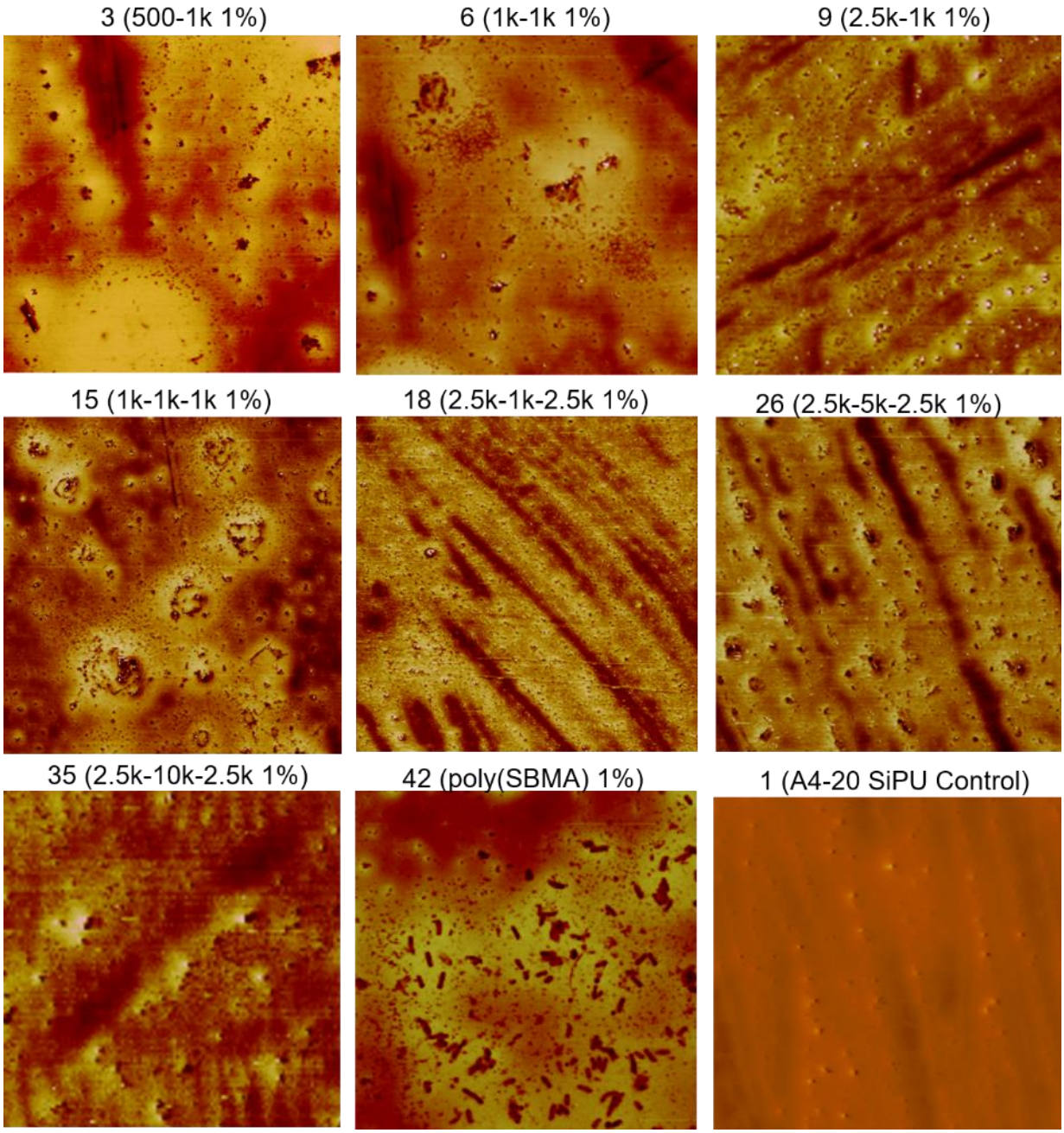

Figure 2.3. AFM phase images of A4-20 systems containing surface-modifying amphiphilic additives for a scan area of 50 µm x 50 µm. Each label reflects the coating number and its additive type and composition.

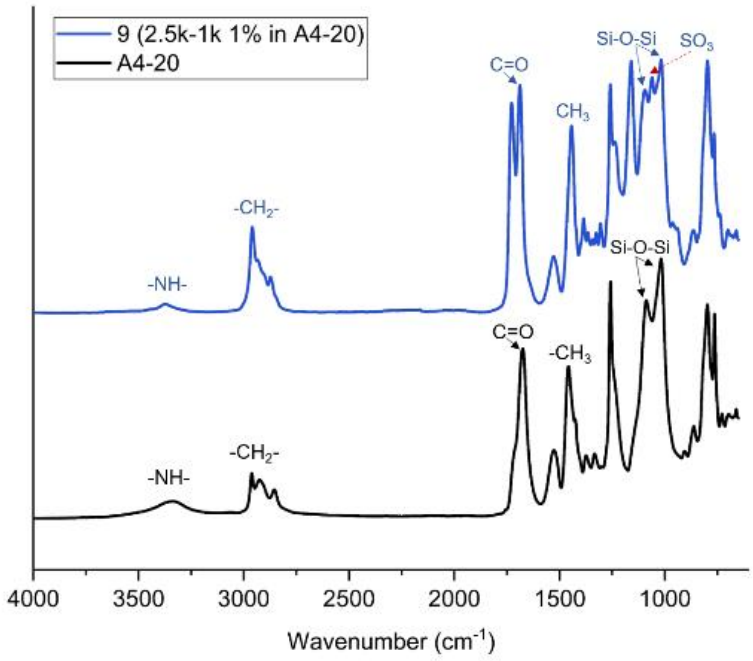

Figure 2.4. ATR-FTIR spectra for coating 9 containing 2.5k-1k additive at 1.0 wt. % (blue line) and A4-20 coating (black line).

All biological laboratory experiments to evaluate fouling-release performance of marine coatings, using five representative marine fouling organisms, were conducted after 28 days of water immersion. Before any experiments, the toxicity of coatings leachates was assessed to ensure coatings a were non-toxic (using *C. lytica* and *N. incerta*) as described elsewhere.[42] Briefly, overnight extracts of the coatings were gathered and inoculated with algae and bacteria. The growth of algae and bacteria was quantified after 48 hours by fluorescence of chlorophyll and crystal violet absorbance, respectively. The measurements were compared against positive and negative growth controls. Bioassay of leachates from the coatings was negative (data not reported), and the coatings underwent further evaluations.

Ulva linza has been widely reported as a common biofouling macroalga. Multiwall plates containing coating formulations were utilized to assess their performance against *U. linza* sporelings. Wettability of a surface influences growth and adhesion strength of *U. linza*.[43-45] The literature reports that *U. linza* generally adheres more strongly to moderately hydrophilic surfaces than on hydrophobic surfaces. Although all the amphiphilic surfaces were more hydrophilic than the unmodified A4-20 coating, the inclusion of the extremely hydrophilic zwitterions may have a destabilizing effect on the adhesive

bond. In order for the algal adhesive to form a bond with the substrate, water must be displaced from the joining surfaces and this can be difficult to achieve around extremely hydrophilic surface groups such as ones containing zwitterions. Fouling-release data for *U. linza* are presented in Figure 2.5, displaying growth (red color) and release at two water pressure levels (blue and green colors). Growth data supports the reported literature that the settlement of spores of *U. linza* is lower on amphiphilic surfaces (all additive-containing coatings). Also, the release performance for all modified coatings was superior to the original A4-20 coating, indicating that incorporation of poly(SBMA)-PDMS-based additives did contribute to better FR properties. A significant difference between the types of additives was not observed, disregarding the effect of number and size of polymeric blocks. All the modified SiPU A4 coatings also showed less initial settlement of *U. linza* than the commercial controls. Release of *U. linza* for all the modified coatings reached a comparable and desirable performance similar to the top-performing commercial controls such as T2 at 10 psi or IS 1100 at both 10 psi and 16 psi water pressures. Analysis of variance (ANOVA), considering the formulations as completely randomized design, indicated that all of the additive-containing SiPU A4 coatings (systems 3, 6, 9, 15, 18, 26, 35, and 42) had significantly improved fouling release for *U. linza* in comparison to A4-20 coating control system (comparison P-values <0.05, Tukey's method, Figure A11).

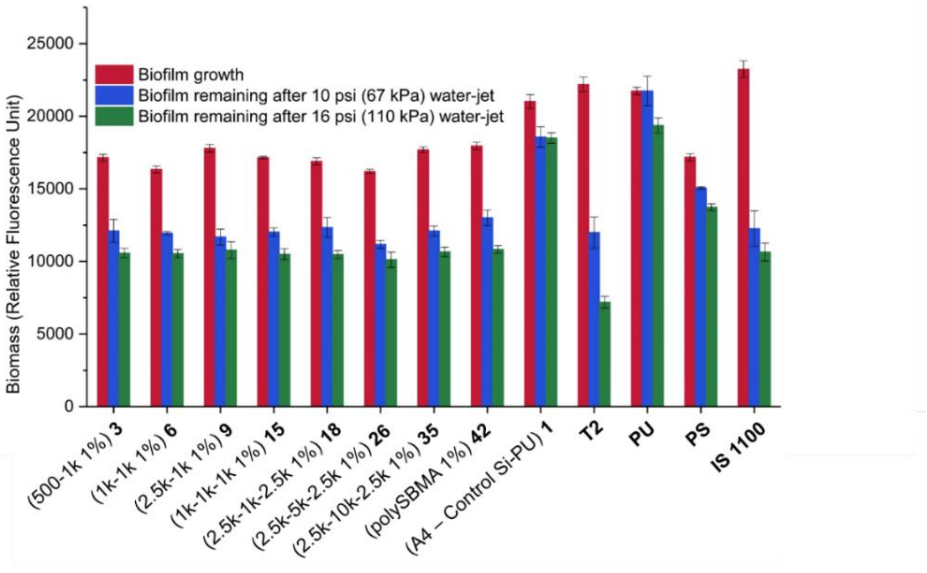

Figure 2.5. *U. linza* data for coatings, showing biofilm growth (red bars) and its biomass remaining after waterjet at 10 psi (blue bars) and 16 psi (green bars). The X-axis is labeled to name both experimental and control coatings; additive composition is mentioned for each experimental system as well.

Diatom (*N. incerta*) is a slime-forming microalga and has a higher attachment rate and strength of adhesion on hydrophobic surfaces than hydrophilic surfaces.[43, 46] The extent of diatom biofouling and its release appeared to be relatively unchanged for all formulated coatings after introducing the amphiphilic additives to the coating system (Figure 2.6). This can be attributed to the fact that all the coatings are intrinsically hydrophobic while a small amount of hydrophilicity is introduced to a surface. The release of diatoms from the modified surfaces was similar, or slightly less, than the control A4-20 system. The observed trend was that as the hydrophilic portion on an additive increased, the release of diatoms for modified coatings decreased slightly. Coatings with 500-1k, 1k-1k, 2.5k-1k, and 1k-1k-1k additives (systems 3, 6, 9, and 15) exhibited a performance comparable to several commercial systems including T2 and IS 700. However, fewer diatoms were released from coatings that contained additives 2.5k-5k-2.5k, 2.5k-10k-2.5k, and poly(SBMA) (systems 26, 35, and 42). The incorporated additives in coatings 26 and 35 contained higher content of PDMS (lower poly(SBMA) content); thus, it may be posited that the higher hydrophobicity of the additive repressed the desired hydrophilic effect as outlined in Table 2.2. To summarize, most of the amphiphilic additives did not have a detrimental impact on the FR performance of SiPU A4-20 system against *N. incerta*.

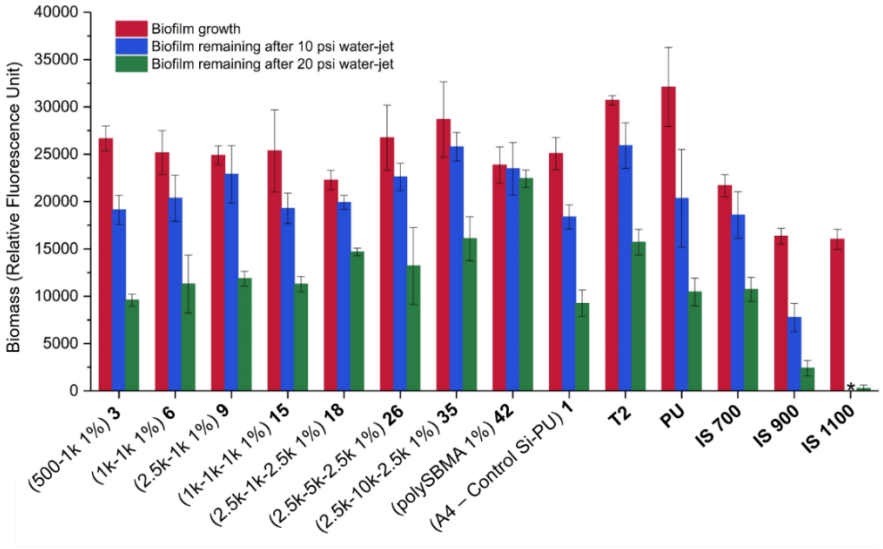

Figure 2.6. *N. incerta* data for coatings, showing biofilm growth (red bars) and its biomass remaining after waterjet at 10 psi (blue bars) and 20 psi (green bars). The X-axis is labeled to name both experimental and control coatings; additive composition is mentioned for each experimental system as well. *Data missing due to processing error.

C. lytica is another marine biofouling organism (bacterium) and known to attach to a wide range of hydrophilic and hydrophobic surfaces.[3] The collected data in Figure 2.7 indicates the extent of biofouling and release of the shortlisted systems. The growth of *C. lytica* film for coatings with additives composed of 1000 $\bar{M}_n$ PDMS in their backbone (coatings 3, 6, 9, 15, and 18) was similar to the A4-20 control system, while systems containing 5000 $\bar{M}_n$ or 10,000 $\bar{M}_n$ PDMS showed relatively higher biofouling. The *C. lytica* film grew considerably more on commercial controls such as IS 700, IS 900, and IS 1100. The release of biofilm at both 10 psi and 20 psi water-jetting pressure showed promising performance. At 10 psi, all modified coatings had a similar or slightly better performance (except coatings 35 and 42) than the A4-20 control system, while demonstrating a better performance than outlined commercial controls. Changing the water pressure to 20 psi did not increase the release of *C. lytica* from the surface of investigated coatings, except for IS 1100. These results suggest that the introduction of amphiphilic additives caused a slight improvement in the performance of A4-20 system (i.e. coatings 3, 6, 9, 15, and 18). This data implies that the ratio of hydrophilic and hydrophobic moieties on a surface affects fouling-release performance. The hydrophilic portion on an additive is a key factor for tuning the surfaces of a hydrophobic system.

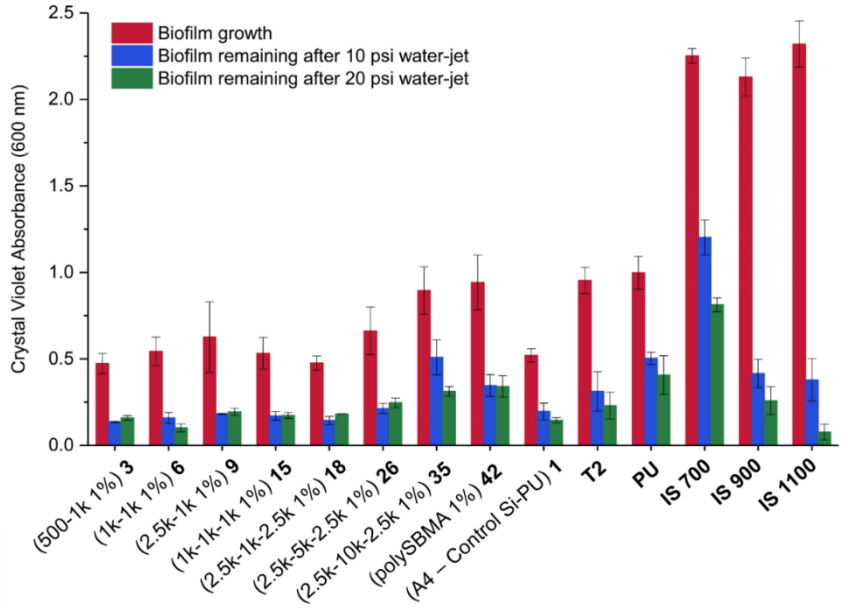

Figure 2.7. *C. lytica* data for coatings, showing biofilm growth (red bars) and its biomass remaining after waterjet at 10 psi (blue bars) and 20 psi (green bars). The X-axis is labeled to name both experimental and control coatings; additive composition is mentioned for each experimental system as well.

Macrofouling organisms such as barnacles and mussels are major marine biofouling organisms.[2, 47, 48] Different species of barnacle have different affinities for surfaces, limiting options to basic surface affinity rule.[3, 49-52] For example, *Amphibalanus amphitrite* prefers hydrophilic surfaces while it still can settle on hydrophobic surfaces.[37, 38, 53, 54] Adhesion strength of barnacles (measured by a push-off test) was substantially lower on the additive-containing coatings compared to the unmodified A4-20 system (Figure 2.8). Also, the number of reattached barnacles on a coating differed among systems. This is shown in Figure 2.8 as the ratio of the number of reattached barnacles over the six barnacles used for evaluation. Several systems such as coatings 6, 9, and 15 demonstrated similar performance to commercial coatings. No barnacle on any coatings was broken as a result of the push-off test. Coating 42, containing the poly(SBMA) additive, deterred the settlement of barnacles, outperforming all investigated and commercial coatings. Analysis of variance (ANOVA), considering the formulations in a completely randomized design, revealed that several systems (coatings 6, 9, 15, 26, 35, and 42) had significantly improved fouling-release properties for barnacles compared to the unmodified SiPU A4-20 control system (comparison P-values <0.05, Fisher's method, Figure A12). Furthermore, we noticed that the number of reattached barnacles on a surface differed with the ratio of hydrophilic content in the backbone of the amphiphilic additive (Figure 2.9). As the hydrophilic content of an additive increased, the number of reattached barnacles decreased. Once the additive was 100% hydrophilic (the poly (SBMA) additive), no barnacles re-attached. This trend may be a useful tool for designing coating systems that deter initial settlement of barnacles. The hydrophilic content of the additives is outlined in Table 2.2.

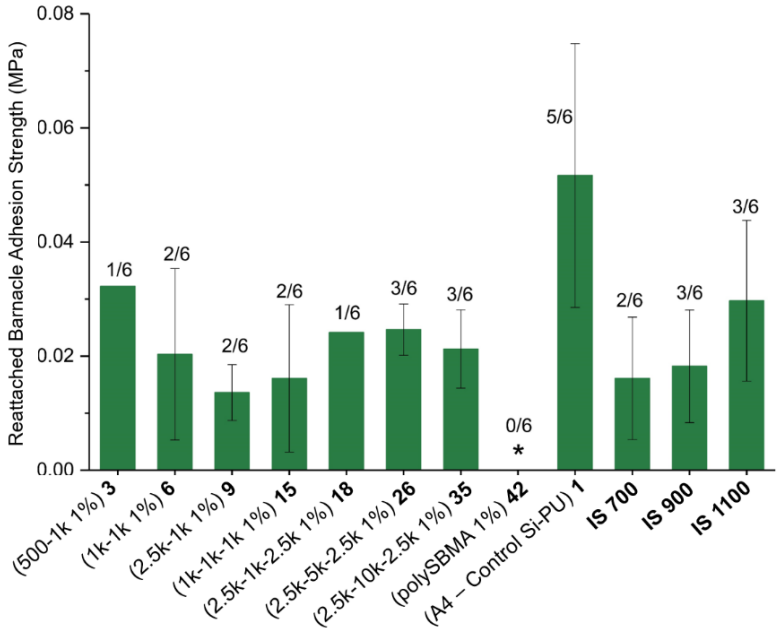

Figure 2.8. Reattached barnacle (*A. amphitrite*) adhesion strength data. Six barnacles were used for each reattachment study. The number of reattached barnacles out of six is labeled for each system as a ratio (* indicates no barnacle was attached). The X-axis is labeled to name both experimental and control coatings; additive composition is mentioned for each experimental system as well.

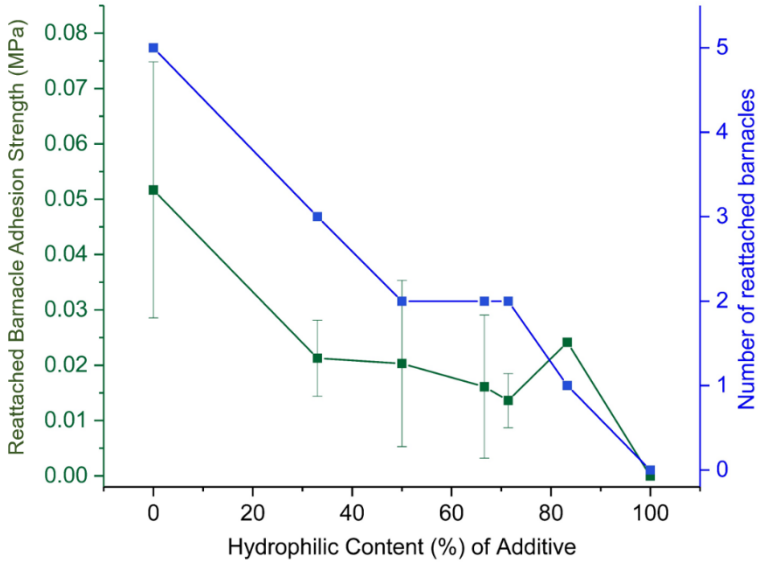

Figure 2.9. Relationship between number of reattached barnacles (*A. amphitrite*) and hydrophilic content of the additives. Blue line displays number of barnacles. Green line shows average adhesion strength based on the number of successfully reattached barnacles (with a standard deviation).

Adult mussels preferentially attach by byssus adhesion to hydrophilic over hydrophobic surfaces.[3, 16] All of the additive-modified and unmodified A4-20 coating systems prevented mussel attachment (Figure 2.10). This suggests that amphiphilic additives did not alter the already good performance of the A4-20 coating, indicating no detrimental effect. In comparison, the commercial coatings, IS 700 and IS 1100, did not perform as well.

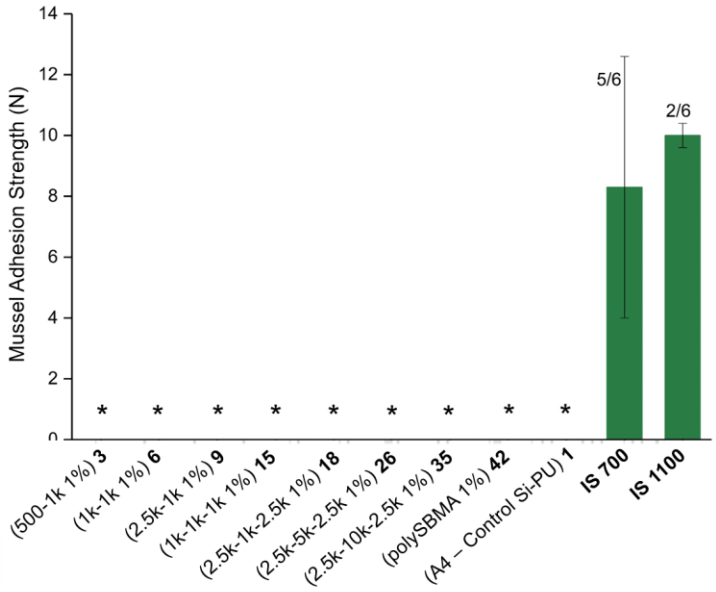

Figure 2.10. Marine mussel (*G. demissa*) adhesion strength data. Six mussels were used for each coating. The number of attached mussels out of six is labeled for each system as a ratio (* indicates no mussel was attached). Each bar shows the average adhesion strength based on the number of successfully attached mussels. The X-axis is labeled to name both experimental and control coatings; additive composition is mentioned for each experimental system as well.

Conclusions

A series of block copolymer amphiphilic additives containing poly(SBMA) and PDMS blocks were prepared utilizing the ARGET ATRP technique. The additives were incorporated into a hydrophobic marine siloxane-polyurethane coating system, known as A4-20. The objective was to attain an amphiphilic surface for the A4-20 system by introducing the synthesized additives that offer some portion of hydrophilicity. Contact angle experiments indicated that the amphiphilic additives were present on the surface and did not leach out of the coating after 28 days of water immersion, as the values remained unchanged. AFM images for additive-containing systems illustrated the presence of heterogeneous microdomains on the surface that were absent for the A4-20 coating due to its homogenous surface

composed of PDMS. Also, ATR-FTIR further substantiated the self-stratification of the amphiphilic additives into a surface by showing a signal for the SO_3 signature of poly(SBMA). In general, considering the performance of modified coatings versus A4-20 and commercial controls, it can be summarized that coatings with additives 1k-1k, 2.5k-1k, 1k-1k-1k, and 2.5k-1k-2.5k (systems 6, 9, 15, 18) offered a desirable performance against all assessed organisms including macroalgae (*U. linza*), bacteria (*C. lytica*), diatom (*N. incerta*), barnacle (*A. amphitrite*), and mussel (*G. demissa*). All the incorporated additives in these systems contained PDMS with a molecular weight of 1000 $\bar{M}_n$ and a hydrophilic ratio within ~50-80%. Thus, it can be concluded that several factors should be considered when amphiphilic additives based on poly(SBMA) and PDMS are being designed to improve the performance of hydrophobic marine coatings: 1) the use of a PDMS block with a molecular weight of 1000 $\bar{M}_n$ is in preference to higher molecular weights; 2) the hydrophilic portion should be between 50% and 80% to provide the desired amphiphilicity on a surface; and 3) the poly(SBMA) block size does not necessarily affect the effectiveness of an amphiphilic additive.

References

1. Callow, J. A.; Callow, M. E., Trends in the development of environmentally friendly fouling-resistant marine coatings. *Nature Communications* **2011,** *2* (1), 244-244.

2. Callow, M. E.; Callow, J. E., Marine biofouling: a sticky problem. *Biologist* **2002,** *49* (1), 10-14.

3. Lejars, M.; Margaillan, A.; Bressy, C., Fouling Release Coatings: A Nontoxic Alternative to Biocidal Antifouling Coatings. *Chemical Reviews* **2012,** *112* (8), 4347-4390.

4. Magin, C. M.; Cooper, S. P.; Brennan, A. B., Non-toxic antifouling strategies. *Materials Today* **2010,** *13* (4), 36-44.

5. Champ, M. A., A review of organotin regulatory strategies, pending actions, related costs and benefits. *Science of the total Environment* **2000,** *258* (1-2), 21-71.

6. Konstantinou, I. K.; Albanis, T. A., Worldwide occurrence and effects of antifouling paint booster biocides in the aquatic environment: a review. *Environment International* **2004,** *30* (2), 235-248.

7. Yebra, D. M.; Kiil, S.; Dam-Johansen, K., Antifouling technology—past, present and future steps towards efficient and environmentally friendly antifouling coatings. *Progress in Organic Coatings* **2004,** *50* (2), 75-104.

8. Sommer, S.; Ekin, A.; Webster, D. C.; Stafslien, S. J.; Daniels, J.; VanderWal, L. J.; Thompson, S. E. M.; Callow, M. E.; Callow, J. A., A preliminary study on the properties and fouling-release performance of siloxane–polyurethane coatings prepared from poly(dimethylsiloxane) (PDMS) macromers. *Biofouling* **2010,** *26* (8), 961-972.

9. Bodkhe, R. B.; Thompson, S. E. M.; Yehle, C.; Cilz, N.; Daniels, J.; Stafslien, S. J.; Callow, M. E.; Callow, J. A.; Webster, D. C., The effect of formulation variables on fouling-release performance of stratified siloxane–polyurethane coatings. *Journal of Coatings Technology and Research* **2012,** *9* (3), 235-249.

10. Pade, M.; Webster, D. C., Self-stratified siloxane-polyurethane fouling-release marine coating strategies: A review. In *Marine Coatings and Membranes*, Mittal, V., Ed. Central West Publishing: Australia, 2019; pp 1-36.

11. Iguerb, O.; Poleunis, C.; Mazéas, F.; Compère, C.; Bertrand, P., Antifouling properties of poly(methyl methacrylate) films grafted with poly(ethylene glycol) monoacrylate immersed in seawater. *Langmuir* **2008,** *24* (21), 12272-12281.

12. Heuberger, M.; Drobek, T.; Spencer, N. D., Interaction forces and morphology of a protein-resistant poly(ethylene glycol) layer. *Biophysical Journal* **2005,** *88* (1), 495-504.

13. Jeon, S. I.; Lee, J. H.; Andrade, J. D.; De Gennes, P. G., Protein—surface interactions in the presence of polyethylene oxide: I. Simplified theory. *Journal of Colloid and Interface Science* **1991,** *142* (1), 149-158.

14. Szleifer, I., Polymers and proteins: interactions at interfaces. *Current Opinion in Solid State and Materials Science* **1997,** *2* (3), 337-344.

15. Prime, K. L.; Whitesides, G. M. *Adsorption of proteins onto surfaces containing end-attached OHgo(ethylene oxide): A model system using self-assembled monolayers*; 1993; pp 10714-10721.

16. Galhenage, T. P.; Webster, D. C.; Moreira, A. M. S.; Burgett, R. J.; Stafslien, S. J.; Vanderwal, L.; Finlay, J. A.; Franco, S. C.; Clare, A. S., Poly(ethylene) glycol-modified, amphiphilic, siloxane–polyurethane coatings and their performance as fouling-release surfaces. *Journal of Coatings Technology and Research* **2017,** *14* (2), 307-322.

17. Zheng, Z.; Shengfu, C.; Yung Chang, a.; Jiang, S., Surface grafted sulfobetaine polymers via atom transfer radical polymerization as superlow fouling coatings. *Journal of Physical Chemistry B* **2006,** *110* (22), 10799-10804.

18. Jiang, S.; Cao, Z., Ultralow-fouling, functionalizable, and hydrolyzable zwitterionic materials and their derivatives for biological applications. *Advanced Materials* **2010,** *22* (9), 920-932.

19. Wu, C.-J.; Huang, C.-J.; Jiang, S.; Sheng, Y.-J.; Tsao, H.-K., Superhydrophilicity and spontaneous spreading on zwitterionic surfaces: carboxybetaine and sulfobetaine. *RSC Advances* **2016,** *6* (30), 24827-24834.

20. Zhang, Z.; Finlay, J. A.; Wang, L.; Gao, Y.; Callow, J. A.; Callow, M. E.; Jiang, S., Polysulfobetaine-grafted surfaces as environmentally benign ultralow fouling marine coatings. *Langmuir* **2009,** *25* (23), 13516-13521.

21. Dundua, A.; Franzka, S.; Ulbricht, M., Improved antifouling properties of polydimethylsiloxane films via formation of polysiloxane/polyzwitterion interpenetrating networks. *Macromolecular rapid communications* **2016,** *37* (24), 2030-2036.

22. Liu, P.; Huang, T.; Liu, P.; Shi, S.; Chen, Q.; Li, L.; Shen, J., Zwitterionic modification of polyurethane membranes for enhancing the anti-fouling property. *Journal of Colloid and Interface Science* **2016,** *480*, 91-101.

23. Bodkhe, R. B.; Stafslien, S. J.; Daniels, J.; Cilz, N.; Muelhberg, A. J.; Thompson, S. E. M.; Callow, M. E.; Callow, J. A.; Webster, D. C., Zwitterionic siloxane-polyurethane fouling-release coatings. *Progress in Organic Coatings* **2015,** *78*, 369-380.

24. Wu, J.; Chen, S., Investigation of the hydration of nonfouling material poly(ethylene glycol) by low-field nuclear magnetic resonance. *Langmuir* **2012,** *28* (4), 2137-2144.

25. Wu, J.; Lin, W.; Wang, Z.; Chen, S.; Chang, Y., Investigation of the hydration of nonfouling material poly(sulfobetaine methacrylate) by low-field nuclear magnetic resonance. *Langmuir* **2012,** *28* (19), 7436-7441.

26. Galhenage, T. P.; Hoffman, D.; Silbert, S. D.; Stafslien, S. J.; Daniels, J.; Miljkovic, T.; Finlay, J. A.; Franco, S. C.; Clare, A. S.; Nedved, B. T., Fouling-release performance of silicone oil-modified siloxane-polyurethane coatings. *ACS applied materials & interfaces* **2016,** *8* (42), 29025-29036.

27. Bodkhe, R. B.; Webster, D. C., Synthesis and characterization of novel polysiloxane based aba-type triblock copolymers using atrp. *e-Polymers* **2013,** *13* (1).

28. Jakubowski, K.; Min, K.; Matyjaszewski, K., Activators regenerated by electron transfer for atom transfer radical polymerization of styrene. *Macromolecules* **2006,** *39* (1), 39-45.

29. Min, K.; Gao, H.; Matyjaszewski, K., Use of ascorbic acid as reducing agent for synthesis of well-defined polymers by ARGET ATRP. *Macromolecules* **2007,** *40* (6), 1789-1791.

30. Owens, D. K.; Wendt, R. C., Estimation of the surface free energy of polymers. *Journal of Applied Polymer Science* **1969,** *13* (8), 1741-1747.

31. Cassé, F.; Stafslien, S. J.; Bahr, J. A.; Daniels, J.; Finlay, J. A.; Callow, J. A.; Callow, M. E., Combinatorial materials research applied to the development of new surface coatings V. Application of a spinning water-jet for the semi-high throughput assessment of the attachment strength of marine fouling algae. *Biofouling* **2007,** *23* (2), 121-130.

32. Utex, S. R. Z. J. A., The Culture Collection of Algae at the University of Texas at Austin. *J. Phycol. 1987 ₩ 23*, 1-47.

33. Stafslien, S. J.; Bahr, J. A.; Daniels, J. W.; Wal, L. V.; Nevins, J.; Smith, J.; Schiele, K.; Chisholm, B., Combinatorial materials research applied to the development of new surface coatings VI: An automated spinning water jet apparatus for the high-throughput characterization of fouling-release marine coatings. *Review of Scientific Instruments* **2007,** *78* (7), 072204-072204.

34. Stafslien, S.; Daniels, J.; Mayo, B.; Christianson, D.; Chisholm, B.; Ekin, A.; Webster, D.; Swain, G., Combinatorial materials research applied to the development of new surface coatings IV. A high-throughput bacterial biofilm retention and retraction assay for screening fouling-release performance of coatings. *Biofouling* **2007,** *23* (1), 45-54.

35. Callow, M. E.; Callow, J. A.; Conlan, S.; Clare, A. S., Efficacy testing of nonbiocidal and fouling-release coatings. John Wiley & Sons, Ltd: 2014; pp 291-316.

36. Cassé, F.; Ribeiro, E.; Ekin, A.; Webster, D. C.; Callow, J. A.; Callow, M. E., Laboratory screening of coating libraries for algal adhesion. *Biofouling* **2007,** *23* (4), 267-276.

37. Stafslien, S.; Daniels, J.; Bahr, J.; Chisholm, B.; Ekin, A.; Webster, D.; Orihuela, B.; Rittschof, D., An improved laboratory reattachment method for the rapid assessment of adult barnacle adhesion strength to fouling-release marine coatings. *Journal of Coatings Technology and Research* **2012,** *9* (6), 651-665.

38. Rittschof, D.; Orihuela, B.; Stafslien, S.; Daniels, J.; Christianson, D.; Chisholm, B.; Holm, E., Barnacle reattachment: a tool for studying barnacle adhesion. *Biofouling* **2008,** *24* (1), 1-9.

39. Kitano, H.; Mori, T.; Takeuchi, Y.; Tada, S.; Gemmei-Ide, M.; Yokoyama, Y.; Tanaka, M., Structure of water incorporated in sulfobetaine polymer films as studied by ATR-FTIR. *Macromolecular Bioscience* **2005,** *5* (4), 314-321.

40. Liaw, D.-J.; Lee, W.-F., Thermal degradation of poly[3-dimethyl(methylmethacryloylethyl) ammonium propanesulfonate]. *Journal of Applied Polymer Science* **1985,** *30* (12), 4697-4706.

41. Shultz, A. R.; Flory, P. J., Phase equilibria in polymer—solvent systems1,2. *Journal of the American Chemical Society* **1952,** *74* (19), 4760-4767.

42. Majumdar, P.; Crowley, E.; Htet, M.; Stafslien, S. J.; Daniels, J.; VanderWal, L.; Chisholm, B. J., Combinatorial materials research applied to the development of new surface coatings XV: An investigation of polysiloxane anti-fouling/fouling-release coatings containing tethered quaternary ammonium salt groups. *ACS Combinatorial Science* **2011,** *13* (3), 298-309.

43. Finlay, J. A.; Callow, M. E.; Ista, L. K.; Lopez, G. P.; Callow, J. A., The influence of surface wettability on the adhesion strength of settled spores of the green alga Enteromorpha and the diatom Amphora. *Integrative and Comparative Biology* **2002,** *42* (6), 1116-1122.

44. Callow, J. A.; Callow, M. E.; Ista, L. K.; Lopez, G.; Chaudhury, M. K., The influence of surface energy on the wetting behaviour of the spore adhesive of the marine alga Ulva linza (synonym Enteromorpha linza). *Journal of the Royal Society Interface* **2005,** *2* (4), 319-325.

45. Callow, M. E.; Callow, J. A.; Ista, L. K.; Coleman, S. E.; Nolasco, A. C.; López, G. P., Use of self-assembled monolayers of different wettabilities to study surface selection and primary adhesion processes of green algal (Enteromorpha) zoospores. *Applied Environmental Microbiology* **2000,** *66* (8), 3249-3254.

46. Holland, R.; Dugdale, T. M.; Wetherbee, R.; Brennan, A. B.; Finlay, J. A.; Callow, J. A.; Callow, M. E., Adhesion and motility of fouling diatoms on a silicone elastomer. *Biofouling* **2004,** *20* (6), 323-329.

47. Aldred, N.; Li, G.; Gao, Y.; Clare, A. S.; Jiang, S., Modulation of barnacle (balanus amphitrite darwin) cyprid settlement behavior by sulfobetaine and carboxybetaine methacrylate polymer coatings. *The Journal of Bioadhesion and Biofilm ResearchOnline) Journal* **2010,** *ISSN homepage*, 892-7014.

48. Tan, B. H.; Hussain, H.; Chaw, K. C.; Dickinson, G. H.; Gudipati, C. S.; Birch, W. R.; Teo, S. L. M.; He, C.; Liu, Y.; Davis, T. P., Barnacle repellent nanostructured surfaces formed by the self-assembly of amphiphilic block copolymers. **2009**.

49. Petrone, L.; Di Fino, A.; Aldred, N.; Sukkaew, P.; Ederth, T.; Clare, A. S.; Liedberg, B., Effects of surface charge and Gibbs surface energy on the settlement behaviour of barnacle cyprids (Balanus amphitrite). *Biofouling* **2011,** *27* (9), 1043-1055.

50. Di Fino, A.; Petrone, L.; Aldred, N.; Ederth, T.; Liedberg, B.; Clare, A. S., Correlation between surface chemistry and settlement behaviour in barnacle cyprids (Balanus improvisus). *Biofouling* **2014,** *30* (2), 143-152.

51. Gatley-Montross, C. M.; Finlay, J. A.; Aldred, N.; Cassady, H.; Destino, J. F.; Orihuela, B.; Hickner, M. A.; Clare, A. S.; Rittschof, D.; Holm, E. R., Multivariate analysis of attachment of biofouling organisms in response to material surface characteristics. *Biointerphases* **2017,** *12* (5), 051003.

52. Aldred, N.; Gatley-Montross, C. M.; Lang, M.; Detty, M. R.; Clare, A. S., Correlative assays of barnacle cyprid behaviour for the laboratory evaluation of antifouling coatings: a study of surface energy components. *Biofouling* **2019,** *35* (2), 159-172.

53. Huggett, M. J.; Nedved, B. T.; Hadfield, M. G., Effects of initial surface wettability on biofilm formation and subsequent settlement of Hydroides elegans. *Biofouling* **2009,** *25* (5), 387-399.

54. Rittschof, D.; Costlow, J. D., Bryozoan and barnacle settlement in relation to initial surface wettability: A comparison of laboratory and field studies. *Sci. Mar.* **1989,** *53* (2), 411-416.

CHAPTER 3. DETERMINATION OF CRITICAL AMPHIPHILIC CONCENTRATION: EFFECT OF AMPHIPHILICITY ON MARINE FOULING-RELEASE PERFORMANCE

Introduction

Marine biofouling, the unwanted settlement of marine organisms on the submerged surfaces in seawater, involves about 4000 marine organisms with a complex multi-stage process.[1] The process is non-linear, meaning biofouling can be initiated with either formation of a conditioning bacteria film or attachment of macrofoulants like barnacles or mussels.[2,3] The diversity of adhesion modes and surface affinities among the biofoulants further complicates this problem.[1, 2, 4] The negative impacts of biofouling are many, including but not limited to heightened economic costs, decreased drag, increased fuel consumption, and introduction of invasive species to new destinations.[3, 5] For example, the US Navy spends a $1 billion per year to maintain its ships due to biofouling.[3]

The complex and ambiguous nature of the biofouling problem has required the development of several protective systems throughout history. The initial historical approaches were based on copper alloys and lead sheaths, but these systems were eventually passed over due to the limited mineral resources and corrosion potential as steel ship hulls were introduced. In 1900s, coating systems containing tributyl-tin (TBT)-based moieties demonstrated superior performance; however, these paints were banned in the early 2000s globally because of their non-targeted toxicity on marine organisms and aquatic environments.[2, 6] Therefore, the focus for development of marine coatings has transitioned to non-toxic antifouling (AF) and fouling-release (FR) coatings.

The current AF systems utilize copper and zinc oxide biocides to contend biofouling. Despite the new alternatives are less toxic than tin, but they are not completely non-toxic. FR systems are another approach, known to be non-toxic and more environmentally friendly. While AF coatings function by leaching biocides to deter settlement of marine organisms, FR coatings perform by weakening adhesion of biofoulants on a surface that facilitates their release.[1, 2]

The traditional FR systems are composed of low-surface energy elastomeric materials such as polydimethylsiloxane (PDMS).[7, 2] Nevertheless, the low surface energy materials suffer from weak

adhesion and mechanical properties, resulting in a need for a tie-coat to improve adhesion.[2, 4] Self-stratifying siloxane-polyurethane (SiPU) FR coatings have been explored to address the limitations of the traditional FR systems[8, 9] SiPU and similar hydrophobic systems possess a desirable fouling-release performance against many organisms, but there are many other biofoulants that prefer a hydrophobic system for settlement or better adherence.[4, 10] As a result, amphiphilic coatings composed of both hydrophilic and hydrophobic segments have been investigated to contend with biofouling of a wider range among the 4000 organisms.[2, 11-15]

Despite literature indicates that amphiphilicity contributes to improved fouling-release performance, the extent of amphiphilicity that offers the needed performance is not clear to the best of our knowledge. The answer to this question is very complex as it depends on many factors such as type of the system, targeted aquatic environment, or targeted organisms, to mention a few.

In this work, our goal was to carry out some preliminary experiments of this unexplored area to determine the amount of amphiphilicity that results in desirable fouling-release performance, calling it the *critical amphiphilic content* (CAC). To answer this question and limit the number of variables in this study, we synthesized a novel amphiphilic additive based on only one molecular weight of PDMS and PEG (the optimum chain lengths were selected based on reported literature and our previous work), and the additive was incorporated at increasing amounts in a conventional polyurethane (PU) coating system, assessing the concentration of additive where the PU system converted to possess a desirable amphiphilic fouling-release surface (Figure 3.1). In this study, we discuss three aspects of the investigation: 1) Synthesis and characterization of the amphiphilic additive by Fourier transform infrared spectroscopy (FTIR) and isocyanate titration; 2) Surface characterization of additively-modified PU coatings (by contact angle measurements, ATR (attenuated total reflectance)-FTIR, X-ray photoelectron spectroscopy (XPS), and atomic force microscopy (AFM)) and mechanical evaluations (by coating-related tests); 3) Correlation of the fouling-release performance of the systems to the amount of the introduced additives and a comparison of the results with internal and commercial controls.

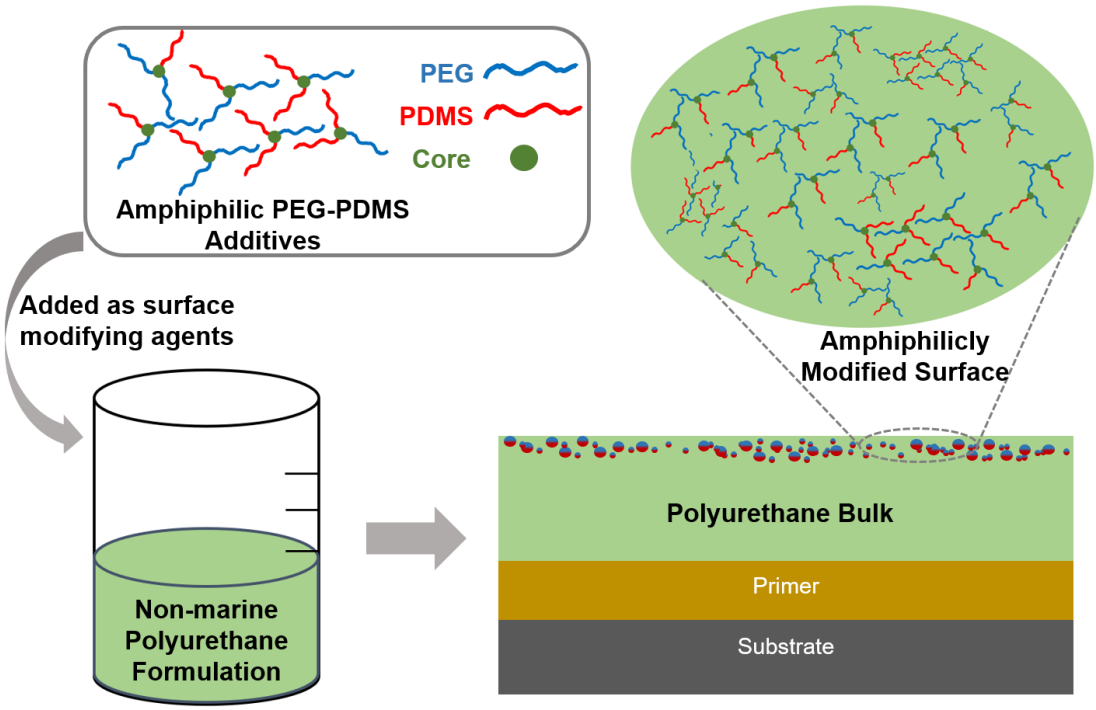

Figure 3.1. Illustration of amphiphilic PEG-PDMS additives as surface-modifying agents, changing the surface of non-marine PU coating system to a marine fouling-release surface.

Experimental

Materials

Isophorone diisocyanate (IPDI) polyisocyanate Desmodur Z4470 BA was provided by Covestro LLC. Monocarbinol-terminated polydimethylsiloxane (PDMS) with molecular weight of 10,000 $\bar{M}_n$ (MCR-C22) was purchased from Gelest, Inc. Poly(ethylene glycol) methyl ether (750 $\bar{M}_n$), ethyl-3-ethoxy propionate, methyl ethyl ketone (MEK), acetylacetone, methyl amyl ketone (MAK), and dibutyltin diacetate (DBTDAc) were purchased from Sigma Aldrich. Toluene and isopropanol were purchased from VWR. Following detailed description elsewhere, an acrylic polyol made of 80% butyl acrylate and 20% 2-hydroxyethyl acrylate was prepared via conventional free radical polymerization and diluted to 50% in toluene.[9]

AkzoNobel International Paint provided the commercial FR standards Intersleek® 700 (IS 700), Intersleek® 900 (IS 900), and Intersleek® 1100SR (IS 1100. Silicone elastomer, Silastic® T2 (T2) was provided by Dow Corning as another commercial standard. Hydrophobic A4-20 coating (A4-20), a siloxane-polyurethane system, was prepared as an internal control following the procedures described

elsewhere.[9] Amphiphilic T-10 coating, internal coating control, was prepared following the procedure elsewhere for a formulation that contained 10 wt.% PEG 750 $\bar{M}_n$ and PDMS 10,000 $\bar{M}_n$.[15] Aluminum panels (4" x 8" in., 0.64 mm thick, type A, alloy 3003 H14) and steel panels (3" x 6" in., 0.51 mm thick, type QD) were purchased from Q-lab and were sandblasted and primed with Intergard 264 (International Paint) using air-assisted spray application. Multi-well microtiter plates were modified using circular disks (1-inch diameter) of primed aluminum.

Experimental Design

An amphiphilic additive based on 10,000 $\bar{M}_n$ PDMS and 750 $\bar{M}_n$ PEG was synthesized and incorporated in a non-marine polyurethane coating system. These molecular weights have shown to offer a desirable fouling-release performance according to literature and previous (un)published work in our lab.[15, 16] This study was designed to evaluate only one variable factor: the amount of the amphiphilic additive in the PU coating system. The additive was added in varying amounts to the system, ranging from 10 wt.% up to 40 wt.% (the highest amount that could be added before the PU film lost its integrity in response to mechanical coating tests). Thus, a total of six formulations were prepared as outlined in Table 3.1. The table outlines amount of additive in each system and wt.% of each PEG and PDMS in the solid content of the final formulation. It should be noted that wt.% of PEG and PDMS as part of the synthesized additive is 41.37 wt.% for each (further details in the following section about synthesis of the additive),thus this value is used to calculate the final weight content of these moieties in a formulation.

Table 3.1. Coating compositions

Formulation	Additive Amount (wt. %)	PDMS Wt.%	PEG Wt.%
F0	0	0	0
F10	10	4	4
F20	20	8	8
F25	25	10	10
F30	30	12	12
F40	40	17	17
F50*	50	21	21

*F50 was not included in surface and biological assays characterizations as the coating with this concentration lacked the desired mechanical integrity.

Control and Standard Coatings

Commercial standards were prepared following the respective manufacturers' guidelines. Internal control SiPU (A4) was prepared following the procedure outlined in a previous study.[9] T-10 coating, internal amphiphilic control, containing 10,000 $\bar{M}_n$ PDMS and 750 $\bar{M}_n$ PEG prepolymer was prepared following directions elsewhere.[15] Similar to experimental coatings all control and standards were also prepared on 4" x 8" primed aluminum panels and multi-well plates. Table 3.2 contains detailed descriptions of the control and standard coatings used for this study.

Table 3.2. List of control coatings

Control Name	Control ID	Description
SiPU A4-20	A4	Internal SiPU FR Control
Amphiphilic SiPU	T-10	Internal Amphiphilic SiPU Control
Commercial Polyurethane	PU	Pure Polyurethane Standard
Commercial Polystyrene	PS	Pure Polystyrene Standard (used for *U. linza* test)
Dow® T2	T2	Silicone Elastomer Standard
Intersleek® 700	IS 700	Intersleek® Commercial FR Standard
Intersleek® 900	IS 900	Intersleek® Commercial FR Standard
Intersleek® 1100	IS 1100	Intersleek® Commercial FR Standard

Synthesis of Amphiphilic Additives

The amphiphilic additive was synthesized by reacting hydroxyl-terminated PEG and PDMS chains with the polyisocyanate IPDI trimer Desmodur Z4470 (Scheme 3.1). The ratio of NCO groups to the combined OH groups was 1:1. Isocyanate groups were fully converted to urethane linkages by attachment of PEG and PDMS chains. PEG and PDMS were added in equal weight ratios to meet the required one molar ratio.

To synthesize the amphiphilic additive (AmpAdd), PEG 750 $\bar{M}_n$ (1.00 g) was diluted in toluene (3.00 g) in a 25-mL flask. PDMS 10,000 $\bar{M}_n$ (1.00 g) was added to the flask and mixed robustly with vortex for 2 minutes. IPDI trimer resin (0.56 g) and DBTDAc catalyst solution (1% by wt. in MAK) (0.128 g) were then added to the flask. The reaction was carried at 80 °C for 2 hours. As another method, the reaction could also be completed at ambient conditions for 24 hours. A reflux condenser was used when heat was

applied. The flask was equipped with a magnetic stirrer, nitrogen inlet, and temperature controller. In theory, the synthesized prepolymer contained 41.37 wt.% PEG and 41.37 wt.% PDMS.

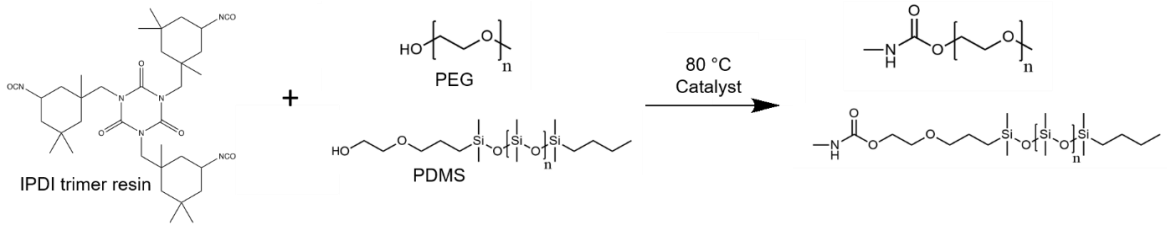

Scheme 3.1. Synthesis of amphiphilic additive based on IPDI trimer containing PDMS 10,000 $\bar{M}_n$ and PEG 750 $\bar{M}_n$.

Isocyanate Titrations

Isocyanate titration was used to confirm the complete conversion of the isocyanate groups after the synthesis of the additive. An additive sample (0.3-0.5 g) was weighed in an Erlenmeyer flask and diluted with isopropanol. Then, 25 mL of 0.1 N dibutyl amine solution and additional 25 mL isopropanol were added to the flask, and the mixture was stirred for 15 minutes. Several drops (3-5 drops) of bromophenol blue indicator were added to the flask. The content of the flask was titrated using a standardized 0.1 N hydrochloric acid until the endpoint blue to yellow was observed. A blank prepared only with 25 mL of dibutyl amine solution was also titrated following the same procedure. The recorded amount of hydrochloric acid for both titrations was used to calculate the amount of isocyanate remaining.

Percent Solids Determination

The non-volatile content of the additive was determined following ASTM D2369. In general, a weighed empty aluminum pan was filled with additive sample (1-2 g). Isopropyl alcohol was used to cover the sample. The pan was placed in an oven at 120 °C for 1 hour. After removal from the oven, the pan was weighed again to determine the percent solids. Three replicates were recorded.

Fourier Transform Infrared Spectroscopy

Fourier transform infrared (FTIR) spectroscopy was used to characterize the additive, using a Thermo Scientific Nicolet 8700 FTIR. The additive was applied as a thin layer on a potassium bromide (KBr) plate to collect the spectrum.

Coatings Preparation

All coating formulations were prepared similarly, except the amount of added additive varied. To prepare the unmodified polyurethane F0 formulation, acrylic polyol (8.00 g; 50% solid) and acetylacetone

(0.62 g) (potlife extender) were added in a vial and stirred ambiently for 24 hours. IPDI isocyanate trimer Desmodur Z4470 BA resin (2.96 g) and DBTDAs catalyst solution (0.25 g) were added to the vial, and the mixture was stirred for another hour before applying it.

To prepare an additive-modified polyurethane formulation, F25 for example here, acrylic polyol (8.00 g; 50% solid), acetylacetone (0.62 g) (potlife extender), and the 10kPDMS-750PEG additive (4.18 g; 60% solid) were added to a vial and stirred ambiently for 24 hours. IPDI isocyanate trimer Desmodur Z4470 BA resin (2.96 g) and DBTDAs catalyst solution (0.25 g) were added to the vial, and the mixture was stirred for another hour before applying it.

Coating formulations were applied on primed 8’ x 4’ aluminum and 6’ x 3’ steel panels using a wire-round drawdown bar with a film thickness of 80 µm. All coatings were allowed to cure ambiently for 24 hours, followed by oven curing at 80 °C for 45 minutes. Coatings were cut out in circular shapes and glued to 24-well plates for biological assays test.

Surface Characterization

A Kruss® DSA 100 (Drop Shape Analyzer) was utilized to measure the surface wettability and surface energy for the coatings. Water and diiodomethane contact angles were measured in 3 replicates for each sample. For each replicate, the static contact angle was measured over 9 minutes. Surface energy for each surface was calculated using the Owens-Wendt method.[17] Slip angle, advancing and receding water contact angles for surface were evaluated using a tilting stage where a 25-µL water droplet was viewed on a coating surface (tilted at 10°/min). The measured angles and surface energies were calculated using Kruss® Advance software.

Attenuated total reflectance Fourier transform infrared spectroscopy (ATR-FTIR) was used to characterize the surfaces of the coatings. A Bruker Vertex 70 with Harrick’s ATR™ accessory using a hemispherical Ge crystal was utilized to collect ATR-FTIR spectra for a coating.

A Thermo Scientific™ K-Alpha™ X-ray photoelectron spectroscopy (XPS) was used to determine the elemental composition of the coatings. The instrument was equipped with a monochromatic Al K_α (1486.68 eV) X-ray source and Ar^+ ion source (up to 4000 eV). Depth profiling of a coating was evaluated using argon ion with 30 etch cycles. For each etch cycle, the ion beam was set to 1,000 eV Monatomic Mode with low current and 30 s etch time. After each etching cycle, survey spectra in 5

replicates were collected at low resolution with a constant analyzer pass energy of 200 eV for a total of 20 ms. For each run, photoemission lines for C1s, N1s, O1s, and Si2p were observed. Spectra were collected at an angle normal to the surface (90°) of a 400-µm area. The chamber pressure was maintained below 1.5 x 10^{-7} torr and samples were analyzed at ambient temperature. Atomic concentrations were quantified by the instrument's software as a representation of the atomic intensities as a percentage of the total intensity of all elements.

Atomic force microscopy (AFM) was utilized to receive insights about the surface topography of the studied coatings. A Dimension 3100 microscope with Nanoscope controller scanned the surface of experimental coatings, collecting images on a sample area of 100 µm x 100 µm in the tapping mode. The experiment condition was in air under ambient conditions, using a silicon probe with a spring constant of 0.1-0.6 N/m and resonant frequency of 15-39 kHz. For each surface, three replicates at varying spots were collected to ensure consistency and accuracy of the data.

Water Aging

All the prepared coatings were pre-leached for 28 days in running tap water. The water tanks were equipped to automatically fill and empty every 4 hours. Water aging of the coatings is carried out to meet two objectives: 1) To leach out any impurities that may deviate with fouling-release assessments; 2) To determine if there are any surface rearrangements of the coatings or the additives leach out. All biological laboratory assays were carried out after the pre-leaching water aging process was completed.

Biological Laboratory Assays

Bacterial (*Cellulophaga lytica*) Biofilm Adhesion

Fouling-release properties towards bacteria was evaluated using retention and adhesion assays described previously.[18, 19] Briefly, a solution of the marine bacterium *Cellulophaga lytica* at 10^7 cells/mL concentration in artificial seawater (ASW) containing 0.5 g/L peptone and 0.1g/L yeast extract was deposited into 24-well plates (1 mL/well). The plates were then incubated statically at 28°C for 24 hours. The ASW growth medium was then removed and the coatings were subjected to water-jet treatments. The first column of each coating was not treated and served as the initial amount of bacterial biofilm growth. The second and third columns were subjected to water-jetting at 10 psi and 20 psi, respectively, for 5 seconds. Following water-jet treatments, the coating surfaces were stained with 0.5 mL of a crystal

violet solution (0.3 wt. % in deionized water) for 15 minutes and then rinsed three times with deionized water. After 1 hour of drying at ambient laboratory conditions, the crystal violet dye was extracted from the coating surfaces by adding 0.5 mL of 33% acetic acid solution for 15 minutes. The resulting eluates were transferred to a 96-well plate (0.15 mL/coating replicate) and subjected to absorbance measurements at 600 nm wavelength using a multi-well plate spectrophotometer. The absorbance values were directly proportional to the amount of bacterial biofilm present on coating surfaces before and after water-jetting treatments. Percent removal of bacterial biofilm was quantified by comparing the mean absorbance values of the non-jetted and water-jetted coating surfaces.[33]

Growth and Release of Microalgae (*Navicula incerta*)

Laboratory biological assay diatom (*Navicula incerta*) was conducted at NDSU following a similar procedure described previously.[1, 20, 21] Briefly, a suspension with 4×10^5 cells/mL of *N. incerta* (adjusted to 0.03 OD at absorbance 660 nm) in Guillard's F/2 medium was deposited into each well (1 mL per well) and cell attachment was stimulated by static incubation for 2 hours under ambient conditions in the dark. Coating surfaces were then subjected to water-jet treatments.[19] First column of wells was not water-jetted so that initial cell attachment could be determined and the next two-column of wells were water-jetted at 10 psi and 20 psi, respectively, for 10 seconds. Microalgae biomass was quantified by extracting chlorophyll using 0.5 mL of DMSO and measuring fluorescence of the transferred extracts at an excitation wavelength of 360 nm and emission wavelength at 670 nm. The relative fluorescence (RFU) measured from the extracts was considered to be directly proportional to the biomass remaining on the coating surfaces after water-jetting. Percent removal of attached microalgae was determined using relative fluorescence of non-jetted and water-jetted wells.

Growth and Release of Macroalgae (*Ulva linza*)

A set of multiwall plates was sent to Newcastle University, following water-immersion for 28 days, to evaluate fouling-release performance of coatings against *U. linza*. The detailed description about the assessment can be found elsewhere.[20] Briefly, after leaching collection, all multiwall plates were equilibrated in 0.22 µm filtered artificial seawater for 2 hours at Newcastle. To each well, 1 mL spores of *U. linza* suspension was added, adjusted to 3.3×10^5 spores/mL (0.05 OD at absorbance 660 nm) in double strength enriched seawater. Spores settled on the discs were grown for 7 days inside an

illuminated incubator at 18°C with a 16:8 light: dark cycle (photon flux density 45 μmol.m^{-2}.s^{-1}). There was no washing to remove unsettled spores after settlement. After 7 days, the biomass generated was assessed from a single row of wells (6) from each plate. The chlorophyll was extracted by adding 1 mL DMSO to each water-pressured well (water pressure of 67 kPa) and followed by measuring the fluorescence at 360 nm excitation and 670 nm emission. Fluorescence is directly proportional to the biomass present on each coating surface. The removal of *U. linza* at each pressure was compared with the unsprayed wells that were used to determine initial growth.

Mechanical Tests

Stability, adhesion, strength, and flexibility are important properties that are desired for organic coatings. Double rub test, according to ASTM D 5402, evaluated the resistance of coatings against solvents. A hammer (0.75 kg) with three-fold cheesecloth wrapped around its head was soaked in MEK or 3.5 wt.% NaCl water solution and rubbed against the coating. The head of hammer was rewet after each 25 double rubs. The number of double rubs was noted when mars were observed on the surface of coatings.

Impact test, according to ASTM D 2794, was used to assess strength of coatings using a Gardner impact tester. The maximum drop height was 43 inches with a weight of 4 pounds. Coated steel panels were placed in testing location, and the load in varying heights was dropped on the coating. The results were recorded in inch-pounds (in-lb). Crazing or loss of adhesion from substrate were observed as a failure point. Coatings that did not fail were reported having an impact strength of >172 in-lb. The test can be carried out in two ways: front and reverse. Front impact directly drops the weight on a coating film, while reverse impact drops the weight on back of a substrate that has a coating film on its other side.

Crosshatch adhesion test, according to ASTM D 3359, assessed the adhesion of coating to substrates by applying and removing pressure-sensitive tape over cuts made in the film. The results were reported on a scale of 0B to 5B, while 0B indicates complete removal of the coating and 5B indicates no removal of the coatings from the substrate as a result of this test.

Conical mandrel test, according to ASTM D 522, was used to determine the flexibility of the coatings on substrates. In principle, ideal flexible coatings should not have any cracks when undergoing

the bending test. The results of flexibility were reported as the length of a formed crack in cm on the coating during the bending test.

Results and Discussions

Amphiphilic coatings have been recognized as a promising path to combat biofouling issues. Despite such systems having been extensively investigated, there is a lack of knowledge about these systems that range from mechanism of performance to design parameters. To this effect, we designed a study to determine if there is a concentration of amphiphilic moieties when a system attains desirable fouling-release performance and then additional amounts of such moieties do not improve the performance. In this study, the AmpAdd additive based on 10,000 $\bar{M}_n$ PDMS and 750 $\bar{M}_n$ was added at increasing amounts to a polyurethane coating system (developed internally with IPDI isocyanate trimer and acrylic polyol) and the relationship between amphiphilicity concentration and fouling-release performance was established accordingly.

The amphiphilic additive, AmpAdd, was prepared by reacting mono-hydroxyl-terminated PEG (750 $\bar{M}_n$) and PDMS (10,000 $\bar{M}_n$) chains with an IPDI isocyanate trimer resin. The complete conversion of the isocyanate groups to urethane linkage was confirmed with FTIR and isocyanate titrations. A FTIR spectrum of the AmpAdd (Figure 3.2) showed the absence of the isocyanate peak at 2250 cm^{-1} and stretching for secondary amine of the formed urethane linkage at 3350 cm^{-1}. Additionally, the appearance of overlapping peaks for PDMS (Si-O-Si) at 1030 cm^{-1} and PEG (C-O-C) at 1105 cm^{-1} confirmed the attachment of amphiphilic chains on the additive. Furthermore, isocyanate titrations validated the complete conversion of the isocyanate groups since the titrations indicated the presence of no isocyanate.

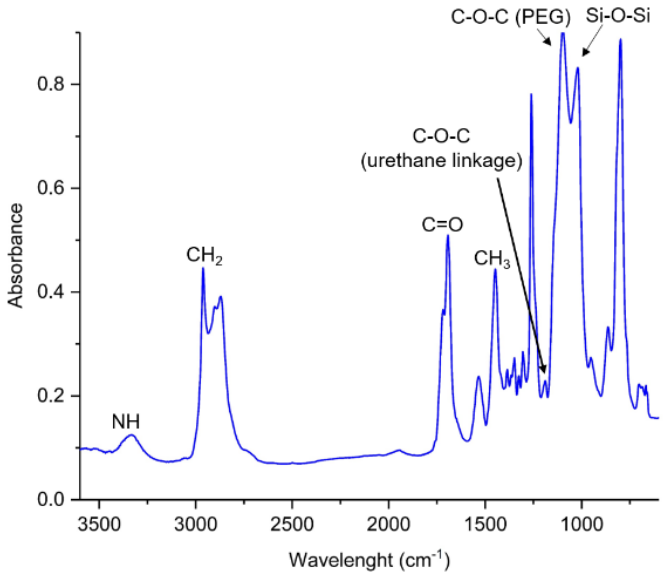

Figure 3.2. FTIR spectrum for the amphiphilic additive based on IPDI trimer containing PDMS 10,000 $\bar{M}_n$ and PEG 750 $\bar{M}_n$.

Surface characterization of the coatings was completed with ATR-FTIR, contact angle measurements, XPS, and AFM. ATR-FTIR was used to assess the presence of the chemical moieties on the surfaces of coatings. Although the spectrum for all the modified PU coatings was similar generally, the only difference was changes to the intensities of peaks associated with PEG at 1030 cm^{-1} and PDMS at 1105 cm^{-1} (Figure 3.3 – red and green highlights, respectively) in respect to ether peak of the urethane linkage (Figure 3.3 – yellow highlight). Also, an overlapped broad stretching for hydroxyl group (due to urethane linkage from the AmpAdd and crosslinking reaction) is present at almost 3350 cm^{-1}. This data indicates the modified PU surfaces are amphiphilic while the unmodified PU lacks such property. Overall, as more amphiphilic additive was present in a system, the intensities for PEG and PDMS peaks increased accordingly as well, signaling a direct correlation between the availability of amphiphilic moieties on the surfaces with the amount of added additive.

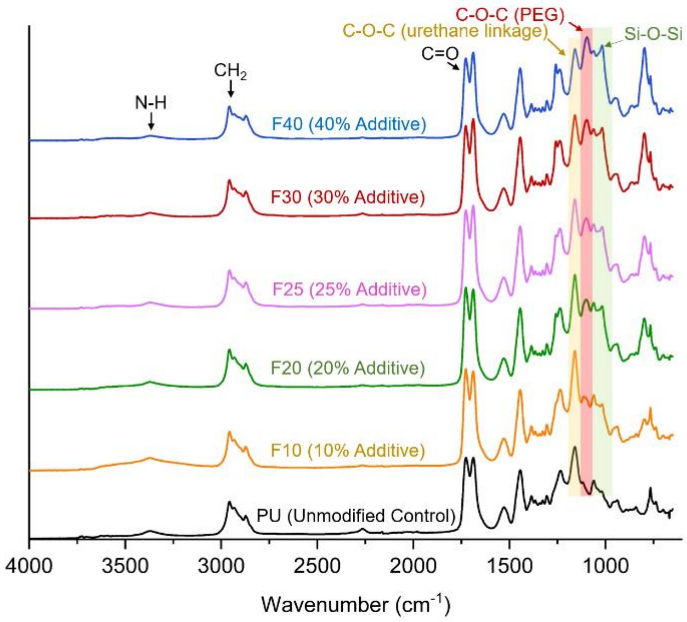

Figure 3.3. ATR-FTIR of the surface of unmodified and modified polyurethane coatings. The spectrum of each coating is labeled to reflect its ID number and amount of added AmpAdd additive, ranging from 0 wt.% to 40 wt.%.

Contact angle measurements were utilized as another method to characterize the surfaces. The contact angle data were collected as static measurements over time and dynamic measurements as a function of tilting stage. The addition of the additives resulted in a dynamic surface, meaning the contact angles for both water and diiodomethane dropped as a function of time (Figure 3.4A). This dynamic nature is attributed to the amphiphilicity of the surfaces where the hydrophilic domains cause the water droplet to spread as they are swollen. The observed dynamic behavior for the additively modified PU coatings was similar to the T-10 amphiphilic control coating, while the hydrophobic A4 system did not possess such feature (due to lack of hydrophilic domains). The change in values was more prominent for water contact angles (WCA) than diiodomethane contact angles (MICA). However, the extent of changes in contact angle values was similar regardless of the amount of additive. Additionally, as the amount of AmpAdd was increased for the modified PU coatings, the initial water contact angle decreased until a plateau was observed for coatings with 25 wt.% or higher amount of the additive (formulations F25, F30, F40). This trend is attributed to the increasing amount of hydrophilic moieties on the surface due to AmpAdd. When the concentration of these moieties on the surface was saturated, the excessive amount

did not greatly impact the surface, displaying the leveled trend. Also, the contact angles of modified PU coatings were generally lower than that of the control coatings, which can be related to the addition of AmpAdd. Surface energy for the experimental and control coatings was calculated using WCA and MICA values (Figure 3.4B). The surface energy values for modified PU coatings was between 40-45 mN/m initially and increased as a function of time, showing a dynamic nature similar to contact angle values. Mostly, the greatest change was observed for coatings with higher amount of AmpAdd (coatings F25 and F40). The surface energy values for the modified coatings were different from the control coatings at 25-30 mN/m. The slip angle (water droplet roll-off angle) for the studied coatings showed a declining trend as the amount of the AmpAdd increased for the systems (Figure 3.4C). Similar to the WCA values, the slip angle becomes relatively constant once it reaches a 25 wt.% concentration of AmpAdd. In comparison, hydrophobic A4 shows considerably higher slip angle while the amphiphilic T-10 displays a value within the range of the assessed coatings. Furthermore, the tilting experiment provided advancing contact angle (Adv CA) and receding contact angle (Rec CA) values, and a trend similar to slip angle was observed (Figure 3.4D). The hysteresis (difference between Adv CA and Rec CA) was higher for coatings F10 and F20 than coatings with higher amounts of AmpAdd in their composition (coatings F25, F30, F40). The lower the hysteresis, the smoother a surface is, and it typically has a better ability to roll off objects from its surface. Relating these results to the control coatings, the A4 system shows a hysteresis like low-containing AmpAdd systems (i.e. F20) and T-10 shows a similar value to high-containing AmpAdd systems (i.e. F30). Contact angle measurements for coatings after 28 days of water aging demonstrated an increase which was relatable to T-10 control system (Figure 3.5). This change was attributed to rearrangement of the surface as hydrophilic and hydrophobic domains interacted with water and to the probability that some amount of AmpAdd may have leached out.

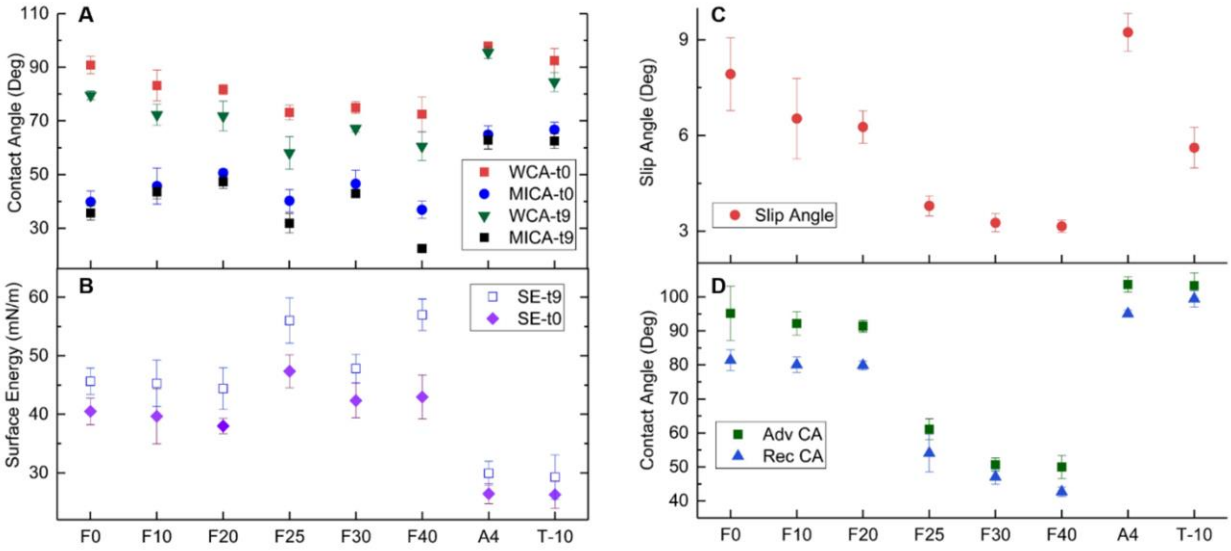

Figure 3.4. Contact angle and surface energy data for coatings. (A) Water contact angles (WCA) and methylene iodide contact angles (MICA) as a function of time at 0 minutes and 9 minutes; (B) Surface energy (SE) of coatings at 0 minute and 9 minutes, calculated by the Owens-Wendt method utilizing the average WCAs and MICAs for each coating; (C) Slip angle of coatings where a water droplet starts to roll off; (D) Advancing contact angle (Adv CA) and receding contact angle (Rec CA) data, measured by tilting method. A4 and T-10 are the internal coatings for comparison.

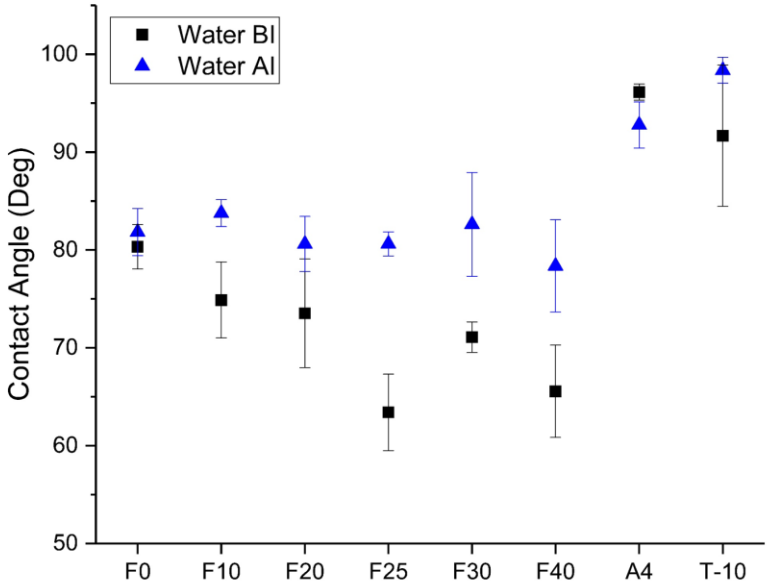

Figure 3.5. Water contact angle data for coatings before immersion (BI) and after immersion (AI) in water for 28 days.

XPS was utilized to quantify the elemental compositions of materials on the surface and as a function of -depth of the coatings. As expected, the results showed that the AmpAdd additive self-stratified onto the surface. As AmpAdd self-stratified, it was observed that there is a higher concentration of Si than C on the surface while this trend was reversed throughout the bulk of a coating (Figure 3.6). The XPS depth profiling analysis implies that the concentration of the amphiphilic moieties on the surface is directly related to the amount of incorporated AmpAdd. The initial Si concentration was higher (C concentration was lower) as the amount of AmpAdd was higher (except for F10). The data indicated the concentration of Si rapidly declined as a function of thickness for F10 coating and plateaued at ~2%. A less severe decreasing trend was also noticed for coatings F20, F25, and F30, and all these systems eventually leveled at a Si concentration around 5-6%. However, the decreasing trend was not observed for coating F40, indicating the concentration of Si atom was almost uniform until the assessed thickness of 36 nm (Figure 3.6B). The XPS data for C atom of these coatings showed an increasing trend for coatings F10, F20, F25, and F30 that is in confirmation with the decreasing Si atom trend for each system. The increasing C atom trend was not observed for coating F40 which was in correlation with the unchanging Si atom concentration of this formulation. As expected, the unmodified PU system showed uniform concentration of C atom throughout the coating while there was no Si in its composition. The XPS data confirms that the amount of AmpAdd has a direct effect on the composition of the system both in surface and bulk.

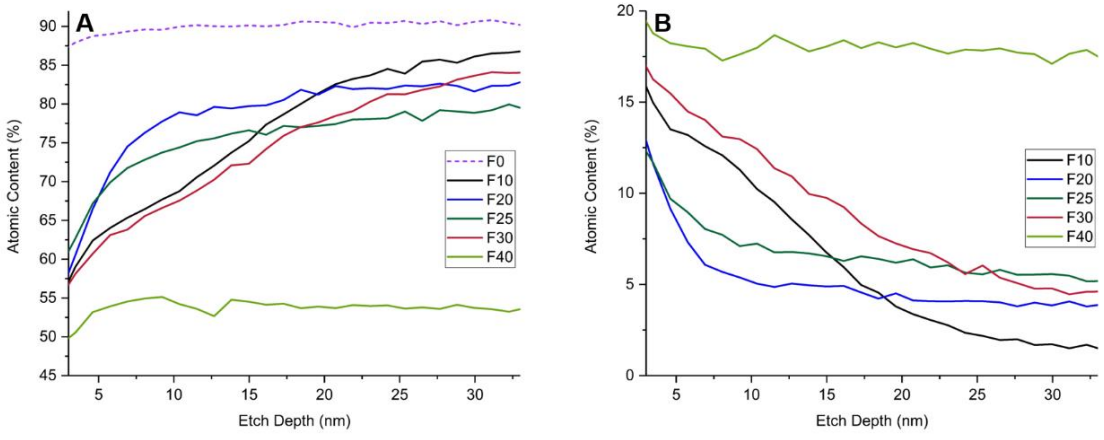

Figure 3.6. XPS data for unmodified and modified PU coatings. (A) XPS depth profiling data for carbon C1s atom; (B) XPS depth profiling data for silicon Si2p atom.

AFM was employed to capture the morphology of the developed surfaces. The general notation is that soft materials like PDMS appear lighter (high phase angles) and harder materials like PEG appear darker (low phase angles). The AmpAdd-modified PU coatings displayed heterogeneous surfaces in both height and phase AFM images that were composed of light and dark patterns, implying the formation of an amphiphilic morphology (Figure 3.7). The unmodified PU system exhibited a uniform homogenous surface (free of patterns) that was relatively similar to the hydrophobic A4 system (since it has solely PDMS on the surface) (Figure A13). As AmpAdd was added to the PU system, the presence of micro-domains on the surface was observed. The AmpAdd-modified coatings displayed a surface that was relatable to the reported morphology of control T-10 amphiphilic coating (Figure A13) – this control system has the same molecular weights of PEG and PDMS that are used for the AmpAdd additive, but instead crosslinked into the system. The sum of these surface domains increased as the concentration of AmpAdd in a formulation increased from 10 wt.% (F10) to 20 wt.% (F20) and 25 wt.% (F25). F30 formulation (containing 30 wt.% AmpAdd) exhibited a very similar morphology to F25, but many smaller domains were seen among the micro-domains. Coating F40 showed domains that were larger in comparison to F25 and F30 which may be due to the saturated surface by AmpAdd (noteworthy that capturing AFM images for F40 coating was more challenging than other systems). The AFM images supports the ATR-FTIR and XPS data that the AmpAdd self-stratified into the surface. Furthermore, the increasing trend of the amount of the observed heterogeneous domains is in direct correlation with the incorporated amount of AmpAdd, the higher the additive amount, the higher sum of domains on the surface. The AFM images for coatings were taken after water immersion. Overall, the coatings experienced a slight decrease in number of the domains on their surface. This change is noticeable in Figure A14, exhibiting the AFM images for F25 coating after and before water immersion. The AFM images indicate the AmpAdd rearranges on the surface as it is not crosslinked into the system and this observation is in confirmation with increased water contact angle values after the water immersion period.

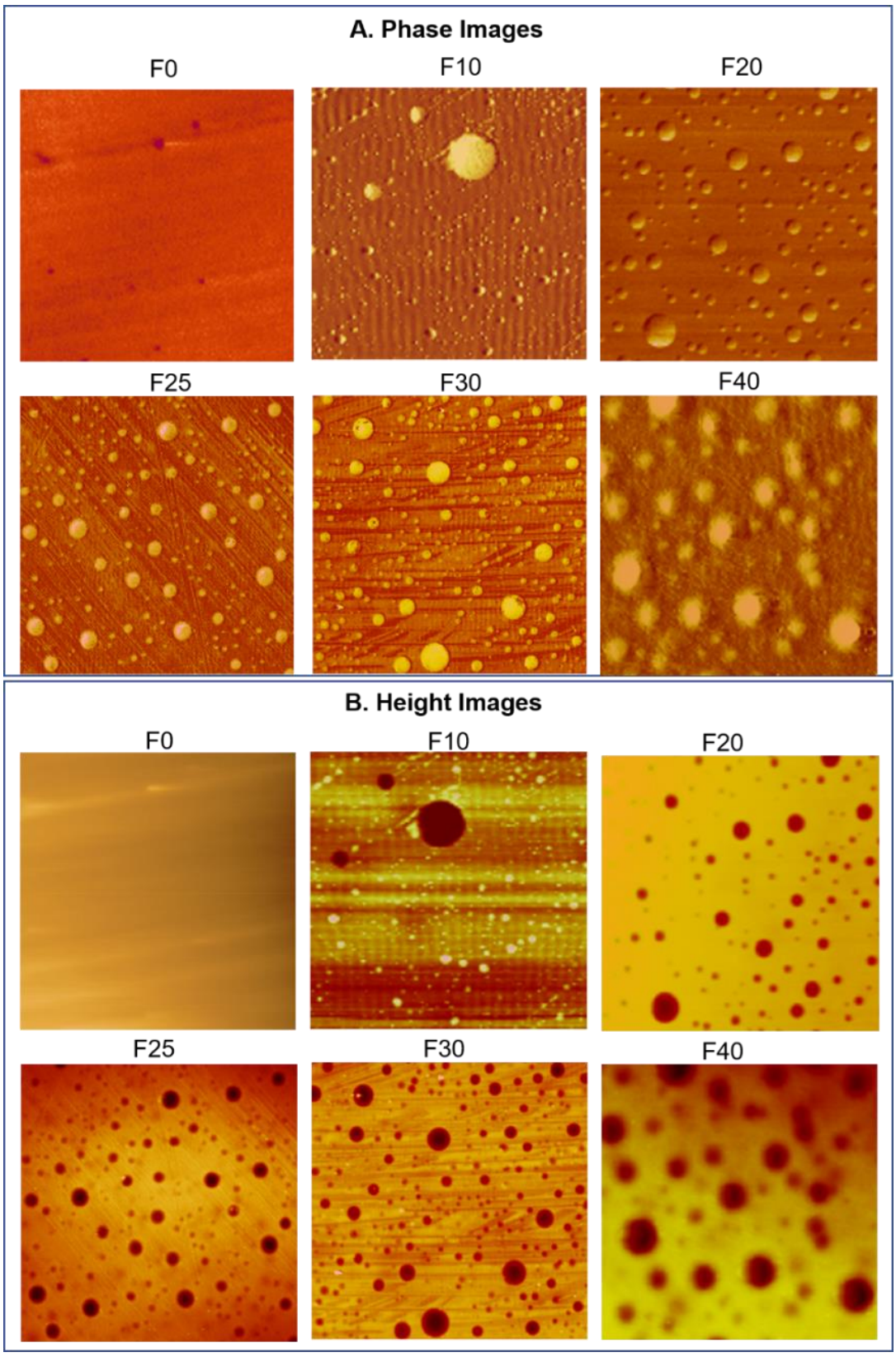

Figure 3.7. AFM phase images (Upper box) and height images (bottom box) for unmodified and modified PU coatings. Each image is for an area of 100 µm x 100 µm. Each label reflects the coating number.

Biological assays were conducted to evaluate fouling-release properties of the studied coatings using a broad number of representative marine fouling organisms, including *U.* linza, *C. lytica*, and *N. incerta*. All the assessments were carried out after 28 days of water leaching to ensure that toxic impurities do not interfere with the results. The coatings were evaluated for leachate toxicity using *C. lytica*, *N. incerta*, and *U. linza* as described elsewhere[20, 22] before any fouling-release experiments. All the coatings were non-toxic, opening the way for biological assessments.

U. linza is a known biofouling macroalgae organism that has a low affinity towards hydrophilic surfaces (with strong adhesion) and shows a high affinity towards hydrophobic surfaces (with weak adhesion).[23-25] The differing affinities and adhesions implies amphiphilic surfaces can be a good fit to overcome biofouling of *U. linza* and similar marine organisms. The extent of *U. linza* biofouling was very similar among the studied and control coatings, except PS coating (Figure 3.8 – red bars; the higher the bar, the higher extent of biofouling). The biofouled surfaces were water-jetted at two pressure levels and the biomass remaining was determined at 10 psi (Figure 3.8 – blue bars) and 16 psi (Figure 3.8 – green bars). The release trend was similar for both water pressures. At 16 psi, a comparison among the modified coatings indicated that the increasing amount of AmpAdd in a system improves fouling-release of *U. linza*. The introduction of 10 wt.% AmpAdd (4 wt.% PEG and PDMS each) and 20 wt.% of AmpAdd (8 wt.% PDMS and PEG each) improved the release of *U. linza* almost two times of the unmodified PU system (F0 coating). The fouling-release was improved further by adding 25 wt.% (10 wt.% PEG and PDMS each) of AmpAdd, and the addition of higher amounts of AmpAdd did not result in further release. At 10 psi, the release in correlation to the amount of AmpAdd followed a similar trend; however, the critical concentration of AmpAdd needed to be at 30 wt.% (12 wt.% PDMS and PEG each) to offer the optimum performance. A comparison between high-performance systems (F25, F30, and F40) with internal and commercial controls implies that the AmpAdd-modified coatings outperformed all the systems. The fouling-release data of *U. linza* suggests that a critical concentration of amphiphilicity (CAC) needed to be observed to deliver a desirable performance. This CAC for contending biofouling of *U. linza* was almost at 10-12 wt.% PEG and PDMS each (25-30 wt.% AmpAdd).

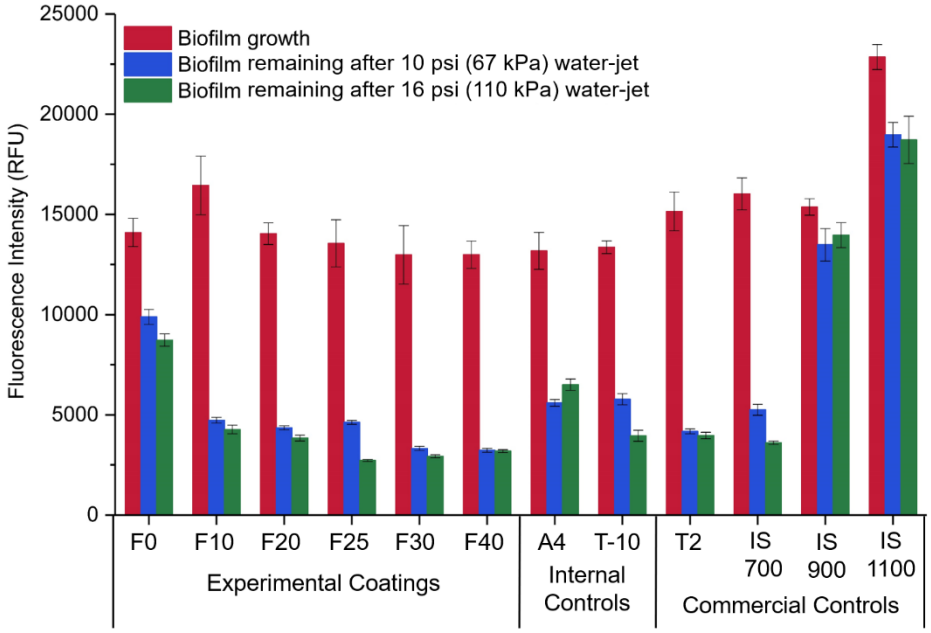

Figure 3.8. *U. linza* fouling-release data for biofilm growth (red bar), biofilm remaining after 10 psi waterjet (blue bar), and biofilm remaining after 16 psi waterjet. The X-axis is labeled to specify the formulations. Each category of assessed coatings is separated with lines.

C. lytica is another biofouling organism that is recognized for its affinity to settle on a variety of surfaces that range from hydrophilic or hydrophobic.[2] The extent of biofouling among the studied and control systems varied greatly (Figure 3.9 – red bars). Overall, studied coatings F0, F30, and F40 and control coatings A4 and T-10 showed the lowest *C. lytica* biofouling, while commercial controls such as IS 700, IS 900, and IS 1100 showed the highest amount of *C. lytica* biofouling. The fouling-release experiments were carried out at two pressure levels and the biomass remaining of *C. lytica* was reported at 10 psi (Figure 3.9 – blue bars) and 20 psi (Figure 3.9 – green bars). Generally, the release of *C. lytica* film was higher at 20 psi than 10 psi, but the trends were alike between the two. At 20 psi, an amount of AmpAdd additive between 10 wt.% to 25 wt.% concentration resulted in improved release of *C. lytica*, but the extent of release was almost the same regardless of the additive amount within this range (comparing coatings F10, F20, and F25 with unmodified F0). Once the amount of AmpAdd additive in a system reached 30 wt.% for F30 coating (12 wt.% PEG and PDMS each), the release of *C. lytica* improved further. The addition of more AmpAdd in F40 system (40 wt.%; 17 wt.% PEG and PDMS each) did not enhance the release and showed a similar performance to F30. At 10 psi, the addition of the AmpAdd

additive did not result in better fouling-release performance up to 25 wt.% of AmpAdd, thus coatings F10, F20, and F25 displayed *C. lytica* release that was comparable to the unmodified F0 system. However, once the amount of AmpAdd reached 30 wt.% and higher, it showed an improved release for the *C. lytica* film. Coatings F30 and F40 were compared with both internal and commercial controls as these two demonstrated the best results among the AmpAdd-modified coatings. The outlined data in Figure 3.9 shows F30 and F40 coatings outperformed both the internal and commercial systems. Like the data of *U. linza*, the fouling-release data of *C. lytica* suggests that a critical amphiphilic concentration (CAC) was needed to be observed to deliver a desired release. This CAC for contending biofouling of *C. lytica* was at 12 wt.% PEG and PDMS each (30 wt.% AmpAdd), being in the range of CAC for *U. linza*.

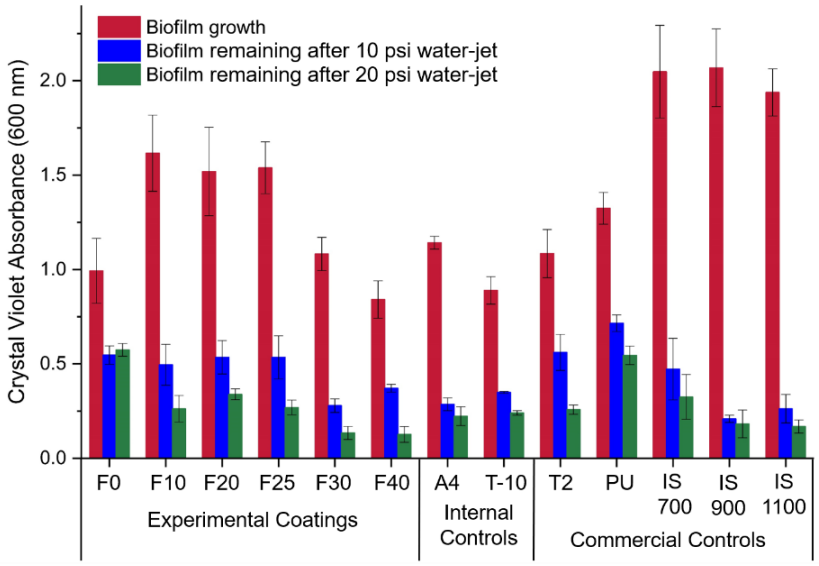

Figure 3.9. *C. lytica* fouling-release data for biofilm growth (red bar), biofilm remaining after 10 psi waterjet (blue bar), and biofilm remaining after 20 psi waterjet. The X-axis is labeled to specify the formulations. Each category of assessed coatings is separated with lines.

N. incerta is well-known as another major biofouling organism that prefers to biofoul hydrophobic surfaces.[23, 24] The extent of *N. incerta* biofouling varied among the studied coatings, internal controls and commercial controls (Figure 3.10 – red bars). Overall, coatings T2, PU and IS 700 showed the highest extent of biofouling; commercial IS 900 and IS 1100 SR showed the lowest amount of biofouling; and studied modified PU coatings showed an intermediate extent of biofouling for *N. incerta*. The release of formed *N. incerta* film was evaluated at two pressure levels and the biofilm remaining of *N. incerta* was

assessed at 10 psi (Figure 3.10 – blue bars) and 20 psi (Figure 3.10 – green bars). The release of the *N. incerta* films was noticeably higher at 20 psi than 10 psi. Even though the extent of release was different due to water pressure level, the observed trends at both levels was similar among the modified PU coatings. At 20 psi, the addition of AmpAdd clearly improves release of the *N. incerta* biofilm. The removal of the film improves until 25 wt.% (10 wt.% PEG and PDMS each) of AmpAdd in the system, and the further addition of the additive after this point resulted in a plateau and negligible improvements. A similar trend was noticed at 10 psi pressure level, except the plateau point was determined to be at 30 wt.% of AmpAdd (12 wt.% PEG and PDMS each). Coating systems F25, F30 and F40 that contained 30 wt.% or more additives released the *N. incerta* films better than internal controls (A4 and T-10), indicating the effect of amphiphilic concentration of the surface on the release performance. The only two systems that outperformed the AmpAdd-modified PU systems were IS 900 and IS 1100. Like the data of *U. linza* and *C. lytica*, *N. incerta* is no exception and follows a similar trend: a critical amphiphilic concentration (CAC) needs to be met for attaining a desired fouling-release performance. This CAC for contending biofouling of *C. lytica* was at 10-12 wt.% PEG and PDMS each (25-30 wt.% AmpAdd).

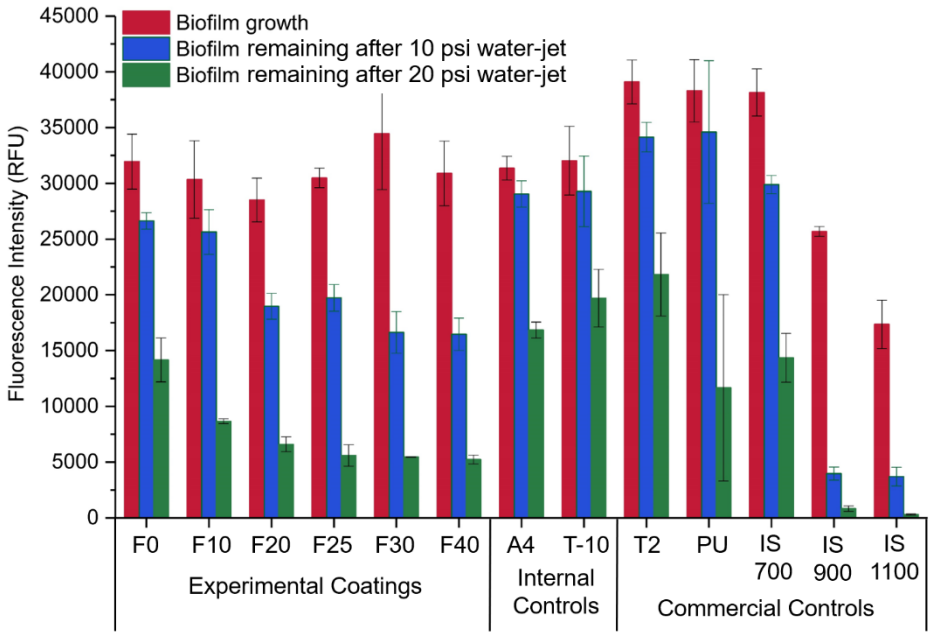

Figure 3.10. *N. incerta* fouling-release data for biofilm growth (red bar), biofilm remaining after 10 psi waterjet (blue bar), and biofilm remaining after 20 psi waterjet. The X-axis is labeled to specify the formulations. Each category of assessed coatings is separated with lines.

Mechanical tests were performed on the PU coatings to assess their integrity as the amount of AmpAdd increased in a system. The properties started to drop at 50 wt.% of the AmpAdd; thus, 40 wt.% concentration of AmpAdd was marked as the highest limit before properties declined (Table 3.3). Coatings showed desirable stability against MEK and salt water double rubs until 40 wt.% of AmpAdd. Additionally, the additive did not impact the performance of the coating in response to rapid deformation, impact test. Conical mandrel bend test showed the additive did not affect the flexibility of the coatings. Despite it was expected the long PEG and PDMS chains will contribute to better flexibility, it potentially did not happen since these moieties were mostly present on the surface of a coating rather than the whole bulk. The adhesion of the coatings to the substrate remained consistent and unchanged until 40 wt.% of AmpAdd. Generally, the introduction of the AmpAdd was not detrimental to the PU system until 40 wt.%. Thus, coatings with 40 wt.% or less amount of AmpAdd were selected to be investigated for this study.

Table 3.3. Results of mechanical tests on unmodified and modified PU coatings

Formulation	MEK Double Rub (Number of rubs)	Water Double rubs (Number of rubs)	Front Impact (in-lb)	Reverse Impact (in-lb)	Conical Mandrel (mm)	Crosshatch Adhesion
F0	>400	>400	64	12	90	4B
F10	>400	>400	68	16	100	5B
F20	>400	>400	72	12	90	5B
F25	>400	>400	68	12	100	4B
F30	>400	>400	68	16	120	5B
F40	380	>400	76	20	130	5B
F50	292	320	76	20	130	3B

Conclusions

The results showed amphiphilic moieties migrate to the surface of a coating and modify it until a point of saturation, and then additional surface-active agents do not change the surface or impact the fouling-release performance, recognizing this point of surface saturation as the critical amphiphilic concentration (CAC). This behavior is like the addition of surfactants to a liquid where they reduce the surface tension until the interface is saturated and then additional surfactants does not change the

surface tension, but they form micelles, known as the critical micelle concentration.[26, 27] This work explored the effect of incorporating an amphiphilic additive into a polyurethane coating system. The amphiphilic additive was made by attaching hydroxyl-terminated PEG and PDMS chains on a polyisocyanate. Amphiphilic coating systems are being widely investigated as marine coatings, but there continues to be a lack of knowledge about these recently developed systems. Thus, this study was designed to determine at what concentration of amphiphilicity a non-marine PU system converts to a marine PU coating having fouling-release properties. Generally, as the amount of the amphiphilic additive in the PU coating increased, the surface of the coating system became more amphiphilic. The fouling release data of the coatings against all biological assays (*C. lytica*, *U. linza*, and *N. incerta*) demonstrated that the systems offered a desirable performance when a specific amount of amphiphilicity was present in a composition (a performance comparable or better than both internal and commercial controls). The amount of amphiphilicity that resulted in the desired performance towards all marine organisms was between 10-12 wt.% PEG and PDMS each (25-30 wt.% AmpAdd), and further amount of AmpAdd after this concentration did not boost the FR performance. Surface characterizations provided further insight into these surfaces as well. ATR-FTIR showed the presence of an amphiphilic surface. Contact angle measurements indicated the amphiphilic concentration had a direct impact on the surface considering that coatings with 25 wt.% AmpAdd or higher were more dynamic, possessed lower slip-off angles, and displayed the lowest contact angle hysteresis (difference between advancing and receding contact angles). XPS showed that the AmpAdd self-stratified onto the surfaces, and the presence of the amphiphilic moieties on the surface was directly correlated to the amount of AmpAdd in a system. XPS data indicated that for coatings with 25 wt.% or higher amount of AmpAdd, the additives were well distributed on the surface and extended to a higher thickness within the bulk of the coating. AFM images clearly showed the presence of heterogenous micro-sized domains after AmpAdd was introduced to the PU system, and the sum of domains increased as the amount of AmpAdd increased in a formulation. Once AmpAdd was introduced at 25 wt.% or higher amounts in a formulation, the surfaces appeared to be saturated by these domains. Mechanical integrity of the coatings was assessed too, and it was determined that the coatings maintained their integrity until 40 wt.% of AmpAdd was added. Overall, the fouling release data and surface characterizations go hand in hand. Both suggest that at a critical

amphiphilic concentration there are noticeable changes in contact angles, surface morphology, and removal extent of the biological films. The critical amphiphilic concentration (CAC) that resulted in the desired FR performance was between 10-12 wt.% PEG and PDMS each (25-30 wt.% AmpAdd). This study opens the door for an unexplored area to understand amphiphilic systems for designing better systems. Future investigations will explore how changes in the amphiphilic balance of the moieties or replacing PEG with other hydrophilic moieties (i.e. zwitterions) impact the FR performance and observed trends. The results of these work will hopefully encourage researchers to further explore and develop a deeper understanding of amphiphilic systems for marine biofouling purposes as well as other applications such as anti-icing coatings, fouling-release membranes, and non-fouling medical devices.

References

1. Callow, J. A.; Callow, M. E., Trends in the development of environmentally friendly fouling-resistant marine coatings. *Nature Communications* **2011,** *2* (1), 244-244.

2. Lejars, M.; Margaillan, A.; Bressy, C., Fouling release coatings: A nontoxic alternative to biocidal antifouling coatings. *Chemical Reviews* **2012,** *112* (8), 4347-4390.

3. Callow, M. E.; Callow, J. E., Marine biofouling: a sticky problem. *Biologist* **2002,** *49* (1), 10-14.

4. Yebra, D. M.; Kiil, S.; Dam-Johansen, K., Antifouling technology—past, present and future steps towards efficient and environmentally friendly antifouling coatings. *Progress in Organic Coatings* **2004,** *50* (2), 75-104.

5. Magin, C. M.; Cooper, S. P.; Brennan, A. B., Non-toxic antifouling strategies. *Materials Today* **2010,** *13* (4), 36-44.

6. Konstantinou, I. K.; Albanis, T. A., Worldwide occurrence and effects of antifouling paint booster biocides in the aquatic environment: a review. *Environment International* **2004,** *30* (2), 235-248.

7. Wyszogrodzka, M.; Haag, R., Synthesis and characterization of glycerol dendrons, self-assembled monolayers on gold: A detailed study of their protein resistance. *Biomacromolecules* **2009,** *10* (5), 1043-1054.

8. Sommer, S.; Ekin, A.; Webster, D. C.; Stafslien, S. J.; Daniels, J.; VanderWal, L. J.; Thompson, S. E. M.; Callow, M. E.; Callow, J. A., A preliminary study on the properties and fouling-release performance of siloxane–polyurethane coatings prepared from poly(dimethylsiloxane) (PDMS) macromers. *Biofouling* **2010,** *26* (8), 961-972.

9. Bodkhe, R. B.; Thompson, S. E. M.; Yehle, C.; Cilz, N.; Daniels, J.; Stafslien, S. J.; Callow, M. E.; Callow, J. A.; Webster, D. C., The effect of formulation variables on fouling-release performance of stratified siloxane–polyurethane coatings. *Journal of Coatings Technology and Research* **2012,** *9* (3), 235-249.

10. Selim, M. S.; El-Safty, S. A.; Azzam, A. M.; Shenashen, M. A.; El-Sockary, M. A.; Abo Elenien, O. M., Superhydrophobic silicone/TiO2–SiO2 nanorod-like composites for marine fouling release coatings. *ChemistrySelect* **2019,** *4* (12), 3395-3407.

11. Iguerb, O.; Poleunis, C.; Mazéas, F.; Compère, C.; Bertrand, P., Antifouling properties of poly(methyl methacrylate) films grafted with poly(ethylene glycol) monoacrylate immersed in seawater. *Langmuir* **2008,** *24* (21), 12272-12281.

12. Rath, S. K.; Chavan, J. G.; Ghorpade, T. K.; Patro, T. U.; Patri, M., Structure–property correlations of foul release coatings based on low hard segment content poly (dimethylsiloxane–urethane–urea). *Journal of Coatings Technology and Research* **2018,** *15* (1), 185-198.

13. Yi, L.; Xu, K.; Xia, G.; Li, J.; Li, W.; Cai, Y., New protein-resistant surfaces of amphiphilic graft copolymers containing hydrophilic poly (ethylene glycol) and low surface energy fluorosiloxane side-chains. *Applied Surface Science* **2019,** *480*, 923-933.

14. Zhang, Z.-P.; Song, X.-F.; Cui, L.-Y.; Qi, Y.-H., Synthesis of polydimethylsiloxane-modified polyurethane and the structure and properties of its antifouling coatings. *Coatings* **2018,** *8* (5), 157-157.

15. Galhenage, T. P.; Webster, D. C.; Moreira, A. M. S.; Burgett, R. J.; Stafslien, S. J.; Vanderwal, L.; Finlay, J. A.; Franco, S. C.; Clare, A. S., Poly(ethylene) glycol-modified, amphiphilic, siloxane–polyurethane coatings and their performance as fouling-release surfaces. *Journal of Coatings Technology and Research* **2017,** *14* (2), 307-322.

16. Bodkhe, R. B.; Stafslien, S. J.; Cilz, N.; Daniels, J.; Thompson, S. E. M.; Callow, M. E.; Callow, J. A.; Webster, D. C., Polyurethanes with amphiphilic surfaces made using telechelic functional PDMS having orthogonal acid functional groups. *Progress in Organic Coatings* **2012,** *75* (1-2), 38-48.

17. Owens, D. K.; Wendt, R. C., Estimation of the surface free energy of polymers. *Journal of Applied Polymer Science* **1969,** *13* (8), 1741-1747.

18. Stafslien, S.; Daniels, J.; Mayo, B.; Christianson, D.; Chisholm, B.; Ekin, A.; Webster, D.; Swain, G., Combinatorial materials research applied to the development of new surface coatings IV. A high-throughput bacterial biofilm retention and retraction assay for screening fouling-release performance of coatings. *Biofouling* **2007,** *23* (1), 45-54.

19. Stafslien, S. J.; Bahr, J. A.; Daniels, J. W.; Wal, L. V.; Nevins, J.; Smith, J.; Schiele, K.; Chisholm, B., Combinatorial materials research applied to the development of new surface coatings VI: An automated spinning water jet apparatus for the high-throughput characterization of fouling-release marine coatings. *Review of Scientific Instruments* **2007,** *78* (7), 072204-072204.

20. Cassé, F.; Stafslien, S. J.; Bahr, J. A.; Daniels, J.; Finlay, J. A.; Callow, J. A.; Callow, M. E., Combinatorial materials research applied to the development of new surface coatings V. Application of a spinning water-jet for the semi-high throughput assessment of the attachment strength of marine fouling algae. *Biofouling* **2007,** *23* (2), 121-130.

21. Cassé, F.; Ribeiro, E.; Ekin, A.; Webster, D. C.; Callow, J. A.; Callow, M. E., Laboratory screening of coating libraries for algal adhesion. *Biofouling* **2007,** *23* (4), 267-276.

22. Majumdar, P.; Crowley, E.; Htet, M.; Stafslien, S. J.; Daniels, J.; VanderWal, L.; Chisholm, B. J., Combinatorial materials research applied to the development of new surface coatings XV: An investigation of polysiloxane anti-fouling/fouling-release coatings containing tethered quaternary ammonium salt groups. *ACS Combinatorial Science* **2011,** *13* (3), 298-309.

23. Finlay, J. A.; Callow, M. E.; Ista, L. K.; Lopez, G. P.; Callow, J. A., The influence of surface wettability on the adhesion strength of settled spores of the green alga Enteromorpha and the diatom Amphora. *Integrative and Comparative Biology* **2002,** *42* (6), 1116-1122.

24. Callow, M. E.; Callow, J. A.; Ista, L. K.; Coleman, S. E.; Nolasco, A. C.; López, G. P., Use of self-assembled monolayers of different wettabilities to study surface selection and primary adhesion processes of green algal (Enteromorpha) zoospores. *Applied Environmental Microbiology* **2000,** *66* (8), 3249-3254.

25. Callow, J. A.; Callow, M. E.; Ista, L. K.; Lopez, G.; Chaudhury, M. K., The influence of surface energy on the wetting behaviour of the spore adhesive of the marine alga Ulva linza (synonym Enteromorpha linza). *Journal of the Royal Society Interface* **2005,** *2* (4), 319-325.

26. Dominguez, A.; Fernandez, A.; Gonzalez, N.; Iglesias, E.; Montenegro, L., Determination of Critical Micelle Concentration of Some Surfactants by Three Techniques. *Journal of Chemical Education* **1997,** *74* (10), 1227.

27. Van Oss, C. J., Acid—base interfacial interactions in aqueous media. *Colloids and Surfaces A: Physicochemical and Engineering Aspects* **1993,** *78*, 1-49.

CHAPTER 4. INTRODUCTION OF SURFACE-MODIFYING, PEG-PDMS ADDITIVES INTO A HYDROPHOBIC MARINE COATING FOR ATTAINING AMPHIPHILIC BALANCE

Introduction

Marine biofouling is defined as the undesirable settlement of marine organisms on surfaces that are immersed in seawater.[1, 2] This problem is considered very ambiguous and complicated since it involves more than 4000 marine organisms with varying modes of adhesion and surface affinities.[2-4] As an example, some organisms settle on hydrophilic surfaces such as *U. linza,* mussels, and barnacles, while some organisms settle on hydrophobic surfaces or a hybrid of both such as *N. incerta* and *C. lytica*, respectively.[1, 2, 5] The accumulation of biofoulants is not a linear process, meaning the micro-organisms and macro-organisms have the potential to settle on a surface in alternation, furthering the complexity of this problem.[1, 2]

The economic and environmental impacts of marine biofouling are severe. The settled biofoulants lead to several drawbacks including increased drag and reduced maneuverability, increased fuel consumption and emission of greenhouse gases, shortened service life, transportation of invasive species to new aquatic environments, and expanded maintenance cost.[2, 6] For example, reports indicate that the US Navy spends on average $1 billion per year to maintain their biofouling-affected ships. The negative consequences of biofouling will appear with as low as 2% of attached biofoulants on a ship, resulting in a significant drop for fuel efficiency.[7] Therefore, a biofouled ship requires frequent hull cleaning and dry-docking, penalizing ship owners with high expenses.

Dry-docking ships is not considered a feasible solution to overcome marine biofouling, especially for Naval carriers during long-term missions or cargo ships. Thus, alternative reliable methods have been explored. Ship hulls made of copper alloys and lead sheaths have been historically used to contend with biofouling, but they were replaced due to limited resources and metallic corrosion. Antifouling paints with active biocides were a promising path in the 19th century, specifically the emergence of tributyl tin-based and self-polishing coatings in 1970s.[2, 8] However, these systems were recognized to be toxic towards and negatively affect non-targeted marine organisms, causing their eventual worldwide ban in early 2000s.

Therefore, there has been a wave of investigations to find non-toxic fouling-release and anti-fouling marine coatings to address the marine biofouling issues in an environmentally friendly way.[2]

Antifouling paints (AF) exploit copper oxide and zinc oxide containing materials as biocides to contend with marine biofouling.[1, 2] AF paints function by preventing settlement of marine organisms through releasing biocides over time. These metal-based biocides are less toxic than tin, but they have the potential to pollute marine ecosystems and deliver non-targeted toxicity. The other highly sought technology is fouling release (FR) surfaces, functioning by decreasing the adhesion strength of biofoulants on the surface and enabling their removal upon ship movement or light cleaning. Traditional FR paints are typically composed of hydrophobic surfaces that contain polydimethylsiloxane (PDMS) or fluoroalkyl polymers, benefiting from the low surface energy of such materials that weakens adhesion of marine organisms.[2, 9] The hydrophobic FR coatings are accompanied with two main challenges. First, these systems typically lack mechanical durability and require a tie-coat to facilitate their adhesion (which is not very effective).[2, 5] Second, some organisms out of the 4000 marine biofoulants prefer hydrophobic surfaces for settlement.[4, 10] To address the former issue, self-stratifying siloxane-polyurethane (SiPU) FR coatings were developed, resulting in an easy-to-apply system with highly desired mechanical durability.[7, 11, 12] The SiPU systems separate into two layers by utilizing thermodynamics of incompatibility between polymer types, providing a PDMS-rich surface and a PU-based bulk.[13]

The surface of hydrophobic coatings needs to be tailored to prevent biofouling of a wider range of organisms to address the latter issue. Recent investigations have reported that amphiphilic coatings, surfaces with both hydrophilic and hydrophobic domains, may offer desirable performance to release a wider range of organisms than the hydrophobic FR coatings.[2, 14-18] Hydrophilic domains on surfaces are usually achieved by the introduction of protein-resistant polymers such as polyethylene glycol (PEG) or zwitterionic-based polymers (i.e. poly (sulfobetaine methacrylate)).[2] Having hydrophilic and hydrophobic domains on a surface is very challenging; thus, requiring a change of the coating matrix and utilizing new chemistries. Even though innovating a new amphiphilic coating system is appealing, there is also high demand for surface-modifying additives that do not necessitate significant changes for an established FR formulation.

Additives offer desired improvements to many well-established systems in many industries, and the marine coating industry is no exception. The additives for marine purposes are mostly designed as surface-modifying agents to tune the surface of coatings and boost their performance as FR or AF coatings. There are many types of additives that have been investigated for marine coatings including copper/zinc-based,[19-21] amphiphilic copolymers (i.e. PEG[22-28] or zwitterionic-based[29-32]), or hydrogel-like polymers.[33] The horizon of explored marine additives also covers silicone oils[34-36] and specialty additives such as sephiolite nanofibers, modified graphite, carbon nanotubes and pigments (i.e. TiO_2 and ZnO).[3, 10, 37-39] Amphiphilic copolymers are explored as a viable additive system, but one of major drawbacks for such additives is that their preparation often involves complex synthesis and purification processes, limiting the implementations on a large scale.

Therefore, we designed this study to prepare a series of easy-to-synthesize amphiphilic additives that could be non-covalently incorporated into a hydrophobic SiPU system for attaining a desirable amphiphilic surface (Figure 4.1). The amphiphilic additives were composed of hydrophilic PEG and hydrophobic PDMS, attached on a polyisocyanate compound. The molecular weights of the PEG and PDMS were selected based on reported literature and our previous work. The weight ratios of the attached PEG and PDMS on the polyisocyanate was systematically varied to obtain additives of differing amphiphilicity, and the amphiphilic additives were added in at 20 wt.% to the SiPU system. This specific amount was selected based on the amount of PDMS present in the base SiPU formulation. Thus, the only variable explored in this study was the overall amphiphilic balance in the SiPU system, attained through addition of the amphiphilic additives. This study will discuss three components including synthesis and characterization of amphiphilic additives, surface characterization of additively-modified SiPU coating systems, and fouling-release assessment of these prepared surfaces using representative marine organisms including *U. linza*, *C. lytica*, *N. incerta*, and barnacles.

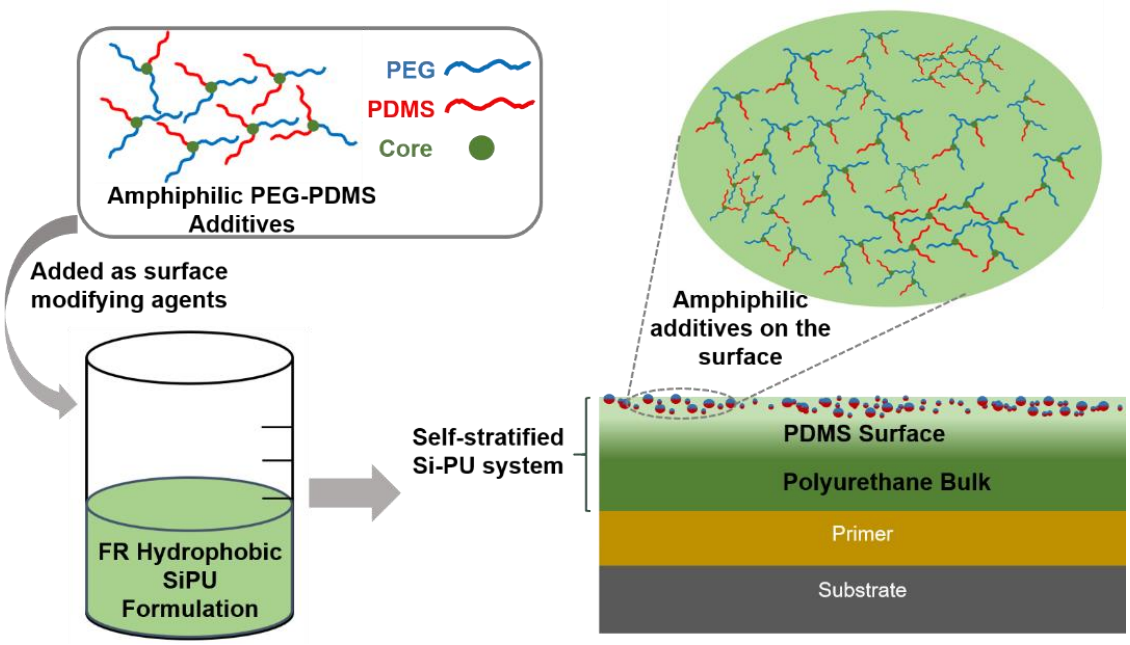

Figure 4.1. Illustration of amphiphilic PEG-PDMS additives as surface-modifying agents, tuning the hydrophobic surface of FR SiPU coating system to an amphiphilic surface.

Experimental

Materials

Isophorone diisocyanate (IPDI)-based polyisocyanate Desmodur Z4470 BA was provided by Covestro LLC. Monocarbinol-terminated polydimethylsiloxane (PDMS) with molecular weight of 10,000 $\bar{M}_n$ (MCR-C22) was purchased from Gelest, Inc. Poly(ethylene glycol) methyl ether (750 $\bar{M}_n$), ethyl-3-ethoxy propionate, methyl ethyl ketone (MEK), acetylacetone, methyl amyl ketone (MAK), and dibutyltin diacetate (DBTDAc) were purchased from Sigma Aldrich. Toluene and isopropanol were purchased from VWR. An acrylic polyol made of 80% butyl acrylate and 20% 2-hydroxyethyl acrylate was prepared via conventional free radical polymerization and diluted to 50% in toluene. Aminopropyl terminated polydimethylsiloxane (APT-PDMS) with molecular weight (MW) of 20,000 $\bar{M}_n$ was also synthesized through a ring-opening equilibration reaction. Both synthesized polymers were prepared following guidelines from elsewhere.[12]

AkzoNobel International Paint provided the commercial FR standards Intersleek® 700 (IS 700), Intersleek® 900 (IS 900), and Intersleek® 1100SR (IS 1100). Silicone elastomer Silastic® T2 and polystyrene were provided by Dow Corning other commercial standards. Hydrophobic siloxane-polyurethane A4 coating (A4) as the base system for this study was prepared following the procedure

elsewhere.[12] Also, a pure polyurethane formulation without APT-PDMS was also prepared to be included as a control. Amphiphilic T-10 coating, internal coating control, was prepared following the procedure elsewhere for a formulation that contained 10 wt.% PEG 750 $\bar{M}_n$ and PDMS 10,000 $\bar{M}_n$.[18] Aluminum panels (4" x 8" in., 0.6 mm thick, type A, alloy 3003 H14) purchased from Q-lab were sandblasted and primed with Intergard 264 (International Paints) using air-assisted spray application. Multi-well plates were modified using circular disks (1-inch diameter) of primed aluminum.

Experimental Design

A series of amphiphilic additives (AmpAdd) based on PDMS and PEG were synthesized and added into a hydrophobic SiPU coating system, called A4. The SiPU A4 system is composed of IPDI trimer isocyanate resin, crosslinked with acrylic polyol and amine-terminated PDMS, resulting in a self-stratified PDMS on the surface and well-adhered PU on the bottom of an applied coating film. In A4, PDMS with 20,000 $\bar{M}_n$ is at 16 wt.% based on total solid content of the formulation (added as 20 wt.% based on solid contents of acrylic polyol and IPDI trimer resin). Thus, hydrophilic moieties that can diffuse into the surface needs to be introduced to attain a coating with amphiphilic surface.

AmpAdds were synthesized by reacting PEG and PDMS with the IPDI trimer polyisocyanate; the ratio of isocyanate groups to the combined OH groups of PEG and PDMS was 1:1 molar ratio. These two were attached in varying weight ratios to meet the required one molar ratio while attaining several types of amphiphilicity. The molecular weights of 10,000 $\bar{M}_n$ for PDMS and 750 $\bar{M}_n$ for PEG were chosen to synthesize amphiphilic additives since desirable FR performance was reported and observed within these ranges.[13, 18] This study varied only the amount of attached PEG and PDMS on an additive, providing five additives that range from the least hydrophilic to most hydrophilic (Table 4.1). It should be noted again that wt.% of PEG and PDMS varies for each of the synthesized additives as varying weight ratios of these two are used to synthesize the additives. There is a wt.% for IPDI isocyanate resin as well since the amphiphilic chains are grafted on its backbone. Thus, these wt.% values of PEG and PDMS on an additive are used to determine the final content of PEG and PDMS moieties in a formulation.

Table 4.1. List of prepared additives and their compositional details

Additive Number	PDMS: PEG (% ratio)	PDMS (wt. %)	PEG (wt. %)	IPDI isocyanate (wt. %)
Amp-1	50: 50	42	42	16
Amp-2	33: 66	26	53	21
Amp-3	20: 80	15	61	23
Amp-4	10: 90	8	67	25
Amp-5	0: 100	0.0	73	27

Preliminary experiments indicated systems having more than 20 wt.% PDMS and PEG each (combined 40 wt.%) lack mechanical integrity as a coating film. Knowing that SiPU A4 system contains up to 16 wt.% PDMS and utilizing our experience on PEG-based additive systems, the AmpAdds of this study were added at 20 wt.% to achieve the desirable amphiphilic nature. As a result, a total of twelve formulations were investigated. Six formulations were the A4 and its additively modified versions as outlined in (Table 4.2) and the other six were the internal and commercial controls (Table 4.3). The table outlines type of added additive, amount of the added additive, wt.% of PEG and PDMS based on the added additive, and overall wt.% of PEG and PDMS in the total formulation (including the 16 wt.% PDMS of A4). The balance of hydrophobic and hydrophilic contents in a formulation becomes more equal going from F1 to F5.

Table 4.2. Coating compositions

Formulation	Added AmpAdd Details				Formulation Details	
	Additive Type	Additive Amount (wt. %)	PDMS (wt.%)	PEG (wt.%)	PDMS (wt.%)	PEG (wt.%)
A4	-	0.0	0.0	0.0	16.0	0.0
F1	Amp-1	20.0	8.2	8.2	24.2	8.2
F2	Amp-2	20.0	5.3	10.5	21.3	10.5
F3	Amp-3	20.0	3.0	12.6	19.0	12.6
F4	Amp-4	20.0	1.6	13.5	17.6	13.5
F5	Amp-5	20.0	0.0	14.6	16.0	14.6

Commercial standards were prepared following the manufacturer's instructions. T-10 coating, internal amphiphilic control, containing 10,000 $\bar{M}_n$ PDMS and 750 $\bar{M}_n$ PEG prepolymer was prepared following directions elsewhere; this formulation was selected since it showed the best performance

among the studied systems.[18] Similar to experimental coatings all control and standards were also prepared on 4” x 8” primed aluminum panels and multi-well plates. Table 4.3 contains detailed descriptions of the control and standard coatings used for this study.

Table 4.3. List of control coatings

Control Name	Control ID	Description
Amphiphilic SiPU	T-10	Internal Amphiphilic SiPU Control
Polyurethane	PU	Pure Polyurethane Standard
Polystyrene	PS	Pure Polystyrene Standard (used for *U. linza* test)
Dow T2	T2	Silicone Elastomer Standard
IS 700	700	Intersleek Commercial FR Standard
IS 900	900	Intersleek Commercial FR Standard
IS 1100	1100 SR	Intersleek Commercial FR Standard

Synthesis of Amphiphilic Additives

The AmpAdd additives were synthesized by reacting hydroxyl-terminated PEG and PDMS chains with the IPDI trimer polyisocyanate (Scheme 4.1). The molar ratio of NCO groups to the combined OH groups of PEG and PDMS was 1:1. Isocyanate groups were fully converted to urethane linkages by attachment of PEG and PDMS chains. PEG and PDMS were added in weight ratios that met the required one molar ratio while accessing additives of varying hydrophilic-hydrophobic balance.

To synthesize Amp-3 (containing weight ratio of PDMS:PEG 20:80), PEG 750 $\bar{M}_n$ (8.00 g) was diluted in toluene (8.00 g) in a 50-mL flask. The flask was equipped with a magnetic stirrer, nitrogen inlet, and temperature controller. Reflux condenser was used when heat was applied. PDMS 10,000 $\bar{M}_n$ (2.00 g) was added to the flask and mixed robustly with vortex for 2 minutes. IPDI trimer resin (4.25 g) and DBTDAc catalyst solution (1% by wt. in MAK) (0.71 g) were then added to the flask. The reaction was carried at 80 °C for 2 hours. As another method, the reaction could also be completed at ambient condition for 24 hours. In theory, the synthesized prepolymer contained 61.0 wt.% PEG and 15.0 wt.% PDMS (Table 4.1). All other AmpAdds were synthesized following the same procedure.

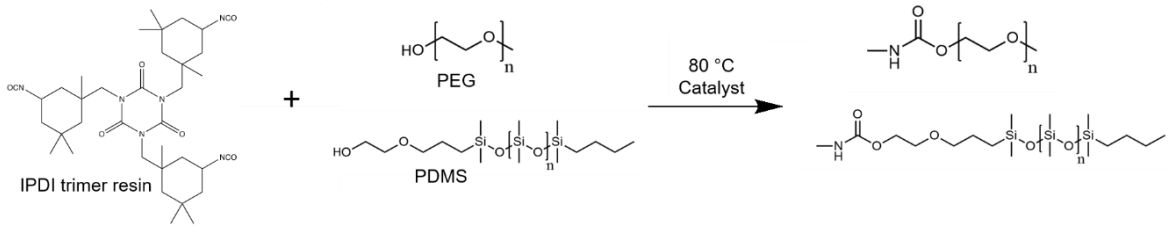

Scheme 4.1. Overall Synthesis Scheme of amphiphilic additives

Isocyanate Titrations

Isocyanate titration was used to confirm the disappearance of isocyanate groups after the synthesis of the additive. An additive sample (0.3-0.5 g) was weighed in an Erlenmeyer flask and diluted with isopropanol. Then, 25 mL of 0.1 N dibutyl amine solution and additional 25 mL isopropanol were added to the flask, and the mixture was stirred for 15 minutes. Several drops (3-5 drops) of bromophenol blue indicator were added to the flask. The content of the flask was titrated using a standardized 0.1 N hydrochloric acid until the endpoint blue to yellow was observed. A blank prepared only with 25 mL of dibutyl amine solution was also titrated following the same procedure. The recorded amount of hydrochloric acid for both titrations was used to calculate the isocyanate content (if any).

Percent Solids Determination

The non-volatile content of the additive was determined following ASTM 2369. In general, a weighed empty aluminum pan was filled with additive sample (1-2 g). Isopropyl alcohol was used to cover the sample. The pan was placed in an oven at 120 °C for 1 hour. After removal from the oven, the pan was weighed again to determine the percent solid. Three replicates were recorded.

Fourier Transform Infrared Spectroscopy

Fourier transform infrared (FTIR) spectroscopy was used to characterize the additive, using a Thermo Scientific Nicolet 8700 FTIR. The additive was applied as a thin layer on a potassium bromide (KBr) plate to collect the spectrum.

Coating Formulations and Curing

A synthesized AmpAdd was added to SiPU A4 system. The A4 system is a hydrophobic marine fouling-release coating that mainly composed of acrylic polyol, IPDI trimer isocyanate resin, and amine-terminated PDMS. The type of additive is the only variable among the formulations; the additives vary based on their degree of hydrophilic and hydrophobic balance.

For example, to formulate coating F3, acrylic polyol (15.06 g; 50% solid), acetylacetone (1.39 g) (potlife extender), amine-terminated PDMS (2.32 g), and Amp-3 additive (5.93 g; 50% solid) were added to a vial and stirred ambiently for 24 hours. IPDI isocyanate trimer Desmodur Z4470 BA resin (5.55 g) and DBTDAs catalyst solution (0.56 g) were added to the vial, and the mixture was stirred for another hour. Coating formulations were drawn on primed 8' x 4' aluminum panels using a wire-round drawdown bar with a film thickness of 80 µm. All coatings were cured ambiently for 24 hours, followed by oven curing at 80 °C for 45 minutes. All experimental coatings were prepared following the same procedure. Coatings were cut out in circular shapes and glued to 24-well plates for biological assays test.

To verify self-stratification of AmpAdd additives into the surface of coatings via X-ray photoelectron spectroscopy (XPS) experiments, two internal model PU systems, one without APT-PDMS (pure model PU) and one with Amp-1 additive in its composition (modified model PU), were also prepared following the same procedure, except no APT- PDMS was introduced as a crosslinker. These controls allowed PDMS signals of A4 to not interfere with PDMS signals of additives for validation purposes.

Surface Characterization

A Kruss® DSA 100 (Drop Shape Analyzer) was utilized to measure the surface wettability and surface energy for the coatings. Water and diiodomethane contact angles were measured in 3 replicates for each sample. For each replicate, the static contact angle was measured over 9 minutes to monitor changes (the values plateaued after 9 minutes). Surface energy for each surface was calculated using the Owens-Wendt method.[40] Slip angle, advancing and receding water contact angles for surface were evaluated using a tilting stage where a 25-µL water droplet was viewed on a coating surface (tilted at 10°/min). The measured angles and surface energies were calculated using Kruss® Advance software.

Attenuated total reflectance Fourier transform infrared spectroscopy (ATR-FTIR) was used to characterize the surfaces of the coatings. A Bruker Vertex 70 with Harrick's ATR™ accessory using a hemispherical Ge crystal was utilized to collect ATR-FTIR spectra for a coating.

A Thermo Scientific™ K-Alpha™ X-ray photoelectron spectrometer (XPS) was used to determine the elemental composition of coatings. The instrument was equipped with monochromatic Al K_α (1486.68 eV) X-ray source and Ar^+ ion source (up to 4000 eV) was utilized for the XPS experiments. Depth profiling of a coating was evaluated using Ar^+ etching with 30 etch cycles. For each etch cycle, the

ion beam was set to 1,000 eV Monatomic Mode with low current and 30 s etch time. After each etching cycle, survey spectra in 5 replicates were collected at low resolution with a constant analyzer pass energy of 200 eV for a total of 20 ms. For each run, photoemission lines for C1s, N1s, O1s, and Si2p were observed. Spectra were collected at an angle normal to the surface (90°) of a 400-µm area. The chamber pressure was maintained below 1.5 x 10^{-7} torr and samples were analyzed at ambient temperature. Atomic concentrations were quantified by the instrument's software as a representation of the atomic intensities as a percentage of the total intensity of all elements. Two internal PU system without (pure PU) and with Amp-1 additive (modified PU) were examined to verify self-stratification of AmpAdd additives into the surface of coatings.

Atomic force microscopy (AFM) was utilized to receive insights about the surface topography of the studied coatings. A Dimension 3100 microscope with Nanoscope controller scanned the surface of experimental coatings, collecting images on a sample area of 100 µm x 100 µm in the tapping mode. The experiment condition was in air under ambient conditions, using a silicon probe with a spring constant (0.1-0.6 N/m) and resonate frequency (15-39 kHz). For each surface, three replicates at varying spots were collected to ensure consistency and accuracy of the data.

Water Aging

All the prepared coatings were pre-leached for 28 days in running tap water. The water tanks were equipped to automatically fill and empty every 4 hours. Water aging of the coatings is carried out to leach out any impurities that may interfere with fouling-release assessments and to determine stability of coatings and surface rearrangements. All biological laboratory assays were carried out after the pre-leaching water aging process was completed.

Biological Laboratory Assays

Growth and Release of Macroalgae (*Ulva linza*)

A set of multiwall plates was sent to Newcastle University, following water-immersion for 28 days, to evaluate fouling-release performance of coatings against *U. linza*. The detailed description about the assessment can be found elsewhere.[41] Briefly, after leaching collection, all multiwall plates were equilibrated in 0.22 µm filtered artificial seawater for 2 hours at Newcastle. To each well, 1 mL spores of *U. linza* suspension was added, adjusted to 3.3 x 10^5 spores/mL (0.05 OD at absorbance 660 nm) in

double strength enriched seawater. Spores settled on the discs were grown for 7 days inside an illuminated incubator at 18°C with a 16:8 light: dark cycle (photon flux density 45 μmol.m^{-2}.s^{-1}). There was no washing to remove unsettled spores after settlement. After 7 days, the biomass generated was assessed from a single row of wells (6) from each plate. The chlorophyll was extracted by adding 1 mL DMSO to each water-pressured well (water pressure of 67 kPa) and followed by measuring the fluorescence at 360 nm excitation and 670 nm emission. Fluorescence is directly proportional to the biomass present on each coating surface. The removal of *U. linza* at each pressure was compared with the unsprayed wells that were used to determine initial growth.

Bacterial (*Cellulophaga lytica*) Biofilm Adhesion

Fouling-release properties towards bacteria was evaluated using retention and adhesion assays described previously.[42-44] Briefly, a solution of the marine bacterium *Cellulophaga lytica* at 10^7 cells/mL concentration in artificial seawater (ASW) containing 0.5 g/L peptone and 0.1g/L yeast extract was deposited into 24-well plates (1 mL/well). The plates were then incubated statically at 28°C for 24 hours. The ASW growth medium was then removed and the coatings were subjected to water-jet treatments. The first column of each coating was not treated and served as the initial amount of bacterial biofilm growth. The second and third columns were subjected to water-jetting at 10 psi and 20 psi, respectively, for 5 seconds. Following water-jet treatments, the coating surfaces were stained with 0.5 mL of a crystal violet solution (0.3 wt. % in deionized water) for 15 minutes and then rinsed three times with deionized water. After 1 hour of drying at ambient laboratory conditions, the crystal violet dye was extracted from the coating surfaces by adding 0.5 mL of 33% acetic acid solution for 15 minutes. The resulting eluates were transferred to a 96-well plate (0.15 mL/coating replicate) and subjected to absorbance measurements at 600 nm wavelength using a multi-well plate spectrophotometer. The absorbance values were directly proportional to the amount of bacterial biofilm present on coating surfaces before and after water-jetting treatments. Percent removal of bacterial biofilm was quantified by comparing the mean absorbance values of the non-jetted and water-jetted coating surfaces.[33]

Growth and Release of Microalgae (*Navicula incerta*)

Laboratory biological assay diatom (*Navicula incerta*) was conducted at NDSU following a similar procedure described previously.[1, 41, 45] Briefly, a suspension with 4×10^5 cells/mL of *N. incerta* (adjusted to

0.03 OD at absorbance 660 nm) in Guillard's F/2 medium was deposited into each well (1 mL per well) and cell attachment was stimulated by static incubation for 2 hours under ambient conditions in the dark. Coating surfaces were then subjected to water-jet treatments.[43] First column of wells was not water-jetted so that initial cell attachment could be determined and the next two-column of wells were water-jetted at 10 psi and 20 psi, respectively, for 10 seconds. Microalgae biomass was quantified by extracting chlorophyll using 0.5 mL of DMSO and measuring fluorescence of the transferred extracts at an excitation wavelength of 360 nm and emission wavelength at 670 nm. The relative fluorescence (RFU) measured from the extracts was considered to be directly proportional to the biomass remaining on the coating surfaces after water-jetting. Percent removal of attached microalgae was determined using relative fluorescence of non-jetted and water-jetted wells.

Adult Barnacle (*Amphibalanus amphitrite*) Adhesion

Adult barnacle reattachment test was carried out to assess fouling-release of coatings against macrofoulants.[46, 47] Coatings prepared on 4" x 8" panels after water aging were utilized for this laboratory assay. Barnacles were dislodged from silicone substrates sent from Duke University and immobilized on experimental coatings (6 barnacles per coating) using a custom-designed immobilization template. The immobilized barnacles were allowed to reattach and grow for 2 weeks while immersed in an ASW aquarium tank system with daily feedings of brine shrimp *Artemia* nauplii (Florida Aqua Farms). After the 2-week attachment period, the number of non-attached barnacles was recorded, and the attached barnacles were pushed off (in shear) using a hand-held force gauge mounted onto a semi-automated stage. Once the barnacles were dislodged, their basal plate areas were determined from scanned images using Sigma Scan Pro 5.0 software program. Barnacle adhesion strength (MPa) was calculated by taking the ratio of peak force of removal to the basal plate area for each reattached barnacle. To ensure consistency, barnacles of similar sizes were tested. The average barnacle adhesion strength for each coating was reported as a function of the number of barnacles released with a measurable force and that exhibited no visible damage to the basis or shell plates. Due to limited source of barnacles, three formulations that ranged in terms of hydrophobicity and hydrophilicity were evaluated to grasp an overall picture for all formulations.

Results and Discussions

Contending with marine biofouling of possibly 4000 organisms has proven to be very complex, considering the requirements to have effective, durable and non-toxic coating systems. One of the primary approaches after the ban of TBT-based marine coatings shifted towards hydrophobic fouling-release (FR) coatings. Despite hydrophobic FR coatings like silicone elastomers or SiPU A4 offer relatively desirable performance, they lack the ability to prevent strong settlement of biofoulants that prefer settling on hydrophobic surfaces. Amphiphilic additives, containing hydrophilic and hydrophobic segments, are sought as a solution to improve the performance of hydrophobic FR coatings against a wider range of organisms. Thus, we prepared and investigated a series of amphiphilic additives (AmpAdd) in this study to obtain better performance of hydrophobic A4 system. The AmpAdds in this study were composed of a polyisocyanate that was modified with chains of 10,000 $\bar{M}_n$ PDMS and 750 $\bar{M}_n$ PEG. These molecular weights of PEG and PDMS were chosen due to their optimal FR performance, following reported literature and our previous works.

The AmpAdds were prepared by reacting OH-terminated PEG and PDMS with the IPDI-based polyisocyanate. The complete disappearance of the isocyanate groups via FTIR and isocyanate titration confirms the formation of urethane linkage and attachment of the amphiphilic chains. FTIR spectra of all five AmpAdds shows the disappearance of the isocyanate signal at 2250 cm^{-1} and a broadened stretching for secondary amine (from the formed urethane linkage) at 3350 cm^{-1} (Figure 4.2), confirming the complete transformation of the available isocyanate groups. Furthermore, the presence of Si-O-Si signal at 1035 cm^{-1} (Figure 4.2; highlighted red) and C-O-C at 1105 cm^{-1} (Figure 4.2; highlighted green) confirm the attachment of PEG and PDMS chains on the additives. The intensity ratio of Si-O-Si and C-O-C peaks changed with the type of AmpAdd. As more amount of PEG was attached on an additive, the ether peak appeared stronger while the siloxane peak became less visible until it completely vanished in Amp-5 (which contained only PEG chains). The FTIR data validates the changes in weight ratio of attached amphiphilic chains resulted in a new additive. Additionally, isocyanate titrations on the synthesized additives showed presence of no remaining isocyanate group. The synthesis was carried out using dried toluene to prevent reaction of isocyanates with water.

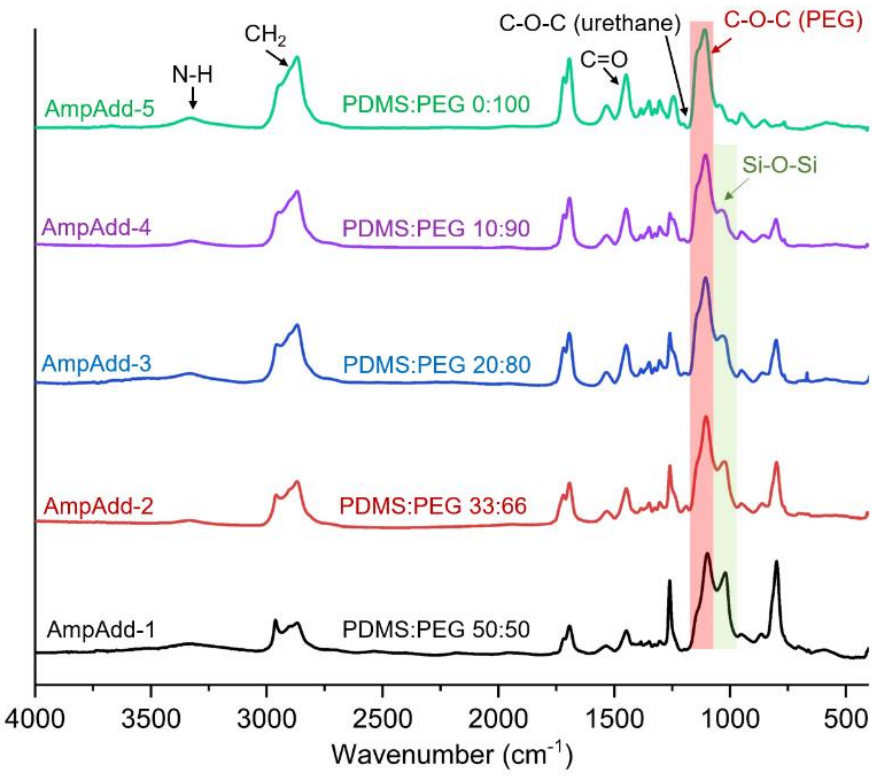

Figure 4.2. FTIR spectra for the five amphiphilic additives. Each spectrum is labeled with the additive ID and its PEG and PDMS compositional ratio.

The surface of coatings was characterized with ATR-FTIR, contact angle measurements, and AFM, while the self-stratification of additives was confirmed with XPS using control coatings. ATR-FTIR of Amp-modified A4 systems show the signal for C-O-C of PEG at 1100 cm^{-1} that is absent for the unmodified A4 coating (Figure 4.3; red highlight). The intensity of the Si-O-Si peak at 1016 cm^{-1} also increases with the addition of AmpAdds. The relative intensity of ether and siloxane peaks correlates with the types of utilized AmpAdd. For example, F1 (having Amp-1) displayed a strong siloxane signal, while F5 (having Amp-5) exhibited the strongest ether (of PEG) signals among all coatings. The remaining signature peaks were present among all systems including ether of urethane (from additives and crosslinked coating) at 1160 cm^{-1}, carboxyl at 1688-1727 cm^{-1}, and urethane NH at 3365 cm^{-1}.

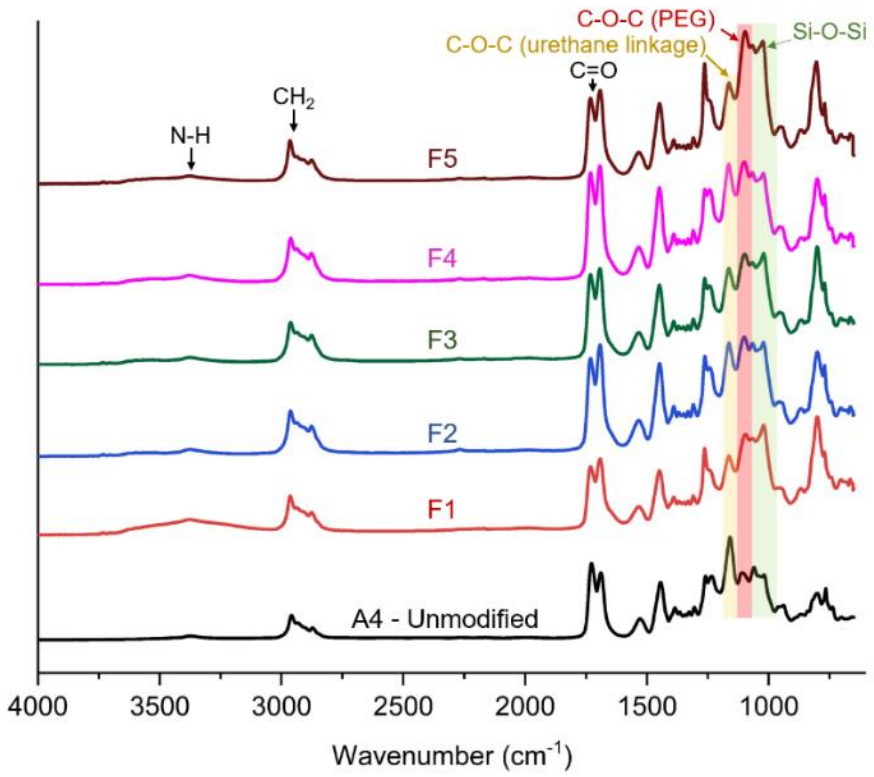

Figure 4.3. ATR-FTIR of the unmodified and modified A4 coatings. Green, red, and yellow highlights reflect the peaks of interest for siloxane, ether (from PEG), and ether (from urethane linkage), respectively. Each spectrum is labeled to reflect the formulation type.

Static and dynamic contact angle measurements were carried out to evaluate interaction of water and diiodomethane with the prepared FR surfaces. The static contact angles surveyed droplets on the coatings over 9 minutes (after this the collected values plateaued). The A4 system did not present any significant changes in water contact angles (WCA) and diiodomethane contact angles (MICA) over time, while Amp-modified A4 coatings demonstrated a decrease in WCAs and MICAs (Figure 4.4A). This dynamic change of contact angles as a function of time is similar to the control amphiphilic T-10, suggesting the hydrophilic domains on the surface of modified SiPU A4 (from added amphiphilic additives) swell upon exposure to water droplet and allow the droplet to spread more on the surface. The comparison of formulations indicate WCAs drops more over time as higher amount of hydrophilicity is introduced in a system, and also the change in values was more noticeable for WCAs than MICAs. Surface energies for the coatings were calculated using WCAs and MICAs (Figure 4.4B). The additives

resulted in a considerable increase in surface energies for the modified coatings in comparison to the unmodified A4. The surface energy (SE) for the Amp-modified coatings initially ranged around 40-50 mN/m and increased by 5-10 mN/m over nine minutes (except F5 coating), while original A4 displayed a relatively stable SE around 27-30 mN/m (which is a typical value for PDMS rich surfaces). Unlike the other modified formulations, F5 showed contact angles and surface energies similar to amphiphilic T-10 control. This different behavior is attributed to similar composition of F5 and T-10 since both contain equal contents of PEG and PDMS. The dynamic WCA experiments using a tilting stage showed that the slip angle (water droplet roll-off angle) of the original A4 significantly decreases upon the introduction of the amphiphilic additives, from 9 degrees to 2-3 degrees (Figure 4.4C). Once the PEG and PDMS balance was equalized in the F5 system, its slip angle was comparable to the amphiphilic T-10 control. Overall, the decreased roll-off data indicates that amphiphilic additives improve the capability of A4 system to remove objects from its surface. Advancing contact angles (Adv CA) and receding contact angles (Rec CA) for the modified A4s (except F5) were in a significantly lower range (around 40-60 degrees) than unmodified A4 coating (95-105 degrees), while F5 system again displayed a behavior similar to T-10 (Figure 4.4D). The low contact angles of modified coatings imply the presence of hydrophilic domains on the surfaces. Typically, a hysteresis lower than 10 degrees is desirable as it is sign of a smooth surface which all the coatings are shown to be, accordingly. After-immersion contact angles (28 days water aging) showed both slightly increasing and decreasing trends (Figure A15). For example, coatings A4 and F5 showed a decrease for WCAs, and the remaining coatings showed an increase for WCAs. The changes may be related to several factors including water absorption, rearrangements of non-bounded amphiphilic domains, and possible leaching of the additives.

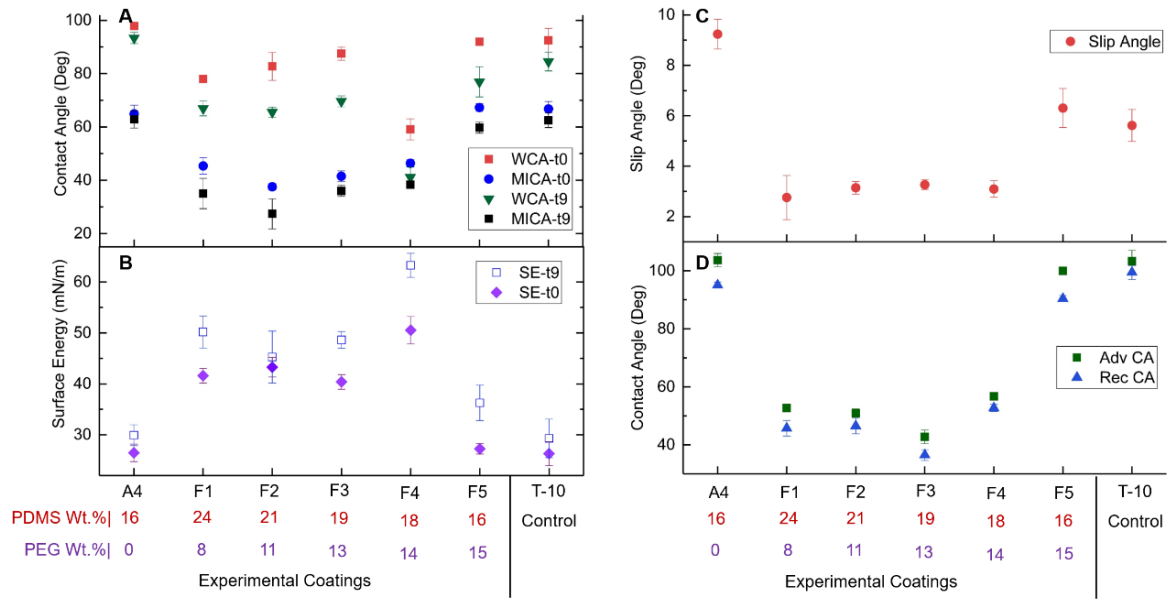

Figure 4.4. Contact angle and surface energy data for coatings. (A) Water Contact Angles (WCA) and methylene iodide contact angles (MICA) as a function of time at 0 minutes and 9 minutes; (B) Surface energy (SE) of coatings at 0 minute and 9 minutes, calculated by Owens-Wendt method utilizing the average WCAs and MICAs for each coating; (C) Slip angle of coatings where a water droplet starts to roll off; (D) Advancing contact angle (Adv CA) and receding contact angle (Rec CA) data, measured by tilting method. T-10 is the internal coating for comparison. The X-axis is labeled to reflect overall content of PEG and PDMS in a formulation.

AFM was employed to capture how the addition of additives modified the morphology of the A4 system on its surface (Figure 4.5). Generally, soft materials like PDMS appear lighter (high phase angles) and harder materials like PEG will appear darker (low phase angles). The A4 system displayed a homogenous surface with no apparent domains which is due to its surface composition being solely PDMS. The additives resulted in the appearance of evident domains on the surface of the modified A4 coatings. (A high-quality AFM image for F5 coating could not be captured due to its surface limitations and noise after many trials, but we could observe the presence of similar domains in partial parts of the images.) The additively-modified A4 coatings possessed a morphology which was comparable to the amphiphilic T-10 control system, confirming the presence of amphiphilic domains on the surface.[18] The morphologies differed among the studied coatings which was potentially related to the type of added additives. As the amount of hydrophilicity in an additive increased, the surface domains appeared to be smaller and well-distributed throughout the surface. This trend can be observed from coatings F1 and F2

to coatings F3 and F4. Furthermore, AFM images were recorded for the coatings after 28 days of water immersion (these images were very hard to capture). As expected from the post-immersion contact angle data, the AFM images supported rearrangement of the domains but there was no remarkable decrease of the domains from the surfaces (Figure A16). The AFM images support the ATR-FTIR data and contact angle measurements that AmpAdds are present on the surface and contribute to the dynamic interaction of the surfaces with assessed droplets.

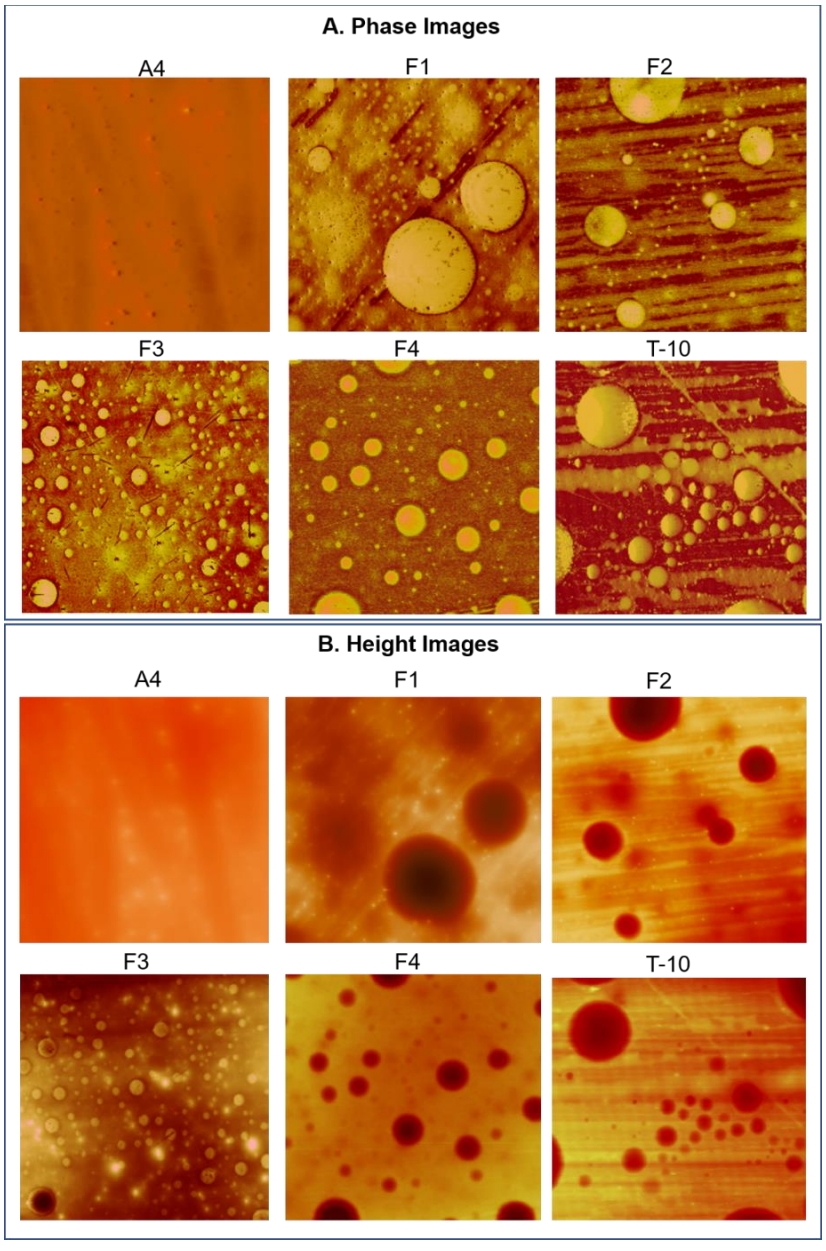

Figure 4.5. AFM phase images (Upper box) and height images (bottom box) of unmodified and modified SiPU A4 and T-10 coatings. Each image is for an area of 100 µm x 100 µm. Each label reflects the coating number.

XPS experiments was used to validate the self-stratification of the amphiphilic additives on the surface of coatings. Initially, the XPS measurements were carried out on modified and unmodified A4 as a function of depth; however, the analysis did not offer substantial conclusions due to difficulties in distinguishing between contents of Si atom from additives and the A4 formulation itself. To this effect, an internal model PU system was utilized to validate diffusion of the additives into the surface. The model PU system was the A4 formulation without amine-terminated PDMS in its composition, and for the validation purpose, Amp-1 was added to the model PU formulation at 20 wt.%. The depth profiling XPS analysis of the model formulations (PU and the Amp-modified PU) confirms that the amphiphilic additives self-stratified into the surface (Figure 4.6). For model PU, concentration of carbon, oxygen, and nitrogen atoms was almost constant throughout the coating, signaling a homogenous network in terms of elemental composition (Figure 4.6A). Alternatively, the model modified PU system contained Si atom (due to the addition of Amp-1) on its surface which gradually dropped as a function of depth, while elemental compositions of carbon and nitrogen increased (related to the bulk of the coating). Therefore, the XPS data substantiated self-stratification of the additives that resulted in amphiphilic surfaces, consistent with data from ATR-FTIR, contact angle assessments, and AFM.

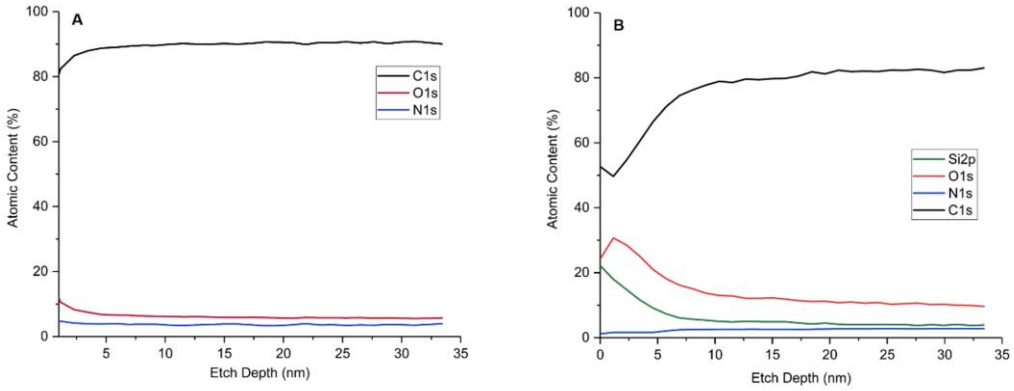

Figure 4.6. XPS data of model PU coatings. (A) XPS depth profiling data for unmodified PU coating; (B) XPS depth profiling data for PU coating containing 20 wt.% Amp-1.

A series of representative marine organism were evaluated on the surfaces of studied and control coatings to determine their fouling-release properties. All the evaluations were conducted after 28 days of water aging. The coatings were assessed for leachate toxicity using *C. lytica*, *N. incerta*, and *U. Linza* as

discussed elsewhere.[41, 48] The leachates from all coatings were non-toxic, allowing for valid fouling-release experiments.

U. Linza is a biofouling macroalgae that prefers to settle on hydrophobic surfaces more than hydrophilic surfaces.[49-51] The extent of *U. linza* biofouling settlement for all systems was relatively same. The biofouled surfaces were water-jetted at two pressure levels and the percent removal/release was plotted at 10 psi (Figure 4.7 – Blue bars) and 16 psi (Figure 4.7 – Green bars). The release trend was similar among coatings at both pressure levels but, not surprisingly, the 16-psi pressure level released more *U. linza* from the surfaces. The introduction of AmpAdds to A4 improved its fouling-release performance as it is evident at both 10 psi and 16 psi (comparing A4 with F1-F5). The extent of release for Amp-modified coatings at 10 psi was very similar, while the extent of release varied among coatings at 16 psi: Coating F3 outperformed all the studied coatings and offered almost 50% improvement. Comparing the performance of coatings with internal and commercial controls indicated that the addition of AmpAdd contributed to desirable performance and boosted the *U. linza* release to be comparable or better than the controls. Coatings F1, F3, F4, and F5 outperformed the well-performing amphiphilic T-10, and coating F2 displayed a comparable performance. Coating F3 also demonstrated a relatively matching performance with commercial paints, namely T2 and 1100 SR. Despite converting the hydrophobic A4 system to an amphiphilic system was attainable and beneficial to A4, the data does not exhibit a noticeably different performance against *U. linza* based on the level of amphiphilic balance (comparing coatings F1-F5 among each other). Overall, the fouling-release data of *U. linza* implies that the addition of amphiphilic additives delivers an advantageous edge to the hydrophobic SiPU A4 system.

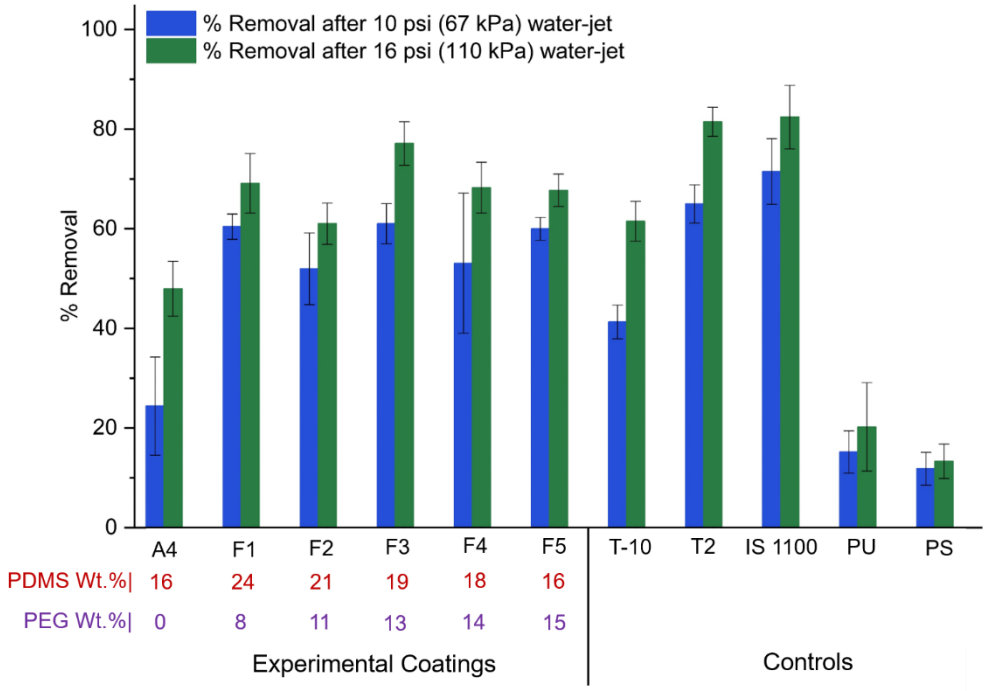

Figure 4.7. *U. linza* fouling-release data for percent removal/release at 10 psi waterjet (blue bar) and at 16 psi waterjet (green bar). The X-axis is labeled to reflect overall content of PEG and PDMS in a formulation. Each category of assessed coatings is separated with lines.

C. lytica is a micro-biofoulant with an affinity to settle on a wide range of surfaces, ranging from hydrophilic to hydrophobic,[2] and amphiphilic surfaces have shown to be a good deterrent against this organism.[18] The biofouling experiments of *C. lytica* showed a relatively similar extent of biofouling among all formulations and control coatings. The biofouled samples were water-jetted at two pressure levels and the percent removal/release of *C. lytica* film was plotted for 10 psi (Figure 4.8 – blue bars) and 20 psi (Figure 4.8 – green bars) water jetting. The higher water pressure level released more *C. lytica*, but the overall trend among the coatings remained unchanged. The addition of Amp-1 and Amp-2 was detrimental to FR performance of A4 (formulations F1 and F2). This undesirable performance may be due to increasing the overall hydrophobic content of the systems (A4 is already hydrophobic) while the hydrophilic content is relatively low for these additives. However, the FR performance for Amp-modified systems improved with adding additives that contain more hydrophilic content, resulting in more amphiphilicly balanced systems. Coatings F4 and F5 remarkably delivered better performance than A4 while coating F3 offered a matching performance to A4. Coatings F4 and F5 contained almost equal

amounts of PEG and PDMS in their composition after adding the AmpAdd additives. The well-balanced amphiphilic systems outperformed the internal amphiphilic control T-10. Also, the performance of F4 and F5 systems matched the top-performing commercial paints such as IS 900 and IS 1100 and outperformed all the other assessed controls. The *C. lytica* data clearly implies the balance of amphiphilicity matters for a coating to offer desirable FR performance. The more balanced the hydrophilic and hydrophobic contents, the more appealing FR performance. Overall, the fouling-release data of *C. lytica* entails that the addition of amphiphilic additives improves the performance of a hydrophobic A4 system.

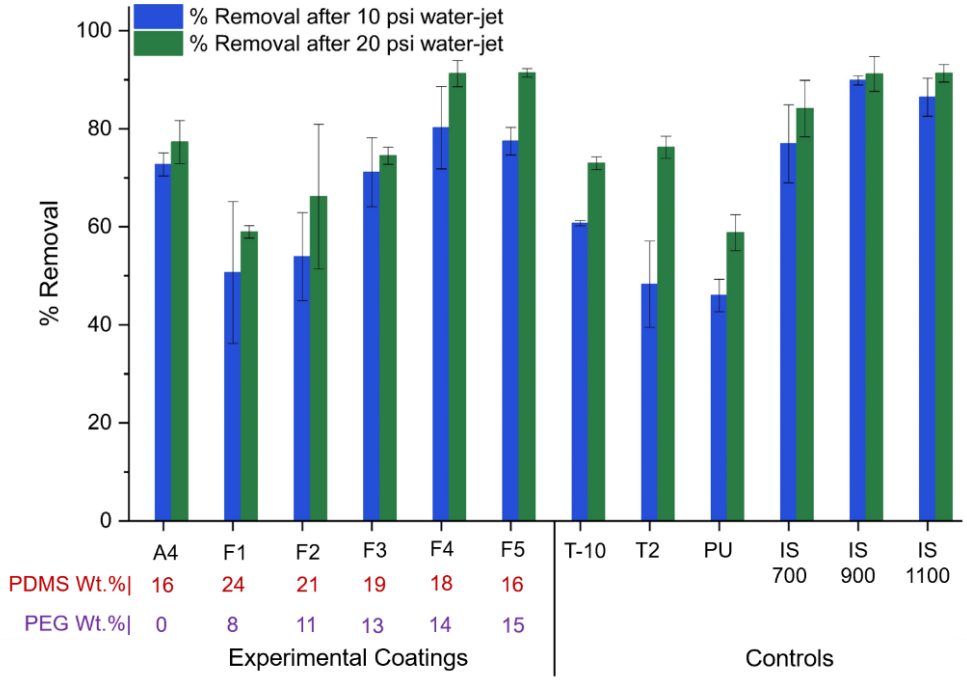

Figure 4.8. *C. lytica* fouling-release data for percent removal/release at 10 psi waterjet (blue bar) and at 20 psi waterjet (green bar). The X-axis is labeled to reflect overall content of PEG and PDMS in a formulation. Each category of assessed coatings is separated with lines.

N. incerta is a recognized biofouling organism that prefers to settle on hydrophobic surfaces.[49, 50] The extent of *N. incerta* biofouling was in a similar range for all the studied and control coatings. Similar to *C. lytica* and *U. linza*, the biofouled surfaces with *N. incerta* were water-jetted at two pressure levels and percent removal/release of *N. incerta* film was reported at 10 psi (Figure 4.9 – blue bars) and 20 psi (Figure 4.9 – green bars). The addition of AmpAdd additives improved the FR performance of the A4 system. The improvements were relatively small at 10 psi for almost all modified coatings (except for F2

coating), while they were observable at 20 psi for all coatings. The FR performance of modified coatings appeared to be slightly better when more amphiphilic balance was met in a system – coatings F2, F3, and F5 showed better performance than the other formulations. These systems offered a matching performance to internal PU and IS 700 commercial coating but were not as good as IS 900 and IS 1100. The *N. incerta* data reveals introducing amphiphilicity to hydrophobic A4 system did contribute to better performance; however, there is no meaningful indication that a particular amphiphilic balance will be preferred over another.

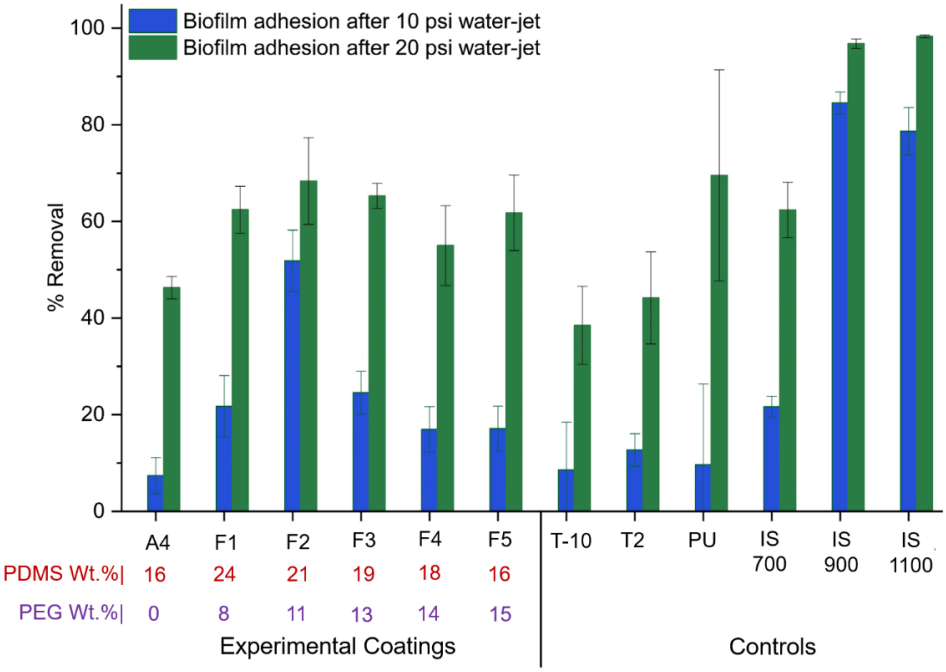

Figure 4.9. *N. incerta* fouling-release data for percent removal/release at 10 psi waterjet (blue bar) and at 20 psi waterjet (green bar). The x-axis is labeled to reflect overall content of PEG and PDMS in a formulation. Each category of assessed coatings is separated with lines.

Macrofouling organisms such as barnacles and mussels are major marine biofouling organisms.[4, 47, 52] Different species of barnacle have different affinities for surfaces, thus it is challenging to propose an underlying rule.[2, 53-56] For example, *Amphibalanus amphitrite* settles on hydrophilic surfaces as well as hydrophobic surfaces.[46, 47, 57, 58] The introduction of AmpAdds has both detrimental and beneficial results for the hydrophobic SiPU A4 system (Figure 4.10). The data showed when an additive solely introduced hydrophilic content to the A4 formulation without adding more hydrophobicity (i.e. Amp-5), this additive

delivered a theoretically well-balanced amphiphilic surface that reduced the adhesion strength of barnacles, which is in correlation with other published results.[18] When amphiphilic balance was more equal in a coating system (i.e. not highly hydrophobic like F1), the FR performance against barnacles was better, improving from F1 to F3 to F5 where the formulations are in order from the least amphiphilicly balanced system to the most amphiphilicly balanced system. The amphiphilic surfaces did not significantly reduce number of reattached barnacles on a surface. Overall, this data indicated that the amphiphilic balance of coatings on the surface plays a major role on its FR performance; thus, it is crucial to introduce such additives to A4 SiPU and other similar hydrophobic systems that do not increase the overall hydrophobicity (because it suppresses the sought effect of introduced hydrophilicity it).

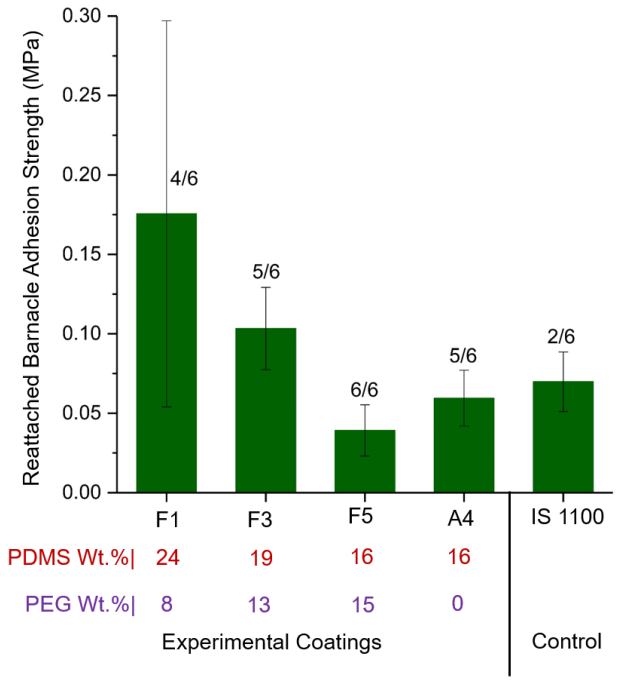

Figure 4.10. Reattached barnacle (*A. Amphitrite*) adhesion strength data. Six barnacles were used for each reattachment study. The number of reattached barnacles out of six is labeled for each system as a ratio. Each bar shows the average adhesion strength based on the number of successfully reattached barnacles. The x-axis is labeled to reflect overall content of PEG and PDMS in a formulation. Each category of assessed coatings is separated with lines.

Conclusions

This study investigated the synthesis of a series of amphiphilic additives by installing PEG and PDMS chains on a polyisocyanate via a facile and easily scalable procedure. The additives were prepared with differences in their amphiphilicity extent, ranging from the least hydrophilic to most

hydrophilic. This study demonstrated that a hydrophobic marine coating can be converted to a desirably performing amphiphilic coating by utilizing amphiphilic additives. The introduction of AmpAdds into the A4 system resulted in an amphiphilic surface as supported by ATR-FTIR, AFM, XPS, and contact angle measurements. ATR-FTIR showed the presence of both PEG and PDMS signals. AFM presented formation of heterogenous microdomains that were missing from the surface of original A4 coating. XPS analysis demonstrated that the additives did self-stratify into the surface of a model coating system, providing an amphiphilic surface, while contact angle measurements supported the presence of amphiphilicity through the dynamic interaction of modified surfaces with assessed droplets. Biological assays strongly supported that the AmpAdds improved FR performance of the SiPU A4 systems and did not have detrimental effects. Generally, fouling-release assessments against *C. lytica, N. incerta, U. linza*, and barnacles suggested coating systems that are well-balanced in terms of PEG and PDMS amount in their composition (i.e. ~15 wt.% PEG and PDMS each in a formulation) performed better than systems that were mainly hydrophobic (i.e. 24 wt.% PDMS and 8 wt.% PEG in a formulation). The FR performance of modified A4 coating systems was in most cases better than or comparable to top-performing commercial marine paints.

References

1. Callow, J. A.; Callow, M. E., Trends in the development of environmentally friendly fouling-resistant marine coatings. *Nature Communications* **2011,** *2* (1), 244-244.

2. Lejars, M.; Margaillan, A.; Bressy, C., Fouling release coatings: A nontoxic alternative to biocidal antifouling coatings. *Chemical Reviews* **2012,** *112* (8), 4347-4390.

3. Beigbeder, A.; Mincheva, R.; Pettitt, M. E.; Callow, M. E.; Callow, J. A.; Claes, M.; Dubois, P., Marine fouling release silicone/carbon nanotube nanocomposite coatings: on the importance of the nanotube dispersion state. *Journal of Nanoscience and Nanotechnology* **2010,** *10* (5), 2972-2978.

4. Callow, M. E.; Callow, J. E., Marine biofouling: a sticky problem. *Biologist* **2002,** *49* (1), 10-14.

5. Yebra, D. M.; Kiil, S.; Dam-Johansen, K., Antifouling technology—past, present and future steps towards efficient and environmentally friendly antifouling coatings. *Progress in Organic Coatings* **2004,** *50* (2), 75-104.

6. Magin, C. M.; Cooper, S. P.; Brennan, A. B., Non-toxic antifouling strategies. *Materials Today* **2010,** *13* (4), 36-44.

7. Pade, M.; Webster, D. C., Self-stratified siloxane-polyurethane fouling-release marine coating strategies: A review. In *Marine Coatings and Membranes*, Mittal, V., Ed. Central West Publishing: Australia, 2019; pp 1-36.

8. Konstantinou, I. K.; Albanis, T. A., Worldwide occurrence and effects of antifouling paint booster biocides in the aquatic environment: a review. *Environment International* **2004,** *30* (2), 235-248.

9. Wyszogrodzka, M.; Haag, R., Synthesis and characterization of glycerol dendrons, self-assembled monolayers on gold: A detailed study of their protein resistance. *Biomacromolecules* **2009,** *10* (5), 1043-1054.

10. Selim, M. S.; El-Safty, S. A.; Azzam, A. M.; Shenashen, M. A.; El-Sockary, M. A.; Abo Elenien, O. M., Superhydrophobic silicone/TiO2–SiO2 nanorod-like composites for marine fouling release coatings. *ChemistrySelect* **2019,** *4* (12), 3395-3407.

11. Sommer, S.; Ekin, A.; Webster, D. C.; Stafslien, S. J.; Daniels, J.; VanderWal, L. J.; Thompson, S. E. M.; Callow, M. E.; Callow, J. A., A preliminary study on the properties and fouling-release performance of siloxane–polyurethane coatings prepared from poly(dimethylsiloxane) (PDMS) macromers. *Biofouling* **2010,** *26* (8), 961-972.

12. Bodkhe, R. B.; Thompson, S. E. M.; Yehle, C.; Cilz, N.; Daniels, J.; Stafslien, S. J.; Callow, M. E.; Callow, J. A.; Webster, D. C., The effect of formulation variables on fouling-release performance of stratified siloxane–polyurethane coatings. *Journal of Coatings Technology and Research* **2012,** *9* (3), 235-249.

13. Bodkhe, R. B.; Stafslien, S. J.; Cilz, N.; Daniels, J.; Thompson, S. E. M.; Callow, M. E.; Callow, J. A.; Webster, D. C., Polyurethanes with amphiphilic surfaces made using telechelic functional PDMS having orthogonal acid functional groups. *Progress in Organic Coatings* **2012,** *75* (1-2), 38-48.

14. Iguerb, O.; Poleunis, C.; Mazéas, F.; Compère, C.; Bertrand, P., Antifouling properties of poly(methyl methacrylate) films grafted with poly(ethylene glycol) monoacrylate immersed in seawater. *Langmuir* **2008,** *24* (21), 12272-12281.

15. Rath, S. K.; Chavan, J. G.; Ghorpade, T. K.; Patro, T. U.; Patri, M., Structure–property correlations of foul release coatings based on low hard segment content poly (dimethylsiloxane–urethane–urea). *Journal of Coatings Technology and Research* **2018,** *15* (1), 185-198.

16. Yi, L.; Xu, K.; Xia, G.; Li, J.; Li, W.; Cai, Y., New protein-resistant surfaces of amphiphilic graft copolymers containing hydrophilic poly (ethylene glycol) and low surface energy fluorosiloxane side-chains. *Applied Surface Science* **2019,** *480*, 923-933.

17. Zhang, Z.-P.; Song, X.-F.; Cui, L.-Y.; Qi, Y.-H., Synthesis of polydimethylsiloxane-modified polyurethane and the structure and properties of its antifouling coatings. *Coatings* **2018,** *8* (5), 157-157.

18. Galhenage, T. P.; Webster, D. C.; Moreira, A. M. S.; Burgett, R. J.; Stafslien, S. J.; Vanderwal, L.; Finlay, J. A.; Franco, S. C.; Clare, A. S., Poly(ethylene) glycol-modified, amphiphilic, siloxane–polyurethane coatings and their performance as fouling-release surfaces. *Journal of Coatings Technology and Research* **2017,** *14* (2), 307-322.

19. Claisse, D.; Alzieu, C., Copper contamination as a result of antifouling paint regulations? *Marine Pollution Bulletin* **1993,** *26* (7), 395-397.

20. Turner, A., Marine pollution from antifouling paint particles. *Marine Pollution Bulletin* **2010,** *60* (2), 159-171.

21. Pérez, M.; Blustein, G.; García, M.; del Amo, B.; Stupak, M., Cupric tannate: a low copper content antifouling pigment. *Progress in Organic Coatings* **2006,** *55* (4), 311-315.

22. Cai, L.; Liu, A.; Yuan, Y.; Dai, L.; Li, Z., Self-assembled perfluoroalkylsilane films on silicon substrates for hydrophobic coatings. *Progress in Organic Coatings* **2017,** *102*, 247-258.

23. Pollack, K. A.; Imbesi, P. M.; Raymond, J. E.; Wooley, K. L., Hyperbranched fluoropolymer-polydimethylsiloxane-poly(ethylene glycol) cross-linked terpolymer networks designed for marine and biomedical Applications: heterogeneous nontoxic antibiofouling surfaces. *ACS Applied Materials & Interfaces* **2014,** *6* (21), 19265-19274.

24. Noguer, A. C., *Experimental investigation of the behaviour and fate of block copolymers in fouling-release coatings*. Technical University of Denmark (DTU): Kgs. Lyngb, Denmark, 2016.

25. Murthy, R.; Bailey, B. M.; Valentin-Rodriguez, C.; Ivanisevic, A.; Grunlan, M. A., Amphiphilic silicones prepared from branched PEO-silanes with siloxane tethers. *Journal of Polymer Science Part A: Polymer Chemistry* **2010,** *48* (18), 4108-4119.

26. Martinelli, E.; Suffredini, M.; Galli, G.; Glisenti, A.; Pettitt, M. E.; Callow, M. E.; Callow, J. A.; Williams, D.; Lyall, G., Amphiphilic block copolymer/poly (dimethylsiloxane)(PDMS) blends and nanocomposites for improved fouling-release. *Biofouling* **2011,** *27* (5), 529-541.

27. Røn, T.; Javakhishvili, I.; Hvilsted, S.; Jankova, K.; Lee, S., Ultralow friction with hydrophilic polymer brushes in water as segregated from silicone matrix. *Advanced Materials Interfaces* **2016,** *3* (2), 1500472.

28. Rufin, M. A.; Barry, M. E.; Adair, P. A.; Hawkins, M. L.; Raymond, J. E.; Grunlan, M. A., Protein resistance efficacy of PEO-silane amphiphiles: Dependence on PEO-segment length and concentration. *Acta biomaterialia* **2016,** *41*, 247-252.

29. Shivapooja, P.; Yu, Q.; Orihuela, B.; Mays, R.; Rittschof, D.; Genzer, J.; López, G. P., Modification of silicone elastomer surfaces with zwitterionic polymers: short-term fouling resistance and triggered biofouling release. *ACS Applied Materials & Interfaces* **2015,** *7* (46), 25586-25591.

30. Liu, Y.; Leng, C.; Chisholm, B.; Stafslien, S.; Majumdar, P.; Chen, Z., Surface structures of PDMS incorporated with quaternary ammonium salts designed for antibiofouling and fouling release applications. *Langmuir* **2013,** *29* (9), 2897-2905.

31. Wan, F.; Pei, X.; Yu, B.; Ye, Q.; Zhou, F.; Xue, Q., Grafting polymer brushes on biomimetic structural surfaces for anti-algae fouling and foul release. *ACS Applied Materials & Interfaces* **2012,** *4* (9), 4557-4565.

32. Yeh, S.-B.; Chen, C.-S.; Chen, W.-Y.; Huang, C.-J., Modification of silicone elastomer with zwitterionic silane for durable antifouling properties. *Langmuir* **2014,** *30* (38), 11386-11393.

33. Ciriminna, R.; Bright, F. V.; Pagliaro, M., Ecofriendly antifouling marine coatings. *ACS Sustainable Chemistry & Engineering* **2015,** *3* (4), 559-565.

34. Galhenage, T. P.; Hoffman, D.; Silbert, S. D.; Stafslien, S. J.; Daniels, J.; Miljkovic, T.; Finlay, J. A.; Franco, S. C.; Clare, A. S.; Nedved, B. T., Fouling-release performance of silicone oil-modified siloxane-polyurethane coatings. *ACS Applied Materials & Interfaces* **2016,** *8* (42), 29025-29036.

35. Wei, C.; Zhang, G.; Zhang, Q.; Zhan, X.; Chen, F., Silicone oil-infused slippery surfaces based on sol–gel process-induced nanocomposite coatings: A facile approach to highly stable bioinspired surface for biofouling resistance. *ACS Applied Materials & Interfaces* **2016,** *8* (50), 34810-34819.

36. Kavanagh, C. J.; Swain, G. W.; Kovach, B. S.; Stein, J.; Darkangelo-Wood, C.; Truby, K.; Holm, E.; Montemarano, J.; Meyer, A.; Wiebe, D., The effects of silicone fluid additives and silicone elastomer matrices on barnacle adhesion strength. *Biofouling* **2003,** *19* (6), 381-390.

37. Beigbeder, A.; Labruyère, C.; Viville, P.; Pettitt, M. E.; Callow, M. E.; Callow, J. A.; Bonnaud, L.; Lazzaroni, R.; Dubois, P., Surface and fouling-release properties of silicone/organomodified montmorillonite coatings. *Journal of Adhesion Science and Technology* **2011,** *25* (14), 1689-1700.

38. Selim, M. S.; El-Safty, S. A.; El-Sockary, M. A.; Hashem, A. I.; Elenien, O. M. A.; El-Saeed, A. M.; Fatthallah, N. A., Smart photo-induced silicone/TiO2 nanocomposites with dominant [110] exposed surfaces for self-cleaning foul-release coatings of ship hulls. *Materials & Design* **2016,** *101*, 218-225.

39. Arukalam, I. O.; Oguzie, E. E.; Li, Y., Fabrication of FDTS-modified PDMS-ZnO nanocomposite hydrophobic coating with anti-fouling capability for corrosion protection of Q235 steel. *Journal of Colloid and Interface Science* **2016,** *484*, 220-228.

40. Owens, D. K.; Wendt, R. C., Estimation of the surface free energy of polymers. *Journal of Applied Polymer Science* **1969,** *13* (8), 1741-1747.

41. Cassé, F.; Stafslien, S. J.; Bahr, J. A.; Daniels, J.; Finlay, J. A.; Callow, J. A.; Callow, M. E., Combinatorial materials research applied to the development of new surface coatings V. Application of a spinning water-jet for the semi-high throughput assessment of the attachment strength of marine fouling algae. *Biofouling* **2007,** *23* (2), 121-130.

42. Stafslien, S.; Daniels, J.; Mayo, B.; Christianson, D.; Chisholm, B.; Ekin, A.; Webster, D.; Swain, G., Combinatorial materials research applied to the development of new surface coatings IV. A high-throughput bacterial biofilm retention and retraction assay for screening fouling-release performance of coatings. *Biofouling* **2007,** *23* (1), 45-54.

43. Stafslien, S. J.; Bahr, J. A.; Daniels, J. W.; Wal, L. V.; Nevins, J.; Smith, J.; Schiele, K.; Chisholm, B., Combinatorial materials research applied to the development of new surface coatings VI: An automated spinning water jet apparatus for the high-throughput characterization of fouling-release marine coatings. *Review of Scientific Instruments* **2007,** *78* (7), 072204-072204.

44. Callow, M. E.; Callow, J. A.; Conlan, S.; Clare, A. S., Efficacy testing of nonbiocidal and fouling-release coatings. John Wiley & Sons, Ltd: 2014; pp 291-316.

45. Cassé, F.; Ribeiro, E.; Ekin, A.; Webster, D. C.; Callow, J. A.; Callow, M. E., Laboratory screening of coating libraries for algal adhesion. *Biofouling* **2007,** *23* (4), 267-276.

46. Stafslien, S.; Daniels, J.; Bahr, J.; Chisholm, B.; Ekin, A.; Webster, D.; Orihuela, B.; Rittschof, D., An improved laboratory reattachment method for the rapid assessment of adult barnacle adhesion strength to fouling-release marine coatings. *Journal of Coatings Technology and Research* **2012,** *9* (6), 651-665.

47. Rittschof, D.; Orihuela, B.; Stafslien, S.; Daniels, J.; Christianson, D.; Chisholm, B.; Holm, E., Barnacle reattachment: A tool for studying barnacle adhesion. *Biofouling* **2008,** *24* (1), 1-9.

48. Majumdar, P.; Crowley, E.; Htet, M.; Stafslien, S. J.; Daniels, J.; VanderWal, L.; Chisholm, B. J., Combinatorial materials research applied to the development of new surface coatings XV: An investigation of polysiloxane anti-fouling/fouling-release coatings containing tethered quaternary ammonium salt groups. *ACS Combinatorial Science* **2011,** *13* (3), 298-309.

49. Finlay, J. A.; Callow, M. E.; Ista, L. K.; Lopez, G. P.; Callow, J. A., The influence of surface wettability on the adhesion strength of settled spores of the green alga Enteromorpha and the diatom Amphora. *Integrative and Comparative Biology* **2002,** *42* (6), 1116-1122.

50. Callow, M. E.; Callow, J. A.; Ista, L. K.; Coleman, S. E.; Nolasco, A. C.; López, G. P., Use of self-assembled monolayers of different wettabilities to study surface selection and primary adhesion processes of green algal (Enteromorpha) zoospores. *Applied Environmental Microbiology* **2000,** *66* (8), 3249-3254.

51. Callow, J. A.; Callow, M. E.; Ista, L. K.; Lopez, G.; Chaudhury, M. K., The influence of surface energy on the wetting behaviour of the spore adhesive of the marine alga Ulva linza (synonym Enteromorpha linza). *Journal of the Royal Society Interface* **2005,** *2* (4), 319-325.

52. Aldred, N.; Li, G.; Gao, Y.; Clare, A. S.; Jiang, S., Modulation of barnacle (Balanus amphitrite Darwin) cyprid settlement behavior by sulfobetaine and carboxybetaine methacrylate polymer coatings. *Biofouling* **2010,** *26* (6), 673-683.

53. Petrone, L.; Di Fino, A.; Aldred, N.; Sukkaew, P.; Ederth, T.; Clare, A. S.; Liedberg, B., Effects of surface charge and Gibbs surface energy on the settlement behaviour of barnacle cyprids (Balanus amphitrite). *Biofouling* **2011,** *27* (9), 1043-1055.

54. Di Fino, A.; Petrone, L.; Aldred, N.; Ederth, T.; Liedberg, B.; Clare, A. S., Correlation between surface chemistry and settlement behaviour in barnacle cyprids (Balanus improvisus). *Biofouling* **2014,** *30* (2), 143-152.

55. Gatley-Montross, C. M.; Finlay, J. A.; Aldred, N.; Cassady, H.; Destino, J. F.; Orihuela, B.; Hickner, M. A.; Clare, A. S.; Rittschof, D.; Holm, E. R., Multivariate analysis of attachment of biofouling organisms in response to material surface characteristics. *Biointerphases* **2017,** *12* (5), 051003.

56. Aldred, N.; Gatley-Montross, C. M.; Lang, M.; Detty, M. R.; Clare, A. S., Correlative assays of barnacle cyprid behaviour for the laboratory evaluation of antifouling coatings: a study of surface energy components. *Biofouling* **2019,** *35* (2), 159-172.

57. Huggett, M. J.; Nedved, B. T.; Hadfield, M. G., Effects of initial surface wettability on biofilm formation and subsequent settlement of Hydroides elegans. *Biofouling* **2009,** *25* (5), 387-399.

58. Rittschof, D.; Costlow, J. D., Bryozoan and barnacle settlement in relation to initial surface wettability: A comparison of laboratory and field studies. *Sci. Mar.* **1989,** *53* (2), 411-416.

CHAPTER 5. EFFECT OF PEG-PDMS ADDITIVES ON SURFACE AND FOULING-RELEASE PROPERTIES OF AMPHIPHILICLY-MODIFIED SILOXANE-POLYURETHANE MARINE COATING SYSTEM

Introduction

The detrimental settlement of marine organisms on submerged surfaces in seawater, marine biofouling is a complex problem that impacts almost any structure such as ships.[1, 2] Besides causing undesired aesthetic effects, the negative impacts of biofouling are many for ships including shortening service life, increasing drag and reducing maneuverability, boosting greenhouse gas emissions, transporting invasive species to new locations, and rising maintenance costs.[1, 3] For instance, the US Navy spends annually $1 billion to maintain its ships from the biofouling phenomena.[4]

Marine biofouling is a very complicated and ambiguous problem as it involves many types of organisms and aquatic environments. There are estimated to be more than 4000 marine organisms that can potentially biofoul a surface in seawater, using different modes of adhesion and preferring various type of surfaces for settlement.[1, 5, 6] As an example, some organisms prefer to settle on hydrophilic surfaces such as *U. linza*, mussels, and barnacles, while some like to settle on hydrophobic surfaces like *N. incerta*.[1] While it is often considered that colonizing microorganisms (i.e. bacteria, diatoms) pre-condition a surface first for macro-biofoulants (i.e. barnacles), it has been found that the marine biofouling process is not linear since organisms may settle on a surface at any time regardless of any pre-conditioning.[1, 7] Therefore, a consideration of these briefly mentioned factors explains why marine biofouling is a very complex problem to solve and tackle.

Many approaches have emerged to fight marine biofouling throughout history. Traditionally, wooden ship hulls were covered with copper alloys and lead sheaths to contend with biofouling; however, lack of resources and inevitable metallic corrosion on steel hulls resulted in their termination. With the development of polymer chemistry and a better understanding of materials, the 19th century observed the advent of antifouling that were mainly based on the incorporation of toxic chemicals into the paint. One of the most effective biocides was tributyl tin (TBT), which was used in free association paints as well as self-polishing coatings. However, the tin-based systems were banned worldwide in the early 2000s due to

their non-targeted toxicity in aquatic environments.[1, 8] Therefore, the endeavors shifted to investigate alternative fouling-release and antifouling marine coating technologies that were non-toxic.[1]

Antifouling (AF) paints prevent the settlement of marine organisms by releasing biocides. The AF biocides are typically composed of copper and zinc oxides.[1, 3] Despite the fact that these biocides are considered to be less toxic than tin, they still pollute the aquatic environments and may be a cause of non-targeted toxicity. Alternatively, fouling-release paints (FR) function by decreasing adhesion of biofoulants on a surface, releasing biofoulants under low hydrodynamic pressures (i.e. when a ship is moving).[1, 9] FR coatings do not exploit active toxic biocides, but they utilize the low surface energy and smoothness of engineered materials on a surface to offer an uninhabitable surface for marine biofoulants. The first generation of FR systems contained mainly polydimethylsiloxane (PDMS) elastomers or fluoroalkyl polymers,[1, 10] known for their low surface energy and hydrophobicity.

The hydrophobic FR systems have two main drawbacks including durability and range of performance.[1] The lack of durability for FR paints originates from weak adhesion of the soft, low-modulus hydrophobic material to ship surfaces and anticorrosion primers. Self-stratified siloxane-polyurethane (SiPU) systems have been investigated to address this issue, increasing durability via crosslinking of the PDMS-based surface to the bulk of coating without requiring any tie-coat.[11] A further issues is that the range of performance for hydrophobic FR coatings is limited since some organisms prefer to settle on hydrophobic surfaces. Surfaces containing both hydrophilic and hydrophobic domains—amphiphilic coatings—have demonstrated promising FR performance against a wider range of organisms.[12] Hydrophilic domains such as poly(ethylene glycol) (PEG) or zwitterionic-based polymers (i.e. poly (sulfobetaine methacrylate))[1] are usually diffused into a surface by attaching them on PDMS-like materials that self-stratify due to their low surface energy and incompatibility with other components in a coating system. Amphiphilic PEG-siloxane-polyurethane (AmpSiPU) system is a recent achievement that crosslinks PEG and PDMS prepolymers in a coating network and delivers desirable FR performance.

While innovating a new amphiphilic coating system is attractive, the use of amphiphilic additives is appealing since they do not require significant changes to a base coating system. To this extent, many types of additives have been developed to boost AF and FR performances of marine coatings. The categories contain additives based on copper/zinc,[13-15] amphiphilic copolymers (i.e. PEG[16-22] or

zwitterionic-based[23-26]), or hydrogel-like polymers.[27] The scope of marine additives also includes silicone oils[28-30] and specialty additives such as sephiolite nanofibers, modified graphite, carbon nanotubes and pigments (i.e. TiO_2 and ZnO).[5, 6, 31-33]

We initiated this study to synthesize amphiphilic additives (AmpAdd) that could be non-covalently incorporated into a marine coating system. While many amphiphilic copolymers have been explored as marine additives, their often-complex synthesis is a major challenge for implementation on a large scale. Thus, we investigated a procedure to prepare a series of easy-to-synthesize amphiphilic additives by combining PEG and PDMS chains on a commercially available polymeric backbone. Several factors were varied including the molecular weights of PEG and PDMS, the hydrophobic-hydrophilic balance of engineered additives, and the incorporated amount of amphiphilic additives in the coating system. In this study, the AmpAdds were added to the AmpSiPU[12] system to assess how further amphiphilicity boosts FR performance. In two other studies (chapters 3 and 4), a series of AmpAdds were introduced to polyurethane and hydrophobic SiPU systems to evaluate critical amphiphilic concentration (the point when a non-marine coating converts to a well-performing marine coating) and effect of attaining amphiphilic balance, respectively. This work discusses the synthesis and characterization of AmpAdds and their effect on the surface and fouling-release properties of the selected AmpSiPU system (Figure 5.1).

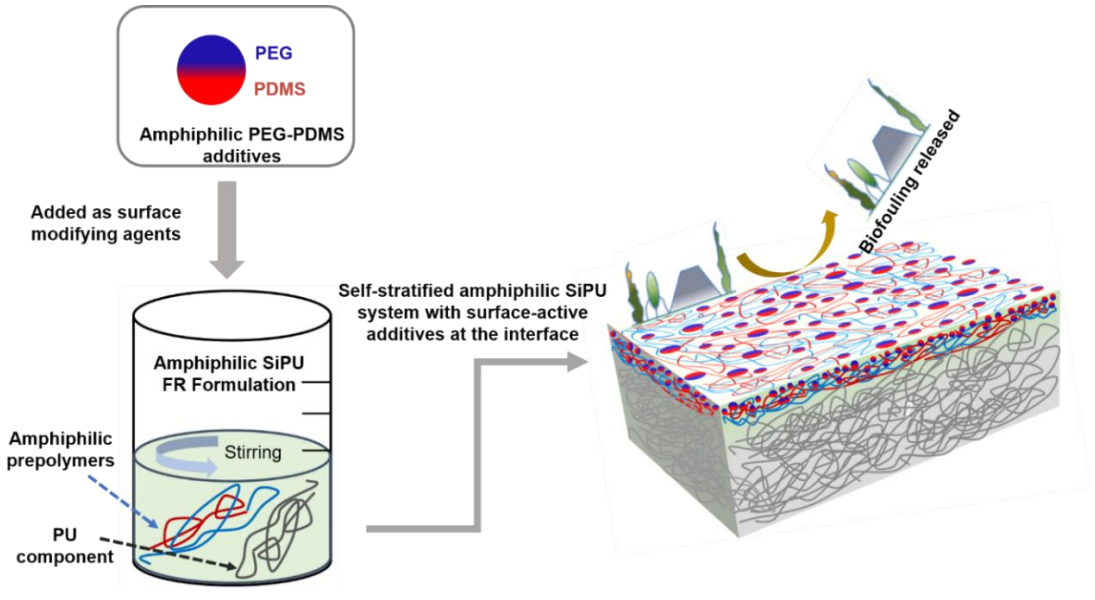

Figure 5.1. Illustration of amphiphilic PEG-PDMS additives as surface-modifying agents, tuning the hydrophobic surface of FR SiPU coating system to an amphiphilic surface.

Experimental

Materials

Isophorone diisocyanate (IPDI) polyisocyanate Desmodur Z4470 BA was provided by Covestro LLC. Monocarbinol-terminated polydimethylsiloxane (PDMS) with molecular weights of 5,000 $\bar{M}_n$ and 10,000 $\bar{M}_n$ were purchased from Gelest, Inc. Poly(ethylene glycol) methyl ether (550 $\bar{M}_n$ and 750 $\bar{M}_n$), ethyl-3-ethoxy propionate, methyl ethyl ketone (MEK), acetylacetone, methyl amyl ketone (MAK), and dibutyltin diacetate (DBTDAc) were purchased from Sigma Aldrich. Toluene and isopropanol were purchased from VWR. An acrylic polyol made of 80% butyl acrylate and 20% 2-hydroxyethyl acrylate was prepared via conventional free radical polymerization and diluted to 50% in toluene. Aminopropyl terminated polydimethylsiloxane (APT-PDMS) with molecular weight (MW) of 20,000 $\bar{M}_n$ was also synthesized through a ring-opening equilibration reaction. Both synthesized polymers were prepared following guidelines from elsewhere.[11] Amphiphilic prepolymer based on PEG 750 $\bar{M}_n$ and PDMS 10,000 $\bar{M}_n$ for the AmpSiPU coating system were also prepared following procedure elsewhere, called R0 in this study.[12]

AkzoNobel International Paint provided the commercial FR standards Intersleek® 700 (IS 700), Intersleek® 900 (IS 900), and Intersleek® 1100 SR (IS 1100). Silicone elastomer Silastic® T2 and polystyrene was provided by Dow Corning as another commercial standard. Hydrophobic siloxane-polyurethane A4 coating (A4), internal control was prepared following the procedure described elsewhere.[11] Also, a pure polyurethane formulation without APT-PDMS was also prepared to be included as a control. Aluminum panels (4” x 8” in., 0.6 mm thick, type A, alloy 3003 H14) purchased from Q-lab were sandblasted and primed with Intergard 264 (International Paints) using air-assisted spray application. Multi-well plates were modified using circular disks (1-inch diameter) of primed aluminum.

Experimental Design

A series of amphiphilic additives (AmpAdd) containing chains of PDMS and PEG were synthesized and added into an amphiphilic siloxane-polyurethane coating system, called AmpSiPU. The AmpSiPU is a system that is formulated with IPDI trimer polyisocyanate, amphiphilic PEG-PDMS-isocyanate prepolymers, and acrylic polyol. The selected AmpSiPU formulation is called R0 in this study,

containing 10 wt.% of 10,000 $\bar{M}_n$ PDMS and 10 wt.% of 750 $\bar{M}_n$ PEG as self-stratifying crosslinked prepolymers; this formulation was selected as it performed the best in the results published elsewhere.[12]

We prepared AmpAdds by installing PEG and PDMS chains on IPDI trimer polyisocyanate resin. The ratio of isocyanate groups to the combined OH groups of PEG and PDMS was a 1:1 molar ratio. To attain types of AmpAdds (Table 5.1), PEG and PDMS were used in varying molecular weights and amounts to complete the required one molar hydroxyl ratio. The molecular weights of 5,000 $\bar{M}_n$ and 10,000 $\bar{M}_n$ for PDMS, and 550 $\bar{M}_n$ and 750 $\bar{M}_n$ for PEG were chosen to synthesize amphiphilic additives in accordance with optimal chain lengths for FR performance.[12, 34] Also, the amount of attached PEG and PDMS on an additive was another variable to access new AmpAdds. For example, "50:50 PDMS: PEG" for Amp1 additive means that both PEG and PDMS were added in equal weight (i.e. 2 g PEG and 2 g PDMS) to synthesize the additive. It should be noted that there was a wt.% for IPDI polyisocyanate resin as part of the additive structure too since the amphiphilic chains were grafted on its backbone. Therefore, the wt.% values of PEG and PDMS on an additive could be calculated and were used to determine the final content of PEG and PDMS moieties in a formulation (Table 5.1).

Table 5.1. List of prepared additives and their compositional details

Additive	PDMS Type ($\bar{M}_n$)	PEG Type ($\bar{M}_n$)	PDMS: PEG (% ratio)	PDMS (wt. %)	PEG (wt. %)	IPDI isocyanate (wt. %)
Amp-1	5,000	750	50: 50	42	42	16
Amp-2	5,000	550	50: 50	42	42	16
Amp-3	10,000	750	50: 50	42	42	16
Amp-4	10,000	550	50: 50	42	42	16
Amp-5	10,000	750	33: 66	15	61	23
Amp-6	10,000	750	10: 90	8	67	25

Knowing that the R0 coating of AmpSiPU contains up to 10 wt.% each PDMS and PEG, we added these additives at 15 wt.%, 10 wt.% and 20 wt.%. A total of 15 formulations were investigated for this study: 8 experimental (Table 5.2) and 7 controls (both internal and commercial) (Table 5.3). For the experimental systems, the first four formulations (R1-R4) were designed as a 2^2 experimental design to evaluate two factors for the designed AmpAdds including the molecular weight of PDMS (5,000 $\bar{M}_n$ and 10,000 $\bar{M}_n$) and molecular weight of PEG (550 $\bar{M}_n$ and 750 $\bar{M}_n$), while keeping the amphiphilic balance

unchanged (amount of hydrophilic and hydrophobic moieties in a system). Formulations R5 and R6 were considered to evaluate the effect of shifting the amphiphilic balance towards more hydrophilicity via AmpAdds, comparing these formulations with R3 and R0. Formulations R7 and R8 were considered to evaluate the effect of the amount of an AmpAdd, comparing these formulations with R3 and R0.

The table outlines type of the added AmpAdd, amount of the added AmpAdd, wt.% of PEG and PDMS based on the added AmpAdd, and overall wt.% of PEG and PDMS in a formulation (including 10 wt.% of each PDMS and PEG in R0 base formulation).

Table 5.2. Coating compositions

Formulation	Added AmpAdd Details				Formulation Details	
	Additive Type	Additive Amount (wt. %)	PDMS (wt.%)	PEG (wt.%)	PDMS (wt.%)	PEG (wt.%)
R0	-	-	-	-	10.0	10.0
R1	Amp-1	15.0	6.2	6.2	16.2	16.2
R2	Amp-2	15.0	6.2	6.2	16.2	16.2
R3	Amp-3	15.0	6.2	6.2	16.2	16.2
R4	Amp-4	15.0	6.2	6.2	16.2	16.2
R5	Amp-5	15.0	5.0	10.0	15.0	20.0
R6	Amp-6	15.0	1.5	13.5	11.5	23.5
R7	Amp-3	20.0	8.3	8.3	18.3	18.3
R8	Amp-3	10.0	4.1	4.1	14.1	14.1

Commercial standards were prepared following the manufacturer's instructions. A4 SiPU coating, internal hydrophobic control, containing 20,000 $\bar{M}_n$ PDMS as crosslinker was prepared following directions elsewhere; this formulation was selected since it showed the best performance among the studied systems.[11] Similar to experimental coatings all control and standards were also prepared on 4" x 8" primed aluminum panels and multi-well plates. Table 5.3 contains detailed descriptions of the control and standard coatings used for this study.

Table 5.3. List of control coatings

Control Name	Control ID	Description
A4 SiPU	A4	Internal Hydrophobic SiPU Control
Polyurethane	PU	Pure Polyurethane Standard
Polystyrene	PS	Pure Polystyrene Standard (used for *U. linza* test)
Dow T2	T2	Silicone Elastomer Standard
Intersleek® 700	IS 700	Intersleek Commercial FR Standard
Intersleek® 900	IS 900	Intersleek Commercial FR Standard
Intersleek® 1100 SR	IS 1100	Intersleek Commercial FR Standard

Synthesis of Amphiphilic Additives

The AmpAdd additives were produced via reacting hydroxyl-terminated PEG and PDMS chains with the IPDI trimer polyisocyanate (Scheme 5.1). The molar ratio of NCO groups to the combined OH groups of PEG and PDMS was 1:1. The functional isocyanate groups were fully converted to urethane linkages by reacting with PEG and PDMS chains. PEG and PDMS were added in weight ratios that met the required molar ratio.

To synthesize Amp-2 (containing weight ratio of PDMS: PEG 50:50), PEG 550 $\bar{M}_n$ (8.00 g) was diluted in toluene (8.00 g) in a 50-mL flask. PDMS 5,000 $\bar{M}_n$ (8.00 g) was added to the flask and mixed robustly with vortex for 2 minutes. IPDI trimer resin (6.32 g) and DBTDAc catalyst solution (1% by wt. in MAK) (1.12 g) were then added to the flask. The reaction was carried out at 80 °C for 2 hours. The reaction could also be carried out at ambient conditions for 24 hours. The flask was equipped with a magnetic stirrer, nitrogen inlet, and temperature controller. The reflux condenser was used when the heat was applied. The synthesized Amp-2 additive contained 42.0 wt.% PEG and 42.0 wt.% PDMS (Table 5.1), calculated based on solid contents utilized to synthesize the additive and the final solid content. All other AmpAdds were synthesized following the same procedure.

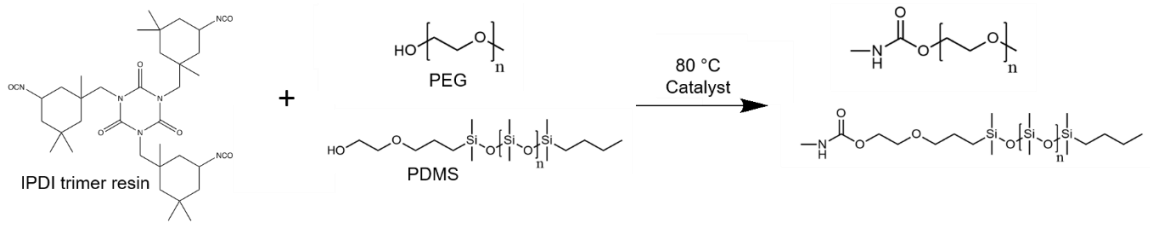

Scheme 5.1. Overall Synthesis Scheme of amphiphilic additives.

Isocyanate Titrations

Isocyanate titration was used to verify the disappearance of isocyanate moieties after the synthesis of the additive. An additive sample (0.3-0.5 g) was weighed in an Erlenmeyer flask and diluted with isopropanol. Then, 25 mL of 0.1 N dibutyl amine solution and additional 25 mL isopropanol were added to the flask, and the mixture was stirred for 15 minutes. Several drops (3-5 drops) of bromophenol blue indicator were added to the flask. The content of the flask was titrated using a standardized 0.1 N hydrochloric acid until the endpoint blue to yellow was observed. A blank prepared only with 25 mL of dibutyl amine solution was also titrated following the same procedure. The recorded amount of hydrochloric acid for both titrations was used to calculate isocyanate content for the additive (if any remained unreacted).

Percent Solids Determination

The non-volatile content of an additive was determined following ASTM 2369. In general, an additive sample (1-2 g) was weighed and placed in a weighed empty aluminum pan. Isopropyl alcohol was used to cover the sample. The pan was placed in an oven at 120 °C for 1 hour. After removal from the oven, the pan was weighed again to determine the percent solids. Three replicates were recorded.

Fourier Transform Infrared Spectroscopy

Fourier transform infrared (FTIR) spectroscopy was used to characterize the additive, using a Thermo Scientific Nicolet 8700 FTIR. The additive was applied as a thin layer on a potassium bromide (KBr) plate to collect the spectrum.

Coating Formulations and Curing

A synthesized AmpAdd was added to R0 (an AmpSiPU formulation). The R0 system is an amphiphilic marine fouling-release coating that mainly composed of acrylic polyol, IPDI trimer isocyanate resin, and amphiphilic PEG-PDMS-isocyanate prepolymers.

For example, to formulate coating R2, acrylic polyol (12.24 g; 50% solid), acetylacetone (1.74 g) (potlife extender), amphiphilic PEG-PDMS-isocyanate prepolymer (5.10 g; 70% solid), and Amp-2 additive (3.73 g; 50% solid) were added to a vial and stirred ambiently for 24 hours. IPDI polyisocyanate trimer Desmodur Z4470 BA resin (2.95 g) and DBTDAs catalyst solution (0.28 g) were added to the vial, and the mixture was stirred for another hour. Coating formulations were drawn down on primed 8’ x 4’

aluminum panels using a wire-round drawdown bar with a film thickness of 80 µm. All coatings were cured at ambient laboratory conditions for 24 hours, followed by oven curing at 80 °C for 45 minutes. All experimental coatings were prepared following the same procedure. Coatings were cut out in circular shapes and glued to 24-well plates for biological assays test.

Furthermore, two internal model PU systems without amphiphilic prepolymers were prepared using the same materials and following the same procedure (except no PEG-PDMS-isocyanate prepolymers were added). One system was the unmodified model PU and the other one was modified model PU with Amp3 additive is its composition. These two model PU systems were used to substantiate the self-stratification of AmpAdd additives into the surface of coatings via X-ray photoelectron spectroscopy (XPS) experiments (these controls avoided interference of PDMS signals of the prepolymer in R0 and PDMS signals of an added AmpAdd).

Surface Characterization

A Kruss® DSA 100 (Drop Shape Analyzer) was employed to determine the surface wettability and surface energy for the coatings. Water and diiodomethane (methylene iodide) contact angles were measured in 3 replicates for each sample. For each replicate, the static contact angle was measured over 9 minutes to monitor changes due to the potential interaction of the moieties (i.e. PEG and PDMS) on the surface with the water droplet as a function of time (the values plateaued after 9 minutes). Surface energy for each surface was calculated using the Owens-Wendt method.[35] Slip angle, advancing and receding water contact angles for surface were evaluated using a tilting stage where a 25-µL water droplet was viewed on a coating surface (tilted at 10°/min). The measured angles and surface energies were calculated using the Kruss® Advance software.

Attenuated total reflectance Fourier transform infrared spectroscopy (ATR-FTIR) was used to characterize the surfaces of the coatings. A Bruker Vertex 70 with Harrick's ATR™ accessory using a hemispherical Ge crystal was utilized to collect ATR-FTIR spectra for a coating.

A Thermo Scientific™ K-Alpha™ X-ray photoelectron spectroscopy (XPS) was used to determine the elemental composition of coatings. The instrument was equipped with monochromatic Al K_α (1486.68 eV) X-ray source and Ar^+ ion source (up to 4000 eV) was utilized for the XPS experiments. Depth profiling of a coating was evaluated with 30 Ar+ etch cycles. For each etch cycle, the ion beam was

set to 1,000 eV Monatomic Mode with low current and 30 s etch time. After each etching cycle, survey spectra in 5 replicates were collected at low resolution with a constant analyzer pass energy of 200 eV for a total of 20 ms. For each run, photoemission lines for C1s, N1s, O1s, and Si2p were observed. Spectra were collected at an angle normal to the surface (90°) of a 400-µm area. The chamber pressure was maintained below 1.5 x 10^{-7} Torr and samples were analyzed at ambient temperature. Atomic concentrations were quantified by the instrument's software as a representation of the atomic intensities as a percentage of the total intensity of all elements. Two internal PU systems without (pure PU) and with AmpAdd-1 additive (modified PU) were examined to verify the self-stratification of AmpAdd additives into the surface of coatings.

Atomic force microscopy (AFM) was utilized to receive insights about the surface topography of the studied coatings. A Dimension 3100 microscope with a Nanoscope controller scanned the surface of experimental coatings, collecting images on a sample area of 100 µm x 100 µm in the tapping mode. The experiment condition was in the air under ambient conditions, using a silicon probe with a spring constant (0.1-0.6 N/m) and resonate frequency (15-39 kHz). For each surface, three replicates at varying spots were collected to ensure the consistency and accuracy of the data.

Water Aging

All the prepared coatings were pre-leached for 28 days in running tap water. The water tanks were equipped to automatically fill and empty every 4 hours. Water aging of the coatings is carried out to leach out any impurities that may interfere with fouling-release assessments and to determine the stability of coatings and surface rearrangements. All biological laboratory assays were carried out after the pre-leaching water aging process was completed.

Biological Laboratory Assays

Bacterial (*Cellulophaga lytica*) Biofilm Adhesion

Fouling-release properties towards bacteria were evaluated using retention and adhesion assays described previously.[36, 37] Briefly, a solution of the marine bacterium *Cellulophaga lytica* at 10^7 cells/mL concentration in artificial seawater (ASW) containing 0.5 g/L peptone and 0.1g/L yeast extract was deposited into 24-well plates (1 mL/well). The plates were then incubated statically at 28°C for 24 hours. The ASW growth medium was then removed and the coatings were subjected to water-jet treatments.

The first column of each coating was not treated and served as the initial amount of bacterial biofilm growth. The second and third columns were subjected to water-jetting at 10 psi and 20 psi, respectively, for 5 seconds. Following water-jet treatments, the coating surfaces were stained with 0.5 mL of a crystal violet solution (0.3 wt. % in deionized water) for 15 minutes and then rinsed three times with deionized water. After 1 hour of drying at ambient laboratory conditions, the crystal violet dye was extracted from the coating surfaces by adding 0.5 mL of 33% acetic acid solution for 15 minutes. The resulting eluates were transferred to a 96-well plate (0.15 mL/coating replicate) and subjected to absorbance measurements at 600 nm wavelength using a multi-well plate spectrophotometer. The absorbance values were directly proportional to the amount of bacterial biofilm present on coating surfaces before and after water-jetting treatments. Percent removal of bacterial biofilm was quantified by comparing the mean absorbance values of the non-jetted and water-jetted coating surfaces.[33]

Growth and Release of Microalgae (*Navicula incerta*)

Laboratory biological assay diatom (*Navicula incerta*) was conducted at NDSU following a similar procedure described previously.[2, 38, 39] Briefly, a suspension with 4×10^5 cells/mL of *N. incerta* (adjusted to 0.03 OD at absorbance 660 nm) in Guillard's F/2 medium was deposited into each well (1 mL per well) and cell attachment was stimulated by static incubation for 2 hours under ambient conditions in the dark. Coating surfaces were then subjected to water-jet treatments.[37] First column of wells was not water-jetted so that initial cell attachment could be determined and the next two-column of wells were water-jetted at 10 psi and 20 psi, respectively, for 10 seconds. Microalgae biomass was quantified by extracting chlorophyll using 0.5 mL of DMSO and measuring the fluorescence of the transferred extracts at an excitation wavelength of 360 nm and emission wavelength at 670 nm. The relative fluorescence (RFU) measured from the extracts was considered to be directly proportional to the biomass remaining on the coating surfaces after water-jetting. Percent removal of attached microalgae was determined using the relative fluorescence of non-jetted and water-jetted wells.

Growth and Release of Macroalgae (*Ulva linza*)

A set of multiwall plates was sent to Newcastle University, following water-immersion for 28 days, to evaluate the fouling-release performance of coatings against *U. linza*. The detailed description of the assessment can be found elsewhere.[38] Briefly, after leaching collection, all multiwall plates were

equilibrated in 0.22 µm filtered artificial seawater for 2 hours at Newcastle. To each well, 1 mL spores of *U. linza* suspension was added, adjusted to 3.3 x 10^5 spores/mL (0.05 OD at absorbance 660 nm) in double strength enriched seawater. Spores settled on the discs were grown for 7 days inside an illuminated incubator at 18°C with a 16:8 light: dark cycle (photon flux density 45 µmol.m^{-2}.s^{-1}). There was no washing to remove unsettled spores after settlement. After 7 days, the biomass generated was assessed from a single row of wells (6) from each plate. The chlorophyll was extracted by adding 1 mL DMSO to each water-pressured well (water pressure of 67 kPa) and followed by measuring the fluorescence at 360 nm excitation and 670 nm emission. Fluorescence is directly proportional to the biomass present on each coating surface. The removal of *U. linza* at each pressure was compared with the unsprayed wells that were used to determine initial growth.

Adult Barnacle (*Amphibalanus amphitrite*) Adhesion

Adult barnacle reattachment test was carried out to assess fouling-release of coatings against macrofoulants.[40, 41] Coatings prepared on 4" x 8" panels after water aging were utilized for this laboratory assay. Barnacles were dislodged from silicone substrates sent from Duke University and immobilized on experimental coatings (6 barnacles per coating) using a custom-designed immobilization template. The immobilized barnacles were allowed to reattach and grow for 2 weeks while immersed in an ASW aquarium tank system with daily feedings of brine shrimp *Artemia* nauplii (Florida Aqua Farms). After the 2-week attachment period, the number of non-attached barnacles was recorded, and the attached barnacles were pushed off (in shear) using a hand-held force gauge mounted onto a semi-automated stage. Once the barnacles were dislodged, their basal plate areas were determined from scanned images using Sigma Scan Pro 5.0 software program. Barnacle adhesion strength (MPa) was calculated by taking the ratio of peak force of removal to the basal plate area for each reattached barnacle. To ensure consistency, barnacles of similar sizes were tested. The average barnacle adhesion strength for each coating was reported as a function of the number of barnacles released with a measurable force and that exhibited no visible damage to the basis or shell plates.

Results and Discussions

Amphiphilic fouling-release (FR) coatings have shown promising results to mitigate marine biofouling. These systems offer better performance than traditional hydrophobic FR coatings. Our work in

Chapter 3 demonstrated that when a critical amphiphilic concentration (CAC) is achieved for a system, its marine performance improves considerably. Thus, we utilized this concept to further investigate how increasing the amphiphilicity for an established amphiphilic marine coating using additives affects its surface and FR properties. Amphiphilic siloxane-polyurethane (AmpSiPU) was selected to be modified by additives in this study, specifically R0 formulation containing 10 wt.% 10,000 $\bar{M}_n$ PDMS and 10 wt.% 750 $\bar{M}_n$ PEG (a top system in another study).[12] A series of amphiphilic additives were introduced to R0 to evaluate their effect on this system.

The amphiphilic additives (AmpAdds) were synthesized by attaching hydroxyl-terminated PEG and PDMS chains on IPDI isocyanate trimer resin through the facile reaction of isocyanate and alcohol. A dried toluene solvent was used to ensure water did not react with isocyanate during the reaction. The complete conversion of isocyanate groups due to the reaction was confirmed with FTIR and isocyanate titration of the additives. All FTIR spectrum displayed disappearance of isocyanate peak at 2250 cm^{-1} and a broadened signal for secondary amine (from the formed urethane linkage) at 3350 cm^{-1} (Figure 5.2), supporting the reaction of isocyanate groups. Also, the signature peaks for Si-O-Si at 1035 cm^{-1} (Figure 5.2 – Green highlights) and C-O-C of PEG at 1105 cm^{-1} (Figure 5.2 – Red highlights) demonstrate the reaction of PDMS and PEG chains onto the isocyanate-based backbone, respectively. The intensity of the C-O-C peak increased, and the intensity of the Si-O-Si signal decreased as a higher amount of PEG and a lower amount of PDMS was attached to an additive, respectively (Figure 5.2A; comparing from bottom to top). Also, 750 $\bar{M}_n$ PEGs appear to show stronger peaks (Amp-1 and Amp-3 additives) than 550 $\bar{M}_n$ PEGs (Amp-2 and Amp-4 additives) in comparison with their neighboring Si-O-Si signals (Figure 5.2B). Overall, the FTIR data qualitatively indicates the amount of PEG and PDMS and their incorporated molecular weights (MW) results in a different additive. Isocyanate titrations were carried out on additives, and the results implied the presence of no remaining isocyanate groups.

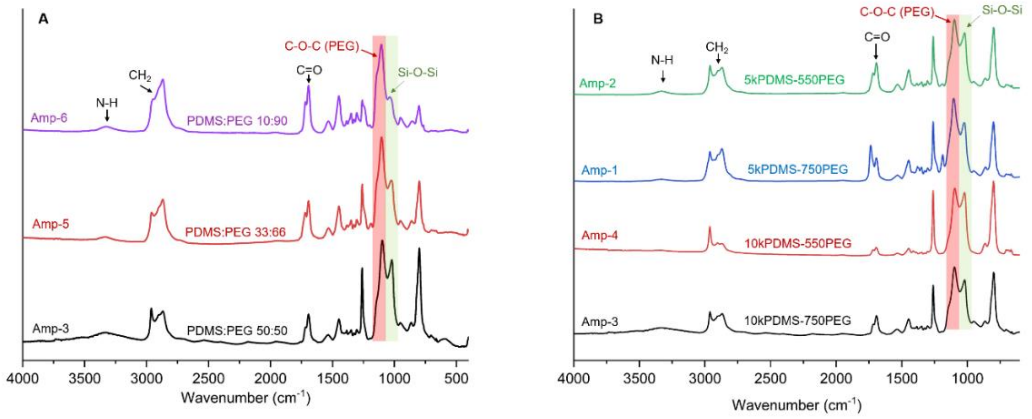

Figure 5.2. FTIR spectra for the amphiphilic additives. Part A reflects spectra for additives with different weight ratios of 750 $\bar{M}_n$ PEG and 10,000 PDMS $\bar{M}_n$. Part B reflects spectra for additives with varying MW of PEG and PDMS with constant weight ratios. Each spectrum is labeled to display details about each spectrum. The signals of interest for C-O-C and Si-O-Si are highlighted in red and green, respectively.

The surfaces of unmodified and modified AmpSiPU R0 coatings were analyzed with a series of techniques including ATR-FTIR, contact angle measurements, and AFM. Also, XPS was used to validate the self-stratification of amphiphilic additives into a surface for model PU coatings. ATR-FTIR of modified coatings showed the signals for both C-O-C (Figure 5.3 – Green highlights) and Si-O-Si (Figure 5.3 – Red highlights) with higher intensity than the unmodified R0 coating. Like additives of different weight ratios of PEG and PDMS, the intensity of ether and siloxane peaks for the coatings followed a similar trend; the C-O-C signal increased as an additive with higher PEG content was used (Figure 5.3A; comparing from bottom to top). The intensity of PEG and PDMS peaks also gradually increased as a higher amount of amphiphilic additives was introduced (Figure 5.3B; comparing from bottom to top). The ATR-FTIR data suggests amphiphilic additives self-stratified into the surface, comparing PEG and PDMS signals of modified and unmodified R0 coatings.

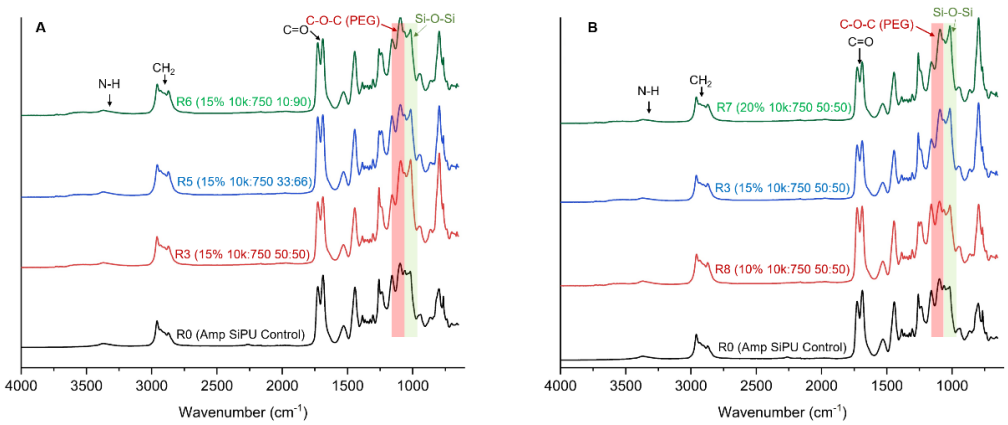

Figure 5.3. ATR-FTIR of the unmodified and modified R0 AmpSiPU coatings. Part A reflects spectra for coatings modified with additives of different weight ratio of 750 $\bar{M}_n$ PEG and 10,000 PDMS $\bar{M}_n$. Part B reflects spectra for coatings modified with varying amounts of Amp-3 additive, ranging from 0 wt.% to 20 wt.%. Green and red highlights reflect the peaks of interest for siloxane and ether (from PEG), respectively. Each spectrum is labeled to reflect the formulation ID number and type.

Contact angle measurements, both static and dynamic, were conducted to assess surface properties of coatings. The static contact angles monitored water and methylene iodide droplets on a surface as a function of time up to 9 minutes (values plateaued at this point). The unmodified R0 AmpSiPU coating shows a dynamic surface, meaning the contact angle values change over time (i.e. droplets spread). In comparison to R0, the initial water contact angle (WCA) and methylene iodide contact angle (MICA) values for all AmpAdd-modified coatings decreased, and the change over time for contact angles was more noticeable than R0 (Figure 5.4A). The dynamic change of contact angles (specially WCA) over time is attributed to the addition of AmpAdds, resulting in a higher density of PEG chains on the surface that facilitates spreading a water droplet. The non-dynamic behavior of hydrophobic A4 (WCA or MICA does not change) due to its PDMS rich surface further reconfirms the surfaces of R0 and its modified versions are amphiphilic. The static data indicates the degree of changes among AmpAdd-modified formulations vary slightly (Figure 5.4A), suggesting the MW of PEG and PDMS or amount of additive in a system does not remarkably impact the dynamic behavior for a system. Surface energies (SE) of coatings were calculated using WCAs and MICAs values (Figure 5.4B); SEs are typically higher when WCA and MICA values are lower than 90°. The data shows SE for R0 jumps significantly after the addition of amphiphilic additives, increasing from 27-30 mN/m to a 40-70 mN/m. The SE for hydrophobic A4 is similar to control R0, suggesting R0 is more hydrophobic on the surface than its modified versions.

Dynamic contact angle experiments were carried out using a tilting stage to determine slip angle (water droplet roll-off angle) and advancing/receding contact angles. The AmpAdds decreased the slip angle of the R0 coating by almost 50%, from nearly 6° to 3°-3.5° (Figure 5.4C). The decrease of the roll-off angle implies that AmpAdds contribute to the easier removal of objects from the surface of R0. There was no significant difference between roll-off angles of modified R0 coatings. In comparison, the hydrophobic A4 system had a slip angle at 9°, implying amphiphilic surfaces improved roll-off performance. Advancing contact angles (Adv CA) and receding contact angles (Rec CA) were remarkably lower for modified R0 coatings (except R7 which held relatively higher values) than both the unmodified R0 and hydrophobic A4 systems (Figure 5.4D). There was no major difference between CA values due to MW of PEG and PDMS or amphiphilicity balance. The hysteresis (numerical difference between Adv CA and Rec CA) remained unchanged and less than 10° for unmodified and modified R0 coatings, demonstrating that the additives did not roughen the surface of R0 system. WCAs were recorded for coatings after water immersion, and the results indicated the modified R0 coatings were as stable as control systems including unmodified R0 and SiPU A4 (Figure A17). Overall, WCAs slightly increased for all systems to a relatively equal extent. The changes are associated with several indicators such as rearrangement of surface domains due to interaction with water.

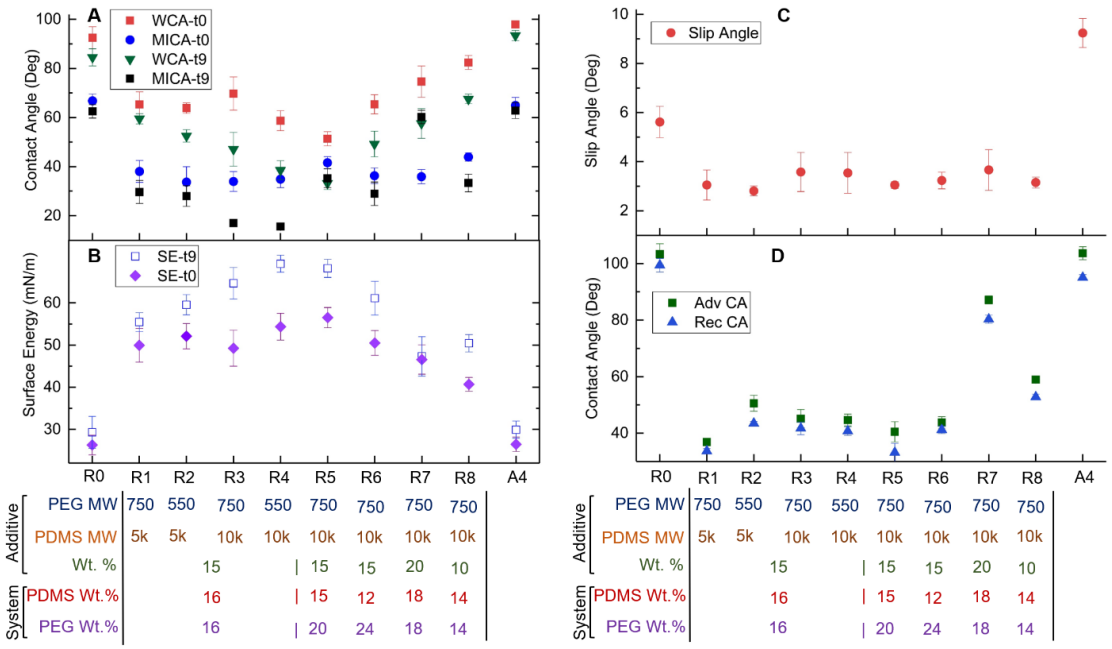

Figure 5.4. Contact angle and surface energy data for coatings. (A) Water contact angles (WCA) and methylene iodide contact angles (MICA) as a function of time at 0 minutes and 9 minutes; (B) Surface energy (SE) of coatings at 0 minute and 9 minutes, calculated by Owens-Wendt method utilizing the average WCAs and MICAs for each coating; (C) Slip angle of coatings where a water droplet starts to roll off; (D) Advancing contact angle (Adv CA) and receding contact angle (Rec CA) data, measured by tilting method. A4 is the internal hydrophobic coating for comparison. The x-axis is labeled to reflect details about utilized additive and the overall content of PEG and PDMS in a formulation.

AFM was used to characterize the surface morphologies of the studied coatings. AFM phase images typically show lighter appearance (high phase angle) for soft materials like PDMS while dark appearance (low phase angle) for harder materials like PEG. AFM images for R0 AmpSiPU (Figure 5.5 – R0; Figure A18 – R0) and A4 SiPU (Figure A19) control systems display a microdomain-containing heterogeneous surface and a microdomain-free homogenous surface, respectively, indicating the amphiphilic R0 system possesses a patterned surface (due to its PEG-PDMS prepolymers).[12] The addition of AmpAdds into R0 further modified its heterogenous surface (Figure 5.5). The data indicates that the MW of PDMS impacts the surface morphology of R0, while MW of PEG does not affect it necessarily – systems with 5k $\bar{M}_n$ PDMS (R1 & R2) contain smaller domains than systems with 10k $\bar{M}_n$ PDMS (R3 & R4). The introduction of AmpAdds with higher contents of PEG (Amp-5 and Amp-6) retained a comparable morphology to R3 and R4 coatings, indicating no major changes (except the images were harder to capture). The amount of additive did alter the morphology of R0, comparing Amp-3 at 10 wt.%

(R8), 15 wt.% (R3), and 20 wt.% (R7). The comparison implies surface of R7 was highly saturated where domains were merged and very near to each other, while R3 and R8 showed fewer domains on their surfaces in the order mentioned. As a sum, AmpAdds appeared to result in the surface domains being more organized and more narrowly dispersed in size. Additionally, AFM images were recorded for coatings after 28-days of water immersion (Figure A20). The comparison of images before and after water-immersion demonstrated the surface domains were stable, slight rearrangements occurred, and no major depletion/leaching of domains was observed. The post-immersion rearrangement of domains may be the reason that contact angle data slightly changed as well (Figure A17). Overall, the AFM images demonstrated that amphiphilic additives modified the surfaces and several factors influence the change such as the MW of moieties or the amount of additive. The AFM images correlate with ATR-FTIR and contact angle data that AmpAdds self-stratified into surfaces and caused a dynamic interaction with assessed droplets.

XPS was utilized to confirm the self-stratification of the amphiphilic additives into the surface of R0. XPS depth analysis was initially conducted on modified and unmodified R0 coatings as a function of coating thickness up to 30 nm, but the data was not conclusive due to difficulties in differentiating between PEG and PDMS of R0 itself and incorporated additives. Therefore, an internal model PU system was used to validate the self-stratification of AmpAdds. The model PU system was similar to the R0 AmpSiPU system but without amphiphilic PEG-PDMS-based prepolymers, and for confirmation purposes, Amp-3 was added to the model PU system at 20 wt.%. XPS depth analysis of unmodified model PU and AmpAdd-modified model PU supported the theory that amphiphilic additives self-stratify into a surface (Figure 5.6). The unmodified model PU showed a constant concentration of carbon (Figure 5.6A) and nitrogen (Figure 5.6B) throughout the evaluated 30 nm depth, indicating a relatively homogenous network by composition. Comparatively, the modified model PU system showed the surface contained silicon which its concentration gradually decreased as a function of depth (Figure 5.6B) while the concentration of nitrogen and carbon atoms increased (Figure 5.6). The depth-dependent concentrations of Si, C, and N supported the self-stratification of amphiphilic additives to the surface, correlating with data from ATR-FTIR, contact angle analysis, and AFM.

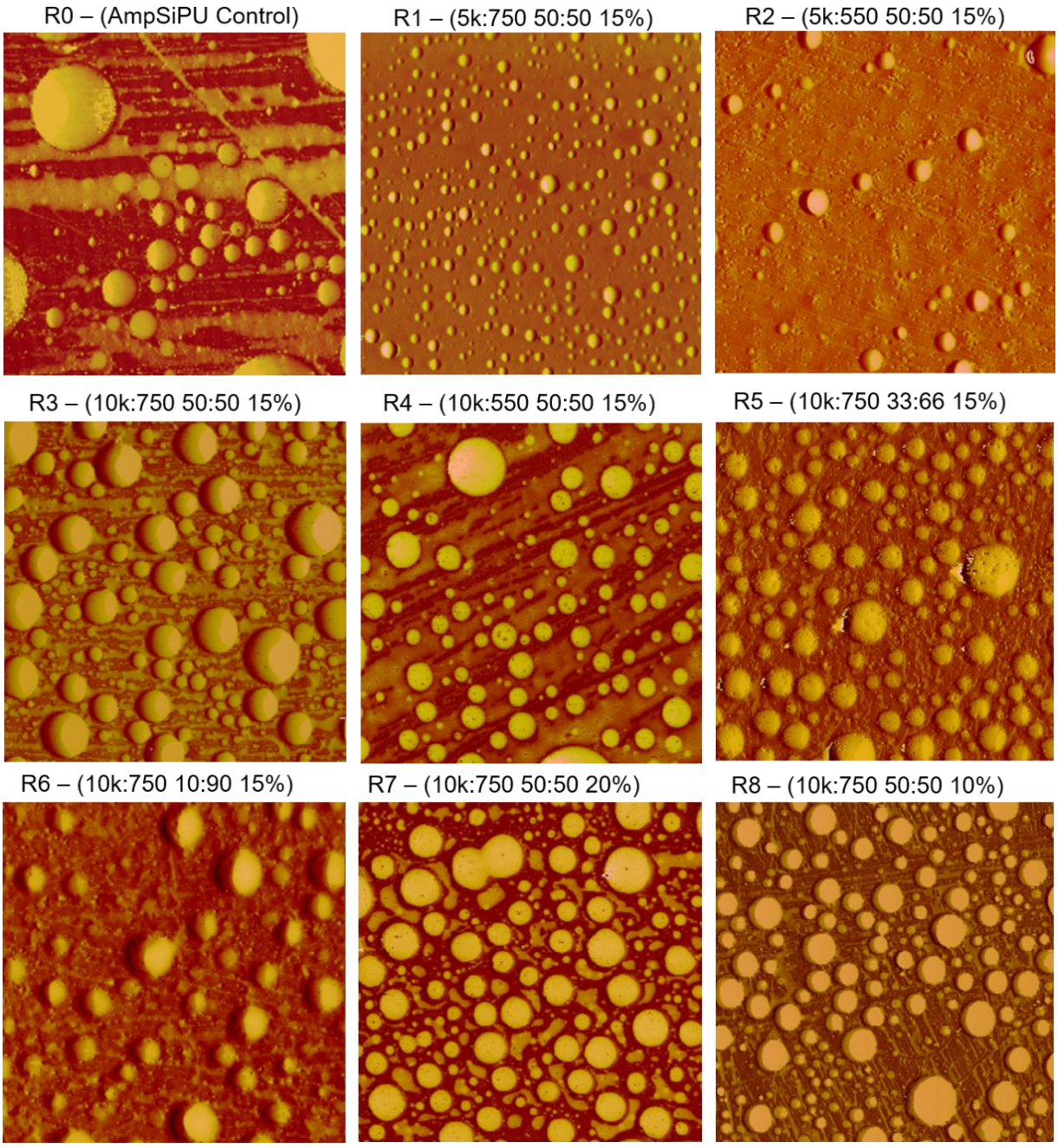

Figure 5.5. AFM phase images of unmodified and modified R0 AmpSiPU coatings. Each image is for an area of 100 µm x 100 µm. Each label reflects the coating number.

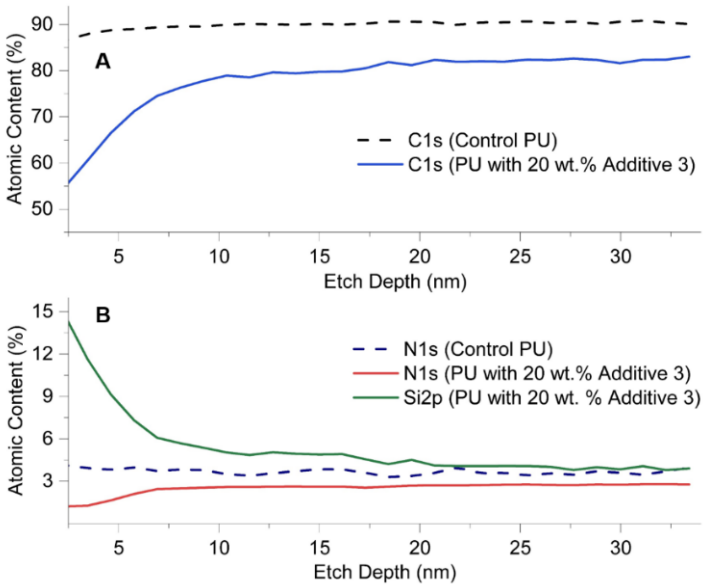

Figure 5.6. XPS depth profiling data for model PU coatings. (A) XPS data for unmodified model PU coating; (B) XPS data for modified model PU coating containing 20 wt.% Amp-3 additive. This data supports self-stratification of the amphiphilic additives to the surface.

To assess the fouling-release performance of the coatings, biological assays using four representative marine fouling organisms were carried out with *U.* linza, *C.* lytica, *N.* incerta, and barnacles. All assessments were carried out after 28 days of water aging. All coatings were non-toxic as they were tested through leachate toxicity of *C. lytica*, *N. incerta*, and *U. linza*, following the procedure described elsewhere.[38, 42]

U. linza is a macroalgae that prefers hydrophobic surfaces for settlement more than hydrophilic surfaces.[43-45] The extent of biofouling among all coatings (both studied and control) was almost equal, and no significant difference was observed. The biofouled surfaces were water-jetted at 10 psi and 16 psi to assess their FR performance under hydrodynamic pressure. The extent of *U. linza* removal (percent removal) was higher at 16 psi (Figure 5.7 – Green bars) than 10 psi (Figure 5.7 – Blue bars), but the overall trend of removal was similar at both pressure levels. Among coatings R1-R4, the MW of PDMS and PEG caused negligible differences in FR performance – Amp-3 composed of 10k $\bar{M}_n$ PDMS and 750 $\bar{M}_n$ PEG was relatively the best-performing additive. Comparing R3, R7, and R8 systems, it is suggested that the amount of added AmpAdd did not have a major impact on FR properties (though Amp-3 at 15 wt.% showed the relative best performance). Alternatively, the data implied that the degree of additive

hydrophilicity influenced the FR performance, where system R6 with the most hydrophilic additive (Amp-6) outperformed R5 and R3 with Amp-5 and Amp-3 additives, respectively. Not only did the AmpAdds improve performance of the R0 coating in respect to the A4 system, some of AmpAdds such as Amp-3, Amp-5, and Amp-6 also pushed FR of R0 system to be on par with well-performing materials such as T2 and IS 1100. Conclusively, the amphiphilic additives improved FR performance of R0 against *U. linza* as the comparison between unmodified and modified R0 systems demonstrated. The FR results of *U. linza* are in correlation with literature that the hydrophilic surfaces weaken the adhesion of this organism.

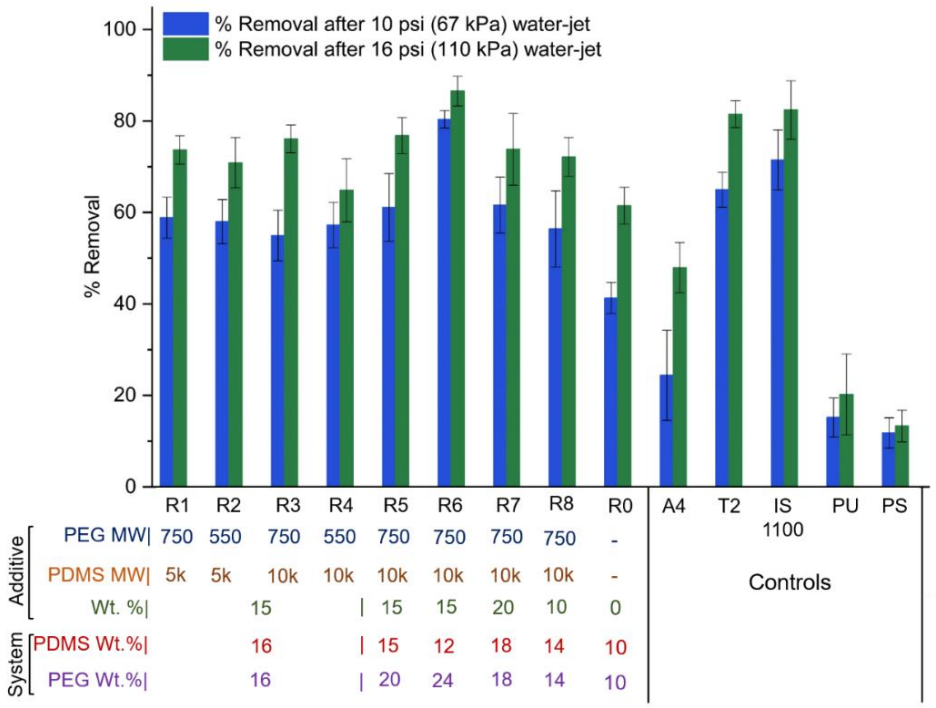

Figure 5.7. *U. linza* fouling-release data, displaying percent removal/release after water jetting at 10 psi (blue bar) and 20 psi (green bar). The x-axis is labeled to reflect details about the utilized additive and the overall content of PEG and PDMS in a formulation. Each category of assessed coatings is separated with lines.

C. lytica is a micro-biofouling bacterium that can settle on both hydrophobic and hydrophilic surfaces, challenging the traditional hydrophobic FR surfaces. Thus, amphiphilic surfaces are considered as a feasible solution to fight against biofouling of *C. lytica*.[1,12] The extent of biofouling among all coatings were relatively similar except for IS 700, IS 900, and IS 1100 that showed almost twice *C. lytica* biofouling, and it was observed AmpAdds did not result in an increased initial film formation. The FR

performance of surfaces was evaluated at two water pressure levels, 10 psi and 20 psi. The biomass remaining of *C. lytica* after 10 psi (Figure 5.8 – Blue bars) and 20 psi (Figure 5.8 – Green bars) water jetting showed that 10 psi water pressure level released less *C. lytica* than the 20 psi but the overall trend for both pressures was similar. Coatings R1 with Amp-1 and R7 and R8 with Amp-3 (at 20 wt.% and 10 wt.%, respectively) displayed better FR performance than unmodified R0 and control A4 systems, while the remaining modified counterparts were comparable to R0 and A4. Additionally, the three systems (R1, R7, and R8) pushed the performance of R0 to be on par with IS 900 and IS 1100, allowing for the least amount of *C. lytica* to remain settled on their surfaces after water jetting. While the removal is greater for IS 900 and IS 1100 systems due to their very high initial biofouling, it should be noted the AmpAdd-modified R0 coatings experienced less initial biofouling. Coating R6 delaminated and could not be tested, which was attributed to its most hydrophilic matrix swollen under water. Overall, AmpAdds did not have a detrimental effect on FR performance of R0; the additives either improved the FR performance or did not alter it.

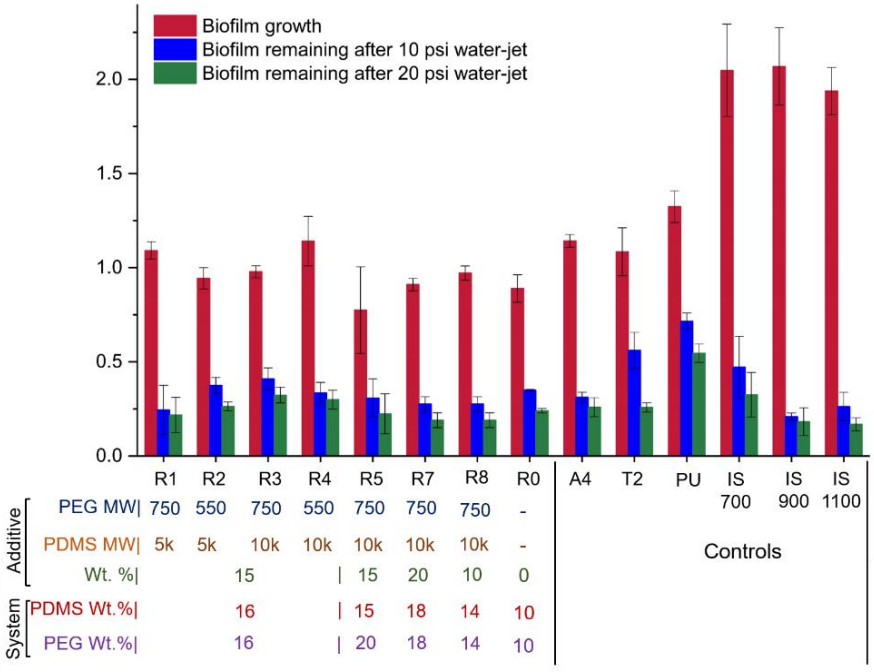

Figure 5.8. *C. lytica* fouling-release data, showing biomass remaining after 10 psi waterjet (blue bar) and 20 psi waterjet (green bar). The x-axis is labeled to reflect details about the utilized additive and the overall content of PEG and PDMS in a formulation. Each category of assessed coatings is separated with lines.

N. incerta is a micro-biofoulant that settles preferably on hydrophobic surfaces.[43, 44] The extent of biofouling settlement was alike among all studied and control coatings, and no remarkable change was noticed due to the addition of AmpAdds. Biofouled surfaces with *N. incerta* were water-jetted at 10 psi and 20 psi pressured levels. The higher water pressure level released more organisms (Figure 5.9 – Green bars) than the lower pressure level (Figure 5.9 – Blue bars), while the overall trends remained alike. The FR data indicates that AmpAdds improved the performance of the R0 base system by almost 60% at both pressure levels. However, the release performance was very similar among the modified R0 coatings, resulting in no substantial conclusion regarding the effect of MW of PEG and PDMS, the extent of additive hydrophilicity, and the amount of additive in a system. All the AmpAdd-modified R0 systems remarkably outperformed several internal and commercial controls including A4, PU, and IS 700. Additionally, several systems including R2, R5, R7, and R8 showed matching performance in respect to the top-performing commercial systems such as IS 900 and 1100 SR. Coating R6 delaminated and could not be tested, which was attributed to its highly hydrophilic matrix swollen underwater (this was the most hydrophilic formulation). The FR data of *N. incerta* suggests that the designed AmpAdds impart better performance to the base AmpSiPU R0 coating, indicating that a higher degree of amphiphilicity for this system is beneficial; however, it could not be concluded which particular AmpAdd was better over another.

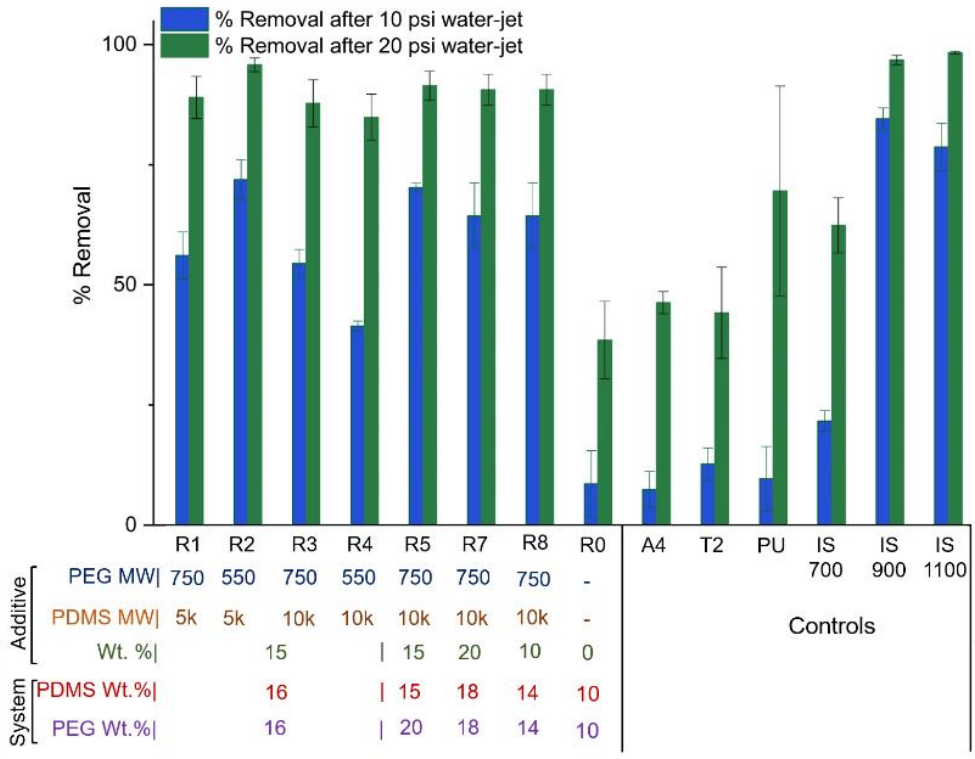

Figure 5.9. *N. incerta* fouling-release data, displaying percent removal/release after water jetting at 10 psi (blue bar) and 20 psi (green bar). The x-axis is labeled to reflect details about the utilized additive and the overall content of PEG and PDMS in a formulation. Each category of assessed coatings is separated with lines.

Barnacles, a macrofoulant, is another known marine organism that is infamous for its detrimental biofouling effects.[3, 46] Different species of barnacle settle on different surfaces, for example, *Amphibalanus amphitrite* settles both hydrophilic and hydrophobic surfaces;[40, 41, 47, 48] Consequently, it is challenging to propose a universal rule predicting their behavior.[1, 49-52] AmpAdds resulted in both beneficial and detrimental effects in terms of the adhesion strength of the reattached barnacles (Figure 5.10). For example, in respect to the unmodified R0 system, Amp-2 at 15 wt.% (R2 formulation) and Amp-3 at 20 wt.% (R7 formulation) reduced the adhesion strength of barnacles, while Amp-3 at 15 wt.% (R3 formulation) increased the adhesion strength of the barnacles. These two additives (Amp-3 and Amp-3) increased the overall amphiphilicity balance of the R0 system equally, meaning the wt.% of PEG and PDMS in solid contents were same. However, when AmpAdds with varying hydrophilic-hydrophobic balance shifted the systems to be more hydrophilic (increasing from R0 to R5 to R6), the adhesion strength of barnacles slightly increased, which may be due to affinity of *A. Amphitrite* to more hydrophilic

surfaces in this case. Overall, this data suggested the amount of an additive or its design parameters influences the performance of a system, which can be either favorable or unfavorable.

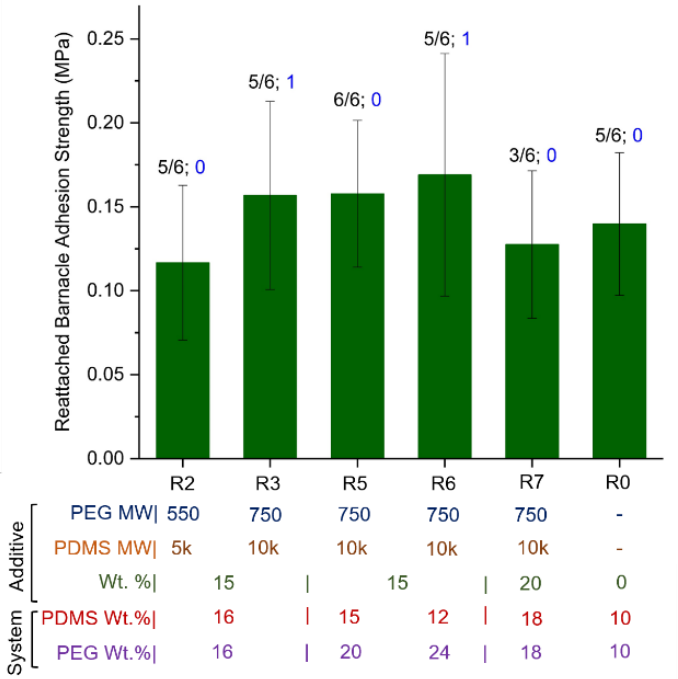

Figure 5.10. Reattached barnacle (*A. Amphitrite*) adhesion strength data. Six barnacles were used for each reattachment study. The number of reattached barnacles out of six is labeled for each system as a ratio. The blue number shows the number of broken barnacles out of the reattached ones during the push-off experiment. Each bar shows the average adhesion strength based on the number of successfully reattached barnacles. The x-axis is labeled to reflect details about the utilized additive and the overall content of PEG and PDMS in a formulation. Each category of assessed coatings is separated with lines.

Conclusions

This study explored a novel series of amphiphilic additives by attaching PEG and PDMS chains on a polyisocyanate resin via the facile isocyanate and alcohol reaction, allowing for the easy synthesis of amphiphilic additives having varied molecular weights of amphiphilic chains and tunable hydrophilic-hydrophobic balance. This study demonstrated that the introduction of amphiphilic additives to an amphiphilic marine coating system, known as the amphiphilic siloxane-polyurethane (AmpSiPU), was beneficial overall, boosting the performance of this system to tackle marine biofoulants better. The surface characterizations confirmed that the amphiphilic additives modified the surface of the control amphiphilic coatings. Contact angle measurements displayed modified AmpSiPU systems were more

dynamic in their interaction with water and methylene iodide droplets in respect to the control AmpSiPU coating. ATR-FTIR confirmed the presence of PEG and PDMS moieties on the surfaces that were attributed to amphiphilic additives. In respect to the base AmpSiPU system, modified surfaces exhibited highly saturated surfaces containing heterogenous microdomains under AFM. Additionally, the XPS experiment on model PU systems confirmed that the additives self-stratified to the surfaces. Biological assays demonstrated that amphiphilic additives improved the fouling-release performance of the base AmpSiPU system. Overall, the PEG-PDMS additives boosted the performance of AmpSiPU system against *U. linza* and *N. incerta* and advanced it slightly against *C. lytica*, while they presented both advantageous and hampering effects against barnacles. The results indicated systems where the hydrophilic balance was slightly more than hydrophobic offered a more desirable performance against some organisms such as *U. linza* and *N. incerta*. This study intrigues the questions to further investigate and understand the effect of amphiphilic balance (ratio of hydrophilic and hydrophobic contents in a system) which may bridge some less understood concepts for the purpose of marine biofouling as well as other applications such as anti-icing and medical devices.

References

1. Lejars, M.; Margaillan, A.; Bressy, C., Fouling release coatings: A nontoxic alternative to biocidal antifouling coatings. *Chemical Reviews* **2012,** *112* (8), 4347-4390.

2. Callow, J. A.; Callow, M. E., Trends in the development of environmentally friendly fouling-resistant marine coatings. *Nature Communications* **2011,** *2* (1), 244-244.

3. Callow, M. E.; Callow, J. E., Marine biofouling: a sticky problem. *Biologist* **2002,** *49* (1), 10-14.

4. Pade, M.; Webster, D. C., Self-stratified siloxane-polyurethane fouling-release marine coating strategies: A review. In *Marine Coatings and Membranes*, Mittal, V., Ed. Central West Publishing: Australia, 2019; pp 1-36.

5. Beigbeder, A.; Mincheva, R.; Pettitt, M. E.; Callow, M. E.; Callow, J. A.; Claes, M.; Dubois, P., Marine fouling release silicone/carbon nanotube nanocomposite coatings: on the importance of the nanotube dispersion state. *Journal of Nanoscience and Nanotechnology* **2010,** *10* (5), 2972-2978.

6. Beigbeder, A.; Labruyère, C.; Viville, P.; Pettitt, M. E.; Callow, M. E.; Callow, J. A.; Bonnaud, L.; Lazzaroni, R.; Dubois, P., Surface and fouling-release properties of silicone/organomodified montmorillonite coatings. *Journal of Adhesion Science and Technology* **2011,** *25* (14), 1689-1700.

7. Genzer, J.; Efimenko, K., Recent developments in superhydrophobic surfaces and their relevance to marine fouling: a review. *Biofouling* **2006,** *22* (5), 339-360.

8. Konstantinou, I. K.; Albanis, T. A., Worldwide occurrence and effects of antifouling paint booster biocides in the aquatic environment: a review. *Environment International* **2004,** *30* (2), 235-248.

9. Magin, C. M.; Cooper, S. P.; Brennan, A. B., Non-toxic antifouling strategies. *Materials Today* **2010,** *13* (4), 36-44.

10. Wyszogrodzka, M.; Haag, R., Synthesis and characterization of glycerol dendrons, self-assembled monolayers on gold: A detailed study of their protein resistance. *Biomacromolecules* **2009,** *10* (5), 1043-1054.

11. Bodkhe, R. B.; Thompson, S. E. M.; Yehle, C.; Cilz, N.; Daniels, J.; Stafslien, S. J.; Callow, M. E.; Callow, J. A.; Webster, D. C., The effect of formulation variables on fouling-release performance of stratified siloxane–polyurethane coatings. *Journal of Coatings Technology and Research* **2012,** *9* (3), 235-249.

12. Galhenage, T. P.; Webster, D. C.; Moreira, A. M. S.; Burgett, R. J.; Stafslien, S. J.; Vanderwal, L.; Finlay, J. A.; Franco, S. C.; Clare, A. S., Poly(ethylene) glycol-modified, amphiphilic, siloxane–polyurethane coatings and their performance as fouling-release surfaces. *Journal of Coatings Technology and Research* **2017,** *14* (2), 307-322.

13. Claisse, D.; Alzieu, C., Copper contamination as a result of antifouling paint regulations? *Marine Pollution Bulletin* **1993,** *26* (7), 395-397.

14. Turner, A., Marine pollution from antifouling paint particles. *Marine Pollution Bulletin* **2010,** *60* (2), 159-171.

15. Pérez, M.; Blustein, G.; García, M.; del Amo, B.; Stupak, M., Cupric tannate: a low copper content antifouling pigment. *Progress in Organic Coatings* **2006,** *55* (4), 311-315.

16. Cai, L.; Liu, A.; Yuan, Y.; Dai, L.; Li, Z., Self-assembled perfluoroalkylsilane films on silicon substrates for hydrophobic coatings. *Progress in Organic Coatings* **2017,** *102*, 247-258.

17. Pollack, K. A.; Imbesi, P. M.; Raymond, J. E.; Wooley, K. L., Hyperbranched fluoropolymer-polydimethylsiloxane-poly(ethylene glycol) cross-linked terpolymer networks designed for marine and biomedical Applications: heterogeneous nontoxic antibiofouling surfaces. *ACS Applied Materials & Interfaces* **2014,** *6* (21), 19265-19274.

18. Noguer, A. C., *Experimental investigation of the behaviour and fate of block copolymers in fouling-release coatings*. Technical University of Denmark (DTU): Kgs. Lyngb, Denmark, 2016.

19. Murthy, R.; Bailey, B. M.; Valentin-Rodriguez, C.; Ivanisevic, A.; Grunlan, M. A., Amphiphilic silicones prepared from branched PEO-silanes with siloxane tethers. *Journal of Polymer Science Part A: Polymer Chemistry* **2010,** *48* (18), 4108-4119.

20. Martinelli, E.; Suffredini, M.; Galli, G.; Glisenti, A.; Pettitt, M. E.; Callow, M. E.; Callow, J. A.; Williams, D.; Lyall, G., Amphiphilic block copolymer/poly (dimethylsiloxane)(PDMS) blends and nanocomposites for improved fouling-release. *Biofouling* **2011,** *27* (5), 529-541.

21. Røn, T.; Javakhishvili, I.; Hvilsted, S.; Jankova, K.; Lee, S., Ultralow friction with hydrophilic polymer brushes in water as segregated from silicone matrix. *Advanced Materials Interfaces* **2016,** *3* (2), 1500472.

22. Rufin, M. A.; Barry, M. E.; Adair, P. A.; Hawkins, M. L.; Raymond, J. E.; Grunlan, M. A., Protein resistance efficacy of PEO-silane amphiphiles: Dependence on PEO-segment length and concentration. *Acta biomaterialia* **2016,** *41*, 247-252.

23. Shivapooja, P.; Yu, Q.; Orihuela, B.; Mays, R.; Rittschof, D.; Genzer, J.; López, G. P., Modification of silicone elastomer surfaces with zwitterionic polymers: short-term fouling resistance and triggered biofouling release. *ACS Applied Materials & Interfaces* **2015,** *7* (46), 25586-25591.

24. Liu, Y.; Leng, C.; Chisholm, B.; Stafslien, S.; Majumdar, P.; Chen, Z., Surface structures of PDMS incorporated with quaternary ammonium salts designed for antibiofouling and fouling release applications. *Langmuir* **2013,** *29* (9), 2897-2905.

25. Wan, F.; Pei, X.; Yu, B.; Ye, Q.; Zhou, F.; Xue, Q., Grafting polymer brushes on biomimetic structural surfaces for anti-algae fouling and foul release. *ACS Applied Materials & Interfaces* **2012,** *4* (9), 4557-4565.

26. Yeh, S.-B.; Chen, C.-S.; Chen, W.-Y.; Huang, C.-J., Modification of silicone elastomer with zwitterionic silane for durable antifouling properties. *Langmuir* **2014,** *30* (38), 11386-11393.

27. Ciriminna, R.; Bright, F. V.; Pagliaro, M., Ecofriendly antifouling marine coatings. *ACS Sustainable Chemistry & Engineering* **2015,** *3* (4), 559-565.

28. Galhenage, T. P.; Hoffman, D.; Silbert, S. D.; Stafslien, S. J.; Daniels, J.; Miljkovic, T.; Finlay, J. A.; Franco, S. C.; Clare, A. S.; Nedved, B. T., Fouling-release performance of silicone oil-modified siloxane-polyurethane coatings. *ACS Applied Materials & Interfaces* **2016,** *8* (42), 29025-29036.

29. Wei, C.; Zhang, G.; Zhang, Q.; Zhan, X.; Chen, F., Silicone oil-infused slippery surfaces based on sol–gel process-induced nanocomposite coatings: A facile approach to highly stable bioinspired surface for biofouling resistance. *ACS Applied Materials & Interfaces* **2016,** *8* (50), 34810-34819.

30. Kavanagh, C. J.; Swain, G. W.; Kovach, B. S.; Stein, J.; Darkangelo-Wood, C.; Truby, K.; Holm, E.; Montemarano, J.; Meyer, A.; Wiebe, D., The effects of silicone fluid additives and silicone elastomer matrices on barnacle adhesion strength. *Biofouling* **2003,** *19* (6), 381-390.

31. Selim, M. S.; El-Safty, S. A.; Azzam, A. M.; Shenashen, M. A.; El-Sockary, M. A.; Abo Elenien, O. M., Superhydrophobic silicone/TiO2–SiO2 nanorod-like composites for marine fouling release coatings. *ChemistrySelect* **2019,** *4* (12), 3395-3407.

32. Selim, M. S.; El-Safty, S. A.; El-Sockary, M. A.; Hashem, A. I.; Elenien, O. M. A.; El-Saeed, A. M.; Fatthallah, N. A., Smart photo-induced silicone/TiO2 nanocomposites with dominant [110] exposed surfaces for self-cleaning foul-release coatings of ship hulls. *Materials & Design* **2016,** *101*, 218-225.

33. Arukalam, I. O.; Oguzie, E. E.; Li, Y., Fabrication of FDTS-modified PDMS-ZnO nanocomposite hydrophobic coating with anti-fouling capability for corrosion protection of Q235 steel. *Journal of Colloid and Interface Science* **2016,** *484*, 220-228.

34. Bodkhe, R. B.; Stafslien, S. J.; Cilz, N.; Daniels, J.; Thompson, S. E. M.; Callow, M. E.; Callow, J. A.; Webster, D. C., Polyurethanes with amphiphilic surfaces made using telechelic functional PDMS having orthogonal acid functional groups. *Progress in Organic Coatings* **2012,** *75* (1-2), 38-48.

35. Owens, D. K.; Wendt, R. C., Estimation of the surface free energy of polymers. *Journal of Applied Polymer Science* **1969,** *13* (8), 1741-1747.

36. Stafslien, S.; Daniels, J.; Mayo, B.; Christianson, D.; Chisholm, B.; Ekin, A.; Webster, D.; Swain, G., Combinatorial materials research applied to the development of new surface coatings IV. A high-throughput bacterial biofilm retention and retraction assay for screening fouling-release performance of coatings. *Biofouling* **2007,** *23* (1), 45-54.

37. Stafslien, S. J.; Bahr, J. A.; Daniels, J. W.; Wal, L. V.; Nevins, J.; Smith, J.; Schiele, K.; Chisholm, B., Combinatorial materials research applied to the development of new surface coatings VI: An automated spinning water jet apparatus for the high-throughput characterization of fouling-release marine coatings. *Review of Scientific Instruments* **2007,** *78* (7), 072204-072204.

38. Cassé, F.; Stafslien, S. J.; Bahr, J. A.; Daniels, J.; Finlay, J. A.; Callow, J. A.; Callow, M. E., Combinatorial materials research applied to the development of new surface coatings V. Application of a spinning water-jet for the semi-high throughput assessment of the attachment strength of marine fouling algae. *Biofouling* **2007,** *23* (2), 121-130.

39. Cassé, F.; Ribeiro, E.; Ekin, A.; Webster, D. C.; Callow, J. A.; Callow, M. E., Laboratory screening of coating libraries for algal adhesion. *Biofouling* **2007,** *23* (4), 267-276.

40. Stafslien, S.; Daniels, J.; Bahr, J.; Chisholm, B.; Ekin, A.; Webster, D.; Orihuela, B.; Rittschof, D., An improved laboratory reattachment method for the rapid assessment of adult barnacle adhesion strength to fouling-release marine coatings. *Journal of Coatings Technology and Research* **2012,** *9* (6), 651-665.

41. Rittschof, D.; Orihuela, B.; Stafslien, S.; Daniels, J.; Christianson, D.; Chisholm, B.; Holm, E., Barnacle reattachment: A tool for studying barnacle adhesion. *Biofouling* **2008,** *24* (1), 1-9.

42. Majumdar, P.; Crowley, E.; Htet, M.; Stafslien, S. J.; Daniels, J.; VanderWal, L.; Chisholm, B. J., Combinatorial materials research applied to the development of new surface coatings XV: An investigation of polysiloxane anti-fouling/fouling-release coatings containing tethered quaternary ammonium salt groups. *ACS Combinatorial Science* **2011,** *13* (3), 298-309.

43. Finlay, J. A.; Callow, M. E.; Ista, L. K.; Lopez, G. P.; Callow, J. A., The influence of surface wettability on the adhesion strength of settled spores of the green alga Enteromorpha and the diatom Amphora. *Integrative and Comparative Biology* **2002,** *42* (6), 1116-1122.

44. Callow, M. E.; Callow, J. A.; Ista, L. K.; Coleman, S. E.; Nolasco, A. C.; López, G. P., Use of self-assembled monolayers of different wettabilities to study surface selection and primary adhesion processes of green algal (Enteromorpha) zoospores. *Applied Environmental Microbiology* **2000,** *66* (8), 3249-3254.

45. Callow, J. A.; Callow, M. E.; Ista, L. K.; Lopez, G.; Chaudhury, M. K., The influence of surface energy on the wetting behaviour of the spore adhesive of the marine alga Ulva linza (synonym Enteromorpha linza). *Journal of the Royal Society Interface* **2005,** *2* (4), 319-325.

46. Aldred, N.; Li, G.; Gao, Y.; Clare, A. S.; Jiang, S., Modulation of barnacle (Balanus amphitrite Darwin) cyprid settlement behavior by sulfobetaine and carboxybetaine methacrylate polymer coatings. *Biofouling* **2010,** *26* (6), 673-683.

47. Huggett, M. J.; Nedved, B. T.; Hadfield, M. G., Effects of initial surface wettability on biofilm formation and subsequent settlement of Hydroides elegans. *Biofouling* **2009,** *25* (5), 387-399.

48. Rittschof, D.; Costlow, J. D., Bryozoan and barnacle settlement in relation to initial surface wettability: A comparison of laboratory and field studies. *Sci. Mar.* **1989,** *53* (2), 411-416.

49. Petrone, L.; Di Fino, A.; Aldred, N.; Sukkaew, P.; Ederth, T.; Clare, A. S.; Liedberg, B., Effects of surface charge and Gibbs surface energy on the settlement behaviour of barnacle cyprids (Balanus amphitrite). *Biofouling* **2011,** *27* (9), 1043-1055.

50. Di Fino, A.; Petrone, L.; Aldred, N.; Ederth, T.; Liedberg, B.; Clare, A. S., Correlation between surface chemistry and settlement behaviour in barnacle cyprids (Balanus improvisus). *Biofouling* **2014,** *30* (2), 143-152.

51. Gatley-Montross, C. M.; Finlay, J. A.; Aldred, N.; Cassady, H.; Destino, J. F.; Orihuela, B.; Hickner, M. A.; Clare, A. S.; Rittschof, D.; Holm, E. R., Multivariate analysis of attachment of biofouling organisms in response to material surface characteristics. *Biointerphases* **2017,** *12* (5), 051003.

52. Aldred, N.; Gatley-Montross, C. M.; Lang, M.; Detty, M. R.; Clare, A. S., Correlative assays of barnacle cyprid behaviour for the laboratory evaluation of antifouling coatings: a study of surface energy components. *Biofouling* **2019,** *35* (2), 159-172.

CHAPTER 6. AMPHIPHILIC, SELF-STRATIFIED GLYCIDYL-CARBAMATE SURFACES AS FOULING-RELEASE MARINE COATING SYSTEMS

Introduction

Marine biofouling is recognized as the undesirable settlement of marine organisms on submerged surfaces in seawater.[1] Marine biofouling causes many issues such as increased drag, reduced maneuverability, high fuel consumption, and even transportation of invasive species.[2,3] As an example, the US Navy spends $1 billion per year to maintain their ships from biofouling.[3,4] Marine biofouling is a complex problem since reports indicate that more than 4000 marine organisms, involving various surface affinities and mechanisms of adhesion, can potentially biofoul a surface.[1, 2, 5]

Ships have been around for thousands of years and humans developed a variety of systems to fight biofouling. Initially, copper alloys and lead sheaths opposed biofouling on hulls of ships, but they had limitations in terms of metallic corrosion and availability of resources. Biocide-containing antifouling paints and tributyltin-based self-polishing coatings were eventually introduced as alternatives in 1900s. Despite their stellar performance, the novel systems caused toxic effects on aquatic environments, resulting in a worldwide ban of tin-containing marine coatings by International Marine Organization (IMO) and motivating the development of non-toxic antifouling and fouling-release coating systems.[2, 6]

Current antifouling (AF) coatings typically contain copper-based biocides with organic booster biocides to contend with biofouling. Copper is less toxic than tin, but it still has potential to poison ecosystems. Alternatively, fouling-release (FR) systems offer non-toxic and environmental-friendly solution to tackle biofouling. Instead of leaching biocides, FR systems function by forbidding strong adhesion of biofoulants to the surface of a structure and facilitating their release under hydrodynamic pressure.[1, 2] Thus, FR systems have been favored due to the absence of biocides in their design.

Traditionally, FR systems are made of elastomeric materials such as polydimethylsiloxane (PDMS) and fluoroalkyl polymers. These materials are widely explored due to their low surface energy that delays biofouling and acts as a driving force for the fouling-release mechanism.[7, 2] Nevertheless, the low surface energy materials suffer from durability (adhesion and mechanical), requiring a tie-coat to

attain proper adhesion to a surface.[2, 5] Hydrophobic siloxane-polyurethane (SiPU) FR coatings have shown promising performance to address the limitations of the traditional FR systems such as durability and the need for a tie-coat. The SiPU FR system takes advantage of self-stratification of the non-polar low-surface-energy PDMS over the polar PU layer, while both layers are connected through covalently bonded crosslinks.[8, 9]

Hydrophobic FR systems like SiPU demonstrate a great potential to fight biofouling, but such systems still lack desirable performance against some organisms.[10-12] There are organisms out of the ~4000 biofoulants in seawater that prefer to settle on a hydrophobic system.[5] For example, diatom (*N. incerta*) attaches strongly to a hydrophobic system while barnacles or mussels prefer a hydrophilic surface. Therefore, amphiphilic systems that contain both hydrophilic and hydrophobic moieties on the surface have been investigated to deter biofouling of a wider range of marine organisms.[2, 13-17]

Amphiphilic surfaces have been explored using many approaches based on layer-by-layer polyanion-polycation,[18, 19] hyperbranched,[20, 21] UV-cured,[22] zwitterionic,[23-25] self-stratification,[8, 26] and polypeptide/peptide-mimic chemistries.[27] Recently, PEG-modified amphiphilic SiPU systems have shown desirable fouling-release performance.[17] The system is founded on an amphiphilic prepolymer: partial functionalization of an isocyanate resin with hydrophobic and hydrophilic moieties. The amphiphilic isocyanate-based prepolymer, isocyanate resin, and acrylic polyol constitute the coating system. Despite the fact that there are health concerns for workers who use isocyanates in 2K coating formulations as a final product,[28-30] it is tough to discard the desired properties that urethane linkages contribute to a coating system. Thus, there is a need for a solution that reduces the exposure of workers to isocyanates as a final product while it still sustains the benefits of isocyanate.

Glycidyl-carbamate (GC) coating systems have been introduced as a viable alternative to deliver both properties of urethane linkage and isocyanate-free formulations.[31-39] GC coatings are composed of a GC resin which can undergo either polycondensation curing with an amine[33] or self-crosslinking.[37] A GC resin is easily synthesized by reaction of an isocyanate resin with glycidol, generating a urethane/carbamate linkage and introducing epoxy functional groups. Thus, a GC resin offers highly sought urethane properties combined with epoxy groups for facile curing chemistries.

In this study, we worked on a solution to achieve an amphiphilic fouling-release coating by utilizing glycidyl-carbamate technology. With this inspiration, we developed a new synthetic method to re-functionalize a commercially available isocyanate resin with epoxy functional groups to access an isocyanate-based epoxy resin and with amphiphilic chains to attain fouling-release performance (Figure 6.1). We applied thermodynamic principles to utilize self-stratification of low surface energy components like PDMS-containing materials to the surface.[9] In addition to efforts to find a facile synthesis for attaching PEG and PDMS chains in the same backbone (which usually requires several steps), we investigated a series of coatings to find answers for three dimensions that would pave the way for effective design of future amphiphilic systems: 1) Optimum molecular weight of PDMS and PEG for a system, 2) Optimum total weight of PEG and PDMS in a system, and 3) Effect of cross-linking agent. To this effect, here we report synthesis and characterization of glycidyl-carbamate (GC)-based resin and amphiphilic prepolymers and their incorporation in developing amphiphilic self-stratified fouling-release coatings.

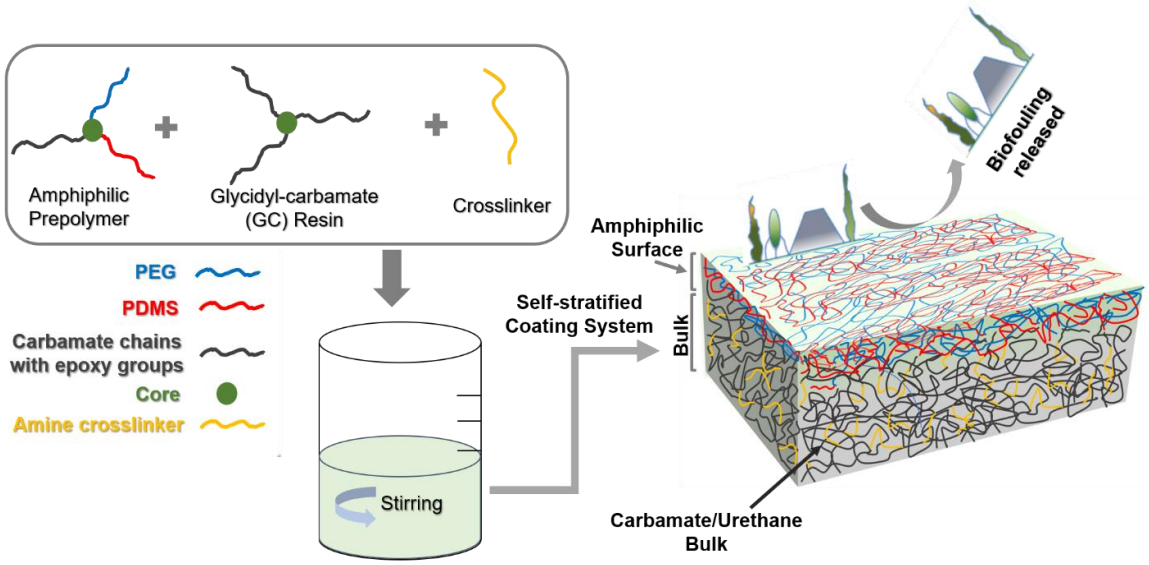

Figure 6.1. Illustration of fouling-release amphiphilic self-stratified glycidyl-carbamate coating system for marine applications.

Experimental

Materials

Isophorone diisocyanate (IPDI) polyisocyanate Desmodur Z4470 BA was supplied by Covestro LLC. Monocarbinol-terminated polydimethylsiloxane (CT-PDMS) with two molecular weights of 5000 $\bar{M}_n$ (MCR-C18) and 10,000 $\bar{M}_n$ (MCR-C22) were purchased from Gelest, Inc. Glycidol, poly(ethylene glycol)

methyl ether (550 $\bar{M}_n$ and 750 $\bar{M}_n$), ethyl-3-ethoxy propionate, methyl ethyl ketone (MEK), methyl amyl ketone (MAK), hydrobromic acid (5.7 M), and dibutyltin diacetate (DBTDAc) were purchased from Sigma Aldrich. Toluene and glacial acetic acid (for epoxy titration) was purchased from VWR. Ancamide® 702B75 and Amicure® PACM crosslinkers were provided by Evonik Industries.

AkzoNobel International Paint provided the commercial FR standards Intersleek® 700 (IS 700), Intersleek® 900 (IS 900), and Intersleek® 1100SR (IS 1100). Silicone elastomer, Silastic® T2 (T2) was provided by Dow Corning as another commercial standard. Hydrophobic A4-20 coating (A4-20), a siloxane-polyurethane system, was prepared as an internal control following the procedures described elsewhere.[9] Amphiphilic T-10 coating was prepared following the procedure elsewhere, an isocyanate-based formulation that contained 10 wt.% PEG 750 $\bar{M}_n$ and PDMS 10,000 $\bar{M}_n$.[17] Aluminum panels (4" x 8" in., 0.6 mm thick, type A, alloy 3003 H14) purchased from Q-lab were sandblasted and primed with Intergard 264 (International Paint) using air-assisted spray application. Multi-well plates were modified using circular disks (1-inch diameter) of primed aluminum.

Experimental Design

This study examined four factors including molecular weight of PEG, molecular weight of PDMS, the amounts of PDMS and PEG in the coating system, and type of crosslinker. To assess these factors, three overlapping designs were utilized.[40] First, an experimental design followed a 2^3 design, involving 8 coating formulations. For this design, each of the three factors had two levels: PEG in two molecular weights of 550 $\bar{M}_n$ and 750 $\bar{M}_n$; PDMS in two molecular weights of 5000 $\bar{M}_n$ and 10,000 $\bar{M}_n$; and PDMS and PEG amounts of 5 wt.% and 10 wt.% each based on solid contents. These eight formulations are F1-F8 in Table 6.1. To further evaluate effect of higher amphiphilic amounts in a system, three formulations that contained between 15 wt.% to 20 wt.% of PEG 550/750 $\bar{M}_n$ and PDMS 10,000 $\bar{M}_n$ were evaluated. These formulations result in comparison of formulations F4, F8, F9, F10, and F11 based on one variable (Table 6.1), amount of PEG and PDMS. To assess effect of crosslinking agent, three additional formulations were introduced that utilized Ancamide®702B75 as a curing agent, allowing coatings F6, F8, F11, F12, F13, and F14 to be compared (Table 6.1).

Table 6.1. Coating compositions

Formulation	Formulation Type	PDMS MW ($\bar{M}_n$)	PDMS Wt.%	PEG MW ($\bar{M}_n$)	PEG Wt.%	Crosslinker
F1	5-5kPDMS-550PEG	5,000	5	550	5	PACM
F2	5-5kPDMS-750PEG	5,000	5	750	5	
F3	5-10kPDMS-550PEG	10,000	5	550	5	
F4	5-10kPDMS-750PEG	10,000	5	750	5	
F5	10-5kPDMS-550PEG	5,000	10	550	10	
F6	10-5kPDMS-750PEG	5,000	10	750	10	
F7	10-10kPDMS-550PEG	10,000	10	550	10	
F8	10-10kPDMS-750PEG	10,000	10	750	10	
F9	15-5kPDMS-750PEG	5,000	15	750	15	
F10	15-10kPDMS-750PEG	10,000	15	750	15	
F11	20-10kPDMS-750PEG	10,000	20	750	20	
F12	10-5kPDMS-750PEG-RT	5,000	10	750	10	Anacamide 702B75
F13	10-10kPDMS-750PEG-RT	10,000	10	750	10	
F14	13-10kPDMS-750PEG-RT	10,000	13	750	13	

Synthesis of Glycidyl Carbamate Resin

Polyisocyanate IPDI trimer Desmodur Z4470 was reacted with glycidol to prepare the glycidyl-carbamate (GC) resin, an epoxidized urethane-linkage-containing resin (Scheme 6.1 – Route 1). The GC

resin was produced by reacting the IPDI trimer resin with glycidol in 1:1 ratio of NCO: OH. To synthesize the resin, 13.00 g of IPDI trimer (NCO eq wt. = 253), 2.92 g glycidol, 0.48 g DBTDAc catalyst solution (1% by wt. in MAK) and 7.95 g toluene were added in a 50-mL three-neck flask, equipped with a magnetic stirrer, nitrogen inlet, and temperature controller. The reaction was carried at 80 °C for 2 hours. As another method, the reaction could also be completed at ambient condition for 24 hours. A reflux condenser was used when heat was applied.

Synthesis of Glycidyl Carbamate Prepolymers

GC-functional prepolymers were synthesized by attaching epoxy functional groups and PEG and PDMS chains on the polyisocyanate IPDI trimer Desmodur Z4470 resin (Scheme 6.1 – Route 2). The ratio of NCO groups to the combined OH groups was 1:1, where glycidol was used to functionalize 33.3 % of the NCO groups and the remaining 66.6% isocyanate groups were converted to urethane linkages by attachment of PEG and PDMS chains. PEG and PDMS were added in equal weight ratios to meet the 66.6% required molar ratio.

As an example, to synthesize prepolymer 5kPDMS-550PEG, PEG 550 $\bar{M}_n$ (2.50 g) was diluted in toluene (2.50 g) in a 50-mL flask. PDMS 10,000 $\bar{M}_n$ (2.50 g) was added to the flask and mixed robustly with vortex for 2 minutes. Glycidol (0.13 g) was added to the flask and mixed for another 2 minutes. IPDI trimer resin (1.84 g) and DBTDAc catalyst solution (1% by wt. in MAK) (0.35 g) were then added to the flask. The reaction was carried at 80 °C for 2 hours. As another method, the reaction could also be completed at ambient condition for 24 hours. A reflux condenser was used when heat was applied. The flask was equipped with a magnetic stirrer, nitrogen inlet, and temperature controller. In theory, the synthesized prepolymer contained 38.5 wt.% PEG and 38.5 wt.% PDMS.

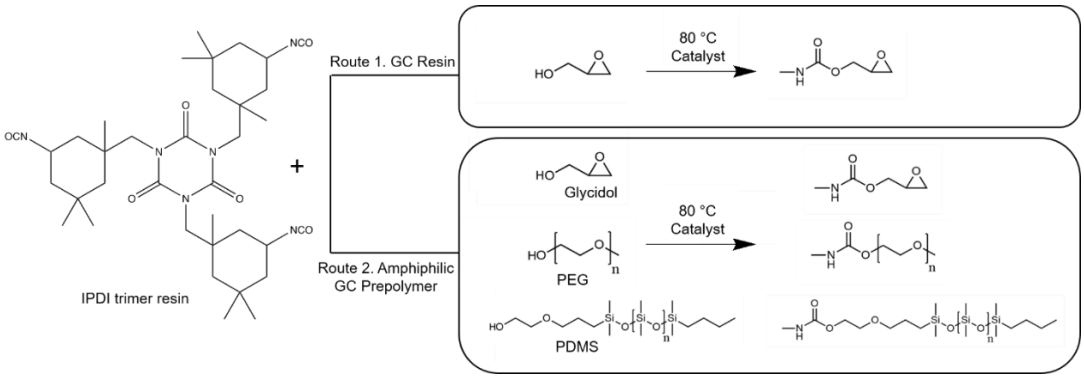

Scheme 6.1. Synthesis of glycidyl carbamate resin (Route 1) and amphiphilic GC prepolymer (Route 2).

Epoxy Equivalent Weight Titrations

Epoxy equivalent weight (EEW) titrations were used to verify EEW content for both resin and prepolymers. The titration was conducted following ASTM D1652. In general, a sample of resin or prepolymer (1-2 g) was weighed in an Erlenmeyer flask. The sample was dissolved in 15 mL of chloroform and an indicator solution of 1% crystal violet in glacial acetic acid was added (4-6 drops). The content of flask was titrated with a standardized solution (0.1 N) of hydrobromic acid in glacial acetic acid until the blue solution displayed a color change to blue-green endpoint. A blank titration was also carried for 15 mL chloroform without any sample in it. Three replicates were recorded for each resin\prepolymer. EEW was calculated using the recorded information and the percent solids content.

Percent Solids Determination

Percent solids procedure was followed to determine the volatile content of resins or prepolymer based on ASTM 2369. In general, a weight empty aluminum pan was filled with resin\prepolymer sample (1-2 g). Isopropyl alcohol was used to cover the sample. The pan was placed in an oven at 120 °C for 1 hour. After removal from the oven, the pan was weighed again to determine the percent solids. Three replicates were recorded for each resin\prepolymer.

Fourier Transform Infrared Spectroscopy

Fourier transform infrared (FTIR) spectroscopy was employed to characterize GC resin and prepolymers, using a Thermo Scientific Nicolet 8700 FTIR. The resin or prepolymer was spread as thin layer on a potassium bromide (KBr) plate to collect the spectrum.

Coating Formulations and Curing

The GC resin and amphiphilic GC prepolymer were mixed in a vial and stirred for 24 hours. Curing agent (i.e. PACM) was then added to the vial and stirred for another 20 minutes. The formulation was let to sit for 15 minutes to sweat-in before application. The formulation was applied to 8” x 4” steel or aluminum substrates using a drawdown bar with a wet film thickness of 80 µm. Coatings with PACM crosslinker were oven-cured at 80 °C for 45 minutes and coatings with 702B75 crosslinker were cured ambiently for 8 hours. Formulation for the resin and prepolymer that was described before is provided here. To formulate coating 5-5kPDMS-550PEG (F1), as an example, 2.85 g amphiphilic GC prepolymer (70.26% solid), 21.57 g GC resin (54.68% solid), and 1.6 g PACM crosslinker were used. All outlined

formulations for this study in Table 1 were prepared in the same way. The highest amount of PEG and PDMS in a system using PACM as crosslinker was 20 wt.% (Formulation F11) and using 702B75 as crosslinker was 13 wt.% (Formulation F14). The highest amounts were determined by running a series of mechanical tests on the coatings such as hardness, impact, and solvent double rubs (data not reported; available upon request).

Surface Characterization

A Kruss® DSA 100 (Drop Shape Analyzer) was used to determine the surface wettability of the coatings and their surface energy. For each surface, water and diiodomethane contact angles were measured in 3 replicates. For each replicate, the static contact angle was measured over 6 minutes to monitor changes due to the potential interaction of the surface with the water droplet as a function of time. Surface energy for each surface was calculated using the Owens-Wendt method.[41] Also, slip angle, advancing and receding water contact angles for surface was measured using a tilting stage where a 25-µL water droplet was watched on a coating surface that was tilted at 10°/min. The measured angles and surface energies were auto-calculated using Kruss® Advance software.

Attenuated total reflectance Fourier transform infrared spectroscopy (ATR-FTIR) was used to further characterize the surfaces of the coatings. A Bruker Vertex 70 with Harrick's ATR™ accessory using a hemispherical Ge crystal was utilized to collect ATR-FTIR spectra for a coating.

A Thermo Scientific™ K-Alpha™ X-ray photoelectron spectroscopy (XPS) was used to determine the surface elemental composition of the coatings. The instrument was equipped with monochromatic Al K_α (1486.68 eV) X-ray source and Ar^+ ion source (up to 4000 eV) was utilized for the XPS experiments. All samples were cleaned to remove trace contaminants; a 2 mm x 2 mm area of the sample was sputtered with a large Ar^+ ion cluster with a power of 4000 eV using the MAGCIS® cluster gun before analysis. Depth profiling of a coating was evaluated with 20 etch cycles. For each etch cycle, the ion beam was set to 1,000 eV Monatomic Mode with low current and 30 s etch time. After each etching cycle, survey spectra in 5 replicates were collected at low resolution with a constant analyzer pass energy of 200 eV for a total of 20 ms. For each run, photoemission lines for C1s, N1s, O1s, and Si2p were observed. Spectra were collected at an angle normal to the surface (90°) of a 400-µm area. The chamber

pressure was maintained below 1.5 x 10^{-7} Torr and samples were analyzed at ambient temperature. Atomic concentrations were quantified by the instrument's software.

Atomic force microscopy (AFM) was utilized to receive insights about the surface topography of the studied coatings. A Dimension 3100 microscope with Nanoscope controller scanned the surface of experimental coatings, collecting images on a sample area of 100 µm x 100 µm in the tapping mode. The experiment condition was in air under ambient conditions, using a silicon probe with a spring constant (0.1-0.6 N/m) and resonant frequency (15-39 kHz). For each surface, two to three replicates were collected to ensure consistency and accuracy of the data.

Water Aging

All the prepared coatings were pre-leached for 28 days in running tap water. The water tanks were equipped to automatically fill and empty every 4 hours. Water aging of the coatings is carried out to leach out any impurities that may interfere with fouling-release assessments and to determine the stability of coatings and surface rearrangements. All biological laboratory assays were carried out after the pre-leaching water aging process was completed.

Biological Laboratory Assays

Growth and Release of Macroalgae (*Ulva linza*)

A set of multiwall plates was used, following water-immersion for 28 days, to evaluate the fouling-release performance of coatings against *U. linza*. The detailed description of the assessment can be found elsewhere.[42] Briefly, after leaching collection, all multiwall plates were equilibrated in 0.22 µm filtered artificial seawater for 2 hours at Newcastle. To each well, 1 mL spores of *U. linza* suspension was added, adjusted to 3.3 x 10^5 spores/mL (0.05 OD at absorbance 660 nm) in double strength enriched seawater. Spores settled on the discs were grown for 7 days inside an illuminated incubator at 18°C with a 16:8 light: dark cycle (photon flux density 45 µmol.m^{-2}.s^{-1}). There was no washing to remove unsettled spores after settlement. After 7 days, the biomass generated was assessed from a single row of wells (6) from each plate. The chlorophyll was extracted by adding 1 mL DMSO to each water-pressured well (water pressure of 67 kPa) and followed by measuring the fluorescence at 360 nm excitation and 670 nm emission. Fluorescence is directly proportional to the biomass present on each coating surface. The

removal of *U. linza* at each pressure was compared with the unsprayed wells that were used to determine initial growth.

Bacterial (*Cellulophaga lytica*) Biofilm Adhesion

Fouling-release properties towards bacteria were evaluated using retention and adhesion assays described previously.[43, 44] Briefly, a suspension consisting of the marine bacterium *Cellulophaga lytica* at 10^7 cells/mL concentration in artificial seawater (ASW) containing 0.5 g/L peptone and 0.1g/L yeast extract was deposited into 24-well plates (1 mL/well). The plates were then incubated statically at 28°C for 24 hours. The ASW growth medium was then removed and the coatings were subjected to water-jet treatments. The first column of each coating (3 replicate wells) was not treated and served as the initial amount of bacterial biofilm growth. The second and third columns (3 replicate wells) were subjected to water-jetting at 10 psi and 20 psi, respectively, for 5 seconds. Following water-jet treatments, the coating surfaces were stained with 0.5 mL of a crystal violet solution (0.3 wt. % in deionized water) for 15 minutes and then rinsed three times with deionized water. After 1 hour of drying at ambient laboratory conditions, the crystal violet dye was extracted from the coating surfaces by adding 0.5 mL of 33% acetic acid solution for 15 minutes. The resulting eluates were transferred to a 96-well plate (0.15 mL/coating replicate) and subjected to absorbance measurements at 600 nm wavelength using a multi-well plate spectrophotometer. The absorbance values were considered to be directly proportional to the amount of bacterial biofilm present on coating surfaces before and after water-jetting treatments. [33]

Growth and Release of Microalgae (*Navicula incerta*)

Laboratory biological assay diatom (*Navicula incerta*) was conducted at NDSU following a similar procedure described previously.[1, 42, 45] Briefly, a suspension with 4×10^5 cells/mL of *N. incerta* (adjusted to 0.03 OD at absorbance 660 nm) in Guillard's F/2 medium was deposited into each well (1 mL per well) and cell attachment was stimulated by static incubation for 2 hours under ambient conditions in the dark. Coating surfaces were then subjected to water-jet treatments.[44] First column of wells (3 wells) were not water-jetted so that initial cell attachment could be determined and the next two-column of wells (3 wells) were water-jetted at 10 psi and 20 psi, respectively, for 10 seconds. Microalgae biomass was quantified by extracting chlorophyll using 0.5 mL of DMSO and measuring fluorescence of the transferred extracts at an excitation wavelength of 360 nm and emission wavelength at 670 nm. The relative fluorescence

(RFU) measured from the extracts was considered to be directly proportional to the biomass remaining on the coating surfaces after water-jetting.

Adult Barnacle (*Amphibalanus amphitrite*) Adhesion

An adult barnacle reattachment and adhesion assay evaluated the fouling-release performance of the coatings towards macrofoulants.[46, 47] Coatings prepared on 4" x 8" panels after water aging were utilized for this laboratory assay. Barnacles were dislodged from silicone substrates sent from Duke University and immobilized on experimental coatings (6 barnacles per coating) using a custom-designed immobilization template. The immobilized barnacles were allowed to reattach and grow for 2 weeks while immersed in an ASW aquarium tank system with daily feedings of brine shrimp *Artemia* nauplii (Florida Aqua Farms). After the 2-week attachment period, the number of non-attached barnacles was recorded, and the attached barnacles were pushed off (in shear) using a hand-held force gauge mounted onto a semi-automated stage. Once the barnacles were dislodged, their basal plate areas were determined from scanned images using Sigma Scan Pro 5.0 software program. Barnacle adhesion strength (MPa) was calculated by taking the ratio of peak force of removal to the basal plate area for each reattached barnacle. To ensure consistency, barnacles of similar sizes were tested. The average barnacle adhesion strength for each coating was reported as a function of the number of barnacles released with a measurable force and that exhibited no visible damage to the basis or shell plates.

Statistical Analysis

Analysis of variance for the 2^3 factorial design (Coating F1-F8 included in this design) and completely randomized design (CRD) (all experimental and control coatings included in this design) were performed in SAS software, version 9.4. The GLM procedure with Tukey's method was utilized to determine the difference mean for each treatment group under the CRD design. The assessed responses for the analysis was the fouling-release extent of *U. linza* organism and adhesion strength of the reattached barnacles.

Results and Discussions

Amphiphilic coatings contain both hydrophobic and hydrophilic domains on their surfaces, and such coatings have shown promising performance as marine coatings. As recent literature has reported the preparation of amphiphilic fouling-release coatings based on isocyanate resin,[17] we developed a

theory to access a system that utilizes a new crosslinking chemistry while still benefiting from the urethane linkages. To this effect, this study explored development of a fouling-release system based on epoxy-amine crosslinking that became accessible through glycidyl-carbamate chemistry, conversion of the isocyanate groups of the IPDI trimer resin to epoxy functional groups using glycidol.

A coating formulation was prepared composed of three parts including glycidyl-carbamate (GC) resin (the IPDI-based epoxy resin), amphiphilic prepolymers, and crosslinking agent. The amphiphilic prepolymer based on IPDI trimer resin is furnished with chains of polydimethylsiloxane (PDMS) and poly (ethylene glycol) (PEG), accounting for 66.6% of the isocyanate groups, while having a partial functionality of 33.3% via its epoxy groups.

Several factors were considered as variables to determine the optimum design strategies for the amphiphilic coatings. Molecular weights of PDMS (5,000 $\bar{M}_n$ and 10,000 $\bar{M}_n$) and PEG (550 $\bar{M}_n$ and 750 $\bar{M}_n$) were assessed at two levels for each component to determine how the molecular weight of amphiphilic chains impact performance. Amounts of PDMS and PEG in a system were investigated at 5 wt.%, 10 wt.%, 15 wt.%, and 20 wt.% to validate effect of amphiphilic concentration on performance. Additionally, the effect of amine crosslinking agents (PACM vs 702B75) on performance was explored.

The complete conversion of the isocyanate IPDI resin to epoxy-functional GC (urethane) resin was confirmed with FTIR and epoxy titrations. FTIR spectrum of the GC resin shows the absence of signature isocyanate peak at 2250 cm^{-1} and appearance of the secondary amine (due to formation of the urethane linkage) and ether peaks at 3350 cm^{-1} and 1128 cm^{-1}, respectively (Figure 6.2 – Red spectrum). For amphiphilic GC prepolymer, in addition to the complete disappearance of the isocyanate signal and advent of the urethane linkage signal, the FTIR displayed overlapping stretching for PDMS at 1030 cm^{-1} and PEG at and 1105 cm^{-1}, confirming attachment of the amphiphilic chains (Figure 6.2 – Blue spectrum). Furthermore, epoxy titrations validated the presence of the epoxy-functional groups on both the resin and the amphiphilic prepolymers. The epoxy equivalent weight (EEW) values for the samples were in correlation with their type (Table 6.2). As expected, the GC resin had a lower EEW value, suggesting the availability of more epoxy functional groups in short segments on the modified isocyanate resin. The value of EEW for the prepolymer was significantly higher as theorized, supporting the limited presence of epoxy functional groups due to the attachment of PEG and PDMS chains on majority of the sites.

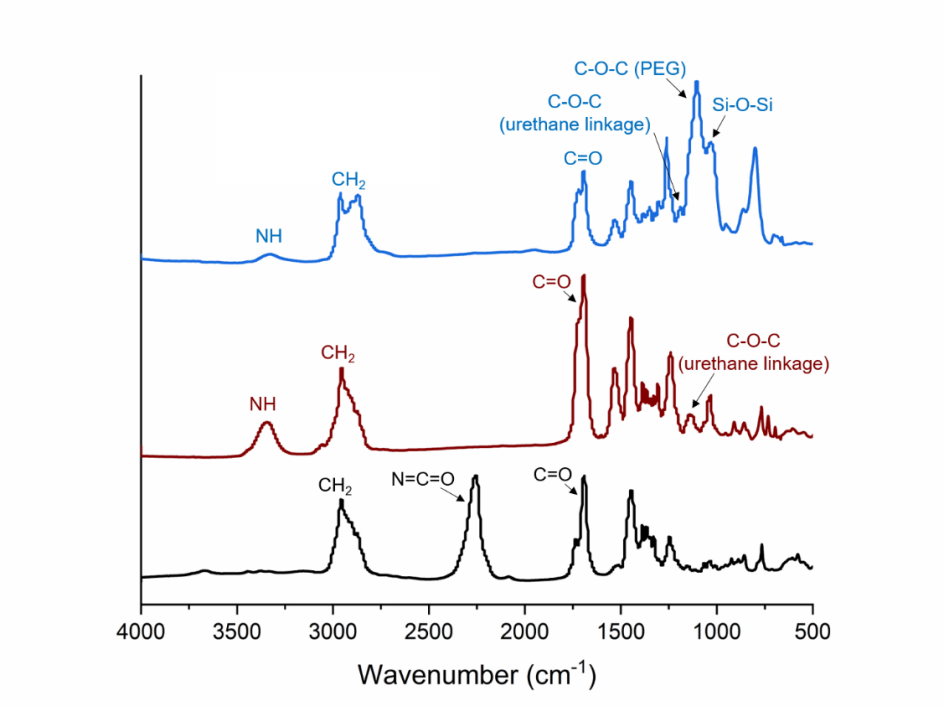

Figure 6.2. FTIR spectrum for the IPDI trimer resin (black line), GC resin (red line), and amphiphilic prepolymer 10kPDMS-750PEG (blue line).

Table 6.2. Epoxy equivalent weight for GC resin and some prepolymers

Material	Theoretical % Epoxy on Structure	Theoretical % PEG and PDMS on Structure	Average EEW ± σ
GC Resin	100.0%	0.0%	320.16 ± 25.20
Prepolymer 10kPDMS-550PEG	33.3%	66.6%	1987.23 ± 135.20
Prepolymer 5kPDMS-750PEG	33.3%	66.6%	1695.20 ± 95.35

The surfaces of the prepared coatings were characterized with a series of experiments. ATR-FTIR was used to qualitatively assess the surface composition of the coatings. The spectrum of all coatings showed similar results and confirmed the amphiphilic nature of explored AmpSiGC systems. The comparison of formulations with varying amphiphilicity of 5 wt.% to 20 wt.% PEG/PDMS displayed the presence of siloxane (Si-O-Si) and ether (C-O-C) peaks at ~1030 cm^{-1} (Figure 6.3A – highlighted green) and ~1105 cm^{-1} (Figure 6.3A – highlighted red), respectively. The intensity of PEG signal in relative to PDMS signal increased as the amphiphilicity content increased, which may be due to the availability of more PEG chains in a system that increase the probability for this moiety to diffuse into the surface. Also,

a broadened overlapped stretching for hydroxyl group (formed due to crosslinking of epoxy and amine groups) and secondary amine (due to urethane linkage) is present at around 3350 cm^{-1}. Furthermore, the FTIR data indicated amphiphilic PEG and PDMS moieties are present on the surface regardless of the used crosslinker, comparing the spectra for coatings F11 and F14 crosslinked with PACM and 702B75, respectively (Figure 6.3B).

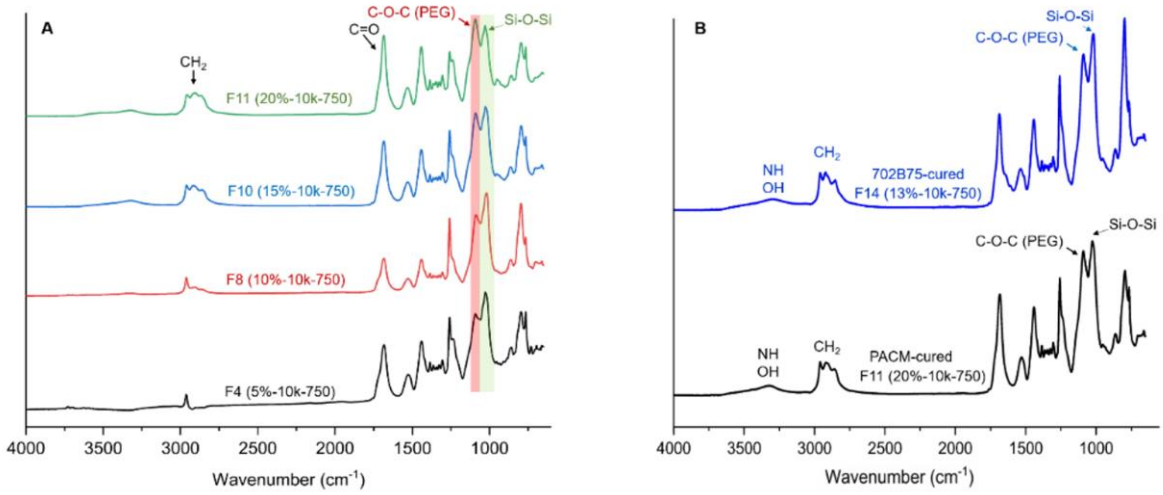

Figure 6.3. ATR-FTIR of the AmpSiGC coating surfaces. (A) Spectra of coatings with ranging degree of amphiphilicity from 5 wt.% to 20 wt.% of 750 $\bar{M}_n$ PEG and 10,000 $\bar{M}_n$ PDMS; and (B) Spectra of F11 and F14 coatings crosslinked with PACM and 702B75 crosslinkers, respectively. Each spectrum is labeled to reflect a coating ID and its composition.

Contact angle measurements were used to further evaluate the surfaces of the coatings. Figure 6.4A shows the static contact angles and surface energies over time for the experimental coatings and control coatings (A-4 and T-10). The coatings overall displayed a dynamic surface as the contact angles (both water and diiodomethane) decreased as a function of time (6 minutes), similar to the T-10 amphiphilic control coating. The decrease for water contact angles (WCA) was more noticeable than methylene iodide contact angles (MICA). The decrease of contact angles was attributed to the presence of hydrophilic domains on the surface that swell due to interaction with the water droplet, facilitating the spread of the droplet, while this phenomenon was not present for the hydrophobic A4-20 control coating that did not contain any PEG. Formulations with 10 wt.% PEG and PDMS showed a higher dynamic nature than formulations with 5 wt.% amphiphilic components. Also, the higher amount of PDMS in a system reflected a higher initial contact angle as the upward trend is observed from formulation F4 with 5 wt.% PDMS to formulations F8, F10, and F11 with 10, 15, and 20 wt. % PDMS, respectively. PACM-

based coatings like F8 and F11 showed lower contact angles than 702B75-based coatings like F13 and F14 (highest amount of PEG and PDMS for F14 was 13 wt.% compared to 20 wt.% for F11). The dynamic nature of contact angles has a direct correlation on surface energy of the surfaces as illustrated in Figure 6.4B. The surface energy of coatings lied between 14 mN/m up to 30 mN/m, depending on amount of PEG and PDMS in a system and type of the curing agent. Overall, the higher the changes in contact angle values over time, the higher change for surface energy as well. The similar comparisons that were mentioned for contact angle values can be noticed for the surface energy data as well. Coatings with 5 wt.% and 10 wt.% PEG and PDMS (cured with PACM) exhibited properties similar to the T-10 control, while this was not the case for coatings with higher amounts of PEG and PDMS or with the 702B75 crosslinker.

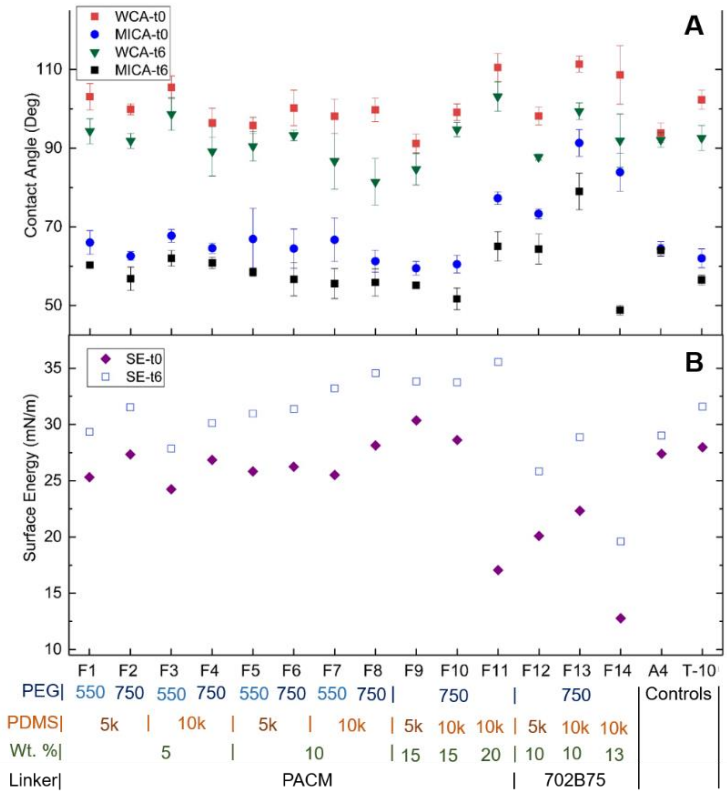

Figure 6.4. Static contact angle data for AmpSiGC coatings. (A) Water contact angles (WCA) and methylene iodide contact angles (MICA) as a function of time at 0 minute and 6 minutes, (B) Surface energy (SE) of the coatings at 0 minute and 6 minutes, calculated by Owens-Wendt method utilizing the average WCAs and MICAs for each coating. The X-axis is labeled to specify the formulations and its components including PEG MW, PDMS MW, wt.% of PEG and PDMS, and crosslinker type.

The surfaces of the coatings were further studied by dynamic contact angle measurements to determine advancing/receding contact angles and slip tilting degree (water droplet roll-off angle). Generally, the roll-off angle for the water droplet was between 4 to 8 degrees (Figure 6.5A), a value like the amphiphilic T-10 coating and significantly different from hydrophobic A4 control system (with slip angle of 11 degrees). The type of crosslinker affected the advancing and receding contact angles for a surface (Figure 6.5B). Coatings with PACM crosslinker showed hysteresis lower than 10 degrees that were comparable to T-10 and A4 control systems, signaling the presence of a smooth surface. Alternatively, coatings with 702B75 crosslinker showed a higher extent of hysteresis, specifically coating F12, indicating the surface is not as smooth as PACM-containing coatings.

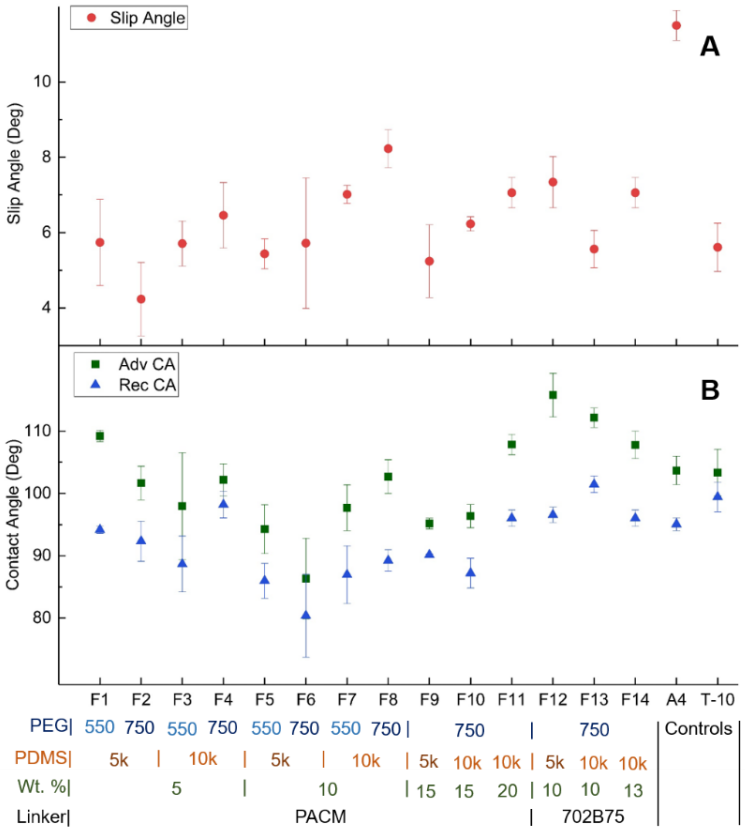

Figure 6.5. Dynamic contact angle data for AmpSiGC coatings. (A) Water droplet slip angle (roll-off angle for water to slide from a surface), (B) Advancing contact angle (Adv CA) and receding contact angle (Rec CA) data, measured by tilting method. The X-axis is labeled to specify the formulations and its components including PEG MW, PDMS MW, wt.% of PEG and PDMS, and crosslinker type.

The surfaces of the amphiphilic systems were characterized by XPS to determine the elemental composition of materials on the surface and in the outer layers of a coating using argon ion milling. The XPS analysis indicated all the coatings are self-stratified where the surface is primarily composed of PDMS-containing materials and the bulk is constructed of the glycidyl-carbamate matrix. As an example, the XPS depth profiling data for coating F8 (Figure 6.6A) displays the concentration of silicon and oxygen atoms on the surface is dominant, but the silicon signal starts to decrease after ~5 nm thickness while the concentration of carbon and nitrogen atoms increase that is related to the crosslinked GC network in the bulk. The XPS depth profiling analysis also suggested that concentration of amphiphilic domains directly is related to the amount of incorporated amphiphilic moieties in a system (Figure 6.6B). This data shows that systems with 15 wt.% and 20 wt.% PDMS have a high concentration of silicone atom on the surface that is well-extended through the bulk of the coating. Comparatively, coatings with lower amounts of amphiphilic chains have less initial concentration of PDMS on the surface; thus, the signal for silicone atom decreases considerably as a function of thickness. As expected, coatings with 10 wt.% amphiphilic moieties have a higher initial concentration of PDMS on the surface than systems with 5 wt.%. Furthermore, XPS data illustrated that self-stratification occurred for all systems regardless of the type of the curing agent (Figure 6.6C). This data shows systems with PACM crosslinking agent have a slightly higher concentration of PDMS on the surface.

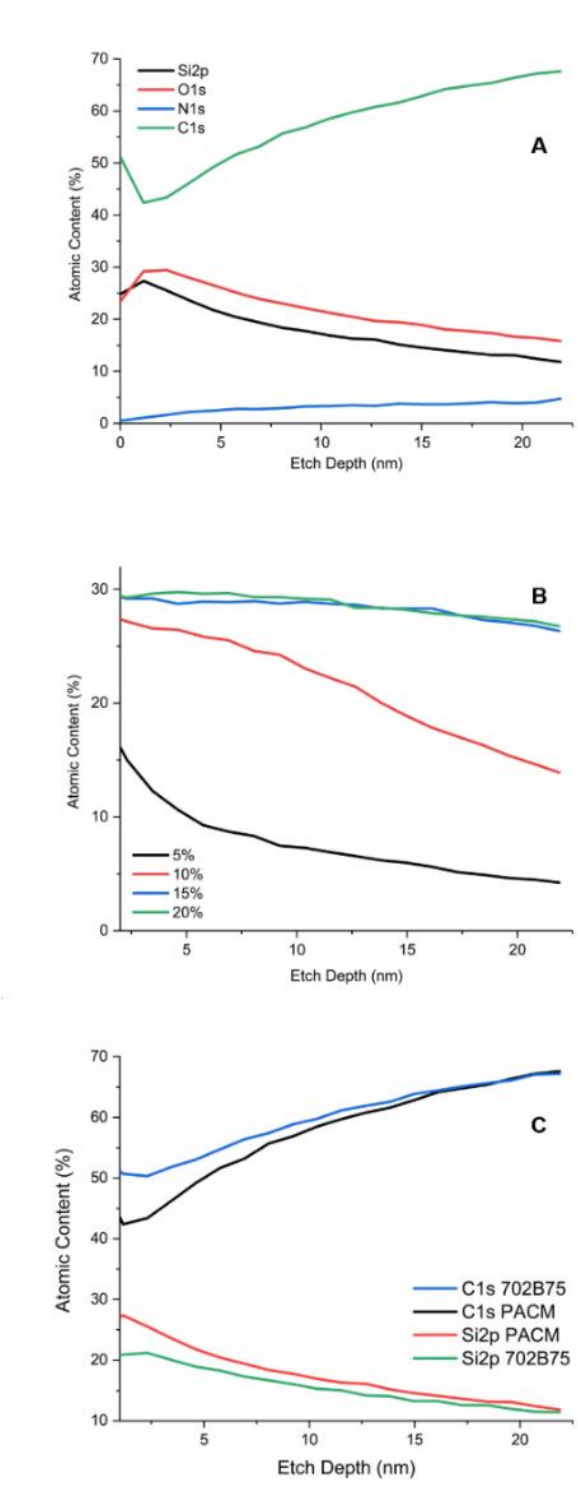

Figure 6.6. XPS data for AmpSiGC coatings. (A) XPS depth profile analysis for coating F8 (10-10kPDMS-750PEG system), indicating self-stratification of the PDMS-based materials into the surface; (B) XPS depth profile data for silicon atom for coatings F4 (5 wt.%), F8 (10 wt.%), F10 (15 wt.%), and F11 (20 wt.%) that demonstrates effect of amount of amphiphilic prepolymers in a system on the surface composition; (C) XPS depth profile data for coatings F8 (PACM-cured) and F13 (702B75-cured), comparing effect of crosslinker type on self-stratification and surface composition.

AFM was utilized as another technique to characterize the morphology of the developed surfaces. Generally, soft materials like PDMS appear lighter (having high phase angles) in AFM phase images and harder materials like PEG appear darker (having low phase angles). The AmpSiGC coatings possessed heterogeneous surfaces composed of light and dark patterns on the surface, signaling the presence of an amphiphilic morphology (Figure 6.7). The AFM phase images (Figure 6.7) are in correlation with AFM height images (Figure A21). Comparing this data with phase AFM image of the control A4 system (Figure A22), it was clearly observed the hydrophobic system lacked the patterns which further supports the amphiphilic nature of the AmpSiGC coatings. Coatings with 5 wt.% amphiphilic prepolymers showed smaller microdomains than systems with higher amounts of amphiphilic moieties. Among the 5 wt.% ones (cured with PACM), it appeared coatings that contain 5,000 $\bar{M}_n$ show a well-distributed pattern as small circular domains, while coatings with 10,000 $\bar{M}_n$ PDMS showed stretched-lines domains that is mixed with circular domains. For systems with 10 wt.% amphiphilic moieties (cured with PACM), several changes were noticed including a higher number of circular domains and a wider range of domain sizes. However, the number and size of the heterogonous domains did remain relatively the same with 15 wt.% of amphiphilicity. The 702B75-cured coatings such as F12 and F13 displayed a different morphology than PACM-cured coatings, suggesting the type of crosslinker impacts the pattern of a surface. AFM images for coating systems F11 and F14 could not be captured due to encountered limitations with the surfaces.

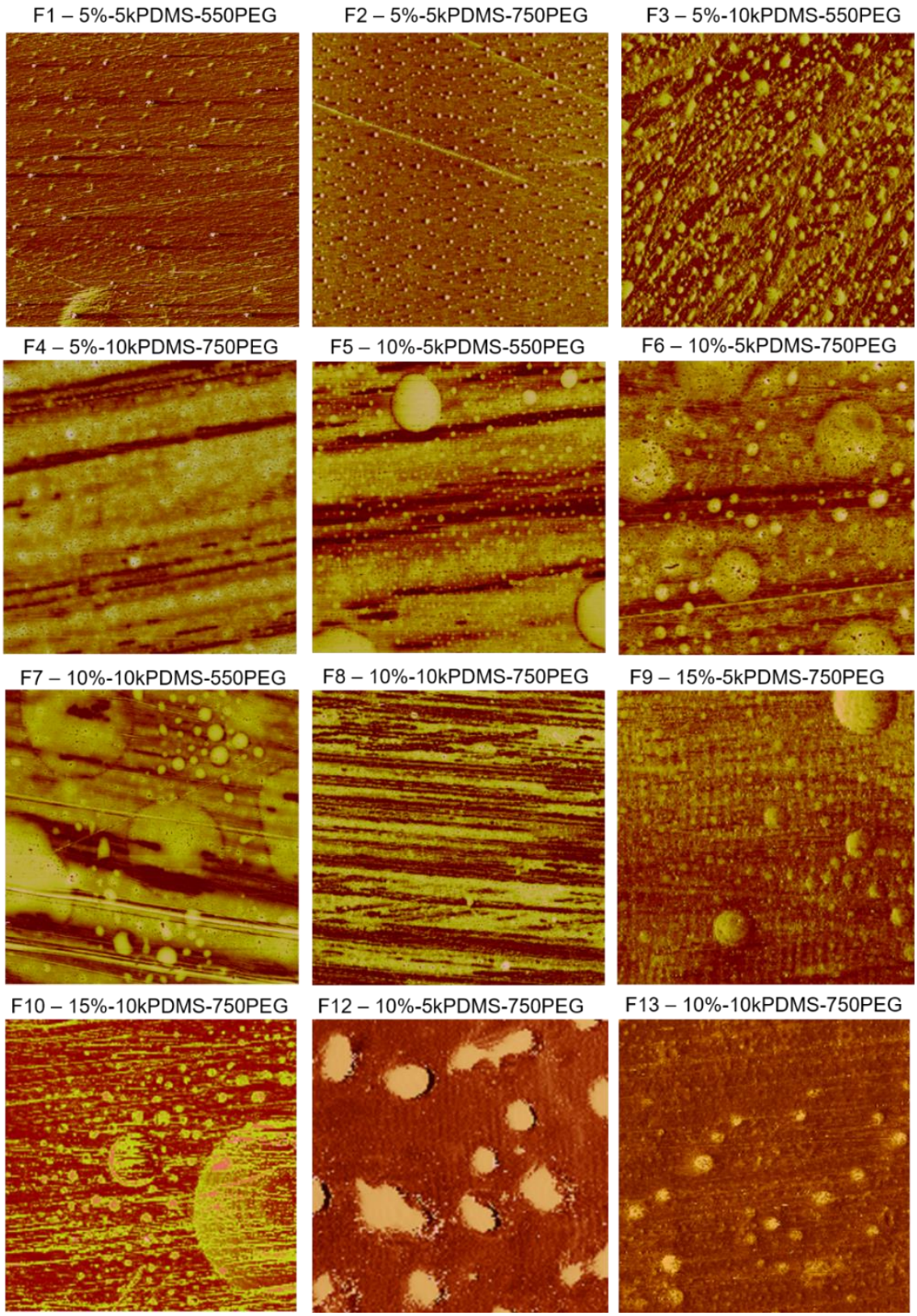

Figure 6.7. AFM phase images of AmpSiGC coatings. Each image is for an area of 100 µm x µm. Each label reflects the coating number and composition of an image.

Biological assays to assess fouling-release performance of the developed coatings were conducted after 28 days of water immersion to ensure coatings are stable and any toxic ingredients were leached out. Before any experiments, the coatings were tested for leachate toxicity using *C. lytica* and *N. incerta* as described elsewhere.[48] All the coatings indicated no sign of toxicity when compared to positive and negative growth controls (data not reported; available upon request), allowing for further biological evaluations.

U. linza is recognized as a potential biofouling macroalgae organism. This organism expresses a low affinity for hydrophilic surfaces but with a stronger adhesion, while it shows higher interest to settle on hydrophobic surfaces but with a weaker adhesion.[49-51] This opposing behavior of *U. linza* suggests that an amphiphilic surface may be a desirable fit to tackle biofouling for it and similar-behaving organisms. Engineered AmpSiGC coatings and all the control coatings showed a relatively similar extent of *U. linza* biofouling (Figure 6.8 – Red bars; the higher the bar level, the higher amount of biofouling). Systems cured with 702B75 and systems with high amounts of amphiphilicity (i.e. 15 wt.% and up) had slightly lower initial biofouling than the other formulations. The release of *U. linza* was assessed at two water pressure levels and the biomass remaining was reported at 10 psi (Figure 6.8 – Blue bars) and 16 psi (Figure A23 – blue bar). At 10 psi, all the systems with 10 wt.% amphiphilic portion or higher showed desirable performance, fouling-release results that were significantly better than A4 control system (tested with Tukey's method for comparison of means; P-values < 0.05). Several AmpSiGC formulations such as F7, F8, F13, and F14 showed even better performance than the top-performing IS 1100 and internal T-10 coatings – each of these four coatings is composed of ~10 wt.% PEG (750 $\bar{M}_n$) and PDMS (10,000 $\bar{M}_n$) PDMS (Figure 6.8). At 16 psi, the fouling-release of coatings followed a similar trend, except the extent of the *U. linza* release was improved due to a higher level of water pressure. The top-performing formulations at 10 psi (F7, F8, F13, and F14) still exhibited a better performance at 20 psi than A4 and T-10 systems while their release was slightly less than the IS 1100 (Figure A23). Overall, *the U.* linza data suggested AmpSiGC systems offer well-performing fouling-release surfaces.

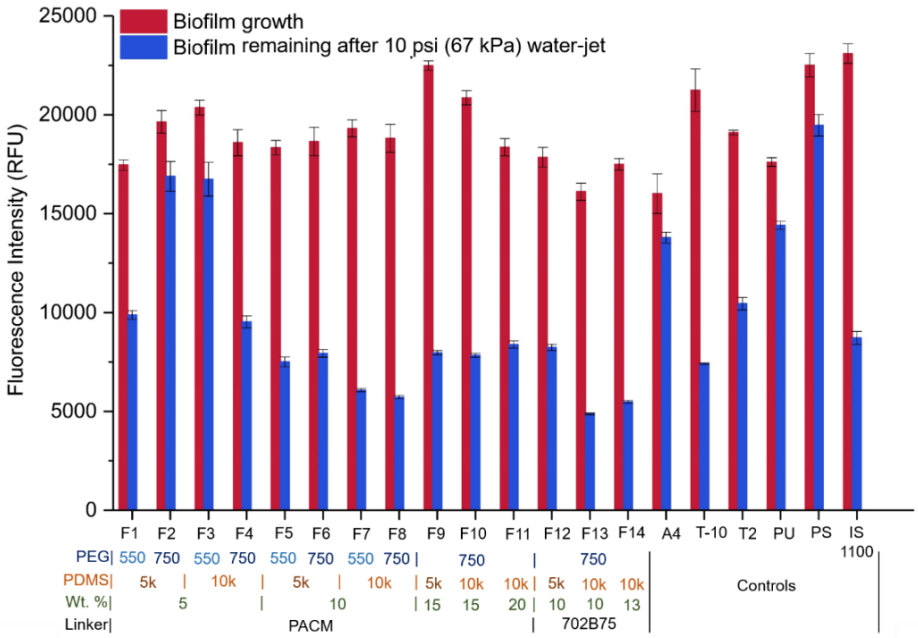

Figure 6.8. *U. linza* fouling-release data for biofilm growth (Red bar) and biomass remaining after water jetting at 10 psi (Blue bar). The X-axis is labeled to specify the formulations and its components including PEG MW, PDMS MW, wt.% of PEG and PDMS, and crosslinker type.

C. lytica is a microorganism that is known for its biofouling with an affinity to a wide range of surfaces, including both hydrophilic and hydrophobic.[2] The extent of biofouling for coatings with 5 wt.% amphiphilicity is the highest and it decreases for coatings with 10 wt.% or higher amphiphilic content. Specifically, coatings F9-F11 that contain more than 15 wt.% PEG and PDMS and 702B75-cured coatings (F12 and F13 systems) demonstrate the least amount of initial biofouling which is comparable to the top-performing controls, suggesting the amount of PEG and PDMS and the type of crosslinker affect the affinity of *U. linza* to a surface. The fouling-release of *C. lytica* film was evaluated at two water pressure levels and the biomass remaining was graphed at 10 psi (Figure 6.9) and 20 psi (Figure A24), and the results for both pressures followed a similar trend. At 10 psi, several coating systems such as formulations F9-F13 outperformed the internal and commercial controls. All these coatings contained 15 wt.% or higher PEG and PDMS for PACM-cured systems (F9, F10, F11) or 10 wt.% PEG and PDMS for 702B75-cured systems (F12 and F13). In comparison, PACM-cured coatings with 10 wt.% amphiphilic chains (F5-F8) did not perform as well as 702B75-cured coatings at the same concentration, indicating choice of crosslinker can help to achieve better fouling-release performance with lower concentration of

amphiphilic moieties in a system. Additionally, coatings F9-F13 outperformed almost all the well-known commercial marine paints, including IS 700, IS 900, and IS 1100 (Figure 6.9). At 20 psi, the top-performing coatings F9-F13 demonstrated matching trends with higher extent of fouling-release due to higher water pressure (Figure A24). The observations for all the comparisons among studied coatings and controls remained unchanged. Generally, the *N. incerta* data implies AmpSiGC surfaces deliver a desirable fouling-release performance which is better than our previously stablished hydrophobic A4 and amphiphilic T-10 systems.

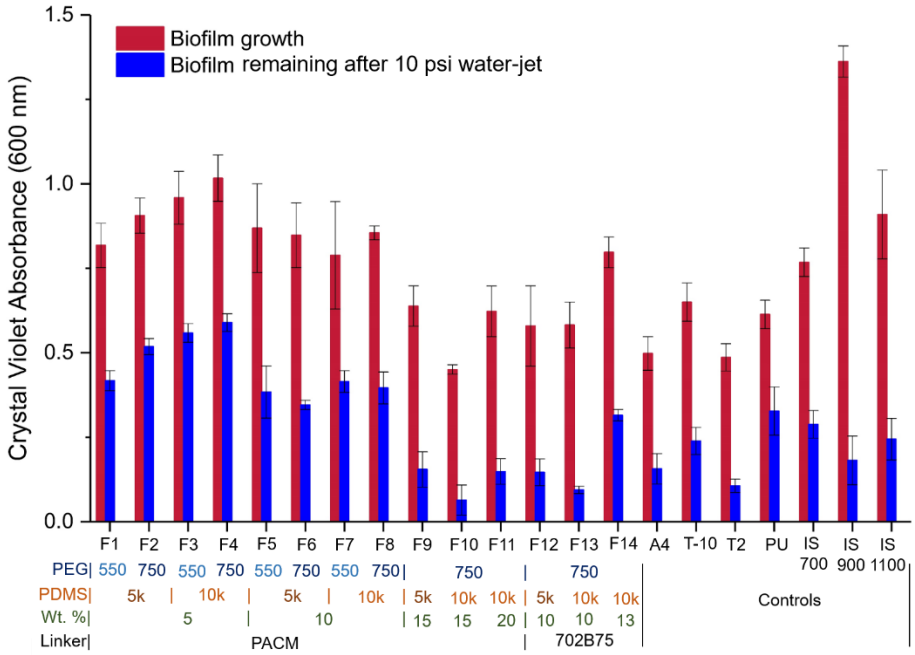

Figure 6.9. *C. lytica* fouling-release data for biofilm growth (Red bar) and biomass remaining after water jetting at 10 psi (Blue bar). The X-axis is labeled to specify the formulations and its components including PEG MW, PDMS MW, wt.% of PEG and PDMS, and crosslinker type.

A slime-forming microalga, diatom (*N. incerta*) is another major biofouling organism that settles on hydrophobic surfaces typically.[49, 50] The extent of diatom biofouling for systems that contained between 5-10 wt.% amphiphilic chains and were cured with PACM was relatively higher than coatings with higher loadings of PEG and PDMS, 702B75-cured systems, or controls. While IS 900 and IS 1100 coatings showed the least diatom biofouling, coatings F10-F14 showed less or similar biofouling than several controls such as A4, T-10, and IS 700. The biomass remaining was evaluated after water jetting at 10 psi and 20 psi pressure levels, and a similar trend was observed in both scenarios. At 20 psi (Figure 6.10),

the results indicated two differing trends for systems depending on type of the used crosslinker. For PACM-cured systems, coatings F1-F3 with least amount of amphiphilic chains of PEG and PMDS at 5 wt.% demonstrated a better or comparable release than several controls including hydrophobic A4, amphiphilic T-10, PU, and IS 700. Alternatively, 702B75-cured coatings F12 and F14 with amphiphilic chains higher than 10 wt.% exhibited a similar performance. These coatings (F1-F3, F12, and F14) offered better performance than several commercial controls such as T2, PU, and IS 700, but not as well as the output of IS 900 and IS 1100 coatings. Overall, it can be summarized that several AmpSiGC coatings offer a promising performance better than both internal control coatings and several commercial systems.

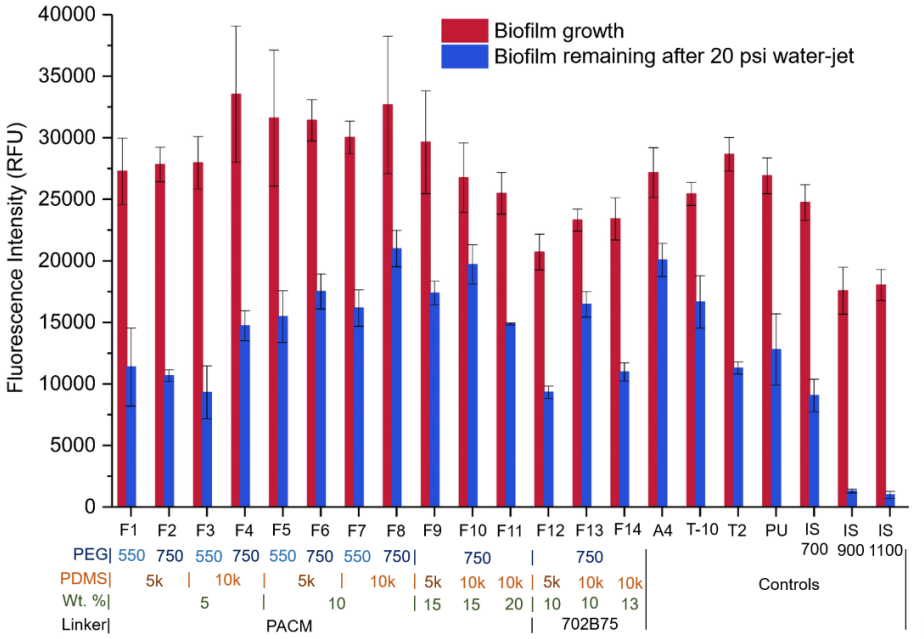

Figure 6.10. *N. incerta* fouling-release data for biofilm growth (Red bar) and biomass remaining after water jetting at 20 psi (Blue bar). The X-axis is labeled to specify the formulations and its components including PEG MW, PDMS MW, wt.% of PEG and PDMS, and crosslinker type**.**

A macrofouling organism, barnacle is another major macrofoulant organism that cause severe biofouling on a surface.[2, 52] There are several types of barnacles and differences in their surface affinities for fouling imposes it challenging to introduce a conclusive rule about barnacles' general behavior (i.e. preference of hydrophilic vs hydrophobic surfaces).[46, 47, 53-58] Due to the limited availability of barnacles, several coatings out of the 14 formulations were selected to be assessed to include features of all the

designed coatings. While AmpSiGC coatings hosted most of the reattached barnacles (probably due to higher hydrophilic domains on the surface), but they mostly showed better barnacle release than the IS 1100 commercial control, suggesting the amphiphilic systems function desirably as fouling-release (FR) surfaces (Figure 6.11).[17, 59] A closer analysis indicate that PACM-cured coatings with concentration of amphiphilic chains between 10-15 wt.% of PEG and PDMS offer desirable performance. However, the amphiphilic amounts lower and higher than this range perform slightly worse, yet better than the commercial control. Also, PACM-cured F14 coating performed better than 702B75-cured F11 coating (both systems contained the highest amount of amphiphilicity in their category), correlating with previous data that the crosslinker impacts FR output. Overall, it can be summed up that systems with PACM crosslinker, 10,000 $\bar{M}_n$ PDMS, 750 $\bar{M}_n$ PEG, and amphiphilicity between 10-15 wt.% provide a desirable performance against barnacles. Analysis of variance (ANOVA) was conducted on the data of barnacles, and the tabulated data was considered as a completely randomized design. The results indicated there was not a significant difference between the mean of performance of these coatings, attributed to the fluctuating standard deviations.

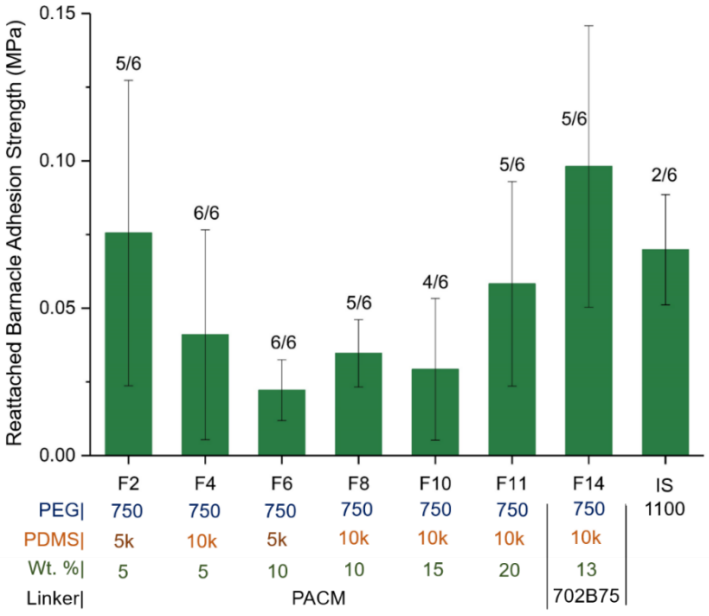

Figure 6.11. Reattached barnacle (*A. Amphitrite*) adhesion strength data. Six barnacles were used for each reattachment. The number of attached barnacles out of six is labeled as a ratio for each system. Each bar shows the average adhesion strength based on the number of successfully reattached barnacles. The X-axis is labeled to specify the formulations and its components including PEG MW, PDMS MW, wt.% of PEG and PDMS, and crosslinker type.

Conclusions

We reported a new method to develop amphiphilic glycidyl-carbamate-based (urethane-based) coatings by converting the isocyanate groups of the IPDI trimer resin to epoxy functional groups and by introducing PEG and PMDS chains to the IPDI resin. This facile synthesis could potentially eliminate the presence of the isocyanate groups from the final product/formulation which may cause health hazards to a worker and coating variability due to environmental humidity. Formulations in this study considered four factors of interest, including molecular weight of PDMS, molecular weight of PEG, amount of PEG and PDMS in a system, and effect of crosslinking agent. The surface characterization of the coatings indicated that the goal to have an amphiphilic surface was met. Contact angle measurements showed the presence of a dynamic amphiphilic surface in comparison to a hydrophobic system. ATR-FTIR showed the presence of PEG and PDMS signals on the surface. XPS displayed the occurrence of self-stratification of PDMS-based moieties in correlation with amount of incorporated amphiphilic prepolymers. Additionally, AFM confirmed the presence of heterogeneous domains on the surface that their presence was attributed due to the amphiphilic nature of the surface (the heterogeneous patterns were missing from the control hydrophobic system). In terms of application, the AmpSiGC coatings demonstrated desirable performance as amphiphilic fouling-release coatings. Considering the fouling-release performance of four studied biological assays, it was generally observed that systems with 15 wt.% or higher concentration of amphiphilic moieties on the surface demonstrate promising performance (better than internal/external standards) against *U. linza*, *C. lytica*, and barnacles, regardless of the crosslinking agent used. For *N. incerta* (diatom), the fouling-release performance was dependent on type of crosslinker which would determine the favorable amphiphilic amount to offer a relatively good performance. In conclusion, it can be summarized that design of amphiphilic siloxane-GC systems can be tuned for a desirable performance by considering the following factors: 1) A 10,000 $\bar{M}_n$ PDMS is favored over lower molecular weights of PDMS – this is in correlation with previously reported work;[9, 17, 60] 2) A 750 $\bar{M}_n$ PEG offers relatively better performance than 550 $\bar{M}_n$ PEG; 3) Amounts of hydrophobic and hydrophilic moieties in a system affects the fouling-release performance – the preferred amount is between 10-15 wt.% or higher depending on type of utilized crosslinker; 4) A crosslinker has remarkable impact on fouling-release performance.

References

1. Callow, J. A.; Callow, M. E., Trends in the development of environmentally friendly fouling-resistant marine coatings. *Nature Communications* **2011,** *2* (1), 244-244.

2. Lejars, M.; Margaillan, A.; Bressy, C., Fouling release coatings: A nontoxic alternative to biocidal antifouling coatings. *Chemical Reviews* **2012,** *112* (8), 4347-4390.

3. Callow, M. E.; Callow, J. E., Marine biofouling: a sticky problem. *Biologist* **2002,** *49* (1), 10-14.

4. Magin, C. M.; Cooper, S. P.; Brennan, A. B., Non-toxic antifouling strategies. *Materials Today* **2010,** *13* (4), 36-44.

5. Yebra, D. M.; Kiil, S.; Dam-Johansen, K., Antifouling technology—past, present and future steps towards efficient and environmentally friendly antifouling coatings. *Progress in Organic Coatings* **2004,** *50* (2), 75-104.

6. Konstantinou, I. K.; Albanis, T. A., Worldwide occurrence and effects of antifouling paint booster biocides in the aquatic environment: a review. *Environment International* **2004,** *30* (2), 235-248.

7. Wyszogrodzka, M.; Haag, R., Synthesis and characterization of glycerol dendrons, self-assembled monolayers on gold: A detailed study of their protein resistance. *Biomacromolecules* **2009,** *10* (5), 1043-1054.

8. Sommer, S.; Ekin, A.; Webster, D. C.; Stafslien, S. J.; Daniels, J.; VanderWal, L. J.; Thompson, S. E. M.; Callow, M. E.; Callow, J. A., A preliminary study on the properties and fouling-release performance of siloxane–polyurethane coatings prepared from poly(dimethylsiloxane) (PDMS) macromers. *Biofouling* **2010,** *26* (8), 961-972.

9. Bodkhe, R. B.; Thompson, S. E. M.; Yehle, C.; Cilz, N.; Daniels, J.; Stafslien, S. J.; Callow, M. E.; Callow, J. A.; Webster, D. C., The effect of formulation variables on fouling-release performance of stratified siloxane–polyurethane coatings. *Journal of Coatings Technology and Research* **2012,** *9* (3), 235-249.

10. Hu, P.; Xie, Q.; Ma, C.; Zhang, G., Silicone-based fouling-release coatings for marine antifouling. *Langmuir* **2020**.

11. Selim, M. S.; El-Safty, S. A.; Azzam, A. M.; Shenashen, M. A.; El-Sockary, M. A.; Abo Elenien, O. M., Superhydrophobic silicone/TiO2–SiO2 nanorod-like composites for marine fouling release coatings. *ChemistrySelect* **2019,** *4* (12), 3395-3407.

12. Selim, M. S.; El-Safty, S. A.; Shenashen, M. A., Chapter 8 - Superhydrophobic foul resistant and self-cleaning polymer coating. In *Superhydrophobic Polymer Coatings*, Samal, S. K.; Mohanty, S.; Nayak, S. K., Eds. Elsevier: 2019; pp 181-203.

13. Iguerb, O.; Poleunis, C.; Mazéas, F.; Compère, C.; Bertrand, P., Antifouling properties of poly(methyl methacrylate) films grafted with poly(ethylene glycol) monoacrylate immersed in seawater. *Langmuir* **2008,** *24* (21), 12272-12281.

14. Rath, S. K.; Chavan, J. G.; Ghorpade, T. K.; Patro, T. U.; Patri, M., Structure–property correlations of foul release coatings based on low hard segment content poly (dimethylsiloxane–urethane–urea). *Journal of Coatings Technology and Research* **2018,** *15* (1), 185-198.

15. Yi, L.; Xu, K.; Xia, G.; Li, J.; Li, W.; Cai, Y., New protein-resistant surfaces of amphiphilic graft copolymers containing hydrophilic poly (ethylene glycol) and low surface energy fluorosiloxane side-chains. *Applied Surface Science* **2019,** *480*, 923-933.

16. Zhang, Z.-P.; Song, X.-F.; Cui, L.-Y.; Qi, Y.-H., Synthesis of polydimethylsiloxane-modified polyurethane and the structure and properties of its antifouling coatings. *Coatings* **2018,** *8* (5), 157-157.

17. Galhenage, T. P.; Webster, D. C.; Moreira, A. M. S.; Burgett, R. J.; Stafslien, S. J.; Vanderwal, L.; Finlay, J. A.; Franco, S. C.; Clare, A. S., Poly(ethylene) glycol-modified, amphiphilic, siloxane–polyurethane coatings and their performance as fouling-release surfaces. *Journal of Coatings Technology and Research* **2017,** *14* (2), 307-322.

18. Zhu, X.; Guo, S.; He, T.; Jiang, S.; Jańczewski, D.; Vancso, G. J., Engineered, robust polyelectrolyte multilayers by precise control of surface potential for designer protein, cell, and bacteria adsorption. *Langmuir* **2016,** *32* (5), 1338-1346.

19. Martinelli, E.; Pretti, C.; Oliva, M.; Glisenti, A.; Galli, G., Sol-gel polysiloxane films containing different surface-active trialkoxysilanes for the release of the marine foulant Ficopomatus enigmaticus. *Polymer* **2018,** *145*, 426-433.

20. Gudipati, C. S.; Finlay, J. A.; Callow, J. A.; Callow, M. E.; Wooley, K. L., The antifouling and fouling-release perfomance of hyperbranched fluoropolymer (HBFP)− poly (ethylene glycol)(PEG) composite coatings evaluated by adsorption of biomacromolecules and the green fouling alga Ulva. *Langmuir* **2005,** *21* (7), 3044-3053.

21. Pollack, K. A.; Imbesi, P. M.; Raymond, J. E.; Wooley, K. L., Hyperbranched fluoropolymer-polydimethylsiloxane-poly(ethylene glycol) cross-linked terpolymer networks designed for marine and biomedical Applications: heterogeneous nontoxic antibiofouling surfaces. *ACS Applied Materials & Interfaces* **2014,** *6* (21), 19265-19274.

22. Wang, Y.; Betts, D. E.; Finlay, J. A.; Brewer, L.; Callow, M. E.; Callow, J. A.; Wendt, D. E.; DeSimone, J. M., Photocurable amphiphilic perfluoropolyether/poly (ethylene glycol) networks for fouling-release coatings. *Macromolecules* **2011,** *44* (4), 878-885.

23. Bodkhe, R. B.; Stafslien, S. J.; Daniels, J.; Cilz, N.; Muelhberg, A. J.; Thompson, S. E. M.; Callow, M. E.; Callow, J. A.; Webster, D. C., Zwitterionic siloxane-polyurethane fouling-release coatings. *Progress in Organic Coatings* **2015,** *78*, 369-380.

24. Jiang, S.; Cao, Z., Ultralow-fouling, functionalizable, and hydrolyzable zwitterionic materials and their derivatives for biological applications. *Advanced Materials* **2010,** *22* (9), 920-932.

25. Liu, P.; Huang, T.; Liu, P.; Shi, S.; Chen, Q.; Li, L.; Shen, J., Zwitterionic modification of polyurethane membranes for enhancing the anti-fouling property. *Journal of Colloid and Interface Science* **2016,** *480*, 91-101.

26. Bodkhe, R. B.; Stafslien, S. J.; Cilz, N.; Daniels, J.; Thompson, S. E. M.; Callow, M. E.; Callow, J. A.; Webster, D. C., Polyurethanes with amphiphilic surfaces made using telechelic functional PDMS having orthogonal acid functional groups. *Progress in Organic Coatings* **2012,** *75* (1-2), 38-48.

27. Van Zoelen, W.; Buss, H. G.; Ellebracht, N. C.; Lynd, N. A.; Fischer, D. A.; Finlay, J.; Hill, S.; Callow, M. E.; Callow, J. A.; Kramer, E. J., Sequence of hydrophobic and hydrophilic residues in amphiphilic polymer coatings affects surface structure and marine antifouling/fouling release properties. *ACS Macro Letters* **2014,** *3* (4), 364-368.

28. Salmon, A. G.; Muir, M. K.; Andersson, N., Acute toxicity of methyl isocyanate: A preliminary study of the dose response for eye and other effects. *Occupational and Environmental Medicine* **1985,** *42* (12), 795-798.

29. Charles, J.; Bernstein, A.; Jones, B.; Jones, D. J.; Edwards, J. H.; Seal, R. M.; Seaton, A., Hypersensitivity pneumonitis after exposure to isocyanates. *Thorax* **1976,** *31* (2), 127-36.

30. Sonnenschein, M. F., *Polyurethanes : science, technology, markets, and trends*. Hoboken, NJ, 2015.

31. Chattopadhyay, D. K.; Webster, D. C., Hybrid coatings from novel silane-modified glycidyl carbamate resins and amine crosslinkers. *Progress in Organic Coatings* **2009,** *66* (1), 73-85.

32. Harkal, U. D.; Muehlberg, A. J.; Li, J.; Garrett, J. T.; Webster, D. C., The influence of structural modification and composition of glycidyl carbamate resins on their viscosity and coating performance. *Journal of coatings technology and research* **2010,** *7* (5), 531-546.

33. Harkal, U. D.; Muehlberg, A. J.; Webster, D. C., Linear glycidyl carbamate (GC) resins for highly flexible coatings. *Journal of Coatings Technology and Research* **2013,** *10* (2), 141-151.

34. Edwards, P. A.; Striemer, G.; Webster, D. C., Novel polyurethane coating technology through glycidyl carbamate chemistry. *JCT research* **2005,** *2* (7), 517-527.

35. Chattopadhyay, D. K.; Zakula, A. D.; Webster, D. C., Organic–inorganic hybrid coatings prepared from glycidyl carbamate resin, 3-aminopropyl trimethoxy silane and tetraethoxyorthosilicate. *Progress in Organic Coatings* **2009,** *64* (2-3), 128-137.

36. Chattopadhyay, D. K.; Muehlberg, A. J.; Webster, D. C., Organic–inorganic hybrid coatings prepared from glycidyl carbamate resins and amino-functional silanes. *Progress in Organic Coatings* **2008,** *63* (4), 405-415.

37. Edwards, P. A.; Striemer, G.; Webster, D. C., Synthesis, characterization and self-crosslinking of glycidyl carbamate functional resins. *Progress in Organic Coatings* **2006,** *57* (2), 128-139.

38. Ravindran, N.; Chattopadhyay, D. K.; Zakula, A.; Battocchi, D.; Webster, D. C.; Bierwagen, G. P., Thermal stability of magnesium-rich primers based on glycidyl carbamate resins. *Polymer Degradation and Stability* **2010,** *95* (7), 1160-1166.

39. Harkal, U. D.; Muehlberg, A. J.; Webster, D. C., UV curable glycidyl carbamate based resins. *Progress in Organic Coatings* **2012,** *73* (1), 19-25.

40. Anderson, V. L.; McLean, R. A., *Design of experiments: a realistic approach*. Routledge: 2018.

41. Owens, D. K.; Wendt, R. C., Estimation of the surface free energy of polymers. *Journal of Applied Polymer Science* **1969,** *13* (8), 1741-1747.

42. Cassé, F.; Stafslien, S. J.; Bahr, J. A.; Daniels, J.; Finlay, J. A.; Callow, J. A.; Callow, M. E., Combinatorial materials research applied to the development of new surface coatings V. Application of a spinning water-jet for the semi-high throughput assessment of the attachment strength of marine fouling algae. *Biofouling* **2007,** *23* (2), 121-130.

43. Stafslien, S.; Daniels, J.; Mayo, B.; Christianson, D.; Chisholm, B.; Ekin, A.; Webster, D.; Swain, G., Combinatorial materials research applied to the development of new surface coatings IV. A high-throughput bacterial biofilm retention and retraction assay for screening fouling-release performance of coatings. *Biofouling* **2007,** *23* (1), 45-54.

44. Stafslien, S. J.; Bahr, J. A.; Daniels, J. W.; Wal, L. V.; Nevins, J.; Smith, J.; Schiele, K.; Chisholm, B., Combinatorial materials research applied to the development of new surface coatings VI: An automated spinning water jet apparatus for the high-throughput characterization of fouling-release marine coatings. *Review of Scientific Instruments* **2007,** *78* (7), 072204-072204.

45. Cassé, F.; Ribeiro, E.; Ekin, A.; Webster, D. C.; Callow, J. A.; Callow, M. E., Laboratory screening of coating libraries for algal adhesion. *Biofouling* **2007,** *23* (4), 267-276.

46. Stafslien, S.; Daniels, J.; Bahr, J.; Chisholm, B.; Ekin, A.; Webster, D.; Orihuela, B.; Rittschof, D., An improved laboratory reattachment method for the rapid assessment of adult barnacle adhesion strength to fouling-release marine coatings. *Journal of Coatings Technology and Research* **2012,** *9* (6), 651-665.

47. Rittschof, D.; Orihuela, B.; Stafslien, S.; Daniels, J.; Christianson, D.; Chisholm, B.; Holm, E., Barnacle reattachment: A tool for studying barnacle adhesion. *Biofouling* **2008,** *24* (1), 1-9.

48. Majumdar, P.; Crowley, E.; Htet, M.; Stafslien, S. J.; Daniels, J.; VanderWal, L.; Chisholm, B. J., Combinatorial materials research applied to the development of new surface coatings XV: An investigation of polysiloxane anti-fouling/fouling-release coatings containing tethered quaternary ammonium salt groups. *ACS Combinatorial Science* **2011,** *13* (3), 298-309.

49. Finlay, J. A.; Callow, M. E.; Ista, L. K.; Lopez, G. P.; Callow, J. A., The influence of surface wettability on the adhesion strength of settled spores of the green alga Enteromorpha and the diatom Amphora. *Integrative and Comparative Biology* **2002,** *42* (6), 1116-1122.

50. Callow, M. E.; Callow, J. A.; Ista, L. K.; Coleman, S. E.; Nolasco, A. C.; López, G. P., Use of self-assembled monolayers of different wettabilities to study surface selection and primary adhesion processes of green algal (Enteromorpha) zoospores. *Applied Environmental Microbiology* **2000,** *66* (8), 3249-3254.

51. Callow, J. A.; Callow, M. E.; Ista, L. K.; Lopez, G.; Chaudhury, M. K., The influence of surface energy on the wetting behaviour of the spore adhesive of the marine alga Ulva linza (synonym Enteromorpha linza). *Journal of the Royal Society Interface* **2005,** *2* (4), 319-325.

52. Aldred, N.; Li, G.; Gao, Y.; Clare, A. S.; Jiang, S., Modulation of barnacle (Balanus amphitrite Darwin) cyprid settlement behavior by sulfobetaine and carboxybetaine methacrylate polymer coatings. *Biofouling* **2010,** *26* (6), 673-683.

53. Huggett, M. J.; Nedved, B. T.; Hadfield, M. G., Effects of initial surface wettability on biofilm formation and subsequent settlement of Hydroides elegans. *Biofouling* **2009,** *25* (5), 387-399.

54. Rittschof, D.; Costlow, J. D., Bryozoan and barnacle settlement in relation to initial surface wettability: A comparison of laboratory and field studies. *Sci. Mar.* **1989,** *53* (2), 411-416.

55. Di Fino, A.; Petrone, L.; Aldred, N.; Ederth, T.; Liedberg, B.; Clare, A. S., Correlation between surface chemistry and settlement behaviour in barnacle cyprids (Balanus improvisus). *Biofouling* **2014,** *30* (2), 143-152.

56. Petrone, L.; Di Fino, A.; Aldred, N.; Sukkaew, P.; Ederth, T.; Clare, A. S.; Liedberg, B., Effects of surface charge and Gibbs surface energy on the settlement behaviour of barnacle cyprids (Balanus amphitrite). *Biofouling* **2011,** *27* (9), 1043-1055.

57. Aldred, N.; Gatley-Montross, C. M.; Lang, M.; Detty, M. R.; Clare, A. S., Correlative assays of barnacle cyprid behaviour for the laboratory evaluation of antifouling coatings: a study of surface energy components. *Biofouling* **2019,** *35* (2), 159-172.

58. Gatley-Montross, C. M.; Finlay, J. A.; Aldred, N.; Cassady, H.; Destino, J. F.; Orihuela, B.; Hickner, M. A.; Clare, A. S.; Rittschof, D.; Holm, E. R., Multivariate analysis of attachment of biofouling organisms in response to material surface characteristics. *Biointerphases* **2017,** *12* (5), 051003.

59. Galhenage, T. P.; Hoffman, D.; Silbert, S. D.; Stafslien, S. J.; Daniels, J.; Miljkovic, T.; Finlay, J. A.; Franco, S. C.; Clare, A. S.; Nedved, B. T., Fouling-release performance of silicone oil-modified siloxane-polyurethane coatings. *ACS Applied Materials & Interfaces* **2016,** *8* (42), 29025-29036.

60. Rasulev, B.; Jabeen, F.; Stafslien, S.; Chisholm, B. J.; Bahr, J.; Ossowski, M.; Boudjouk, P., Polymer coating materials and their fouling release activity: A cheminformatics approach to predict properties. *ACS Applied Materials & Interfaces* **2017,** *9* (2), 1781-1792.

CHAPTER 7. INVESTIGATION OF AMPHIPHILIC SILOXANE-EPOXYPEG SURFACES FOR MARINE APPLICATIONS

Introduction

Marine biofouling is the undesirable colonization of marine organisms on submerged surfaces in seawater such as ships.[1] Biofouling is a non-linear multi-stage problem that involves about 4000 marine organisms, meaning organisms with varying adhesion modes and mechanisms can attach to a surface in any order (regardless of the presence of a conditioning bacteria film).[1, 2] The consequences of biofouling are severe and penalizes the marine industry significantly. For example, the US Navy spends $1 Billion annually to maintain their ships from fouling organisms. Beside economic impacts, marine biofouling results in increased drag and decreased maneuverability, increased fuel consumption, and elevated transportation of invasive species to new aquatic environments.[1-3]

A series of systems have been developed throughout history to contend with marine biofouling. Initially, copper alloys and lead sheaths were utilized extensively but were eventually withdrawn due to limited resources and corrosion potential.[4] With the advent of polymers, coating systems containing biocides such as tributyl-tin (TBT) compounds exhibited great performance but were eventually banned worldwide in the early 2000s due to their non-targeted toxicity on marine species and environment.[5] Since then, the focus has been on exploring marine coatings that are efficient and non-toxic including antifouling (AF) and fouling-release (FR) technologies. AF systems prevent settlement of marine organisms while FR systems weaken the adhesion of biofoulants so they can be easily washed away as a ship moves.[1, 5]

The current AF paints mainly use copper and zinc oxide biocides to fight biofouling.[1] The biocides leach out of the coating over time and prevent the settlement of marine organisms on a coating. These alternative biocides are less toxic than tin, but they are still considered heavy metals and relatively harmful to environments.[6] In comparison, FR marine coatings are non-toxic and do not utilize biocides to tackle biofouling. FR coatings take advantage of intrinsic properties of available polymers on a surface such as hydrophobicity, hydrophilicity, or low surface energy to reduce adhesion strength of biofoulants and facilitate release/removal of organisms under hydrodynamic pressure.[1, 7]

FR marine systems traditionally contain low surface energy elastomeric materials such as polydimethylsiloxane (PDMS). As these systems lack mechanical durability due to their low modulus and weak adhesion as topcoats to the subsequent layers, self-stratifying siloxane-polyurethane (SiPU) systems were introduced to address the limitations for PDMS-based technologies.[8-10] While SiPU and other hydrophobic systems display desirable FR performance, there are still organisms that prefer to settle on hydrophobic surfaces. For example, the diatom *N. incerta* settles on a hydrophobic surfaces while barnacles or mussels prefer a hydrophilic surface.[1, 8] To this extent, amphiphilic surfaces, containing domains of hydrophilic and hydrophobic moieties, have proven to be effective at reducing adhesion of a wider range of marine biofoulants.[3, 11]

Amphiphilic surfaces for marine applications have been explored using various approaches such as utilizing layer-by-layer technique to assemble layers of polyanions and polycations,[12, 13] synthesizing hyperbranched globule-like polymers to access stronger hydration layers at the interface due to steric excluded volume ,[14, 15] developing UV-cured systems to eliminate complex synthesis procedures to attain FR surfaces,[16] introducing zwitterionic-based surfaces to design stable hydrophilic-containing surfaces with up to eight times more water uptake than PEG,[17-20] exploring self-stratified coating systems to reach durable and easily scalable formulations,[10, 21] and assessing polypeptide/polysaccharide-modified surfaces as “natural” systems.[22] Generally, amphiphilic systems usually contain a hydrophilic component such as poly(ethylene glycol) (PEG) or zwitterionic poly (sulfobetaine methacrylate) and a hydrophobic component like PDMS or fluoroalkyl polymers. The hydrophilic moieties are usually attached onto surface-migrating hydrophobic materials due to their low surface energy and incompatibility with other components in a coating system, resulting in amphiphilic domains.

Amphiphilic self-stratifying systems have demonstrated promising FR performance, signaling the potential for commercial applications.[7] An amphiphilic PEG-siloxane-polyurethane (AmpSiPU) system has been recently reported that incorporates self-stratifying PEG and PDMS prepolymers in a coating network and delivers desirable FR performance.[23] A series of self-stratifying amphiphilic siloxane-glycidyl carbamate (AmpSiGC) coatings have also been investigated to deliver the performance of AmpSiPU systems while altering crosslinking chemistry.[7, 24] While the developed systems have been stable in field test lasting up to two years,[25] the urethane linkage of these systems has been questioned for its possible

“low stability” in aquatic environments. Therefore, we pivoted to investigate alternative non-urethane self-stratifying fouling-release marine systems.

In this work, we investigated the preparation and properties of amphiphilic epoxy-based fouling-release coatings. The matrix was an acrylic-epoxy resin with pendant hydrophilic PEG chains as part of its backbone. The hydrophilic epoxy resin was crosslinked with an amine-terminated PDMS and another amine curing agent. We hypothesized that the presence of hydrophilic and hydrophobic moieties as a base resin and crosslinking agent, respectively, would result in an amphiphilic surface (Figure 7.1). Initially, this work explored the effect of crosslinkers on forming a stable coating network and the effect of mixing on surface morphology. With the selection of optimal variables, a series of coating systems were prepared to assess the effect of the amount of amphiphilic moieties in a system on surface morphology and fouling-release performance. The properties of the amphiphilic siloxane-epoxy (AmpSiEpox) coatings were compared against both internal (hydrophobic SiPU and amphiphilic AmpSiPU systems) and commercial systems. The AmpSiEpox surfaces were characterized with contact angle measurements, ATR (attenuated total reflectance)-FTIR, X-ray photoelectron spectroscopy (XPS), and atomic force microscopy (AFM) and the fouling-release performance was evaluated against *C. lytica* and *N. incerta* marine organisms.

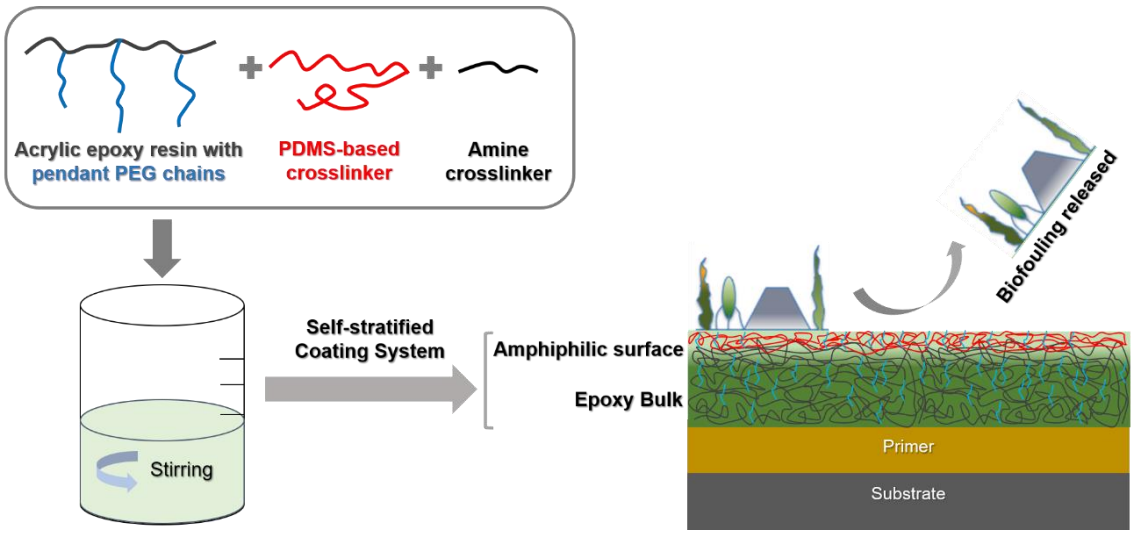

Figure 7.1. Illustration of self-stratifying siloxane-EpoxyPEG system, delivering an amphiphilic fouling-release surface.

Experimental

Materials

Glycidyl methacrylate (GMA), butyl methacrylate (BMA), poly (ethylene glycol) methyl ether methacrylate (PEGMA) of 500 $\bar{M}_n$, hydrobromic acid (5.7 M), and methyl ethyl ketone (MEK) were purchased from Sigma Aldrich. Vazo 64, azo(bis isovaleronitrile) initiator for free radical copolymerization, was provided by Miller-Stephenson and used without further purification. Toluene, chloroform, and glacial acetic acid (for epoxy titration) were purchased from VWR. Ancamide® 702B75, Amicure® PACM, Vestamin® IPDA, and Ancamide® 2353 crosslinkers were provided by Evonik Industries. Aminopropyl terminated polydimethylsiloxane (APT-PDMS) with molecular weight (MW) of 20,000 $\bar{M}_n$ was also synthesized through a ring-opening equilibration reaction as previously reported.[8]

AkzoNobel International Paint provided the commercial FR standards Intersleek® 700 (IS 700), Intersleek® 900 (IS 900), and Intersleek® 1100SR (IS 1100). Silicone elastomer, Silastic® T2 (T2) was provided by Dow Corning as another commercial standard. Hydrophobic A4-20 coating (A4-20), a siloxane-polyurethane system, was prepared as an internal control following the procedures described elsewhere.[8] Also, a PU system without APT-PDMS was prepared as a control. Amphiphilic T-10 coating, internal coating control, was prepared following the procedure elsewhere for a formulation that contained 10 wt.% PEG 750 $\bar{M}_n$ and PDMS 10,000 $\bar{M}_n$.[23] Aluminum panels (4” x 8” in., 0.6 mm thick, type A, alloy 3003 H14) purchased from Q-lab were sandblasted and primed with Intergard 264 (International Paint) using air-assisted spray application. Multi-well plates were modified using circular disks (1-inch diameter) of primed aluminum.

Synthesis of Acrylic Epoxy PEG-containing Resin

Two acrylic-epoxy PEG resins (Resin-A and Resin-B) were prepared via conventional free-radical copolymerization of GMA, BMA, and PEGMA (Scheme 7.1). The synthesis of acrylic resins was carried out in a semi-continuous process using a 250-mL 3-neck round-bottom flask, equipped with an addition funnel, nitrogen inlet, Model 210 J-KEM temperature controller and magnetic stirrer. First, toluene (90.0 g) was placed in the heated to 80 °C while nitrogen gas was slowly flowing in the system. In an Erlenmeyer flask, Vazo-64 initiator (1.8 g) and monomers (GMA, BMA, PEGMA) were mixed until homogeneous. The mixture was added dropwise via an additional funnel to the reaction flask over 90 minutes at 85 °C. The

reaction proceeded for 3 hours at 85 °C, and then chaser, a solution of Vazo-64 (0.5 g) and toluene (2.5 g), was added to the reaction that was let to run for another hour. An ice-bath was used to maintain the temperature constant when needed. For Resin-A, GMA, BMA, and PEGMA were added at 24.0 g, 24.0 g, and 12.0 g, respectively. For Resin-B, GMA, BMA, and PEGMA were added at 24.0 g, 18.0 g, and 18.0 g, respectively. Resin-A was designed to contain less hydrophilic PEG than Resin-B.

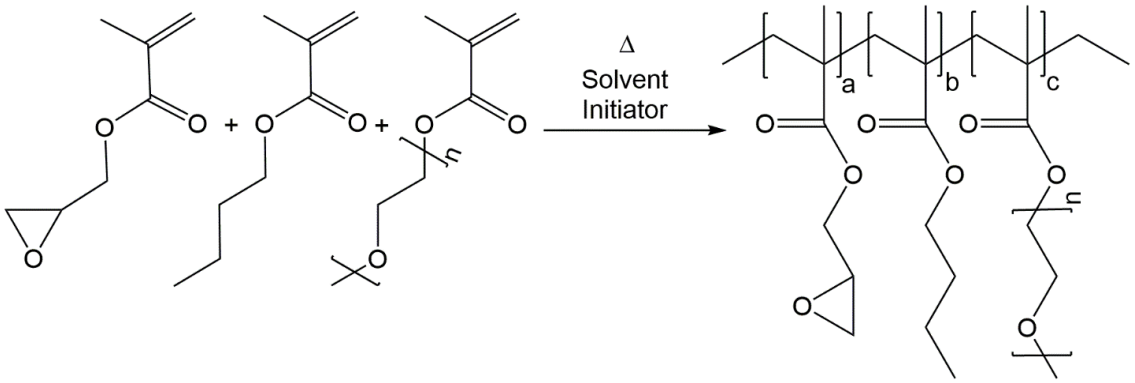

Scheme 7.1. Synthesis of acrylic epoxy PEG-containing resin

Epoxy Equivalent Weight Titrations

Epoxy equivalent weight (EEW) was determined using titration for the acrylic epoxy resins. The titration was conducted following ASTM D1652. In general, a sample of resin or prepolymer (1-2 g) was weighed in an Erlenmeyer flask. The sample was dissolved in 15 mL of chloroform and an indicator solution of 1% crystal violet in glacial acetic acid was added (4-6 drops). The content of the flask was titrated with a standardized solution (0.1 N) of hydrobromic acid in glacial acetic acid until the blue solution displayed a color change to a blue-green endpoint. A blank titration was also carried for 15 mL chloroform without any sample in it. Three replicates were recorded for each resin\prepolymer. EEW (g/eq) was calculated using the recorded information and the percent solids content.

Percent Solids Determination

The non-volatile content of the acrylic resins was determined following ASTM 2369. In general, a weighed empty aluminum pan was filled with the polymer sample (1-2 g). Isopropyl alcohol was used to cover the sample. The pan was placed in an oven at 120 °C for 1 hour. After removal from the oven, the pan was weighed again to determine the percent solid. Three replicates were recorded.

Gel Permeation Chromatography (GPC)

The average molecular weight of acrylic epoxy resins was quantified using GPC (gel permeation chromatography). All samples were analyzed using a GPC system (EcoSEC HLC-8320GPC, Tosoh Bioscience, Japan) with a differential refractometer (DRI) detector. Separations were performed using two TSKgel SuperHM-L 6.00 mm ID× 15 cm columns with an eluent flow rate of 0.4 mL min^{-1}. The columns and detectors were thermally controlled at 40 °C. The eluent used is tetrahydrofuran (THF). Samples were prepared at nominally 1 mg mL^{-1} in an aliquot of the eluent and allowed to dissolve at ambient temperature for several hours and the injection volume was 20 µL for each sample. Calibration was conducted using linear polystyrene standards (Agilent EasiVial PS-H 4 mL).

Fourier Transform Infrared Spectroscopy

Fourier transform infrared (FTIR) spectroscopy was used to characterize the additive, using a Thermo Scientific Nicolet 8700 FTIR. The additive was applied as a thin layer on a potassium bromide (KBr) plate to collect the spectrum.

Coating Formulations and Curing

A coating composition was prepared comprising an acrylic epoxy resin (Resin-A or Resin-B), APT-PDMS (amine-terminated PDMS), and an amine crosslinker. The molar ratio of epoxy to overall two amines was 1:1, where EEW of resins was quantified in our lab through titration and percent solids and amine hydrogen equivalent weights of crosslinkers were provided by the suppliers. For preliminary experiments to select a suitable amine crosslinker, all ingredients were stirred in a vial for 30 minutes, applied, and cured at 80 °C for 45-180 minutes. For the effect of mixing experiments, Resin-A and APT-PDMS were initially stirred for a period (i.e. 4h, 8h, 24h), then Ancamide® 2353 crosslinker (the selected curing agent from initial experiments) was added and the ingredients were mixed for 15 minutes before application (cured at 80 °C for 120 minutes and 120 °C for another two hours). For final formulations, Resin-A/Resin-B and APT-PDMS were stirred in a one-neck round bottom flask at 80 °C for 24 hours, and then, Ancamide® 2353 crosslinker was added to the flask and the ingredients were stirred ambiently for 15 minutes before application. Coatings were cured at 80 °C for two hours, followed by 120 °C for another two hours. Coating formulations and internal controls were drawn down on primed 8’ x 4’ aluminum panels using a wire-round drawdown bar with a film thickness of 80 µm. Final and internal

control coatings were cut out in circular shapes and glued to 24-well plates for biological assays test. All commercial controls were prepared on multi-well plates following manufacturer's guidelines.

Mechanical Tests

The coatings of preliminary experiments were assessed through several tests to determine stability, adhesion, strength, and flexibility of formulated coatings and select which crosslinker offered the optimal mechanical performance. Double rub test, according to ASTM D 5402, evaluated the stability of cured systems and resistance of coatings against solvents. A hammer (0.75 kg) with three-fold cheesecloth wrapped around its head was soaked in MEK and rubbed against the coating. The head of the hammer was rewet after every 25 double rubs. The number of double rubs was noted when mars were observed on the surface of coatings.

Impact test, according to ASTM D 2794, was used to assess the strength of coatings using a Gardner impact tester. The maximum drop height was 43 inches with a weight of 4 pounds. Coated steel panels were placed in a testing location, and the load in varying heights was dropped on the coating. The results were recorded in inch-pounds (in-lb). Crazing or loss of adhesion from the substrate was observed as a failure point. Coatings that did not fail were reported having impact strength of >172 in-lb.

Crosshatch adhesion test, according to ASTM D 3359, assessed the adhesion of a coating to substrates by applying and removing pressure-sensitive tape over cuts made in the film. The results were reported on a scale of 0B to 5B, while 0B indicates complete removal of the coating and 5B indicates no removal of the coatings from the substrate as a result of this test.

KÖnig pendulum test, according to ASTM D 4366, quantified the hardness of coatings in seconds. This test measures the time taken for the amplitude to decrease from 6° to 3°. The pendulum hardness test is based on the principle that the amplitude of the pendulum's oscillation in seconds will decrease more quickly when supported on a softer surface and will last longer when supported on a harder surface. The results are reported in seconds.

Pencil hardness test, according to ASTM D 3363, qualitatively measured the hardness of coatings. A series of pencils from hard (8H) to soft (8B) were pushed at 45o against the coating. The first pencil that does not gauge or scratch the surface was recorded.

Surface Characterization

A Kruss® DSA 100 (Drop Shape Analyzer) was used to assess the surface wettability and surface energy for the coatings. Water and diiodomethane contact angles were measured in 3 replicates for each sample. The static contact angle was measured over 10 minutes to detect changes due to the interaction of a surface with the water droplet as a function of time (the values plateaued after 10 minutes). Surface energy for each surface was calculated using the Owens-Wendt method, having contact angles values of two different liquids (water and diiodomethane) on the same surface.[26] Slip angle and advancing/receding water contact angles for a surface were evaluated using a tilting stage (tilted at 10°/min) where a 25-µL water droplet was viewed on a coating surface. The measured angles and surface energies were calculated using the Kruss® Advance software.

Attenuated total reflectance Fourier transform infrared spectroscopy (ATR-FTIR) was used to characterize the surfaces of the coatings. A Bruker Vertex 70 with Harrick's ATR™ accessory using a hemispherical Ge crystal was utilized to collect ATR-FTIR spectra for a coating.

A Thermo Scientific™ K-Alpha™ X-ray photoelectron spectroscopy (XPS) was used to determine the elemental composition of coatings. The instrument was equipped with monochromatic Al K_α (1486.68 eV) X-ray source and Ar^+ ion source (up to 4000 eV) was utilized for the XPS experiments. Depth profiling of a coating was evaluated with 30 Ar^+ etch cycles. For each etch cycle, the ion beam was set to 1,000 eV Monatomic Mode with low current and 30 s etch time. After each etch cycle, survey spectra in 5 replicates were collected at low resolution with a constant analyzer pass energy of 200 eV for a total of 20 ms. For each run, photoemission lines for C1s, N1s, O1s, and Si2p were observed. Spectra were collected at an angle normal to the surface (90°) of a 400-µm area. The chamber pressure was maintained below 1.5×10^{-7} Torr and samples were analyzed at ambient temperature. Atomic concentrations were quantified by the instrument's software.

Atomic force microscopy (AFM) was utilized to receive insights about the surface topography of the studied coatings. A Dimension 3100 microscope with a Nanoscope controller scanned the surface of experimental coatings, collecting images on a sample area of 100 µm x 100 µm in the tapping mode. The experiment condition was in the air under ambient conditions, using a silicon probe with a spring constant

(0.1-0.6 N/m) and resonate frequency (15-39 kHz). For each surface, three replicates at varying spots were collected to ensure the consistency and accuracy of the data.

Water Aging

All the final coatings for biological assessments were pre-leached for 28 days in running tap water. The water tanks were equipped to automatically fill and empty every 4 hours. Water aging of the coatings is carried out to meet two objectives including leaching out any impurities that may deviate with fouling-release assessments and determining the stability of coatings. All biological laboratory assays were carried out after the water aging process was completed.

Biological Laboratory Assays

Bacterial (*Cellulophaga lytica*) Biofilm Adhesion

Fouling-release property towards bacteria was evaluated using retention and adhesion assays described previously.[27, 28] Briefly, a solution of the marine bacterium *Cellulophaga lytica* at 10^7 cells/mL concentration in artificial seawater (ASW) containing 0.5 g/L peptone and 0.1g/L yeast extract was deposited into 24-well plates (1 mL/well). The plates were then incubated statically at 28°C for 24 hours. The ASW growth medium was then removed and the coatings were subjected to water-jet treatments. The first column of each coating was not treated and served as the initial amount of bacterial biofilm growth. The second and third columns were subjected to water-jetting at 10 psi and 20 psi, respectively, for 5 seconds. Following water-jet treatments, the coating surfaces were stained with 0.5 mL of a crystal violet solution (0.3 wt. % in deionized water) for 15 minutes and then rinsed three times with deionized water. After 1 hour of drying at ambient laboratory conditions, the crystal violet dye was extracted from the coating surfaces by adding 0.5 mL of 33% acetic acid solution for 15 minutes. The resulting eluates were transferred to a 96-well plate (0.15 mL/coating replicate) and subjected to absorbance measurements at 600 nm wavelength using a multi-well plate spectrophotometer. The absorbance values were directly proportional to the amount of bacterial biofilm present on coating surfaces before and after water-jetting treatments. Percent removal of bacterial biofilm was quantified by comparing the mean absorbance values of the non-jetted and water-jetted coating surfaces.[33]

Growth and Release of Microalgae (*Navicula incerta*)

Laboratory biological assay diatom (*Navicula incerta*) was conducted at NDSU following a similar procedure described previously.[3, 29, 30] Briefly, a suspension with 4×10^5 cells/mL of *N. incerta* (adjusted to 0.03 OD at absorbance 660 nm) in Guillard's F/2 medium was deposited into each well (1 mL per well) and cell attachment was stimulated by static incubation for 2 hours under ambient conditions in the dark. Coating surfaces were then subjected to water-jet treatments.[28] The first column of wells was not water-jetted so that initial cell attachment could be determined and the next two-column of wells were water-jetted at 10 psi and 20 psi, respectively, for 10 seconds. Microalgae biomass was quantified by extracting chlorophyll using 0.5 mL of DMSO and measuring the fluorescence of the transferred extracts at an excitation wavelength of 360 nm and emission wavelength at 670 nm. The relative fluorescence (RFU) measured from the extracts was considered to be directly proportional to the biomass remaining on the coating surfaces after water-jetting. Percent removal of attached microalgae was determined using the relative fluorescence of non-jetted and water-jetted wells.

Results and Discussions

Our recent work has focused on amphiphilic siloxane-polyurethane, amphiphilic fouling-release (FR) marine coatings. While the urethane-based systems have shown great stability in field tests for extended periods (i.e. 2 years), the possible hydrolysis of urethane linkage in aquatic environments has been questioned. Therefore, we investigated the preparation of a novel urethane-free amphiphilic FR epoxy-based coating, which contained acrylic epoxy-PEG resin, APT-PDMS, and amine crosslinker. Initially, a series of acrylic epoxy-PEG resins were synthesized and cured with 702B75 curing agent to evaluate the ideal content of glycidyl methacrylate (GMA), and it was determined a resin with 40 parts GMA in its backbone is optimal for film formation. Thus, Resin-A was synthesized to conduct initial experiments for selecting a crosslinker and ideal mixing condition. Resin-A contained 20 parts poly (ethylene glycol) methacrylate (PEGMA) with 357 ± 5 EEW, 12,000 $\bar{M}_n$, and 1.89 PDI. Also, Resin-B was synthesized later to prepare coatings for further fouling-release experiments; the resin contained 30 parts of PEGMA, with 318 ± 5 EEW, 25,000 $\bar{M}_n$, and 1.53 PDI. As expected, the molecular weight of Resin-B was higher than Resin-A since it contained a higher content of PEGMA chains in its backbone. FTIR spectra of the acrylic epoxy-PEG resins (Figure 7.2) showed signals indicative of ether (C-O-C) at 1140

cm^{-1} and C-O of the oxirane group at 906 cm^{-1}, confirming the presence of expected moieties on the resin. Also, percent solids analysis confirmed the free radical polymerization had a conversion of 99% (dividing experimental % solids over theoretical % solids).

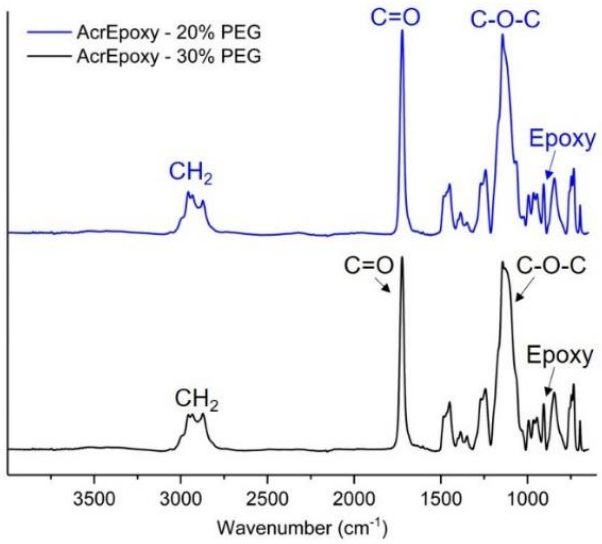

Figure 7.2. FTIR spectrum for the acrylic epoxy-PEG resin. Blueline shows spectra for Resin-A, containing 20 parts PEGMA. Blackline shows spectra for Resin-B, containing 30 parts PEGMA.

Ancamide® 702B75, Ancamide® 2353, Amicure® PACM, and Vestamin® IPDA crosslinkers were used to crosslink Resin-A either ambiently or oven-cured. As stated by the supplier, the chemical nature of 702B75 and 2353 crosslinkers was based on a modified polyamide structure while the structure of PACM and IPDA crosslinkers was based on cycloaliphatic amines. Coatings that contained polyamide-based crosslinkers (702B75 and 2353) could tolerate >400 MEK DR (an indication of a well-crosslinked network), exhibited defect-free and smooth surfaces, and possessed values of desired durability (i.e. 80 in-lb or higher impact resistance; 5B crosshatch adhesion; 85-110 s König pendulum hardness; >5H pencil hardness). Alternatively, coatings with PACM and IPDA crosslinkers did not offer such properties; for examples, their surfaces had defects (i.e. crates and orange peel) or showed MEK DR less than 250. Consequently, 702B75 and 2353 crosslinkers were shortlisted, and each was used simultaneously with amine-terminated PDMS (APT-PDMS) for curing Resin-A. Coatings with 2353 crosslinker displayed better and smoother surfaces than the ones with 702B75 crosslinker (i.e. craters or raptured bubbles on the surface); thus, the 2353 crosslinker was selected for future experiments.

The extent of mixing and pre-reaction affects the surface morphology of marine FR coatings.[31] Hence, it may be beneficial to react functional PDMS chains partially to access a better network otherwise the PDMS might totally phase separate. We started by mixing all ingredients (Resin-A, APT-PDMS, and 2353 curing agent) for 30 minutes, four hours, eight hours, and 24 hours before drawing down formulations on a panel, but there was no observable difference in terms of mechanical properties and AFM images. In another set of experiments, we let Resin-A and APT-PDMS initially stir at ambient conditions between 30 mins to 24 hours before adding 2353 curing agent and applying the formulations. Though no observable differences were noticed among the surfaces, AFM images displayed slightly better well-defined domains as the initial mixing period increased (Figure 7.3A-D). Finally, we stirred Resin-A and APT-PDMS at 80 °C for 24 hours to speed up the reaction of epoxy and amine groups which could have been potentially hindered due to long chains of APT-PDMS. The AFM image of this approach (Figure 7.3E) exhibited a morphology of organized domains that were narrowly dispersed in size compared to other formulations, suggesting this stirring procedure delivers a desirable surface texture.[23] Additionally, water/toluene (0.5-1 mL) was placed on the surface of the coating that was prepared via heated stirring (80 °C 24 hours) for ten minutes to evaluate changes to surface domains due to interaction with each liquid. AFM images demonstrated that the surface domains slightly swelled and merged under both toluene (Figure 7.4A) and water (Figure 7.4C), signaling the presence of an amphiphilic surface similar to the T-10 control system (Figure 7.4E).[23] Hydrophilic chains like PEG swell in water and hydrophobic chains like PDMS swell in toluene.

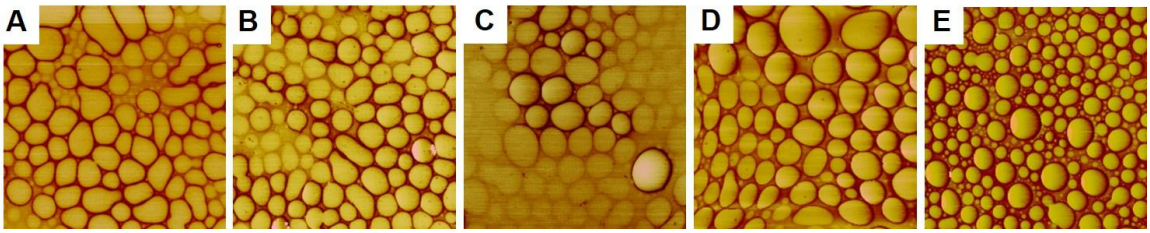

Figure 7.3. AFM images displaying the effect of stirring extent of acrylic Epoxy-PEG (Resin-A) and APT-PDMS on surface morphology. (A) 30 mins, (B) 4 hours, (C) 8 hours, (D) 24 hours, and (E) 24 hours 80 °C. Each image is an area of 100 µm x 100 µm.

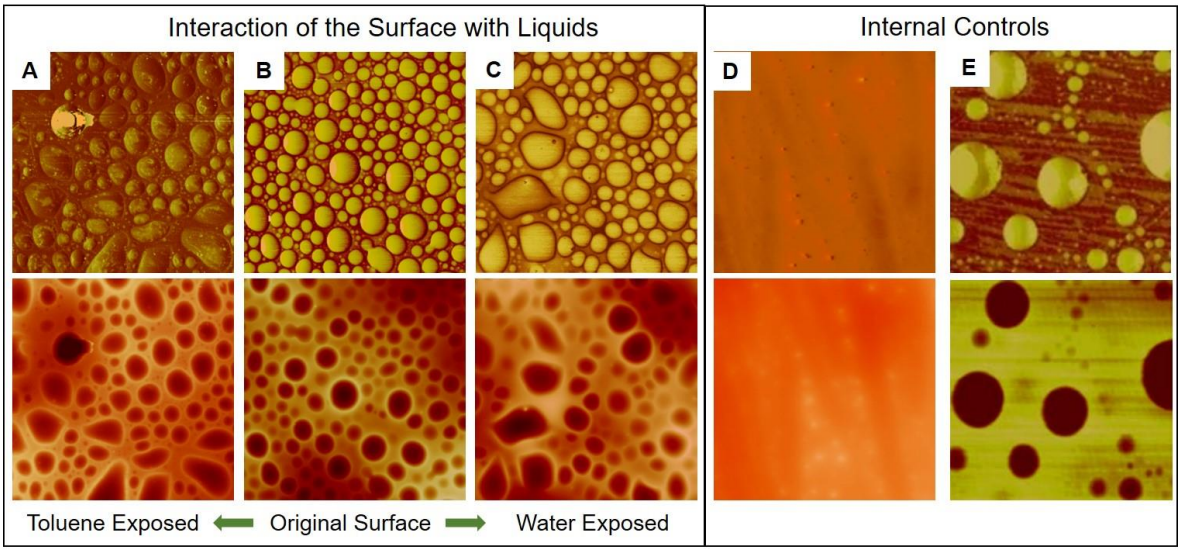

Figure 7.4. AFM images displaying the effect of solvent exposure on surface morphology. (A) Surface after exposure to toluene for 10 minutes; (B) Original surface of coating; (C) Surface after exposure to water for 10 minutes. Control coatings are presented for comparison as well: (D) A4 system – a siloxane-polyurethane formulation with a PDMS-rich surface, known for its hydrophobic nature and homogenous composition on the surface; (E) T-10 system – an amphiphilic siloxane-polyurethane system with a surface composed of PEG and PDMS. Each image is for an area of 100 µm x 100 µm.

We designed four formulations with a 2^2 design of experiment to gauge the fouling-release performance of this novel siloxane-epoxy-PEG system. The two factors for the formulations were the content of PEG and PDMS in a system with 2 levels for each. PEG levels were attained by changing its content in the backbone of acrylic epoxy resin at 20 and 30 parts, and PDMS levels were controlled by changing its molar ratio as a crosslinker. Table 7.1 outlines details about the four formulations and highlights how PEG and PDMS levels contribute to their overall content in a system. The overall content of PEG and PDMS for each system was calculated based on the solid contents of all ingredients.

Table 7.1. Investigated formulations for fouling-release performance

Formulation ID	PEG Parts in Acrylic Epoxy Resin	PDMS Molar Equivalent %	Overall PEG Content in the formulation (Wt. %)	Overall PDMS Content in the formulation (Wt. %)
F1	20	1.25	12.0	10.0
F2	20	2.50	12.0	20.0
F3	30	1.25	18.0	10.0
F4	30	2.50	18.0	20.0

Surface characterization of the four coatings was completed with ATR-FTIR, contact angle measurements, XPS, and AFM. The coatings visually appeared smooth and similar to both hydrophobic SiPU A4 and amphiphilic T-10. ATR-FTIR spectra for coatings F1-F4 presented signature signals for siloxane (Si-O-Si) at 1019 cm^{-1} and ether (C-O-C) at 1130 cm^{-1}, suggesting the availability of an amphiphilic surface (Figure 7.5). The signals for siloxane and PEG were in correlation with amphiphilic T-10 control coating, further supporting the amphiphilicity of the prepared surfaces. Also, an overlapped broad stretching for the hydroxyl group (due to epoxy and amine reaction) was present at ~3500 cm^{-1}.

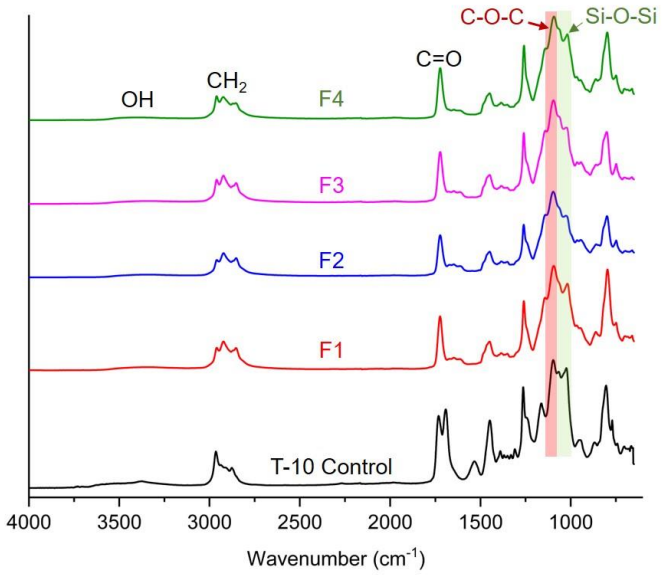

Figure 7.5. ATR-FTIR of prepared coatings for fouling-release investigations. Each spectrum is labeled to reflect the coating type.

Contact angle measurements were carried out to collect data both statically as a function of time and dynamically as a function of a tilting stage. The static data presented that the siloxane-epoxy-PEG (AmpSiEpox) systems possessed a dynamic surface since the water contact angles (WCA) and methylene iodide contact angles (MICA) changed over time (Figure 7.6A). For example, WCA for all AmpSiEpox coatings dropped from ~100° to ~80° in ten minutes. The dynamic nature of AmpSiEpox coatings, similar to amphiphilic T-10 coatings, was associated with amphiphilicity of surfaces. The initial WCA was in hydrophobic range and it decreased as hydrophilic PEG domains swelled, letting the water droplet spread more on the surface. Coatings F3 and F4 exhibited a relatively more dynamic surface than F1 and F2 coatings which may be due to higher PEG content in their composition. The dynamic behavior

is not observed for the A4 coating since its surface is composed of PDMS, a hydrophobic surface with no moieties to swell. Surface energy (SE) values were calculated using static WCAs and MICAs for each coating (Figure 7.6B). A comparison of SE values before water immersion and after water immersion for 28 days showed a slight change overall, indicating that the coatings were stable. The SE change was attributed to the potential rearrangement of surface domains in water as it was previously observed in AFM experiments (Figure 7.4). Using the dynamic tilting state, the slip angle of water droplet for the AmpSiEpox coatings was between 4.5°-6.5°, similar to the amphiphilic T-10 while the A4 slip angle was around 9°. The lower slip angle indicates surfaces facilitate the removal of objects from their surfaces easier (Figure 7.6C). Advancing (Adv) and receding (Rec) contact angles values for all AmpSiEpox coatings was between 95°-110°, showing the hydrophobic nature of the surfaces before swelling occurs (Figure 7.6D). The overall hysteresis (the difference between Adv CA and Rec CA) was less than or equal to 10°, similar to A4 and T-10 controls, which is an indication of a smooth surface and the ability to let objects roll-off from it – a property desired for marine fouling-release coatings.

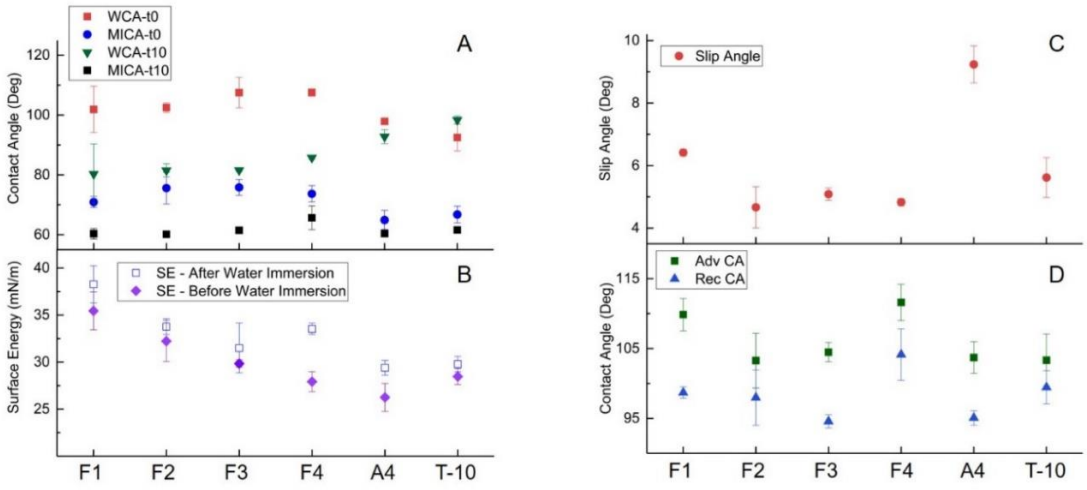

Figure 7.6. Contact angle and surface energy data for coatings. (A) Water Contact Angles (WCA) and methylene iodide contact angles (MICA) as a function of time at 0 minutes and 10 minutes; (B) Surface energy (SE) of coatings before and after 28-day water immersion, calculated by Owens-Wendt method utilizing the average WCAs and MICAs for each coating; (C) Slip angle of coatings where a water droplet starts to roll off; (D) Advancing contact angle (Adv CA) and receding contact angle (Rec CA) data, measured by tilting method. Hydrophobic A4 and amphiphilic T-10 are the internal coatings for comparison.

XPS was utilized to quantify the elemental compositions of materials on the surface. XPS depth profiling analysis confirmed the self-stratification of PDMS onto the surface. For example, XPS depth analysis for coating F2 showed the concentration of Si and O atoms gradually dropped after 5 nm depth, while the elemental composition of C increased (Figure 7.7A). The decrease of Si atom suggests PDMS is mainly present on the surface and the increase of C atom suggests the bulk of coating is constituted of the epoxy network.[8, 32] The self-stratification was present for all AmpSiEpox coatings as the Si atom graph for each system shows (Figure 7.7B). All systems show the concentration of PDMS decreases as a function of depth into the coating.

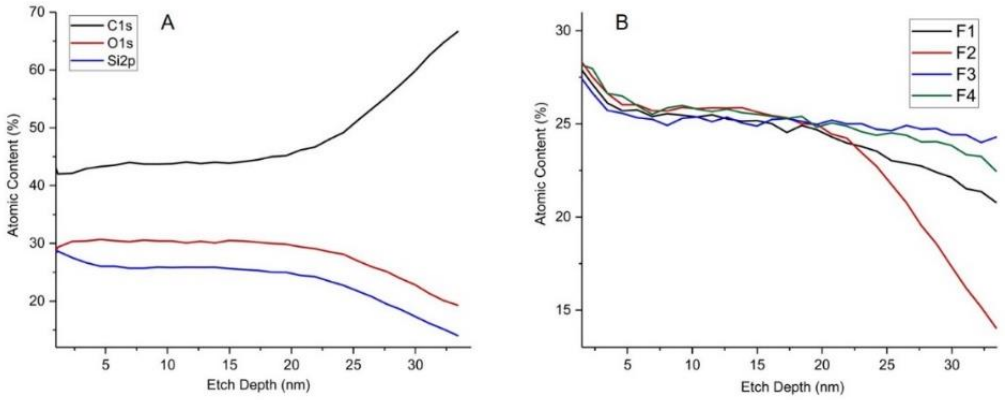

Figure 7.7. XPS data of the designed marine coatings. (A) XPS depth analysis for coating F2, composed of Resin-A; (B) XPS depth analysis of silicon atom for all AmpSiEpox coatings.

AFM was used to capture the morphology of surfaces for the coatings. AFM indicates soft materials like PDMS appear lighter (high phase angles) than relatively harder materials like PEG. The AmpSiEpox coatings exhibited heterogeneous phase patterns (backed by height images) that indicated the presence of both hard and soft moieties on the surfaces (Figure 7.8), suggesting the amphiphilic nature of these coatings that is similar to the T-10 control while A4 control lacked such features (Figure 7.4). AFM data did not suggest any observable difference in morphology between the AmpSiEpox coatings, and no substantial conclusion could be drawn based on PEG or PDMS content in a formulation. This lack of substantial differences may be attributed to the factor that despite the variation in the amount of PEG and PDMS, the MW of incorporated PEG and PDMS is the same for all coatings. Previous studies indicate similar findings where changes of MW of amphiphilic moieties impacts the surface morphology.[23]

Overall, a series of small domains, in the shape of circles or stretched lines, are present throughout the surfaces.

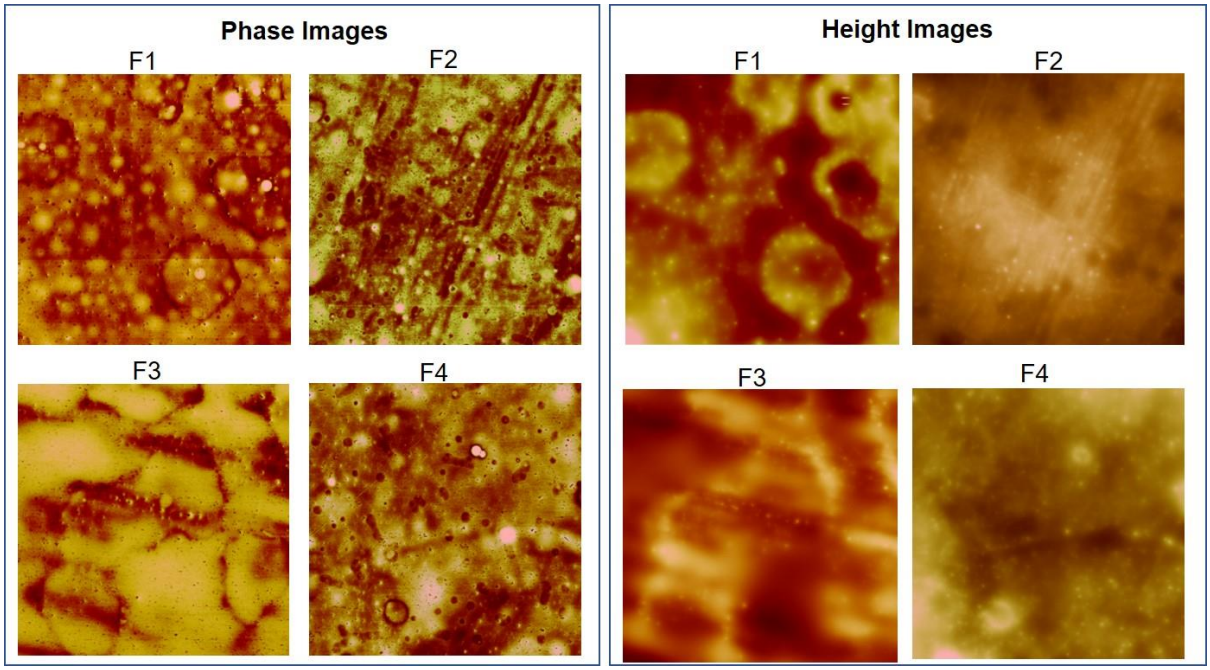

Figure 7.8. AFM phase images (upper box) and height images (bottom box) of AmpSiEpox and internal control coatings. Each image is for an area of 100 µm x 100 µm. Each label reflects the coating number.

Two representative marine biological assays were conducted to evaluate the fouling-release performance of the AmpSiEpox coatings. All the assessments were carried out after 28 days of water leaching to ensure impurities do not interfere with the results. The coatings were assessed for leachate toxicity using *C. lytica* and *N. incerta* as described elsewhere[29, 33] before any fouling-release experiments. All the coatings were non-toxic (data not reported), allowing for biological assessments.

C. lytica is a biofouling organism that usually settles on a variety of surfaces that range from hydrophilic or hydrophobic[1]; thus, amphiphilic surfaces are looked upon desirably to contend with its biofouling. The extent of biofouling among AmpSiEpox coatings and internal controls was similar but it was significantly less than commercial control systems such as IS 700, IS 900, and IS 1100SR (Figure 7.9 – Red bars). The fouling-release experiments were completed at two water pressure levels of 10 psi (Figure 7.9 – Blue bars) and 20 psi (Figure 7.9 – Green bars), and the extent of release is reflected in terms of biomass remaining after water-jetting. As expected, the amount of biomass remaining on a surface was less for coatings water-jetted at 20 psi, but overall trends at both pressure levels were alike.

Although no apparent changes were observed for FR performance among AmpSiEpox coatings against *C.* lytica, systems with more PEG (systems F3 and F4) displayed slightly better performance than the ones with less PEG (systems F1 and F2). The AmpSiEpox coatings showed comparable performance to our internal coatings including hydrophobic A4 and amphiphilic T-10, suggesting the new systems deliver a desirable performance. The AmpSiEpox systems outperformed several commercial coatings including IS 700 and IS 900 while they delivered comparable performance to top-performing IS 1100. Overall, *C. lytica* data shows AmpSiEpox coatings have the potential for marine fouling-release applications.

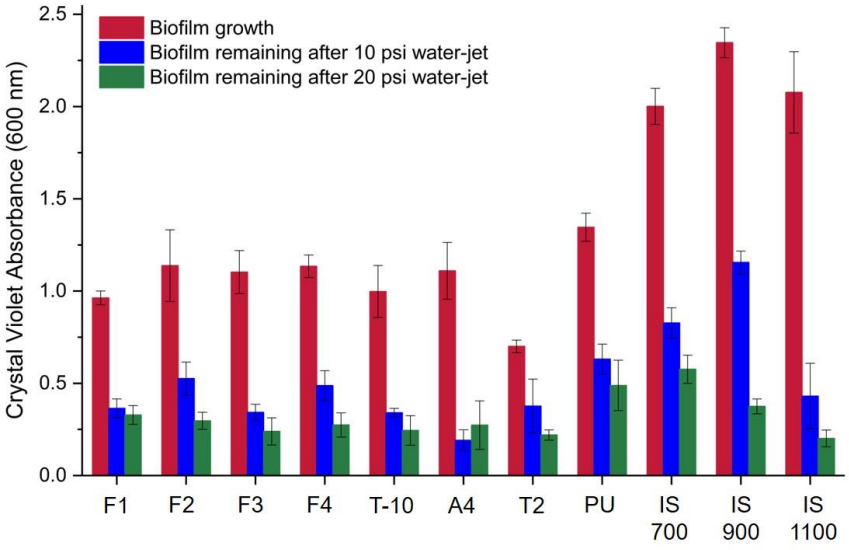

Figure 7.9. *C. lytica's* fouling-release data for biofilm growth (Red bar) and biomass remaining after water jetting at 10 psi (blue bar) and at 20 psi. The x-axis is labeled to specify the formulations.

N. incerta is another micro-biofouling organism that prefers settling on hydrophobic surfaces.[34, 35] The extent of biofouling was alike between all AmpSiEpox, internal controls, and external controls. The release experiments of *N. incerta* fouling film was carried out at 10 psi and 20 psi, and percent removal/release at each level is graphed in Figure 7.10 as blue bars and green bars, respectively. Percent removal was higher for 20 psi pressure level than 10 psi, not surprisingly. Similar to *C. lytica* data, there was no distinguishable FR trend between AmpSiEpox coatings, suggesting the modified content of PEG and PDMS did not result in a noticeable difference – though coatings F3 and F4 with more PEG performed slightly better at 20 psi. The percent removal of AmpSiEpox coatings was in par with internal

control systems T-10 and A4, suggesting these coatings possess similar FR performance. The AmpSiEpox coatings also delivered comparable performance to several control systems including T2 and PU. However, these coatings, like A4 and T-10, lacked the great performance of Intersleek® coatings against *N. incerta*. Overall, *N. incerta* and *C. lytica* data demonstrated AmpSiEpox coatings are comparable to well-established A4 and T-10 internal coatings, supporting the potential of AmpSiEpox systems for marine fouling-release applications.

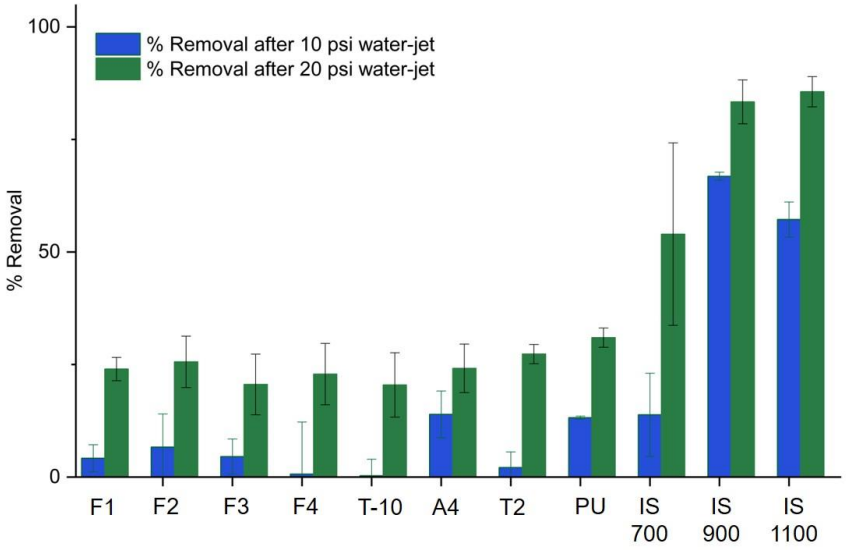

Figure 7.10. *N. incerta* percent removal/release after water jetting at 10 psi (blue bars) and at 20 psi (green bars). The x-axis is labeled to specify the formulations.

Conclusions

This study explored the introduction of a new epoxy coating system for fouling-release marine applications, called amphiphilic siloxane-epoxyPEG (AmpSiEpox) which was composed of acrylic epoxy resin with PEG in its backbone, amine-terminated PDMS, and amine crosslinker. A series of initial experiments resulted in selecting optimal content of 30 parts glycidyl methacrylate on resin backbone, 2353 as crosslinker, and 80 °C 24 hours for mixing condition. Surface characterization of AmpSiEpox coatings demonstrated the presence of an amphiphilic surface. AFM images showed the availability of heterogeneous microdomains that swelled and rearranged under both water and toluene. ATR-FTIR presented the presence of both PEG and PDMS moieties on the surfaces. Contact angle data suggested

AmpSiEpox coatings possess a dynamic surface that interacts with water (or other liquids) over time due to swelling of polymeric chains like PEG. XPS validated the self-stratification of the systems where the surface is mainly composed of PDMS and bulk is made of the epoxy-based network. The fouling-release (FR) assessment of AmpSiEpox coatings against *C. lytica* and *N. incerta* was similar to well-established internal controls including hydrophobic SiPU A4 and amphiphilic SiPU T-10, suggesting this novel system has potential to deliver the same level of performance. This initial investigation of AmpSiEpox coatings concluded this urethane-free epoxy-based approach is feasible and the new utilized chemistry did not affect the desired FR output. Future investigations of the AmpSiEpox system will study the effect of MW of incorporated PEG and PDMS on FR and surface properties, and the system will be assessed against a wider range of marine organisms including barnacles and *U. linza*.

References

1. Lejars, M.; Margaillan, A.; Bressy, C., Fouling release coatings: A nontoxic alternative to biocidal antifouling coatings. *Chemical Reviews* **2012,** *112* (8), 4347-4390.

2. Callow, M. E.; Callow, J. E., Marine biofouling: a sticky problem. *Biologist* **2002,** *49* (1), 10-14.

3. Callow, J. A.; Callow, M. E., Trends in the development of environmentally friendly fouling-resistant marine coatings. *Nature Communications* **2011,** *2* (1), 244-244.

4. Magin, C. M.; Cooper, S. P.; Brennan, A. B., Non-toxic antifouling strategies. *Materials Today* **2010,** *13* (4), 36-44.

5. Yebra, D. M.; Kiil, S.; Dam-Johansen, K., Antifouling technology—past, present and future steps towards efficient and environmentally friendly antifouling coatings. *Progress in Organic Coatings* **2004,** *50* (2), 75-104.

6. Konstantinou, I. K.; Albanis, T. A., Worldwide occurrence and effects of antifouling paint booster biocides in the aquatic environment: a review. *Environment International* **2004,** *30* (2), 235-248.

7. Pade, M.; Webster, D. C., Self-stratified siloxane-polyurethane fouling-release marine coating strategies: A review. In *Marine Coatings and Membranes*, Mittal, V., Ed. Central West Publishing: Australia, 2019; pp 1-36.

8. Bodkhe, R. B.; Thompson, S. E. M.; Yehle, C.; Cilz, N.; Daniels, J.; Stafslien, S. J.; Callow, M. E.; Callow, J. A.; Webster, D. C., The effect of formulation variables on fouling-release performance of stratified siloxane–polyurethane coatings. *Journal of Coatings Technology and Research* **2012,** *9* (3), 235-249.

9. Sommer, S. A.; Byrom, J. R.; Fischer, H. D.; Bodkhe, R. B.; Stafslien, S. J.; Daniels, J.; Yehle, C.; Webster, D. C., Effects of pigmentation on siloxane–polyurethane coatings and their performance as fouling-release marine coatings. *Journal of Coatings Technology and Research* **2011,** *8* (6), 661-670.

10. Sommer, S.; Ekin, A.; Webster, D. C.; Stafslien, S. J.; Daniels, J.; VanderWal, L. J.; Thompson, S. E. M.; Callow, M. E.; Callow, J. A., A preliminary study on the properties and fouling-

release performance of siloxane–polyurethane coatings prepared from poly(dimethylsiloxane) (PDMS) macromers. *Biofouling* **2010,** *26* (8), 961-972.

11. Galli, G.; Martinelli, E., Amphiphilic polymer platforms: surface engineering of films for marine antibiofouling. *Macromolecular rapid communications* **2017,** *38* (8), 1600704.

12. Zhu, X.; Guo, S.; He, T.; Jiang, S.; Jańczewski, D.; Vancso, G. J., Engineered, robust polyelectrolyte multilayers by precise control of surface potential for designer protein, cell, and bacteria adsorption. *Langmuir* **2016,** *32* (5), 1338-1346.

13. Martinelli, E.; Pretti, C.; Oliva, M.; Glisenti, A.; Galli, G., Sol-gel polysiloxane films containing different surface-active trialkoxysilanes for the release of the marine foulant Ficopomatus enigmaticus. *Polymer* **2018,** *145*, 426-433.

14. Gudipati, C. S.; Finlay, J. A.; Callow, J. A.; Callow, M. E.; Wooley, K. L., The antifouling and fouling-release perfomance of hyperbranched fluoropolymer (HBFP)− poly (ethylene glycol)(PEG) composite coatings evaluated by adsorption of biomacromolecules and the green fouling alga Ulva. *Langmuir* **2005,** *21* (7), 3044-3053.

15. Pollack, K. A.; Imbesi, P. M.; Raymond, J. E.; Wooley, K. L., Hyperbranched fluoropolymer-polydimethylsiloxane-poly(ethylene glycol) cross-linked terpolymer networks designed for marine and biomedical Applications: heterogeneous nontoxic antibiofouling surfaces. *ACS Applied Materials & Interfaces* **2014,** *6* (21), 19265-19274.

16. Wang, Y.; Betts, D. E.; Finlay, J. A.; Brewer, L.; Callow, M. E.; Callow, J. A.; Wendt, D. E.; DeSimone, J. M., Photocurable amphiphilic perfluoropolyether/poly (ethylene glycol) networks for fouling-release coatings. *Macromolecules* **2011,** *44* (4), 878-885.

17. Bodkhe, R. B.; Stafslien, S. J.; Daniels, J.; Cilz, N.; Muelhberg, A. J.; Thompson, S. E. M.; Callow, M. E.; Callow, J. A.; Webster, D. C., Zwitterionic siloxane-polyurethane fouling-release coatings. *Progress in Organic Coatings* **2015,** *78*, 369-380.

18. Jiang, S.; Cao, Z., Ultralow-fouling, functionalizable, and hydrolyzable zwitterionic materials and their derivatives for biological applications. *Advanced Materials* **2010,** *22* (9), 920-932.

19. Liu, P.; Huang, T.; Liu, P.; Shi, S.; Chen, Q.; Li, L.; Shen, J., Zwitterionic modification of polyurethane membranes for enhancing the anti-fouling property. *Journal of Colloid and Interface Science* **2016,** *480*, 91-101.

20. Wu, J.; Lin, W.; Wang, Z.; Chen, S.; Chang, Y., Investigation of the hydration of nonfouling material poly(sulfobetaine methacrylate) by low-field nuclear magnetic resonance. *Langmuir* **2012,** *28* (19), 7436-7441.

21. Bodkhe, R. B.; Stafslien, S. J.; Cilz, N.; Daniels, J.; Thompson, S. E. M.; Callow, M. E.; Callow, J. A.; Webster, D. C., Polyurethanes with amphiphilic surfaces made using telechelic functional PDMS having orthogonal acid functional groups. *Progress in Organic Coatings* **2012,** *75* (1-2), 38-48.

22. Van Zoelen, W.; Buss, H. G.; Ellebracht, N. C.; Lynd, N. A.; Fischer, D. A.; Finlay, J.; Hill, S.; Callow, M. E.; Callow, J. A.; Kramer, E. J., Sequence of hydrophobic and hydrophilic residues in amphiphilic polymer coatings affects surface structure and marine antifouling/fouling release properties. *ACS Macro Letters* **2014,** *3* (4), 364-368.

23. Galhenage, T. P.; Webster, D. C.; Moreira, A. M. S.; Burgett, R. J.; Stafslien, S. J.; Vanderwal, L.; Finlay, J. A.; Franco, S. C.; Clare, A. S., Poly(ethylene) glycol-modified, amphiphilic, siloxane–

polyurethane coatings and their performance as fouling-release surfaces. *Journal of Coatings Technology and Research* **2017,** *14* (2), 307-322.

24. Pade, M. Influence of Surface Topography and Curing Chemistry on Fouling-Release Performance of Self-Stratified Siloxane-Polyurethane Coatings. North Dakota State University, 2017.

25. Stafslien, S. J.; Sommer, S.; Webster, D. C.; Bodkhe, R.; Pieper, R.; Daniels, J.; Vander Wal, L.; Callow, M. C.; Callow, J. A.; Ralston, E., Comparison of laboratory and field testing performance evaluations of siloxane-polyurethane fouling-release marine coatings. *Biofouling* **2016,** *32* (8), 949-968.

26. Owens, D. K.; Wendt, R. C., Estimation of the surface free energy of polymers. *Journal of Applied Polymer Science* **1969,** *13* (8), 1741-1747.

27. Stafslien, S.; Daniels, J.; Mayo, B.; Christianson, D.; Chisholm, B.; Ekin, A.; Webster, D.; Swain, G., Combinatorial materials research applied to the development of new surface coatings IV. A high-throughput bacterial biofilm retention and retraction assay for screening fouling-release performance of coatings. *Biofouling* **2007,** *23* (1), 45-54.

28. Stafslien, S. J.; Bahr, J. A.; Daniels, J. W.; Wal, L. V.; Nevins, J.; Smith, J.; Schiele, K.; Chisholm, B., Combinatorial materials research applied to the development of new surface coatings VI: An automated spinning water jet apparatus for the high-throughput characterization of fouling-release marine coatings. *Review of Scientific Instruments* **2007,** *78* (7), 072204-072204.

29. Cassé, F.; Stafslien, S. J.; Bahr, J. A.; Daniels, J.; Finlay, J. A.; Callow, J. A.; Callow, M. E., Combinatorial materials research applied to the development of new surface coatings V. Application of a spinning water-jet for the semi-high throughput assessment of the attachment strength of marine fouling algae. *Biofouling* **2007,** *23* (2), 121-130.

30. Cassé, F.; Ribeiro, E.; Ekin, A.; Webster, D. C.; Callow, J. A.; Callow, M. E., Laboratory screening of coating libraries for algal adhesion. *Biofouling* **2007,** *23* (4), 267-276.

31. Majumdar, P.; Webster, D. C., Surface microtopography in siloxane–polyurethane thermosets: The influence of siloxane and extent of reaction. *Polymer* **2007,** *48* (26), 7499-7509.

32. Galhenage, T. P.; Hoffman, D.; Silbert, S. D.; Stafslien, S. J.; Daniels, J.; Miljkovic, T.; Finlay, J. A.; Franco, S. C.; Clare, A. S.; Nedved, B. T., Fouling-release performance of silicone oil-modified siloxane-polyurethane coatings. *ACS Applied Materials & Interfaces* **2016,** *8* (42), 29025-29036.

33. Majumdar, P.; Crowley, E.; Htet, M.; Stafslien, S. J.; Daniels, J.; VanderWal, L.; Chisholm, B. J., Combinatorial materials research applied to the development of new surface coatings XV: An investigation of polysiloxane anti-fouling/fouling-release coatings containing tethered quaternary ammonium salt groups. *ACS Combinatorial Science* **2011,** *13* (3), 298-309.

34. Finlay, J. A.; Callow, M. E.; Ista, L. K.; Lopez, G. P.; Callow, J. A., The influence of surface wettability on the adhesion strength of settled spores of the green alga Enteromorpha and the diatom Amphora. *Integrative and Comparative Biology* **2002,** *42* (6), 1116-1122.

35. Callow, M. E.; Callow, J. A.; Ista, L. K.; Coleman, S. E.; Nolasco, A. C.; López, G. P., Use of self-assembled monolayers of different wettabilities to study surface selection and primary adhesion processes of green algal (Enteromorpha) zoospores. *Applied Environmental Microbiology* **2000,** *66* (8), 3249-3254.

CHAPTER 8. OVERALL CONCLUSIONS AND FUTURE WORK

This work reported in this dissertation investigated several approaches for attaining amphiphilic marine surfaces to meet two goals: 1) Enhancing the (FR) fouling-release performance of previously developed coating systems; 2) Introducing novel fouling-release marine coatings with set criteria. To this effect, chapters two through five studied the effect of prepared amphiphilic additives on modified marine coating systems and chapters six and seven explored designing of new amphiphilic coating networks.

Zwitterionic-based Additives

In the second chapter, amphiphilic zwitterionic additives, based on poly(sulfobetaine methacrylate) (poly(SBMA)) and polydimethylsiloxane (PDMS), were synthesized and introduced to the established hydrophobic siloxane-polyurethane (SiPU) coating formulation.[1] The poly(SBMA)-PDMS additives were synthesized using ARGET-ATRP (activator regenerated by electron transfer - atom transfer radical polymerization) technique, enabling to access additives of defined molecular weights. The zwitterionic additives self-stratified to the surface of SiPU coating and modified its surface properties as surface characterizations by atomic force microscopy (AFM), ATR-FTIR (attenuated total reflectance - Fourier transform infrared spectroscopy), and contact angle measurements indicated. These additives enhanced the FR performance of base SiPU systems towards several marine biofoulants such as *U. linza*, *C. lytica*, and barnacles and presented no detrimental effects towards *N. incerta* and mussels. This study suggested several considerations may result in effective zwitterionic additives including a PDMS block with 1,000 $\bar{M}_n$ and a hydrophilic content between 50%-80% of the total molecular weight of additive, while some factors may not be as influential such as the number of polymeric blocks (2 vs 3).

Utilizing the recent literature, the future investigations of additive and coating systems can explore incorporating alternative zwitterions. The zwitterionic additives in this study contained sulfobetaine moieties as the neutrally charged group. As recent studies have shown the type of zwitterionic moiety influences its performance for protein-resistance or marine biofouling applications. The zwitterionic types can be categorized based on varying molecular structures (i.e. Y-shaped, linear-shaped)[2] or molecular formula (sulfobetaine,[3] carboxybetaine,[4] phosphorylcholine,[5] or recently developed trimethylamine *N*-oxide-derived[6]). Exploring these groups will further develop the understanding of self-stratifying zwitterionic-based FR systems.

Poly (ethylene glycol)-based Additives

Chapters three, four, and five examined another class of amphiphilic additives based on poly (ethylene glycol) and PDMS. The study in chapter three added an amphiphilic additive to a non-marine polyurethane coating system and determined the amphiphilic concentration when desirable fouling-release performance was observed, calling it “critical amphiphilic concentration” (CAC). The amphiphilic additive for this study contained 10,000 $\bar{M}_n$ PDMS and 750 $\bar{M}_n$ chains installed on a polyisocyanate. The surface characterizations with AFM, ATR-FTIR, contact angle analysis, and XPS (X-ray photoelectron spectroscopy) clearly showed a correlation between the amount of added additive and surface properties. The surfaces delivered desirable FR performance (comparable/better to/than internal and commercial controls) towards assessed biofoulants including *N. incerta*, *C. lytica*, and *U. linza*. These FR data indicated once CAC was met at around 10-12 wt.% PEG and PDMS each, the FR performance plateaued and more additive did not boost the output. Surface data was in correlation with FR data as well, and it was noted an additional amount of additive after CAC did not modify the surface properties considerably.

In chapter four, considering the facile tunability of PEG-PDMS additives in terms of hydrophilic-hydrophobic balance (and their easy synthesis which is helpful for scale-up and commercialization purposes), these amphiphilic additives were introduced to hydrophobic SiPU formulation to attain an amphiphilic balance on its surface which was composed of PDMS solely. Knowing that SiPU contains 20 wt.% PDMS in its solid content composition, the amphiphilic additives of varying hydrophilic-hydrophobic balance were added at a constant concentration to this system, enabling the opportunity to calculate the extent of hydrophilic and hydrophobic contents as a whole in the formulation. The comparison of these calculations against the collected surface and FR data indicated that the balance of amphiphilicity has a role in surface patterns and FR performance. Overall, the formulations where the concentration of hydrophilic and hydrophobic moieties was almost equal presented the most desirable FR performance.

As amphiphilic additives contributed beneficial effects to the hydrophobic SiPU system, the question arose regarding what will be the effect of such additives on an amphiphilic marine coating. Thus, chapter five studied the effect of PEG-PDMS additives on an established amphiphilic SiPU system[7] by exploring several factors such as molecular weights of PEG/PDMS, amphiphilicity balance, or

amphiphilicity concentration. Similar to previous studies, the additives segregated to the surfaces and modified them as confirmed by AFM, ATR-FTIR, XPS, and contact angle measurements. Additionally, the data showed amphiphilic additives boosted the performance of the amphiphilic SiPU system noticeably against *N. incerta* and *U. linza*, suggesting these additives offer desirable effects for amphiphilic-based formulations as well.

Future studies of PEG-PDMS amphiphilic additives can follow many routes. A study can examine the leaching extent of the additives from the coating systems over time. For example, select formulations (i.e. polyurethane system with 25 wt.% of a PEG-PDMS additive) can undergo water aging for 1, 3, 6, 12, and 24 months. For each period, surfaces and FR properties can be assessed and compared against each other over time. For another examination, similar to chapter three, amphiphilic additives with a varying balance of hydrophilic-hydrophobic contents can be added to a non-marine polyurethane system, but this time at a constant concentration (~12 wt.% of PEG and PDMS each), for assessing the direct effect of amphiphilic balance of the whole system on surface and FR characteristics (unlike the study in chapter four where the base SiPU system already contained PDMS). Additionally, the effect of PEG-PDMS amphiphilic additives can be evaluated on glycidyl-carbamate marine coatings[8, 9] similar to studies in chapters four and five. To utilize more stable hydrophilic moieties on the design of PEG-PDMS additives, one may think of replacing PEG chains with polyzwitterionic chains (not monomeric zwitterionic units since previous unpublished work showed their ineffectiveness) on a polyisocyanate. It should be noted the synthesis of PEG-PDMS additives in this dissertation is keyed to the facile reaction of hydroxyl groups of PEG/PDMS with isocyanate functional groups, thus it may be required to find chemistry where hydroxyl-terminated polyzwitterions can be synthesized in order to facilitate the suggested replacement of PEG moieties. The suggested future work implies the abundant directions one may pursue to design novel amphiphilic surfaces.

Amphiphilic Glycidyl-carbamate Coating Systems

By introducing amphiphilic glycidyl-carbamate (GC) coatings, the sixth chapter aimed to address the limitations of all the previously prepared FR marine systems, including hydrophobic SiPU,[1] amphiphilic SiPU,[7] and glycidyl-carbamate.[9] These systems either were questioned for their effects on workers' health due to the presence of isocyanate resins in a final formulation or their lack of desirable

performance towards a wide range of marine organisms. Therefore, amphiphilic GC system combined the overall competitive advantages of these systems, namely availability of urethane linkage in the network, presence of epoxy groups instead of isocyanates for crosslinking chemistry, and highly desired fouling-release performance towards all the assessed biofoulants (*N. incerta*, *U. linza*, *C. lytica*, and barnacles) in respect to all the internal controls as well as commercial controls. This study assessed several factors to select optimal design parameters for this novel system such as molecular weights of PEG/PDMS, amphiphilicity concentrations, and crosslinking agents.

The future studies for this system are many, of which several will be suggested here. An approach can be assessing the stability of these networks over time as mentioned earlier – select formulations are exposed to water aging for 1, 3, 6, 12, and 24 months. For each period, surfaces and FR properties can be assessed and compared against each other over time. Also, other studies can evaluate the effect of additives on the amphiphilic GC coatings, where the additives can be the assessed ones in chapters two-five, silicone oil,[10] or other alternatives.

Amphiphilic Urethane-free Epoxy Marine Coating Systems

Chapter seven aimed to create a urethane-free FR marine system since urethane linkages constitute the bulk network of assessed FR coatings in this dissertation and previous works such as SiPU,[1] amphiphilic SiPU,[7] and marine GC.[9] Although urethane linkages are highly desired for their inherent properties, there has been comments about their stability in aquatic environments (the field tests up to two years did not indicate such defects).[11] Therefore, this study explored a novel amphiphilic coating network composed of acrylic epoxy resin with pendant PEG chains, amine-terminated PDMS, and an amine crosslinker. After involved initial experiments, several variables such as optimum epoxy resin, crosslinking agent, and coating preparation procedure were shortlisted to formulate amphiphilic surfaces for FR assessment. The formulated coatings displayed amphiphilic nature under surface characterizations (AFM, ATR-FTIR, contact angle analysis, and XPS) and delivered FR performance which was comparable to both hydrophobic SiPU and amphiphilic SiPU control systems.

As the amphiphilic urethane-free epoxy marine coating system is new, many questions need to be answered to access a well-tuned and well-performing FR formulation. This study was designed as an initial concept for a future researcher's studies. As a few examples out of many, to access amphiphilicity

through an alternative route, one may think of crosslinking an epoxy resin with amine-terminated PEG and PDMS instead of having PEG in the backbone of acrylic resin. This study will compare the behavior of PEG chains as pendant moieties on acrylic epoxy resin vs PEG chains as crosslinking agents which may be tightly bonded to the network – a previous study informs about such differences in another system.[12] Additionally, one should investigate the effect of variables like solvent or varying molecular weights of PDMS crosslinker. It is recommended to review the early work on the development of SiPU system for further ideas.[1, 13-17]

Overall Remarks

This dissertation investigated several domains by not only preparing and introducing novel amphiphilic additives and fouling-release marine coating systems by varying variables like the molecular weight of amphiphilic moieties, crosslinker type, or curing conditions but also answering fundamental questions about some less understood concepts such as the effect of amphiphilicity concentration or effect of amphiphilicity balance for future design considerations. The avenues for future research directions on finding solutions to marine biofouling are boundless (i.e. examples of future work in this chapter), thus a curious mind should dare to imagine the impossible while aiming to contribute more understanding to the marine biofouling field than solely “developing” formulations.

References

1. Bodkhe, R. B.; Thompson, S. E. M.; Yehle, C.; Cilz, N.; Daniels, J.; Stafslien, S. J.; Callow, M. E.; Callow, J. A.; Webster, D. C., The effect of formulation variables on fouling-release performance of stratified siloxane–polyurethane coatings. *Journal of Coatings Technology and Research* **2012,** *9* (3), 235-249.

2. Koc, J.; Schönemann, E.; Amuthalingam, A.; Clarke, J.; Finlay, J. A.; Clare, A. S.; Laschewsky, A.; Rosenhahn, A., Low-fouling thin hydrogel coatings made of photo-cross-linked polyzwitterions. *Langmuir* **2019,** *35* (5), 1552-1562.

3. Zhang, Z.; Finlay, J. A.; Wang, L.; Gao, Y.; Callow, J. A.; Callow, M. E.; Jiang, S., Polysulfobetaine-grafted surfaces as environmentally benign ultralow fouling marine coatings. *Langmuir* **2009,** *25* (23), 13516-13521.

4. Chien, H.-W.; Cheng, P.-H.; Chen, S.-Y.; Yu, J.; Tsai, W.-B., Low-fouling and functional poly(carboxybetaine) coating via a photo-crosslinking process. *Biomaterials Science* **2017,** *5* (3), 523-531.

5. Lee, I.; Kobayashi, K.; Sun, H. Y.; Takatani, S.; Zhong, L. G., Biomembrane mimetic polymer poly (2-methacryloyloxyethyl phosphorylcholine-co-n-butyl methacrylate) at the interface of polyurethane surfaces. *Journal of Biomedical Materials Research Part A* **2007,** *82A* (2), 316-322.

6. Li, B.; Jain, P.; Ma, J.; Smith, J. K.; Yuan, Z.; Hung, H.-C.; He, Y.; Lin, X.; Wu, K.; Pfaendtner, J.; Jiang, S., Trimethylamine N-oxide–derived zwitterionic polymers: A new class of ultralow fouling bioinspired materials. *Science Advances* **2019,** *5* (6), eaaw9562.

7. Galhenage, T. P.; Webster, D. C.; Moreira, A. M. S.; Burgett, R. J.; Stafslien, S. J.; Vanderwal, L.; Finlay, J. A.; Franco, S. C.; Clare, A. S., Poly(ethylene) glycol-modified, amphiphilic, siloxane–polyurethane coatings and their performance as fouling-release surfaces. *Journal of Coatings Technology and Research* **2017,** *14* (2), 307-322.

8. Pade, M.; Webster, D. C., Self-stratified siloxane-polyurethane fouling-release marine coating strategies: A review. In *Marine Coatings and Membranes*, Mittal, V., Ed. Central West Publishing: Australia, 2019; pp 1-36.

9. Pade, M. Influence of Surface Topography and Curing Chemistry on Fouling-Release Performance of Self-Stratified Siloxane-Polyurethane Coatings. North Dakota State University, 2017.

10. Galhenage, T. P.; Hoffman, D.; Silbert, S. D.; Stafslien, S. J.; Daniels, J.; Miljkovic, T.; Finlay, J. A.; Franco, S. C.; Clare, A. S.; Nedved, B. T., Fouling-release performance of silicone oil-modified siloxane-polyurethane coatings. *ACS applied materials & interfaces* **2016,** *8* (42), 29025-29036.

11. Stafslien, S. J.; Sommer, S.; Webster, D. C.; Bodkhe, R.; Pieper, R.; Daniels, J.; Vander Wal, L.; Callow, M. C.; Callow, J. A.; Ralston, E., Comparison of laboratory and field testing performance evaluations of siloxane-polyurethane fouling-release marine coatings. *Biofouling* **2016,** *32* (8), 949-968.

12. Wang, Y.; Betts, D. E.; Finlay, J. A.; Brewer, L.; Callow, M. E.; Callow, J. A.; Wendt, D. E.; DeSimone, J. M., Photocurable amphiphilic perfluoropolyether/poly (ethylene glycol) networks for fouling-release coatings. *Macromolecules* **2011,** *44* (4), 878-885.

13. Ekin, A.; Webster, D. C.; Daniels, J. W.; Stafslien, S. J.; Cassé, F.; Callow, J. A.; Callow, M. E., Synthesis, formulation, and characterization of siloxane–polyurethane coatings for underwater marine applications using combinatorial high-throughput experimentation. *Journal of Coatings Technology and Research* **2007,** *4* (4), 435-451.

14. Majumdar, P.; Webster, D. C., Surface microtopography in siloxane–polyurethane thermosets: The influence of siloxane and extent of reaction. *Polymer* **2007,** *48* (26), 7499-7509.

15. Sommer, S.; Ekin, A.; Webster, D. C.; Stafslien, S. J.; Daniels, J.; VanderWal, L. J.; Thompson, S. E. M.; Callow, M. E.; Callow, J. A., A preliminary study on the properties and fouling-release performance of siloxane–polyurethane coatings prepared from poly(dimethylsiloxane) (PDMS) macromers. *Biofouling* **2010,** *26* (8), 961-972.

16. Majumdar, P.; Webster, D. C., Influence of solvent composition and degree of reaction on the formation of surface microtopography in a thermoset siloxane–urethane system. *Polymer* **2006,** *47* (11), 4172-4181.

17. Sommer, S. A.; Byrom, J. R.; Fischer, H. D.; Bodkhe, R. B.; Stafslien, S. J.; Daniels, J.; Yehle, C.; Webster, D. C., Effects of pigmentation on siloxane–polyurethane coatings and their performance as fouling-release marine coatings. *Journal of Coatings Technology and Research* **2011,** *8* (6), 661-670.

APPENDIX

Chapter 2. Supplemental Information

Table A1. List of formulated coatings

Formulation Title	Assigned ID Number	Incorporated Additive			
		Blocks	PDMS MW (MW)	SBMA (MW)	Amount (wt. %)
A4-20	1				
500-1k 0.2%	2	2	1000	500	0.2
500-1k 1.0%	3	2	1000	500	1
500-1k 5.0%	4	2	1000	500	5
1k-1k 0.2%	5	2	1000	1000	0.2
1k-1k 1%	6	2	1000	1000	1
1k-1k 5%	7	2	1000	1000	5
2.5k-1k 0.2%	8	2	1000	2500	0.2
2.5k-1k 1%	9	2	1000	2500	1
2.5k-1k 5%	10	2	1000	2500	5
500-1k-500 0.2%	11	3	1000	1000	0.2
500-1k-500 1%	12	3	1000	1000	1
500-1k-500 5%	13	3	1000	1000	5
1k-1k-1k 0.2%	14	3	1000	2000	0.2
1k-1k-1k 1%	15	3	1000	2000	1
1k-1k-1k 5%	16	3	1000	2000	5
2.5k-1k-2.5k 0.2%	17	3	1000	5000	0.2
2.5k-1k-2.5k 1%	18	3	1000	5000	1
2.5k-1k-2.5k 5%	19	3	1000	5000	5
500-5k-500 0.2%	20	3	5000	1000	0.2
500-5k-500 1%	21	3	5000	1000	1
1k-5k-1k 0.2%	22	3	5000	2000	0.2
1k-5k-1k 1%	23	3	5000	2000	1
1k-5k-1k 5%	24	3	5000	2000	5
2.5k-5k-2.5k 0.2%	25	3	5000	5000	0.2
2.5k-5k-2.5k 1%	26	3	5000	5000	1
2.5k-5k-2.5k 5%	27	3	5000	5000	5
500-10k-500 0.2%	28	3	10000	1000	0.2
500-10k-500 1%	29	3	10000	1000	1
500-10k-500 5%	30	3	10000	1000	5
1k-10k-1k 0.2%	31	3	10000	2000	0.2
1k-10k-1k 1%	32	3	10000	2000	1
1k-10k-1k 5%	33	3	10000	2000	5
2.5k-10k-2.5k 0.2%	34	3	10000	5000	0.2
2.5k-10k-2.5k 1%	35	3	10000	5000	1
2.5k-10k-2.5k 5%	36	3	10000	5000	5
2.5k-1k 10%	37	2	1000	2500	10
2.5k-1k-2.5k 10%	38	3	1000	5000	10
All di-block of 1k PDMS Together 1%	39	2	N/A	N/A	1
All tri-block of 1k PDMS Together 1%	40	3	N/A	N/A	1
ARR-2-120 p(SBMA) 0.2%	41	1	0	5000	0.2
ARR-2-120 p(SBMA) 1%	42	1	0	5000	1
ARR-2-120 p(SBMA) 5%	43	1	0	5000	5

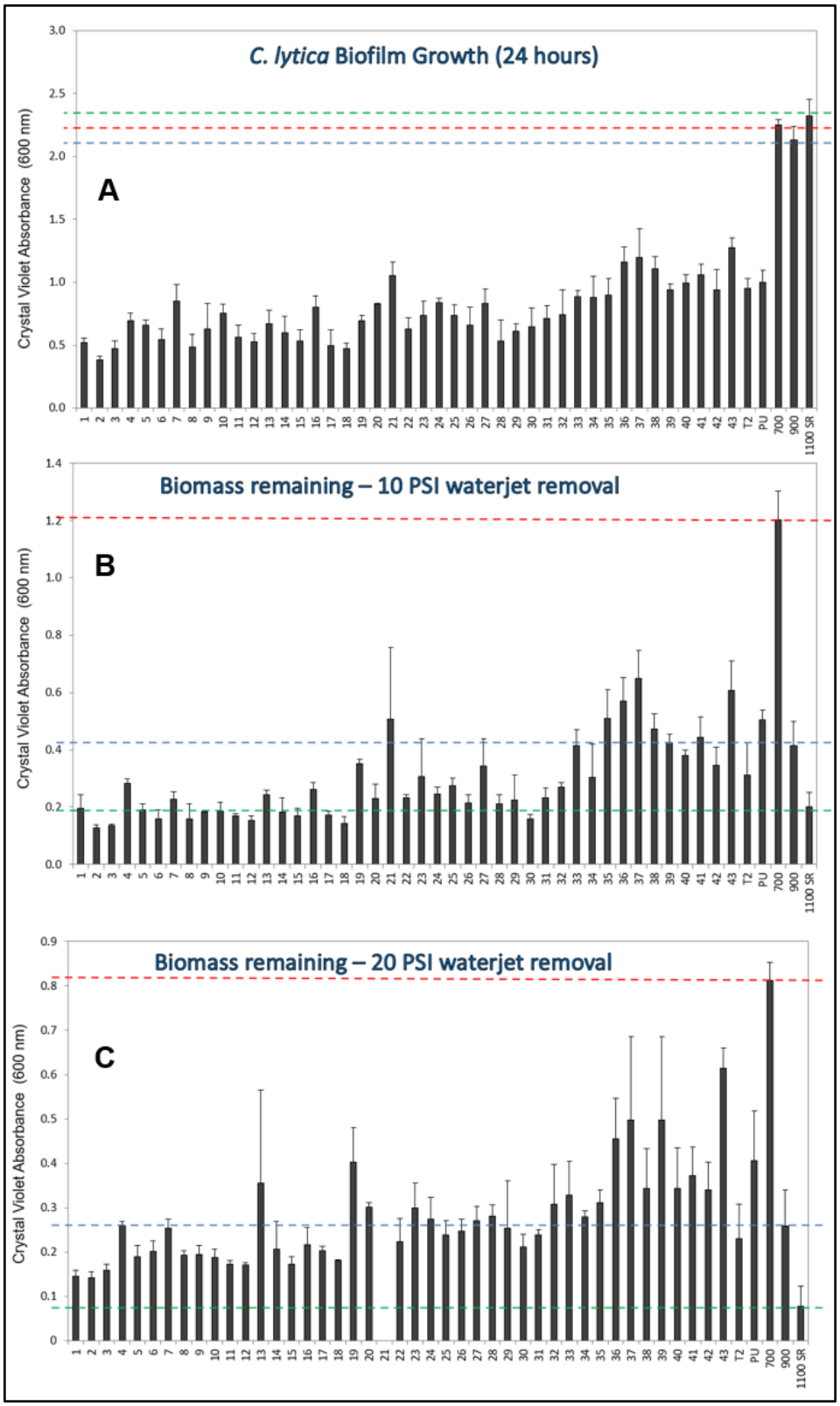

Figure A1. *C. lytica* growth (A) and biomass remaining after 10 psi waterjet (B) and 20 psi waterjet (C). The X-axis is labeled to contain coating number.

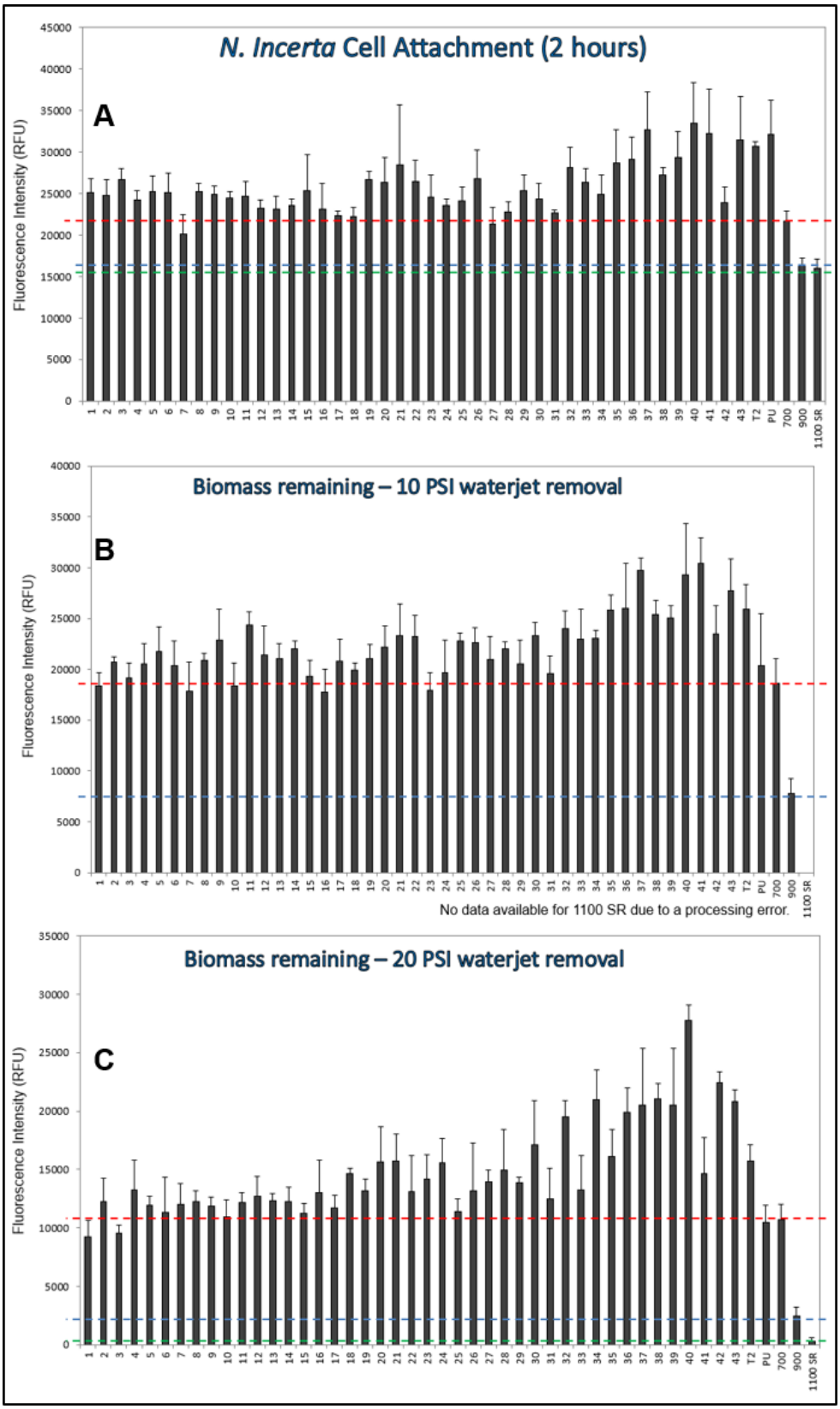

Figure A2. *N. incerta* growth (A) and biomass remaining after 10 psi waterjet (B) and 20 psi waterjet (C). The X-axis is labeled to contain coating number.

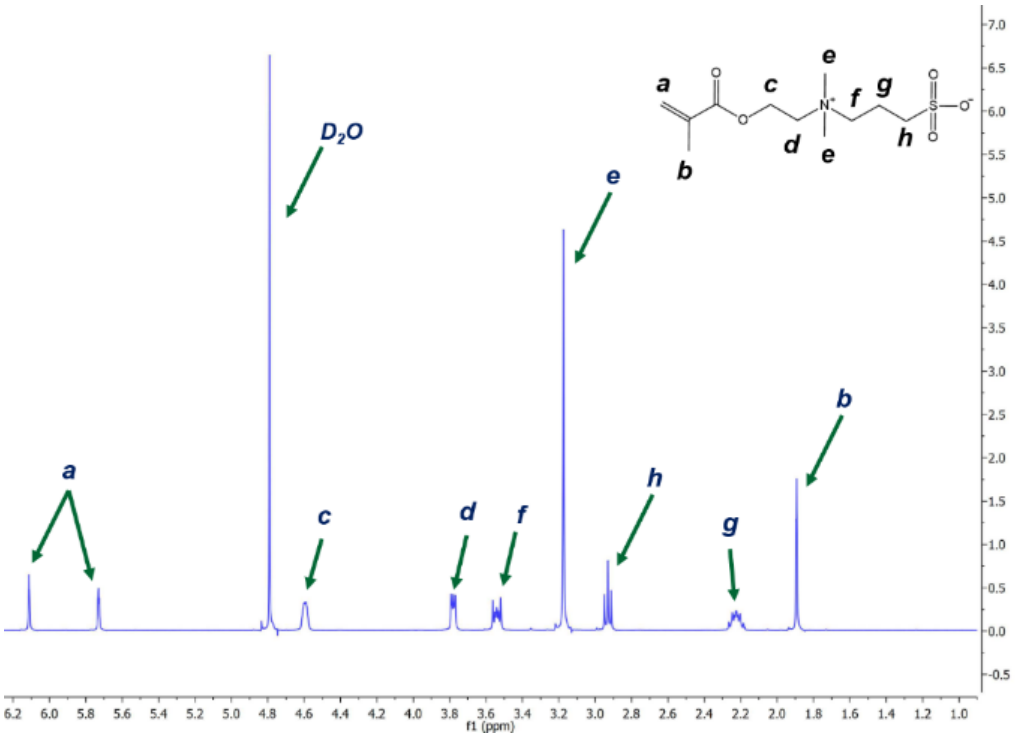

Figure A3. ^{1}H-NMR of sulfobetaine methacrylate (SBMA) monomer

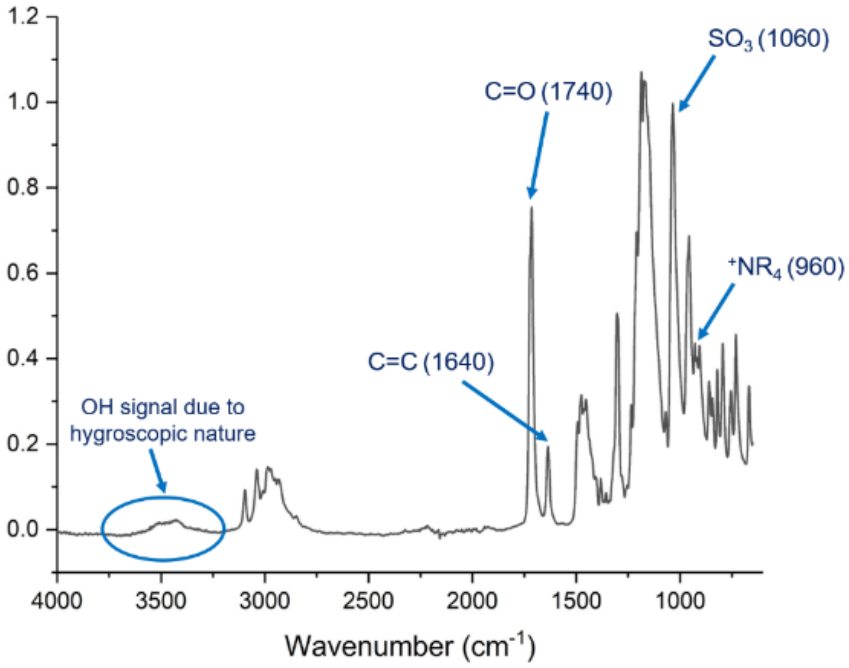

Figure A4. FTIR of sulfobetaine methacrylate (SBMA) monomer

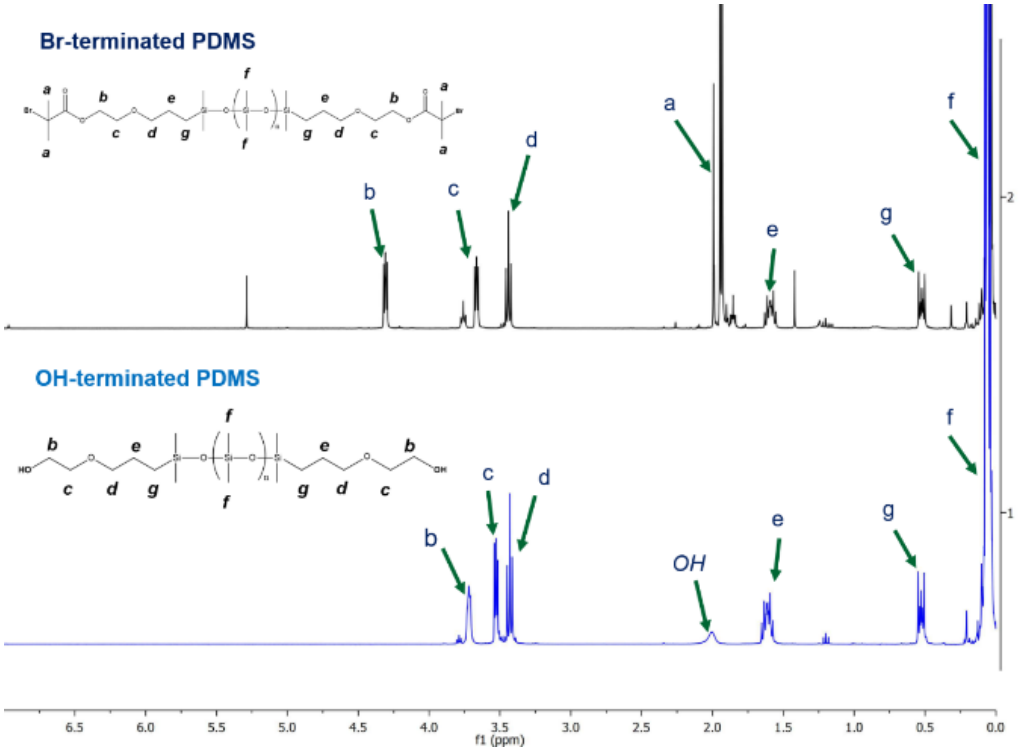

Figure A5. ^{1}H-NMR of virgin and modified PDMS as macroinitiator

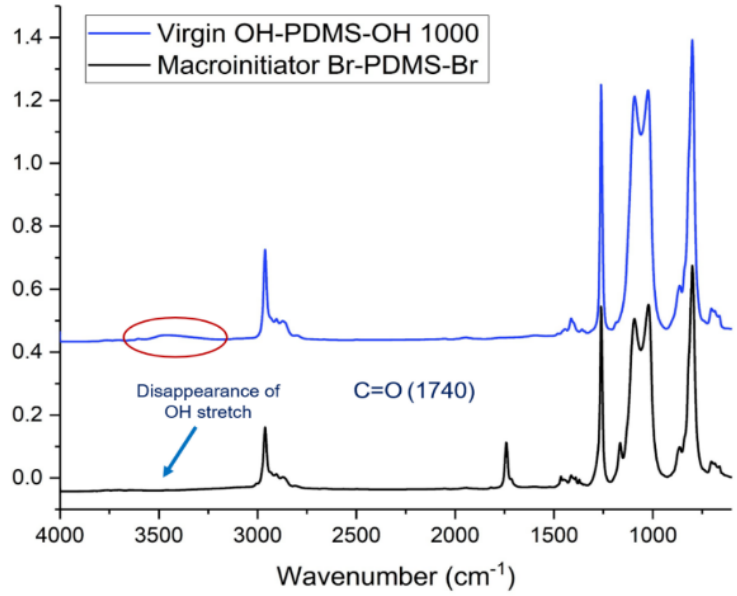

Figure A6. FTIR of virgin and modified PDMS as macroinitiator

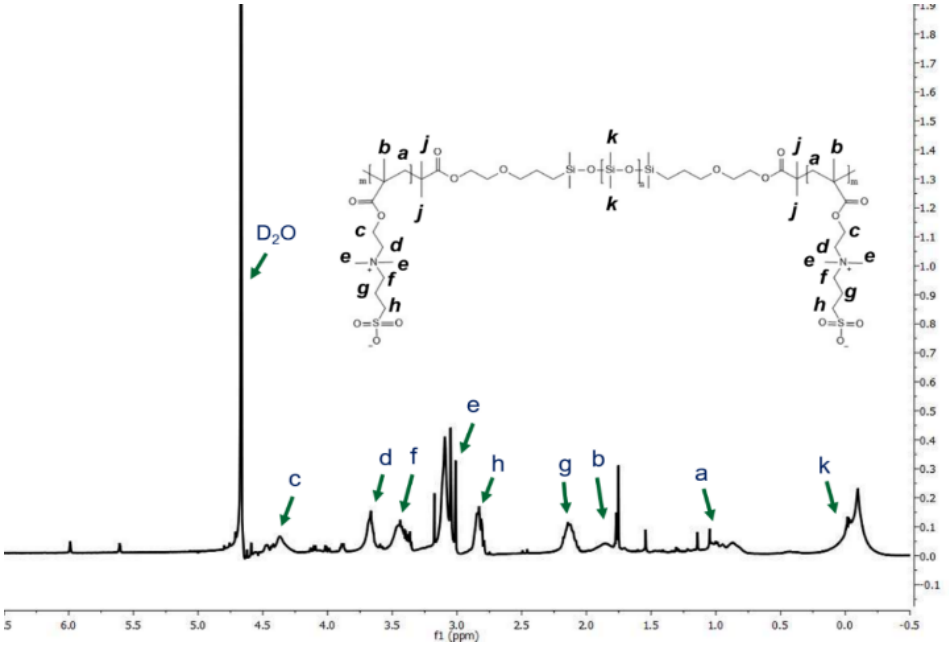

Figure A7. ^{1}H-NMR spectrum of poly(SBMA)-PDMS-poly(SBMA) triblock in D_2O

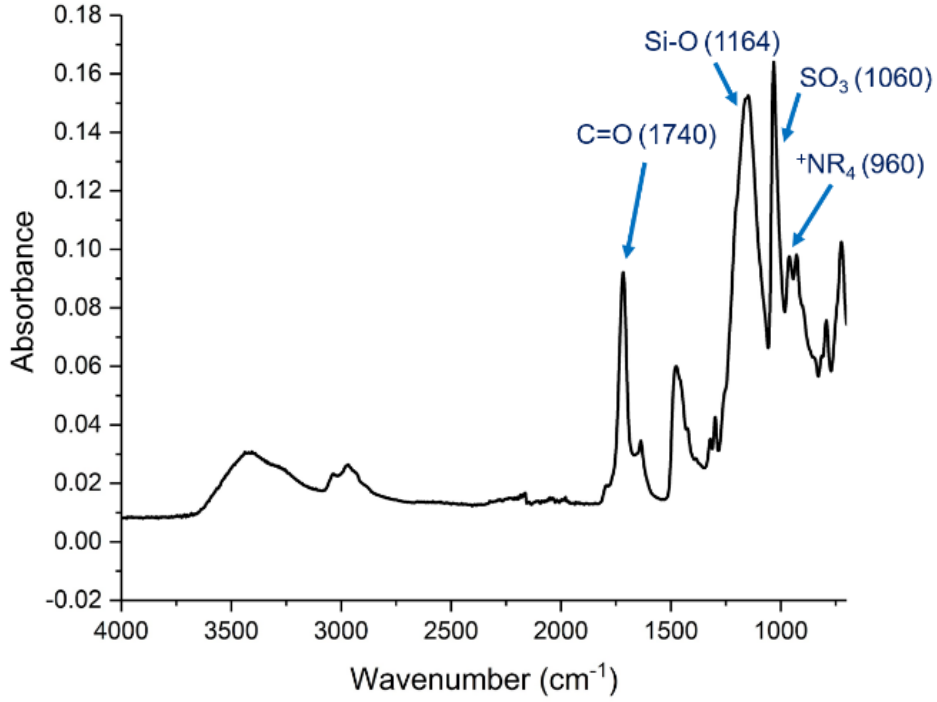

Figure A8. FTIR spectrum of poly(SBMA)-PDMS-poly(SBMA) triblock

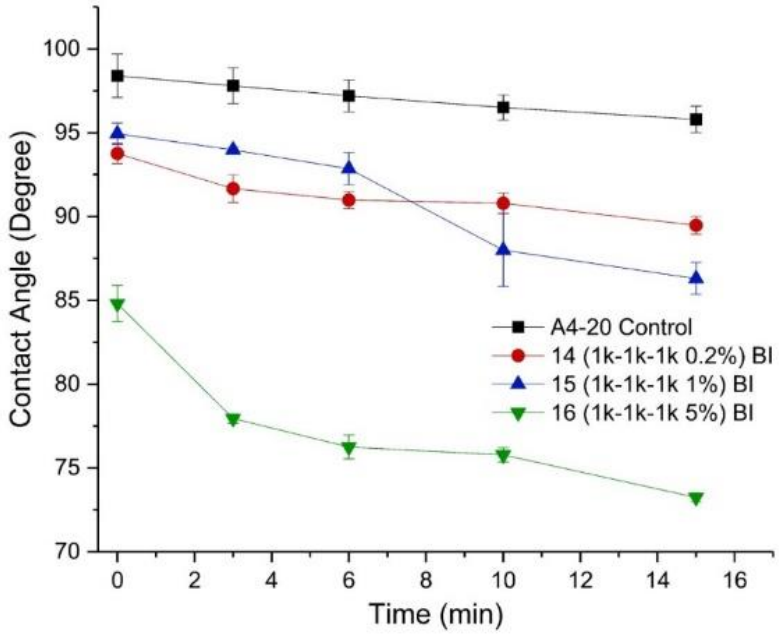

Figure A9. Water contact angle data for additive 1k-1k-1k until 15 minutes, indicating effect of amount of the additive on contact angle values.

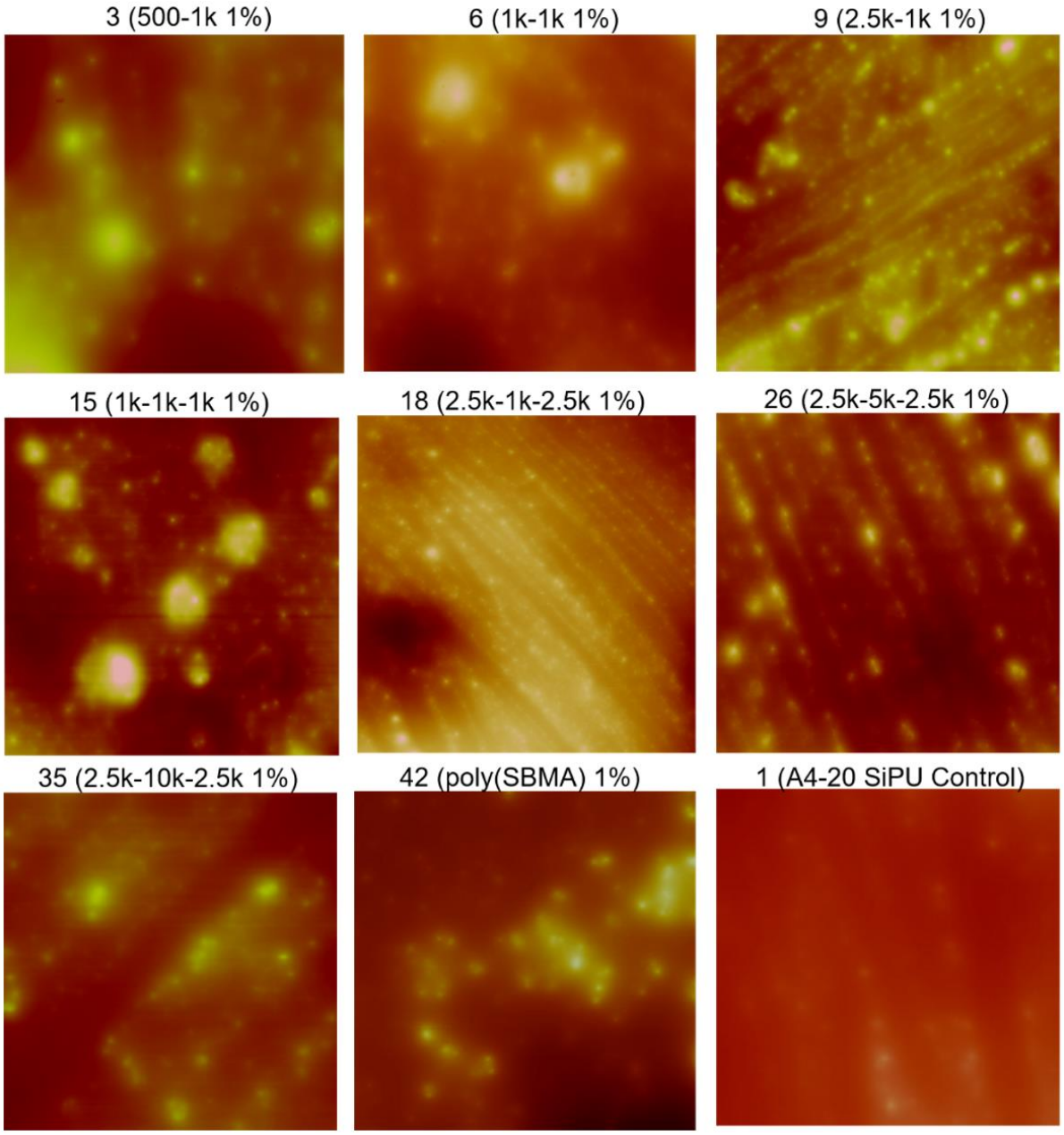

Figure A10. AFM height images.

One-way ANOVA: ***U linza*** biomass remaining at 110 kPa versus coating Type

Factor	Levels	Values
coating	12	1, 3, 6, 9, 15, 18, 26, 35, 42, 700, 900, 1100

Analysis of Variance

Source	DF	Adj MS	F-Value	P-Value
coating	11	21142555.2375	142.838	0.0000
Error	25	148017.7447		
Total	36			

Means

coating	N	Mean	StDev
1	18501.6	388.172	1
42	10826.0	262.034	42
3	10577.0	330.680	3
6	10542.0	284.264	6
9	10780.1	585.811	9
15	10502.8	374.895	15
18	10474.1	278.612	18
26	10122.9	523.541	26
35	10662.6	319.924	35
1100 SR	10045.9	621.068	1100 SR
PU	19365.4	520.841	PU
T2	7192.8	400.186	T2

Tukey Pairwise Comparisons

Groups	Means Upper and Lower	Mean Difference	95% Confidence Interval		P-Value
1 vs 15	[18501.6, 10502.8]	7998.8	6898.1271	9099.4729	0.0000
1 vs 18	[18501.6, 10474.1]	8027.5	6926.8271	9128.1729	0.0000
1 vs 26	[18501.6, 10122.9]	8378.7	7278.0271	9479.3729	0.0000
1 vs 3	[18501.6, 10577]	7924.6	6823.9271	9025.2729	0.0000
1 vs 35	[18501.6, 10662.6]	7839	6738.3271	8939.6729	0.0000
1 vs 42	[18501.6, 10826]	7675.6	6574.9271	8776.2729	0.0000
1 vs 6	[18501.6, 10542]	7959.6	6858.9271	9060.2729	0.0000
1 vs 9	[18501.6, 10780.1]	7721.5	6620.8271	8822.1729	0.0000

Figure A11. Statistical analysis of variance for *U. linza*.

One-way ANOVA: **Barnacle** adhesion versus coating Type

Factor	Levels	Values
coating	12	1, 3, 6, 9, 15, 18, 26, 35, 42, 700, 900, 1100

Analysis of Variance

Source	DF	Adj SS	Adj MS	F-Value	P-Value
coating	11	0.005058	0.000460	2.07	0.090
Error	16	0.003555	0.000222		
Total	27	0.008613			

Means

coating	N	Mean	StDev	95% CI
1	5	0.0517	0.0231	(0.0375, 0.0658)
3	1	0.03230	*	(0.00070, 0.06390)
6	2	0.0203	0.0150	(-0.0020, 0.0426)
9	2	0.01365	0.00488	(-0.00869, 0.03599)
15	2	0.01610	0.01287	(-0.00624, 0.03844)
18	1	0.02410	*	(-0.00750, 0.05570)
26	3	0.02463	0.00451	(0.00639, 0.04288)
35	3	0.02130	0.00687	(0.00306, 0.03954)
42	1	0.000000	*	(-0.031599, 0.031599)
700	2	0.01610	0.01075	(-0.00624, 0.03844)
900	3	0.01823	0.00988	(-0.00001, 0.03648)
1100	3	0.02190	0.01671	(0.00366, 0.04014)

Fisher Pairwise Comparisons

Difference of Levels	Difference of Means	SE of Difference	95% CI	T-Value	Adjusted P-Value
3 - 1	-0.0194	0.0163	(-0.0540, 0.0153)	-1.19	0.253
6 - 1	-0.0314	0.0125	(-0.0578, -0.0049)	-2.51	0.023
9 - 1	-0.0380	0.0125	(-0.0644, -0.0116)	-3.05	0.008
15 - 1	-0.0356	0.0125	(-0.0620, -0.0091)	-2.85	0.012
18 - 1	-0.0276	0.0163	(-0.0622, 0.0071)	-1.69	0.111
26 - 1	-0.0270	0.0109	(-0.0501, -0.0039)	-2.48	0.025
35 - 1	-0.0304	0.0109	(-0.0534, -0.0073)	-2.79	0.013
42 - 1	-0.0517	0.0163	(-0.0863, -0.0170)	-3.16	0.006
700 - 1	-0.0356	0.0125	(-0.0620, -0.0091)	-2.85	0.012
900 - 1	-0.0334	0.0109	(-0.0565, -0.0103)	-3.07	0.007
1100 - 1	-0.0298	0.0109	(-0.0528, -0.0067)	-2.73	0.015

Dunnett Multiple Comparisons with a Control 1 (A4-20)

Difference of Levels	Difference of Means	SE of Difference	95% CI	T-Value	Adjusted P-Value
3 - 1	-0.0194	0.0163	(-0.0715, 0.0327)	-1.19	0.902
6 - 1	-0.0314	0.0125	(-0.0712, 0.0084)	-2.51	0.178
9 - 1	-0.0380	0.0125	(-0.0778, 0.0018)	-3.05	0.066
15 - 1	-0.0356	0.0125	(-0.0754, 0.0042)	-2.85	0.096
18 - 1	-0.0276	0.0163	(-0.0797, 0.0245)	-1.69	0.604
26 - 1	-0.0270	0.0109	(-0.0618, 0.0077)	-2.48	0.188
35 - 1	-0.0304	0.0109	(-0.0651, 0.0044)	-2.79	0.108
42 - 1	-0.0517	0.0163	(-0.1038, 0.0004)	-3.16	0.053
700 - 1	-0.0356	0.0125	(-0.0754, 0.0042)	-2.85	0.096
900 - 1	-0.0334	0.0109	(-0.0682, 0.0013)	-3.07	0.063

Figure A12. Statistical analysis of variance for barnacles

Chapter 3. Supplemental Information

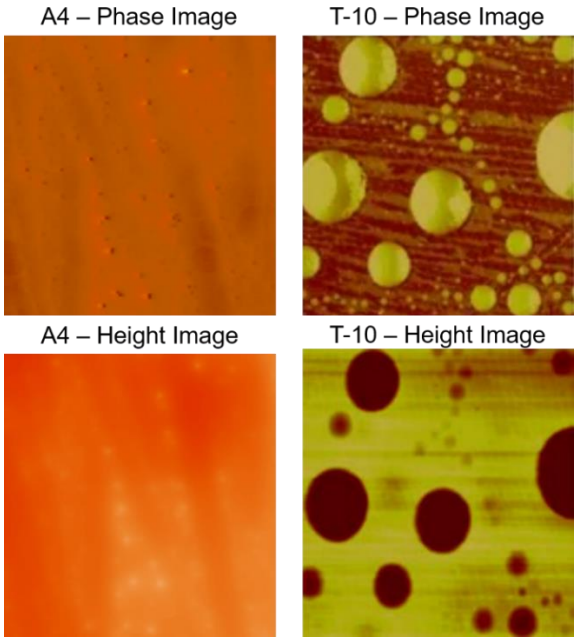

Figure A13. Internal control coatings phase and height AFM images. A4 has a hydrophobic surface composed of sole PDMS. T-10 has an amphiphilic surface composed of both 750 $\bar{M}_n$ PEG and 10,000 $\bar{M}_n$ PDMS (each at 10 wt.%) crosslinked to the coating network.

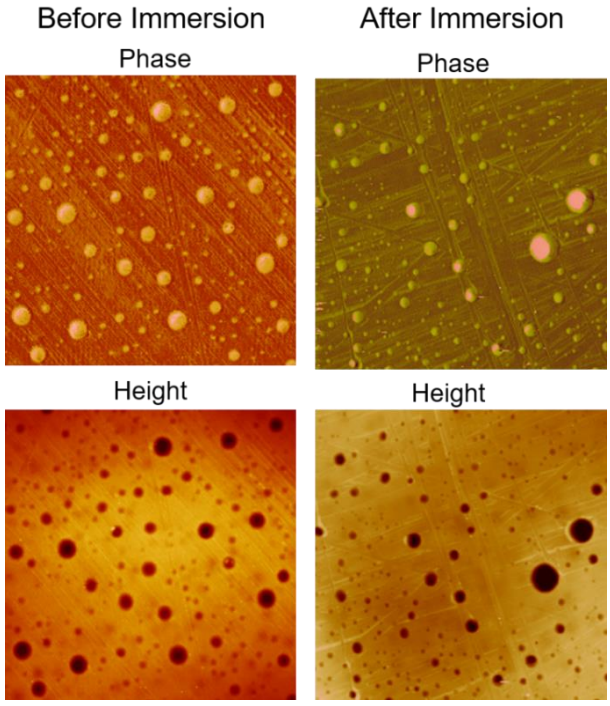

Figure A14. AFM analysis of F25 coating before and after water immersion, displaying phase images (Upper) and height images (bottom). Each image is for an area of 100 µm x 100 µm.

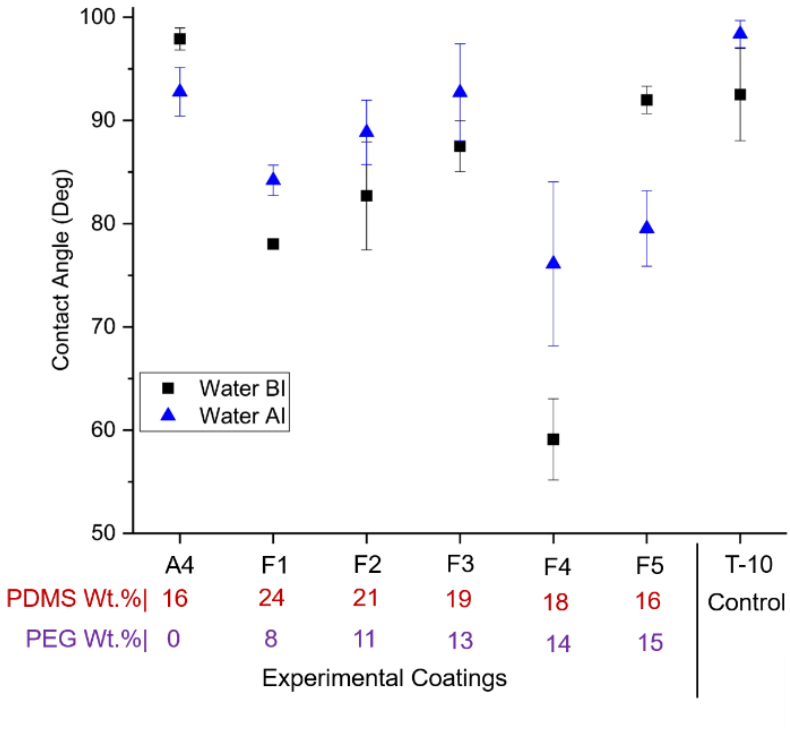

Figure A15. Water contact angle data for coatings before immersion (BI) and after immersion (AI) in water for 28 days.

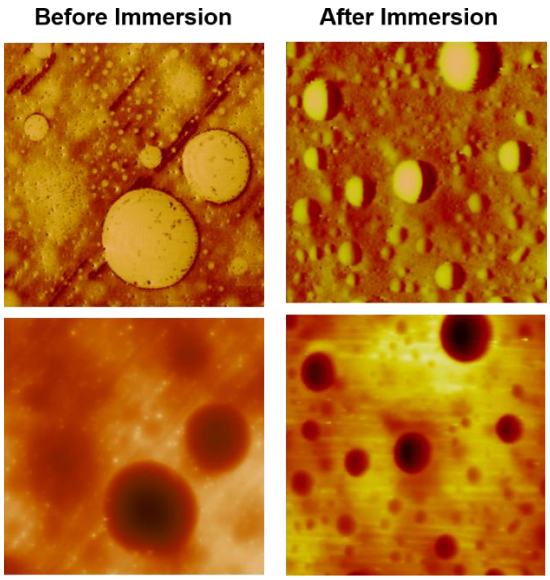

Figure A16. AFM analysis of F1 coating before and after water immersion, displaying phase images (Upper) and height images (bottom). Each image is for an area of 100 µm x 100 µm.

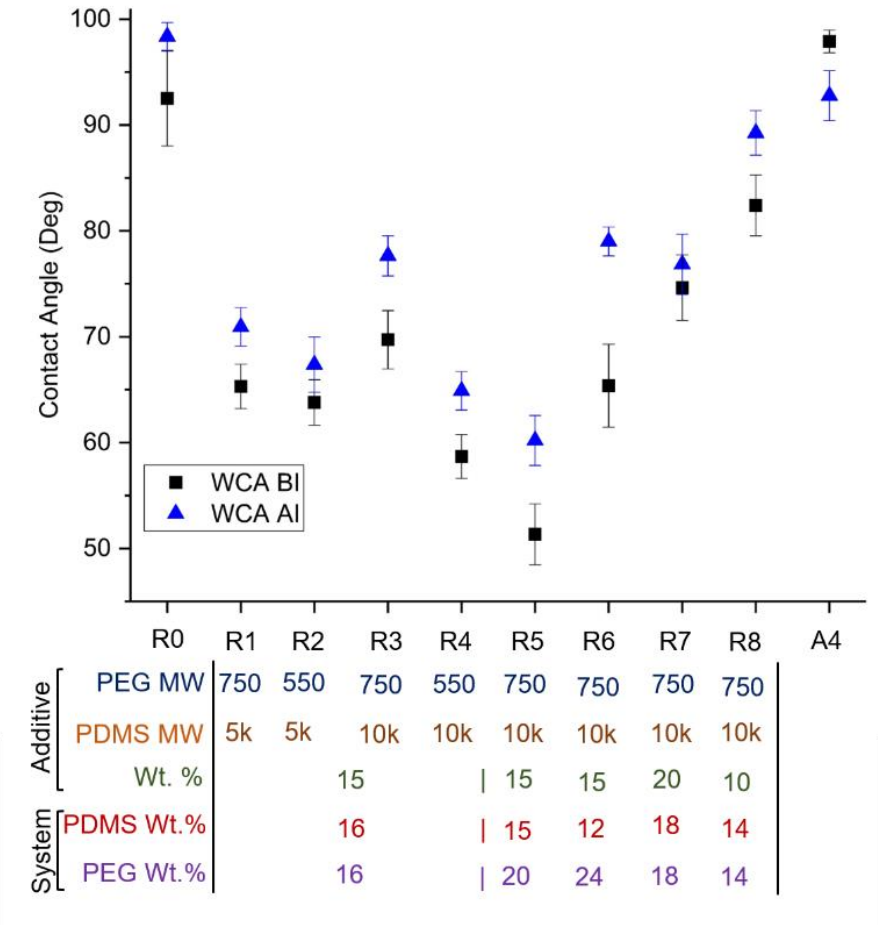

Figure A17. Water contact angle data for coatings before immersion (BI) and after immersion (AI) in water for 28 days. The x-axis is labeled to reflect details about utilized additive and the overall content of PEG and PDMS in a formulation.

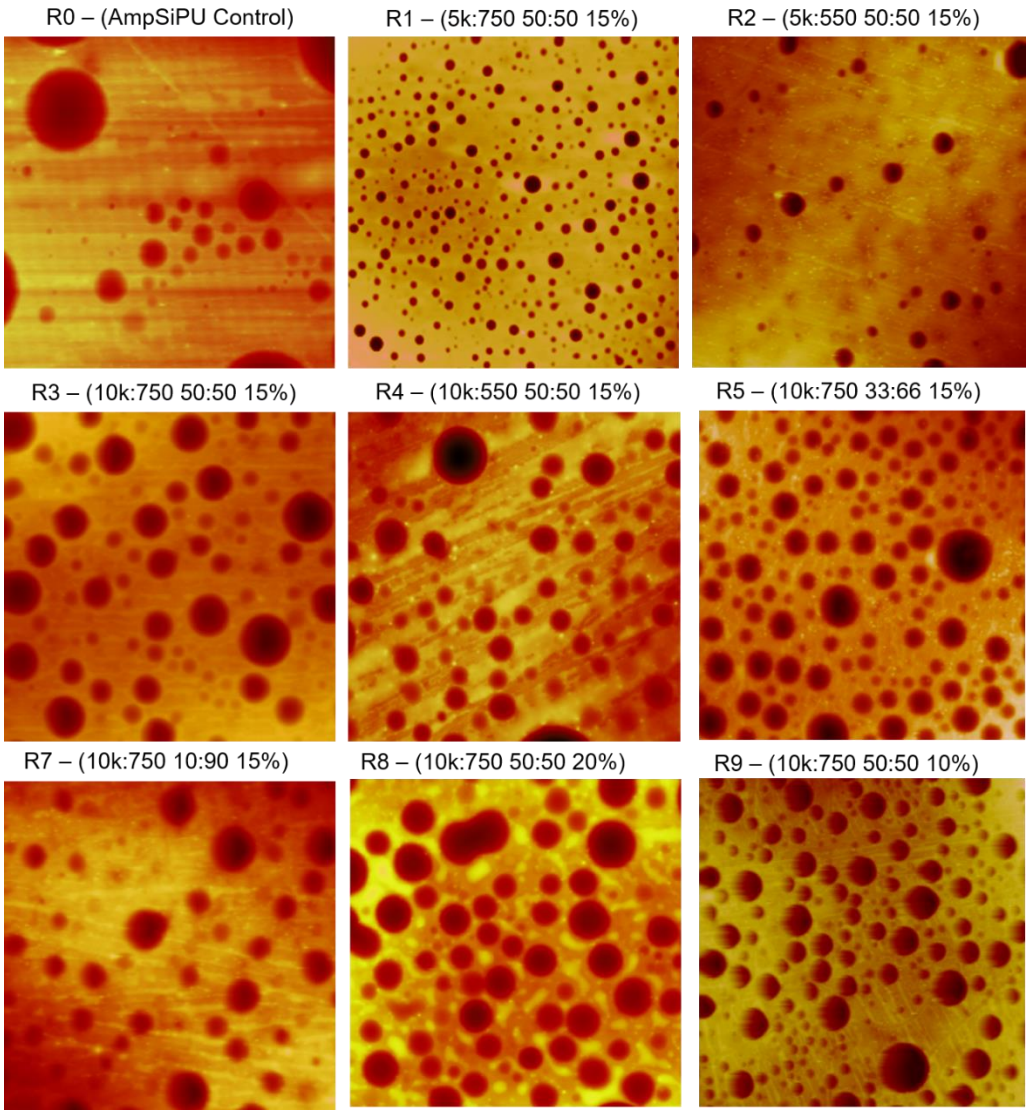

Figure A18. AFM height images of unmodified and modified R0 AmpSiPU coatings. These images are in correlation with phase images in Figure 5. Each image is for an area of 100 µm x 100 µm. Each label reflects the coating number.

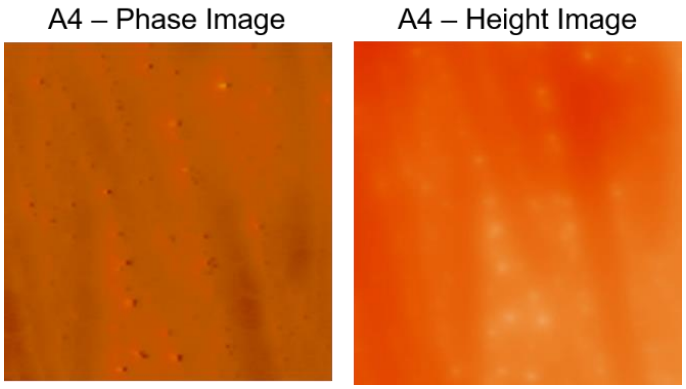

Figure A19. AFM images of hydrophobic A4 SiPU system.

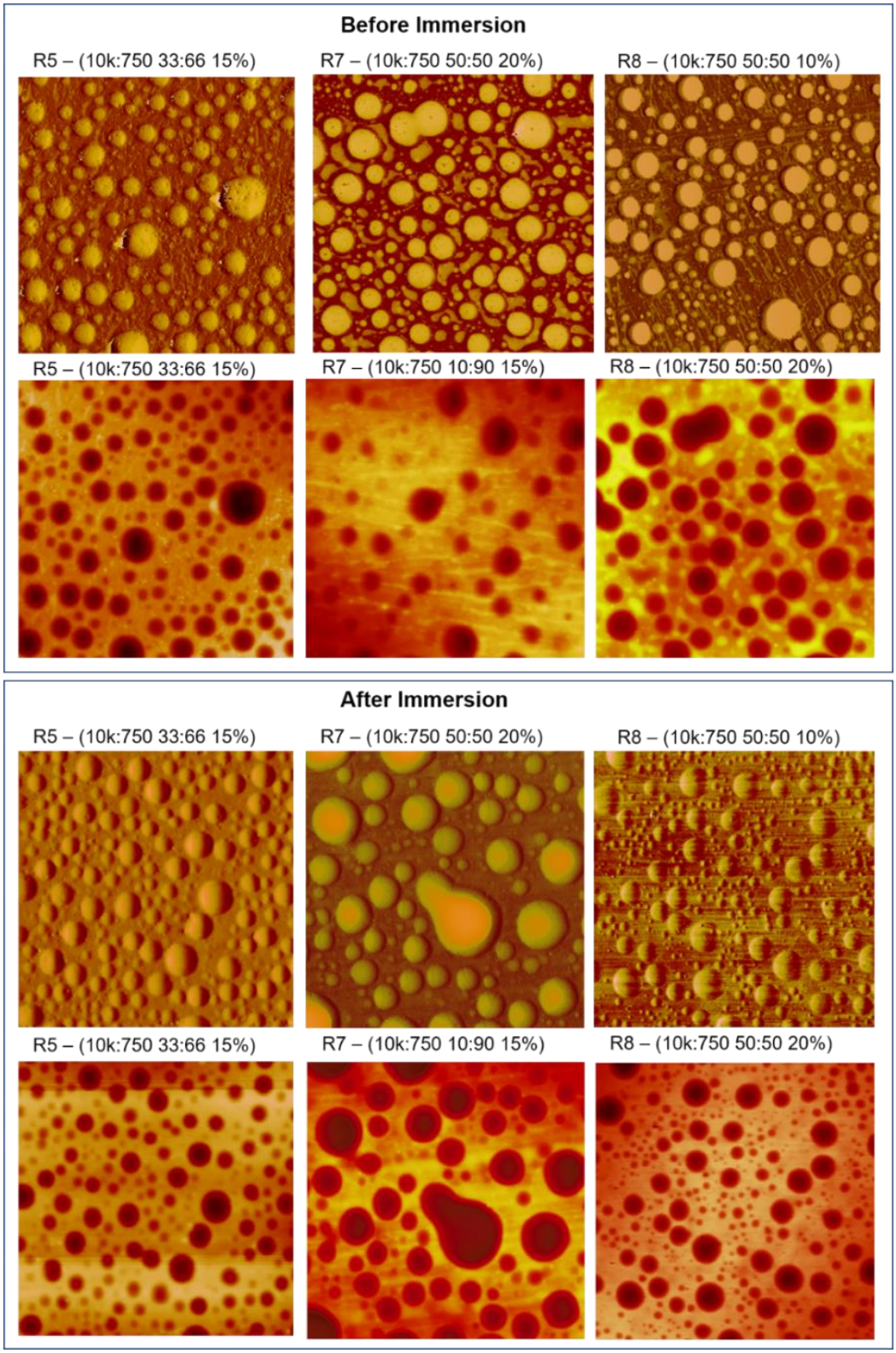

Figure A20. AFM analysis of R5, R7, and R8 coatings before and after water immersion, displaying phase images (Upper) and height images (bottom) under each section. Each image is for an area of 100 µm x 100 µm.

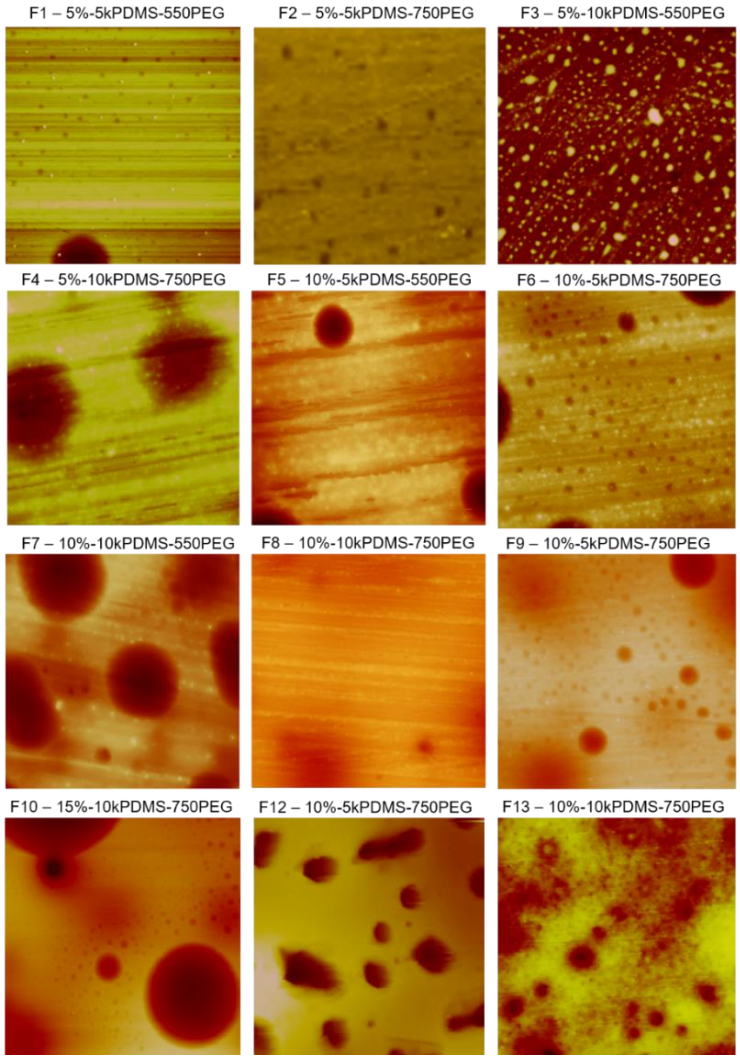

Figure A21. AFM height images of AmpSiGC coatings. Each image is for an area of 100 µm x µm. Each label reflects the coating number and composition of an image.

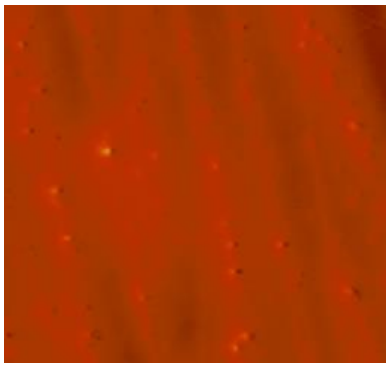

Figure A22. SiPU A4 control coating phase AFM image. The system has a hydrophobic surface composed of sole PDMS.

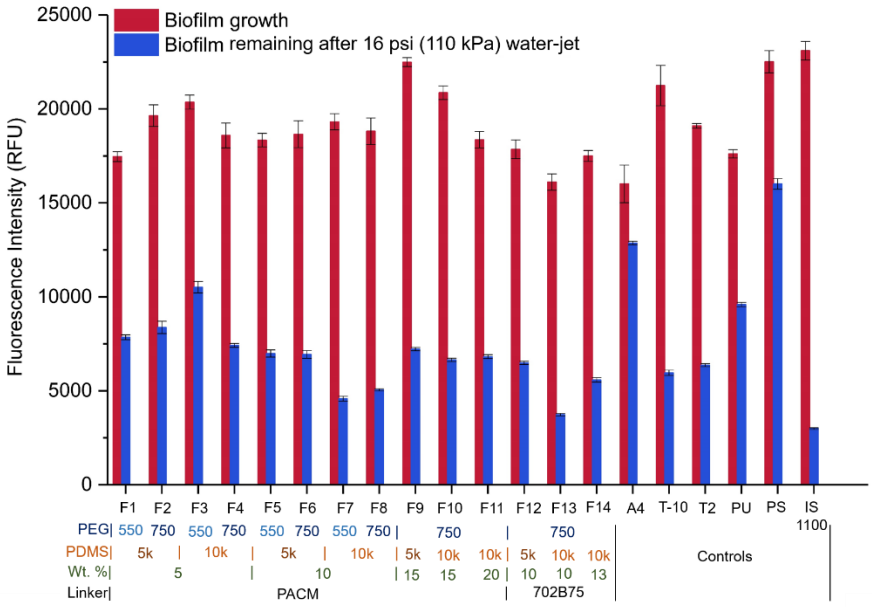

Figure A23. *U. linza* fouling-release data for biofilm growth (Red bar) and biomass remaining after water jetting at 16 psi (blue bar). The x-axis is labeled to specify the formulations and its components including PEG MW, PDMS MW, wt.% of PEG and PDMS, and crosslinker type.

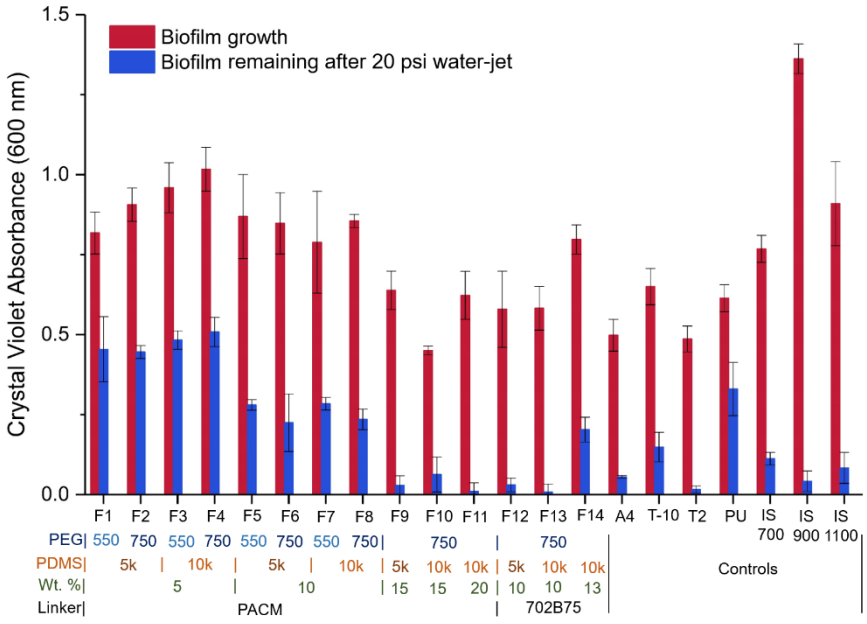

Figure A24. *C. lytica* fouling-release data for biofilm growth (Red bar) and release after 20 psi water jetting (blue bar). The x-axis is labeled to specify the formulations and its components including PEG MW, PDMS MW, wt.% of PEG and PDMS, and crosslinker type.